

Institut für Chemie

DISSERTATION

The Crystal Structures and Thermal Behavior of Hydrogen Monofluorophosphates and Basic Monofluorophosphates with Alkali Metal and N-containing Cations

zur Erlangung des akademischen Grades

doctor rerum naturalium

(Dr. rer. nat.)

Mathematisch-Naturwissenschaftlichen Fakultät I

der Humboldt-Universität zu Berlin

Diplom-Chemikerin Hillary A. Prescott

geboren am 07.09.1971 in San Francisco, California, USA

Dekan der Mathematisch-Naturwissenschaftlichen Fakultät I

Prof. Dr. Bernhard Ronacher

Gutachter: 1. Prof. Dr. E. Kemnitz
 2. Prof. Dr. H. Hartl
 3. Prof. Dr. J. Pickardt

eingereicht: 11. September 2001

Datum der Promotion: 30. November 2001

Table of Contents

1	Introduction	1
1.1	Literature Survey	2
2	Experimental Section	7
2.1	Methods	7
2.2	Chemicals	11
2.3	Preparation	11
3	Synthesis	22
4	The Crystal Structures and their Hydrogen Bonding	30
4.1	The Structures with Infinite Chains	31
4.1.1	$\text{NaHPO}_3\text{F} \cdot 2.5 \text{H}_2\text{O}$	32
4.1.2	$[\text{NH}_2(\text{CH}_2\text{CH}_3)_2]\text{HPO}_3\text{F}$	34
4.1.3	$[\text{NH}_2(\text{CH}_2\text{CH}_2)_2\text{NH}_2][\text{HPO}_3\text{F}]_2$	35
4.2	The Structure with Branched Chains	36
4.2.1	KHPO_3F	37
4.3	The Structure with Isolated Dimers	39
4.3.1	$\text{K}_3[\text{H}(\text{PO}_3\text{F})_2]$	39
4.4	The Structures with Cyclic Dimers	40
4.4.1	CsHPO_3F	41
4.4.2	$[\text{NH}(\text{CH}_2\text{CH}_3)_3]\text{HPO}_3\text{F}$	42
4.4.3	$[\text{C}(\text{NH}_2)_3]\text{HPO}_3\text{F}$	44
4.4.4	$\{\text{HOC}[\text{NH}(\text{CH}_3)_2]\}\text{HPO}_3\text{F}$	45
4.5	The Structures with Cyclic Tetramers	47
4.5.1	$\alpha\text{-NH}_4\text{HPO}_3\text{F}$	47
4.5.2	$\beta\text{-NH}_4\text{HPO}_3\text{F}$	48

4.5.3 α -RbHPO ₃ F	50
4.6 The Complex Structures and Hydrates	51
4.6.1 Cs ₃ (NH ₄) ₂ (HPO ₃ F) ₃ (PO ₃ F)	52
4.6.2 [N(CH ₃) ₄]HPO ₃ F·H ₂ O	55
4.6.3 Na ₂ PO ₃ F·10H ₂ O	57
4.6.4 Na ₅ [N(CH ₃) ₄](PO ₃ F) ₃ ·18H ₂ O	59
4.6.5 [C(NH ₂) ₃] ₂ PO ₃ F	62
4.7 The Structure of β -RbHPO ₃ F	63
4.8 Summary	66
5 Thermal Analysis	69
5.1 The Sodium Salts: NaHPO ₃ F and NaHPO ₃ F·2.5H ₂ O	70
5.1.1 The Thermal Behavior of NaHPO ₃ F	71
5.1.2 The Thermal Behavior of NaHPO ₃ F·2.5H ₂ O	75
5.1.3 Comparison	80
5.2 The Thermal Behavior of CsHPO ₃ F	81
5.3 The Thermal Behavior of [NH(CH ₂ CH ₃) ₃]HPO ₃ F	83
5.4 Summary	85
6 Discussion	87
6.1 A Structural Comparison to the Hydrogen Chalcogenates and Other Oxoacid Salts.....	87
6.2 Structural Features	93
6.3 Fluorine	94
6.4 The Tetrahedral Bonding	97
6.5 The Hydrogen Bonding	99
7 Summary and Conclusions	104
Zusammenfassung	107
Appendix	110
A.1 Selected Experimental Data for the Single Crystal Analysis	110
A.2 Atomic Coordinates and Equivalent Isotropic Displacement Parameters	114
A.3 Selected Bond Lengths	125
A.4 ¹⁹ F, ³¹ P, and ¹ H MAS NMR Data and Spectra.....	129
References	132
Acknowledgements	

Table of Abbreviations, Acronyms, and Symbols

a, b, c, α , β , γ	lattice constants and angles
A	hydrogen acceptor of the hydrogen bond
Å	Ångstrom, 10 pm, 10^{-10} m
aq	aqueous
avg.	average
calcd	calculated
Cs/NH ₄	Cs ₃ (NH ₄) ₂ (HPO ₃ F) ₃ (PO ₃ F) ₂
$\frac{1}{2}$ D + $\frac{1}{2}$ A	$\frac{1}{2}$ hydrogen donor and $\frac{1}{2}$ hydrogen acceptor
d	bond length
D	hydrogen donor of the hydrogen bond
Diet	diethyl ammonium hydrogen monofluorophosphate
di or disd	disordered
DTA	differential thermal analysis
DTG	differential thermogravimetric analysis
Et	ethyl group, $-\text{CH}_2\text{CH}_3$
EtOH	ethanol
Et ₂ O	diethyl ether
<i>GooF</i>	goodness of fit defined as $GooF = S = \{\Sigma[w(F_o^2 - F_c^2)^2]/(n-p)\}^{1/2}$
(H)PO ₃ F	hydrogen monofluorophosphate or monofluorophosphate
H _{(H)PO₃F}	hydrogen atom of OH group in the (H)PO ₃ F tetrahedron
H _N	hydrogen atom on nitrogen
IC	ion current
M	Na ⁺ , K ⁺ , Rb ⁺ , Cs ⁺ , or NH ₄ ⁺ , unless otherwise defined
Me	methyl group, $-\text{CH}_3$
med	medium
MeOH	methanol
Na/[NMe ₄]	Na ₅ [NMe ₄](PO ₃ F) ₃ ·18H ₂ O
N,N'-dmu	N,N'-dimethyl urea
N,N'-dmuH ⁺	N,N'-dimethyl uronium cation, {HOC[NH(CH ₃) ₂]} ⁺
O _A	hydrogen acceptor oxygen atom

Occ.	occupancy
O _D	hydrogen donor oxygen atom
O _w	oxyge. atom of crystal water
O _(w)	oxygen atom of crystal water or (H)PO ₃ F tetrahedron
PE	polyethylene
PipzH ₂ ²⁺	piperazinium cation, [NH ₂ (CH ₂ CH ₂) ₂ NH ₂] ²⁺
Pipz	piperazinium hydrogen monofluorophosphate
PTA	pulse thermal analysis
R_I	residual factor defined as $R_I = \Sigma F_{\text{obs}} - F_{\text{calc}} / \Sigma F_{\text{obs}} $
RT	room temperature
Sect.	section
STA	simultaneous thermal analysis (DG, DTA, TG)
TG	thermogravimetry
wR_2	residual factor defined as $wR_2 = \{ \Sigma [w(F_o^2 - F_c^2)^2] / \Sigma [w(F_o^2)^2] \}^{1/2}$
V	unit cell volume
V_F	total fluorine bond valency
X	oxygen or fluorine atom, unless defined otherwise
XRD	X-ray powder diffraction
Z	number of formula units in the cell
μ	absorption coefficient
ρ _{calc}	density, calculated
∠	bond angle

Chapter 1

Introduction

Strong acids such as H_3PO_4 , H_2SO_4 , and HClO_4 are known to supply hydrated protons for proton conductivity. Even in the absence of H_2O , proton conductivity has been observed in these acids due to self-dissociation [1]. Acid salts of these and other acids have been examined for proton conductivity, because they offer a solid form of the acid, which is easier to handle and less corrosive. Only small proton conductivities were observed in acid salts, until a systematic search found that acidic iodates and CsHSO_4 had particularly high conductivities [1, 2]. Most acid salts undergo phase transitions to produce temperature-dependent modifications with different physical properties. Proton conductivity is largely dependent on the hydrogen bonding and the geometry of the tetrahedra in the structure. The conductivity of the H_3O^+ and OH^- ions (350 and $192 \text{ } \Omega^{-1}\text{cm}^2\text{mol}^{-1}$, respectively) in a hydrogen-bonded media is higher than other ions because of proton-transfer mechanisms. The processes leading to proton conductivity are described by the Grotthus and vehicle mechanisms [3, 4].

The acid salts, MHXO_4 ($\text{X} = \text{S}, \text{Se}$), have been investigated indepth crystallographically and thermally for phase transitions and their consequent physical properties, such as ferroelectricity and superionicity. Some of them have successive phase transitions and superionicity has been found in their high temperature modifications [5]. These phase

transitions are often irreversible and affected by moisture [6]. CsHSO_4 undergoes several phase transitions from a low temperature phase through an intermediate phase at 333-370 K to a superionic phase at 410-414 K based on the dynamic reorientational disorder of the sulfate tetrahedra [2]. Other salts with this composition also exhibit ferroelectric activity. RbHSO_4 and NH_4HSO_4 both have ferroelectric phases with transitions below 260 K. The ammonium salt goes from being nonferroelectric above 270 K through a ferroelectric phase and back to being nonferroelectric below 155 K [7]. RbHSO_4 is paraelectric at room temperature and ferroelectric at lower temperatures with $T_c = 265$ K [8]; the corresponding KHSO_4 is not ferroelectric [9]. Other compositions, such as $\text{M}_3\text{H}(\text{XO}_4)_2$ ($\text{M} = \text{Na}, \text{K}, \text{Rb}$ and $\text{X} = \text{S}, \text{Se}$), have also been studied [10]. The structures and thermal behavior of acid salts with both sulfate and phosphate tetrahedra [11] and acid adducts of sulfuric acid [10, 12] have also been examined. Although the hydrogen sulfates, selenates, and these salts have been investigated extensively, the acid salts of the monofluorophosphoric acid, $\text{H}_2\text{PO}_3\text{F}$, have hardly been studied at all. The monofluorophosphate and sulfate anions are isoelectronic due to the replacement of one of the oxygens by fluorine on phosphorus to form a PO_3F^{2-} ion. Often isosterism between compounds results in similar chemical and physical properties [13]. Thus, it could be speculated that the acid salts of $\text{H}_2\text{PO}_3\text{F}$ and H_2SO_4 have similar crystal structures (hydrogen bonding) and consequently common physical properties. Therefore, the

- synthesis
- crystal structure
- thermal behavior

of the hydrogen monofluorophosphates with alkali metal cations and cations containing nitrogen were studied. Structural correlations and differences between the hydrogen monofluorophosphates and hydrogen sulfates were then established. The investigations led to conclusions on the hydrogen bonding and the influence of fluorine on the bonding in the acid salts of monofluorophosphoric acid.

1.1 Literature Survey

Monofluorophosphoric Acid and the Monofluorophosphates

Monofluorophosphoric acid, $\text{H}_2\text{PO}_3\text{F}$, is an oxo acid, in which one of the OH groups on phosphorus has been substituted by fluorine. The monofluorophosphates have been known for over 100 years. The first "hydrogen monofluorophosphates" with rubidium and

potassium were synthesized by the reaction of the phosphate with the hydroxide and hydrofluoric acid (Reaction 1) [14,15, 16].



The compounds were characterized by elemental analysis. The constitution of these salts was suggested to be similar to that of the phosphates with one of the OH groups replaced by a fluorine atom to form a PO_3F^{2-} anion [14, 15], but it was not proven at the time. The general constitution of the PO_3F^{2-} anion was later confirmed by ^{31}P and ^{19}F NMR spectroscopy. Both the ^{31}P and ^{19}F NMR spectra show 1-1 doublets for the tetrahedral orthophosphate group with one oxygen atom substituted by a fluorine atom [17]. This substitution of one O/OH group on phosphorus creates an anion isoelectronic to the sulfate anion, SO_4^{2-} . Similarities between the basic monofluorophosphates and sulfates were noted in [18]. The monofluorophosphoric acid, $\text{H}_2\text{PO}_3\text{F}$, like sulfuric acid, is a strong, diprotic acid. It is commercially available, but not in pure form. This is due to the hydrolysis and decomposition of the monofluorophosphoric acid to orthophosphoric acid (Reaction 2). The hydrolysis is complete in dilute solution [16]. The rate of hydrolysis is pH-dependent with the monofluorophosphate anion hydrolyzing rapidly at very low and high pH values [19]. The equilibrium of the hydrolysis of $\text{H}_2\text{PO}_3\text{F}$ (Reaction 2) has been studied in detail [16].



Basic salts of the monofluorophosphoric acid are stable in a neutral or weakly alkaline aqueous solution [19], which is reflected in the literature. A variety of basic monofluorophosphates have been published in the last century; some of which are mentioned in [16, 17, 20]; the thermal behavior of $\text{CaPO}_3\text{F} \cdot 2\text{H}_2\text{O}$ [21, 22], $\text{SrPO}_3\text{F} \cdot \text{H}_2\text{O}$ [23, 24], and $\text{Mg}(\text{NH}_4)_2(\text{PO}_3\text{F})_2 \cdot 2\text{H}_2\text{O}$ [25] has also been investigated. On the other hand, the hydrogen monofluorophosphates have remained practically unknown. In 1968, J. Neels and W. Grunze published the synthesis of the following hydrogen monofluorophosphates: NaHPO_3F , KHPO_3F , and $\text{NH}_4\text{HPO}_3\text{F}$ [26]. The products were characterized by Guinier exposures and NMR spectroscopy (^{31}P and ^{19}F); their crystal structures were not determined. The thermal behavior of KHPO_3F was later investigated by paper chromatography [27]. Since then, only the crystal structure of anilinium hydrogen monofluorophosphate, $[\text{C}_6\text{H}_5\text{NH}_3]\text{HPO}_3\text{F}$ [28], has been determined. Consequently, very little is known about the hydrogen bonding in the hydrogen monofluorophosphates.

Hydrogen Bonding

Hydrogen bonding, which involves weak interactions between hydrogen atoms and electronegative atoms, influences the structure and properties of compounds. The hydrogen bond is defined as the interaction of a hydrogen atom with two of its nearest electronegative neighbors, such as oxygen, nitrogen, and/or fluorine. The atom, X, with the shorter distance to hydrogen below 1.0 Å is defined as the hydrogen donor; whereas, the second neighbor, Y, with the weaker interaction with hydrogen is referred to as a hydrogen acceptor. This interaction forms a bond with the X...Y interatomic distance ranging from about 2.26-3.20 Å [29, 30], when X and Y are oxygen, nitrogen, and/or fluorine. Physical properties of compounds are dependent on the strength of the hydrogen bond, which is determined by the length of the X...Y distance. The hydrogen bonds can be classified as very strong (< 2.50 Å), strong (2.50-2.65 Å), medium (2.65-2.80 Å), or weak (>2.80 Å) based on O...O distances [31]. The geometry of the hydrogen bond can be asymmetrical, as described above, or symmetrical, when very short separations are found between the two electronegative elements and the hydrogen atom is involved in two equivalent bonds to X and Y. The geometry of the hydrogen bond is dependent on the potential surfaces of the possible positions for the hydrogen atom. Hydrogen bonds with two equivalent hydrogen positions (two minima on the potential curve) are disordered, either statistically or dynamically. Theoretically, the hydrogen atom lies on a line between the two neighbors forming a linear bond, X-H...Y with an $\angle XHY$ of 180°. However, angles found in structures tend to deviate to lower values. Some example lengths found for the different hydrogen bonds are: F-H...F 2.27-2.49 Å in NaHF₂, KH₄F₅, and HF; O-H...O 2.40-2.63 in acid salts and 2.7-2.9 Å in ice, hydrates, and hydroxo compounds; N-H...O 2.86 in (NH₄)₂H₃IO₆; and N-H...F 2.6-2.96 Å in NH₄F and (N₂H₆)SiF₆ [30]. The mixed hydrogen bond, O-H...F, has lengths of 2.56 and 2.87 Å found in the hydrates of metal fluorides [30]. No length is given for this type of hydrogen bond in an inorganic acid salt, in which the fluorine atom is covalently bonded to another atom, such as P.

Structural Features of the Hydrogen Sulfates

A variety of structural patterns have been found for hydrogen-bonded HSO₄ tetrahedra in the crystal structures of the hydrogen sulfates on the basis of the strong O...O hydrogen bonds [10, 32]. These patterns or structural features include isolated dimers, cyclic dimers, infinite chains, branched chains, cyclic tetramers, and layer structures depending on the H/SO₄ ratio. The type of structure formed is also dependent on the cation. In the case of a H/SO₄ ratio of 1:1, infinite chains, cyclic dimers, and/or branched chains have been found.

Structures with this H/SO₄ ratio have one hydrogen donor, O_D, and one hydrogen acceptor, O_A, for every HSO₄ tetrahedron. Infinite chains have been observed in the following structures: RbHSO₄ [8, 33], CsHSO₄ [6], CsHSeO₄ [34], and [C(NH₂)₃]HSO₄ [35]. Two types of geometry are seen in the structures with infinite zigzag chains of HSO₄ depending on the angle between the tetrahedra (\angle SSS). Tetrahedral angles were found in RbHXO₄ [8, 33] and CsHXO₄ [6, 34] with X = S or Se with smaller angles observed in structures with larger cations [32]. Cyclic dimers formed by two HSO₄ tetrahedra (2O_A+2O_D/dimer) were observed in the isotypic structures of β -NaHSO₄ [36] and NaHSeO₄ [37] and a superprotonic phase of CsHSO₄ [2, 38], but according to [32] they are rather rare for the structures of the hydrogen sulfates. The cyclic dimers in these structures have two different hydrogen bonds holding them together. The structure of KHSO₄ [9, 39] and KHSeO₄ [40] consists of separate units of cyclic dimers and infinite chains. In comparison with the cyclic dimers in the β -modification of NaHSO₄, branched chains were found in the α -NaHSO₄ [41]. Two types of branched chains were observed in hydrogen sulfates depending on the linear or zigzag symmetry of the chain [32]: the branched tetrahedra are situated on one side of the linear chains and alternate sides of zigzag chains. Whether infinite or branched chains form in the structure seems to be dependent on the size of the metal cation [32]. An additional structural motif is the cyclic tetramers found along with separate infinite chains in the structure of AgHSO₄ [42, 43]. This type of tetrameric bonding had not previously been observed in the hydrogen sulfates. Isolated dimers are formed in structures with the composition: M₃[H(SO₄)₂], where the H/SO₄ ratio is less than one. Such dimers were found in the sulfate and selenate structures with M = K [44, 45] and Rb [46, 47, 48], Cs₃H(SeO₄)₂ [49, 50], and the sulfate structures with Na [51] and NH₄ [52]. All of which are isostructural except for the sodium salt. The composition, [H(SO₄)₂], has a H/SO₄ ratio of 1/2 which implies: 1/2D + 1/2A. The hydrogen atom is shared by two SO₄ tetrahedra connected to each other by either a symmetrical or an asymmetrical hydrogen bond. The symmetrical hydrogen bond in the NH₄, K, Rb, and Cs structures was formed by disordered hydrogen atoms; an asymmetrical hydrogen bond was found in Na₃H(SO₄)₂. Disorder was observed in strong O...O bonds with two minima and, for the most part, an O...O interatomic distance of 2.45-2.55 Å in the M₃H(SO₄)₂ structures [32].

In comparison to the alkali metal hydrogen sulfates, the hydrogen sulfates with N-containing cations other than ammonium have hardly been studied crystallographically. One exception is the hydrogen sulfate with guanidinium, already mentioned, based on the discovery of ferroelectricity in the guanidinium sulfates, [C(NH₂)₃]Al(SO₄)₂·6H₂O [53]

and $[\text{C}(\text{NH}_2)_3]\text{UO}_2(\text{SO}_4)_2 \cdot 3\text{H}_2\text{O}$ [54].

Chapter 2

Experimental Section

The compounds synthesized (Sect. 2.3) were characterized by the following methods.

2.1 Methods

Freeze drying

Freeze drying is a widely used method of sublimation drying, in which a frozen material is dried in high vacuum by subliming the solvent. The method is advantageous for the mild drying and conservation of sensitive products. Originally, the method was used in the manufacturing of instant products: foods, pharmaceuticals, biological and medical materials (blood plasma, serums, viruses). However, freeze drying is also being carried out in the laboratory to isolate unstable compounds, for example, in the synthesis of free radicals in concentrated form. In this case, the solid solvent acts as a stabilizer during freeze drying. A recombination does not take place after freeze drying, because of the absence of the reaction medium [55].

The eluate solutions (200–500 mL) of partially neutralized $\text{H}_2\text{PO}_3\text{F}$ were evaporated completely by a Christ Alpha 2-4 freeze dryer (LDC-1M control system). The solutions were frozen by liquid N_2 prior to freeze drying. The chamber was then evacuated and the

freeze drying started. Freeze drying was carried out at 0.04 mbar until the product had a constant temperature between 379-388 K. The dried powder/oil was then removed and recrystallized. Sublimation was observed for the amine salts, but did not affect the later compositions of the crystallized salts.

Fluoride Analysis

Fluoride analysis included two types of sample preparation and the measurement of the fluoride contents by a fluoride-sensitive electrode. In the first case, the sample was decomposed according to the Seel method [56] enabling the measurement of fluoride from F^- and PO_3F^{2-} in the sample. The aqueous solution of the decomposed sample was then measured for its total fluoride content. In a second analysis, a sample of the same compound was simply dissolved in 50 mL. In this case, only the free fluoride in the sample was measured and not the fluoride bonded to phosphorus. The use of these two sample preparations proved to be an excellent method for checking product purity. In cases where enough sample was available, both variations were carried out and compared. The measured fluoride contents are given in Sect. 2.3, where the method of sample preparation is indicated by Seel or H_2O .

^{31}P and ^{19}F NMR Spectroscopy

Samples for NMR measurements were dissolved in H_2O/D_2O and measured in FEP NMR tubes. The spectra were recorded on a Bruker DPX 300 spectrometer at frequencies of 121.5 and 282.4 MHz for ^{31}P and ^{19}F , respectively, with internal standards of 85% H_3PO_4 and Freon-11. The amount of phosphate ($\%H_2PO_4^-$) was estimated by the signal ratio of the integrated phosphate and monofluorophosphate signals in the ^{31}P -NMR spectrum.

^{19}F , ^{31}P , and 1H MAS NMR Spectroscopy

The ^{19}F , ^{31}P , and 1H MAS NMR spectra (Appendix A.4) of the powdered sample were recorded on a Bruker Solid State ASX 400 spectrometer equipped with a Bruker MAS 4 mm probe head at frequencies of 376.46, 161.9, and 400.13 MHz, respectively, with a rotation of 12 kHz. The following pulse programs were used: pulse time 2 μs with a relaxation time of 60 s for ^{31}P (32 scans), pulse time 1 μs with a relaxation time of 30 s for ^{19}F (80 scans), and pulse time 2 μs with a relaxation time of 30 s for 1H (40 scans).

Single Crystal X-ray Diffraction

Measured single crystals were selected under paraffin oil using a polarization microscope. The crystals were mounted on glass fibers and measured at a specific temperature (Appendix A.1) on either the four-circle Stoe STADI-4 diffractometer or the Stoe Imaging Plate Diffraction System (IPDS) area detector. In both cases, Mo-K α radiation was employed with a graphite monochromator ($\lambda = 0.71073$ Å). The four-circle diffractometer was used to measure larger crystals of high quality with smaller cells. The measurement method was a $2\theta/\omega$ -scan with a ratio of 1.0 or 0.5. Smaller crystals with larger lattice parameters and/or poorer quality were measured on the IPDS with rotation and oscillation about the ϕ -axis. During the measurements, the crystal were cooled to lower temperatures by a Oxford CRYOSTREAM using liquid nitrogen. An absorption correction was applied to the data by one of the following methods: Psi scan, numerical, or X-Shape [57]. The structures were solved with direct methods using SHELXS-86 [58] or SHELXS-97 [59] and refined with SHELXL-93 [60] or SHELXL-97 [61]. Non-hydrogen atoms were refined anisotropically. Distinction between oxygen and fluorine was accomplished by first refining the structure to a low R_I -factor with oxygen occupying all of the atoms on phosphorus. One position on phosphorus was then assigned to fluorine based on typical P–O/F bond lengths and the location of hydrogen bonds. The assignment was confirmed by a decrease in the R_I and wR_2 -factors after a final refinement of the structure. The hydrogen atoms were found with difference Fourier syntheses and refined isotropically. Experimental data for the measurements can be found in Appendix A.1 and in the corresponding crystal structure sections.

Bond Valence Calculations

The bond valence model [62, 63] was used to calculate valency of fluorine, check bonding, and verify the correctness of the structure. The model is derived from the concept of bond strength suggested by Pauling [64]. The bond valency, v , is calculated from the bond length, d_{ij} , between the ion, i , and its coordination partner, j , by the following formula:

$$v_{ij} = \exp[(R_{ij} - d_{ij})/b].$$

R_{ij} is referred to as the bond valence parameter, which has been averaged for each type of bond [62]. The difference, $R_{ij} - d_{ij}$, is normalized with a constant, b [Å], which varies depending on i and j . The total valency, V_i , of the ion, i , is then calculated by drawing the sum of all bond valencies for that ion: $\sum_j v_{ij} = V_i$.

X-ray Powder Diffraction

X-ray powder diffraction patterns were measured by a XRD 7 Seiffert-FPM diffractometer (Cu-K α radiation, Ni-filter, 5-65°, 0.05 step, 10s/step). The patterns were then compared with data from the PDF databank [65] for known compounds or with the generated pattern from the single crystal data for new compounds.

Differential Thermal Analysis

The conventional STA graphs (T, DTA, TG, DTG) were obtained by a Netzsch STA 429 thermoanalyzer. MS-coupled investigations (TG-MS) were performed using a Netzsch STA 409 C skimmer-coupled system. In the case of the STA 429 thermoanalyzer, the sample (10-20 mg) was measured by a mini-sample carrier system featuring a Pt/PtRh10-thermocouple, Pt crucible, and α -Al₂O₃ as reference. A purge gas of air or N₂ (100 mL/min) and a heating rate of 5 K/min were used. A DTA/TG-sample carrier system (Pt/PtRh10-thermocouple, Pt crucible, sample mass of about 15 mg against an empty crucible, purge gas, air or N₂, 30 mL/min, and a heating rate of 10 K/min) was integrated into the STA 409 C skimmer-coupled system.

The sample was pulverized in an agate mortar before measurement. The raw data obtained by the STA 429 and STA 409 C were interpreted with the Netzsch-Software (Version SW/STA/531.123_2) and Netzsch *Proteus* v. 4.0+, respectively, without further data processing. The determination and assignment of the characteristic temperatures in the STA graphs (T_i - *initial*, T_e - *extrapolated onset*, T_p - *peak temperature*) was carried out by following international recommendations [66]. The precision of the measurement was checked regularly by measuring recommendation standards, such as Sn, Li₂SO₄, Al [67, 68]. The enthalpimetric analysis of the DTA graphs (maximum accuracy of 10-15%) were calibrated by an appropriate standard following the recommendations in [68, 69].

IR Spectroscopy

IR spectra were recorded as KBr disks (tablets) in the range of 450-4000 cm⁻¹ on a Perkin-Elmer 1600 FT-IR spectrometer.

2.2 Chemicals

Solids

Amberlite IR-120+ ion-exchange resin	Aldrich
Ammonium hydrogen difluoride	Fluka, 98.5%
Cesium carbonate	Aldrich, 99%
Guanidinium carbonate	Riedel-de-Haën, 98%
Monofluorophosphoric acid	ABCR/Avocado, 95%
Potassium carbonate	Fluka, 99%
Phosphorus pentoxide	Merck, 98%
Piperazine	Aldrich, 99%
Rubidium carbonate	Merck, 98%
Sodium monofluorophosphate	BK Giulini Chemie GmbH. & Co.
Uronium phosphate	Fluka, 98%
N, N'-Dimethyl urea	Merck, 98%

Liquids

Diethylamine	Fluka, 99.5%
Diethylether	Fluka, $\geq 99\%$
Ethanol, abs.	Bundesmonopolverwaltung f. Branntwein, 99.8%
Fluoric acid	Fluka, 100%
Methanol	Aldrich, 99+%
Tetramethylammonium hydroxide	Aldrich, 25wt% in H ₂ O
Tetramethylammonium hydroxide	Aldrich, 25wt% in MeOH
Triethylamine	Fluka, 98%

2.3 Preparation

The compounds introduced here were synthesized by cation exchange, in which the eluant, an aqueous solution of Na₂PO₃F (see Sect. 2.2 Chemicals) or (NH₄)₂PO₃F (synthesized according to [70]), was passed through a chromatography column of 150-200 g Amberlite IR 120+ ion-exchange resin. Cation exchange was carried out in H₂O despite the risk of hydrolysis of H₂PO₃F because of the insolubility of the basic monofluorophosphates in other solvents. The rate of cation exchange was adjusted for an effective, but accelerated exchange to avoid extended hydrolysis of the acid in the column. The acidic eluate of H₂PO₃F was collected after its detection with Litmus paper. An aqueous solution of the corresponding base (carbonate, amine, monofluorophosphate, see Sect. 2.2 Chemicals) was added to the acidic eluate dropwise after collection of the first few drops. The rate of

neutralization was regulated to achieve a pH between 3-5 in the eluate-base solution to impede hydrolysis. Cation exchange was over when the pH of the solution remained constant and the drops coming off the column were neutral. After cation exchange, the partially neutralized, dilute, aqueous solution was evaporated completely by freeze drying, unless otherwise indicated. This method of sublimation drying was carried out to avoid the escape of HF and consequent condensation of phosphate. Yields were calculated after freeze drying for powders that were easy to handle. Oils obtained were recrystallized directly from the tray without being weighed.

Characterization

The compounds were characterized by elemental analysis and ^{31}P and ^{19}F NMR spectroscopy (Sect. 2.1). The NMR data and elemental analyses are given below for the different compounds. Analyses could not be carried out for compounds that were difficult to obtain in crystalline form. Deviations were also observed in the elemental analyses of compounds. These discrepancies were based on product impurity due to partial hydrolysis of the HPO_3F^- anion and difficulties with product isolation and recrystallization (Sect. 3.1). The measured fluoride contents, in particular, tend to deviate from calculated values and a complete fluoride analysis with the two types of sample preparation (H_2O and Seel) was not always possible. The type of sample preparation used for the fluoride analysis is indicated by H_2O and/or Seel (Sect. 2.3 Fluoride analysis).

^{31}P and ^{19}F NMR spectroscopy enabled an estimate of the amount of the phosphate impurity in the eluate solution before freeze drying or in the recrystallized product after dissolution in H_2O . Once again, whether the eluate solution or the solution of the recrystallized product were measured, depended on product purity and the ease and success of recrystallization. The ^{31}P and ^{19}F NMR spectra could be recorded for almost all of the compounds as an eluate solution or the dissolved freeze dried product. In fewer cases, spectra of crystals were measured. Therefore, the type of sample used for the NMR measurement is given (neut. eluate, crystals, residue from tray, MeOH solution, or freeze dried powder) with the NMR data. Singulets in ^{31}P and ^{19}F NMR spectra at about 0.7 and -125 ppm confirmed the presence of phosphate and fluoride impurities, respectively, based on the partial hydrolysis of the PO_3F anion. Other signals are discussed when appropriate.

The system of Na / PO₃F

NaHPO₃F·2.5H₂O (M = 167.01 g/mol)

After cation exchange of the eluant of sodium monofluorophosphate (15.8 g, 110 mmol), the eluate was partially neutralized with Na₂PO₃F (15.8 g, 110 mmol). The final pH was 2.5. Ten grams of the freeze-dried, white powder of NaHPO₃F [26, 71] (91% yield) were dissolved in about 5 mL H₂O. Recrystallization was carried out by the addition of portions of EtOH (1mL). The cloudy solution was refrigerated overnight. Slightly hygroscopic crystals of NaHPO₃F·2.5H₂O (58% yield) were filtered, dried, and characterized.

³¹P-NMR (121.5 MHz, crystals in H₂O/D₂O, δ): -3.7 (d, *J*(P,F) = 909 Hz, HPO₃F⁻), 0.7 (s, H₂PO₄⁻), 11% H₂PO₄⁻.

¹⁹F-NMR (282.4 MHz, crystals in H₂O/D₂O, δ): -74.7 (d, *J*(P,F) = 909 Hz, HPO₃F⁻).

Anal. Found (Calcd): H 3.30 (3.59), F 0.3 (H₂O)/ 9.2 (Seel) (11.38)%.

Na₂PO₃F·10H₂O (M = 324.11 g/mol)

The decahydrate of Na₂PO₃F was synthesized by (a) cation exchange and (b) direct recrystallization of Na₂PO₃F.

(a) In the first, Na₂PO₃F (5 g, 35 mmol) was passed through the cation exchange column and neutralized by a second portion (7.5 g, 52 mmol) reaching a pH of 4.90. The freeze dried powder was isolated in high yield. The raw product (2.13 g) was dissolved in H₂O–acetone and placed in the freezer. The partially frozen solution was then moved to the refrigerator and acetone (2 mL) was added. A frozen sludge was found on the bottom of the flask. On examination of this sludge under the microscope, single crystals were found, which melted at room temperature. A single crystal of Na₂PO₃F·10H₂O was then picked out under a cold stream of N₂ for measurement. Crystals of NaHPO₃F·2.5H₂O were also found in the sludge.

³¹P-NMR (121.5 MHz, freeze dried powder in H₂O/D₂O, δ): 0.1 (d, *J*(P,F) = 881 Hz, PO₃F²⁻), 0.8 (s, H₂PO₄⁻), 9% H₂PO₄⁻.

¹⁹F-NMR (282.4 MHz, freeze dried powder in H₂O/D₂O, δ): -74.2 (d, *J*(P,F) = 881 Hz, PO₃F²⁻), -120.8 (s, F⁻).

(b) The decahydrate was also isolated by crystallization of Na₂PO₃F from aqueous

solution. $\text{Na}_2\text{PO}_3\text{F}$ (8.4 g, 58 mmol) was dissolved in H_2O (10 mL) under stirring. A fine white precipitate formed and the mixture was left to stand overnight. The solution was then decanted and refrigerated. After five days without crystal formation, a crystal of $\text{Na}_2\text{SO}_4 \cdot 10\text{H}_2\text{O}$ was added to the solution. Single crystals of $\text{Na}_2\text{PO}_3\text{F} \cdot 10\text{H}_2\text{O}$ were obtained after the solution was left to stand overnight.

The thermal stability of the $\text{Na}_2\text{PO}_3\text{F} \cdot 10\text{H}_2\text{O}$ crystals was investigated directly on the IPDS diffractometer between 230 and 285 K. The same unit cell was determined by exposures taken up to 280 K. The exposure at 285 K showed the crystal had broken down to a powder. Powder rings at higher d-values were too diffuse to interpret; however, the d-values observed in the range of 2.00 - 1.356 Å could be assigned to $\text{Na}_2\text{PO}_3\text{F}$ [72]. The crystals had an incongruent melting point of 283 ± 2 K.

$\text{Na}_5[\text{N}(\text{CH}_3)_4](\text{PO}_3\text{F})_3 \cdot 18\text{H}_2\text{O}$ (M = 807.3 g/mol)

Long, hygroscopic needles of $\text{Na}_5[\text{N}(\text{CH}_3)_4](\text{PO}_3\text{F})_3 \cdot 18\text{H}_2\text{O}$ were crystallized from H_2O by slow evaporation on a tray or by the addition of EtOH to an aqueous solution and refrigeration. The white, hygroscopic powder was obtained by freeze drying after partial cation exchange of $\text{Na}_2\text{PO}_3\text{F}$ (10g, 69 mmol) and the addition of $\text{N}(\text{CH}_3)_4\text{OH}$ in MeOH (29.2 ml, 69 mmol).

^{31}P -NMR (121.5 MHz, crystals in $\text{H}_2\text{O}/\text{D}_2\text{O}$, δ): 1.3 (d, $J(\text{P},\text{F}) = 871$ Hz, PO_3F^{2-}).

^{19}F -NMR (282.4 MHz, crystals in $\text{H}_2\text{O}/\text{D}_2\text{O}$, δ): -74.3 (d, $J(\text{P},\text{F}) = 871$ Hz, PO_3F^{2-}).

Anal. Found (Calcd): F 0.0 (H_2O)/6.5 (Seel) (7.06)%.

The system of K / PO_3F

KHPO_3F (M = 138.08 g/mol) [26]

The KHPO_3F salt was obtained with $\text{Na}_2\text{PO}_3\text{F}$ (8.5 g, 59 mmol) and K_2CO_3 (4.1 g, 29 mmol) with a final pH 4.14 after cation exchange and partial neutralization. Slow evaporation was not successful in obtaining single crystals from the freeze dried, powder. Branched clusters of crystals of the freeze dried powder were instead formed from concentrated, aqueous solution by slowly adding MeOH (1 mL); the solution was then refrigerated. High amounts of phosphate and low yields of the KHPO_3F crystals as the minor phase prevented phase analysis.

K₃[H(PO₃F)₂] (M = 314.24 g/mol)

The 3:1 potassium hydrogen monofluorophosphate was synthesized by cation exchange of (NH₄)₂PO₃F (1.5 g, 11 mmol) and the addition of K₂CO₃ (0.8 g, 6 mmol). The eluate solution (50 mL) was concentrated in vacuum at a bath temperature of 20-25°C to 25 mL. Crystals in the solution were filtered and the solution was hung on the freeze dryer. The dried product was dissolved in a mixture of H₂O/MeOH (2:1) at 50°C. After refrigeration, MeOH (3 mL) was added. No crystals were formed. Single crystals were then obtained by recrystallization from aqueous solution. The solution was evaporated in a desiccator. These several block crystals characterized as K₃[H(PO₃F)₂] formed had a pH of 4.86 in aqueous solution.

³¹P-NMR (121.5 MHz, neut. eluate in H₂O/D₂O, δ): -0.9 (d, *J*(P,F) = 888 Hz, H(PO₃F)₂³⁻), 0.8 (s, H₂PO₄⁻), 15% H₂PO₄⁻.

¹⁹F-NMR (282.4 MHz, neut. eluate in H₂O/D₂O, δ): -74.4 (dd, *J*(P,F) = 888 Hz, *J*(H,F) = 8 Hz, H(PO₃F)₂³⁻).

Anal. Found (Calcd): F 11.9 (H₂O) (6.05)%.

The system of Rb / PO₃F**α-RbHPO₃F (M = 184.45 g/mol)**

α-RbHPO₃F was obtained using Na₂PO₃F (7.5 g, 52 mmol) and Rb₂CO₃ (7.4 g, 32 mmol) with cation exchange. The neutralized eluate had pH 4.01 after cation exchange and was then back titrated with H₂PO₃F to pH 3.5. The solution (300 mL) was freeze dried obtaining a product in high yield. Crystals were obtained from an aqueous solution (1 mL) of the raw product (1.3 g).

³¹P-NMR (121.5 MHz, freeze dried powder in H₂O/D₂O, δ): -3.3 (d, *J*(P,F) = 905 Hz, HPO₃F⁻), 0.8 (s, H₂PO₄⁻), 13% H₂PO₄⁻.

¹⁹F-NMR (282.4 MHz, freeze dried powder in H₂O/D₂O, δ): -74.7 (d, *J*(P,F) = 906 Hz, HPO₃F⁻).

Anal. Found (Calcd): F 1.1 (H₂O)/ 9.4 (Seel) (10.30)%.

β -RbHPO₃F (M = 184.45 g/mol)

The β -modification of RbHPO₃F was synthesized using Na₂PO₃F (13.8 g, 96 mmol) and Rb₂CO₃ (10.8 g, 47 mmol). The pH was kept between 3 and 5 during cation exchange and neutralization with a final pH of 4.43. The freeze dried powder was obtained in 90% yield. Recrystallization involved the dissolution of the raw product (7 g) in H₂O (2 mL). The saturated solution was then filtered and left to stand. After three days, block crystals were found, removed from the solution, and dried on a tile (8.5% yield).

³¹P-NMR (121.5 MHz, neut. eluate in H₂O/D₂O, δ): -2.2 (d, $J(\text{P},\text{F}) = 897$ Hz, HPO₃F⁻), 0.8 (s, H₂PO₄⁻), 12% H₂PO₄⁻.

¹⁹F-NMR (282.4 MHz, neut. eluate H₂O/D₂O, δ): -74.5 (dd, $J(\text{P},\text{F}) = 897$ Hz, $J(\text{H},\text{F}) = 3.5$ Hz, HPO₃F⁻).

Anal. Found (Calcd): H 0.53 (0.53), F 0.5 (H₂O)/9.2 (Seel) (10.30)%.

The system of Cs / PO₃F**CsHPO₃F** (M = 231.89 g/mol)

After cation exchange of an eluant of Na₂PO₃F (5 g, 35 mmol), the eluate was partially neutralized with Cs₂CO₃ (5.7 g, 17 mmol) to a pH 3.8. The freeze dried, hygroscopic, white powder (81% yield) was recrystallized from H₂O by pipetting EtOH slowly along the walls of the PE flask. Crystals formed on the walls. The H₂O/EtOH solution was refrigerated overnight. Hygroscopic crystals were measured and characterized.

³¹P-NMR (121.5 MHz, neut. eluate in H₂O/D₂O, δ): -3.3 (d, $J(\text{P},\text{F}) = 905$ Hz, HPO₃F⁻), 0.8 (s, H₂PO₄⁻), 12% H₂PO₄⁻.

¹⁹F-NMR (282.4 MHz, neut. eluate in H₂O/D₂O, δ): -74.4 (d, $J(\text{P},\text{F}) = 905$ Hz, HPO₃F⁻).

Anal. Found (Calcd): H 0.48 (0.43), F 8.1 (Seel) (8.19)%.

Cs₃(NH₄)₂(HPO₃F)₃(PO₃F) (M = 829.72 g/mol)

Cs₃(NH₄)₂(HPO₃F)₃(PO₃F) was prepared using (NH₄)₂PO₃F (1.6 g, 12 mmol) and Cs₂CO₃ (2.0 g, 6 mmol) in combination with partial cation exchange. The eluate (pH 4.31) was evaporated to 20 mL. The solution was then freeze dried to give a 4.5% yield of a hygroscopic, white powder. The substance was placed in a desiccator overnight.

Recrystallization was carried out from a mixture of H₂O/MeOH of 2:1 at 323 K. The solution was then evaporated in air forming crystals of (NH₄)₂PO₃F·H₂O [73]. The crystals were kept in a desiccator and rechecked after one month. Rectangular and block crystals for two phases were observed. The rectangular crystals were again (NH₄)₂PO₃F·H₂O; the block crystals were characterized as Cs₃(NH₄)₂(HPO₃F)₃(PO₃F).

³¹P-NMR (121.5 MHz, freeze dried powder in H₂O/D₂O, δ): -1.5 (d, *J*(P,F) = 891 Hz, HPO₃F⁻/PO₃F²⁻), 0.8 (s, H₂PO₄⁻), 17% H₂PO₄⁻.

¹⁹F-NMR (282.4 MHz, freeze dried powder in H₂O/D₂O, δ): -74.5 (d, *J*(P,F) = 891 Hz, HPO₃F⁻/PO₃F²⁻).

Anal. Found (Calcd): F 8.2 (H₂O) (9.16)%.

The system of NH₄/PO₃F [26]

α-NH₄HPO₃F (M = 117.02 g/mol)

α-Ammonium hydrogen monofluorophosphate was obtained by two different methods.

(a) The α-modification was first prepared from (NH₄)₂PO₃F synthesized according to [70]. (NH₄)₂PO₃F (1.5 g, 11 mmol) was protonated by grinding it together with NH₄HSO₄ (1.3 g, 11 mmol) in MeOH. The NH₄HPO₃F formed was separated from the byproduct, (NH₄)₂SO₄, by filtration. The (NH₄)₂SO₄ was washed several times with MeOH until more or less neutral. The NH₄HPO₃F/MeOH solution (pH 2.8) and the washings were collected and concentrated slightly. NH₄HPO₃F was precipitated by the addition of ether, filtered, and recrystallized from MeOH.

³¹P-NMR (121.5 MHz, MeOH solution with D₂O, δ): -4.3 (d, *J*(P,F) = 909 Hz, HPO₃F⁻), 0.7 (s, H₂PO₄⁻), 62% H₂PO₄⁻.

¹⁹F-NMR (282.4 MHz, MeOH solution with D₂O, δ): -75.9 (d, *J*(P,F) = 908 Hz, HPO₃F⁻).

Anal. Found (Calcd): F 14.2 (H₂O) (16.24)%.

(b) α-NH₄HPO₃F was also obtained by cation exchange using a H₂PO₃F/(NH₄)₂PO₃F ratio of 1:1. Recrystallization from aqueous solution at room temperature yielded α-NH₄HPO₃F.

β -NH₄HPO₃F (M = 117.02 g/mol)

Two syntheses were used to obtain the β -modification of ammonium hydrogen monofluorophosphate.

(a) The H₂PO₃F/(NH₄)₂PO₃F molar ratio was decreased from 1:1 to 2:3. Cation exchange was done with an aqueous solution of Na₂PO₃F (7 g, 49 mmol). The eluate was neutralized with (NH₄)₂PO₃F (9.8 g, 73 mmol) placed in the beaker prior to cation exchange. After cation exchange, a final pH of 3.4 was reached by adding a second portion of (NH₄)₂PO₃F (0.65 g, 5 mmol). After freeze drying, the white powder was dissolved in H₂O–MeOH. The saturated solution was left to stand and after two days, crystals were formed.

³¹P-NMR (121.5 MHz, crystals in H₂O/D₂O, δ): -3.6 (d, $J(\text{P},\text{F}) = 908$ Hz, HPO₃F⁻).

¹⁹F-NMR (282.4 MHz, crystals in H₂O/D₂O, δ): -74.8 (d, $J(\text{P},\text{F}) = 908$ Hz, HPO₃F⁻).

Anal. Found (Calcd): N 12.08 (11.96), H 3.96 (4.28), F 0.4 (H₂O)/15.7 (Seel) (16.24)%.

(b) β -NH₄HPO₃F was also obtained by recrystallizing the raw product of a 1:1 H₂PO₃F/(NH₄)₂PO₃F synthesis from H₂O at 333 K.

The system of [N(CH₃)₄] / PO₃F**[N(CH₃)₄]HPO₃F·H₂O** (M = 191.14 g/mol)

Tetramethylammonium hydrogen monofluorophosphate monohydrate was synthesized via cation exchange with the reagents, Na₂PO₃F (7.95 g, 55 mmol) and N(CH₃)₄OH in H₂O (21.78 g, 60 mmol). The final 300 mL solution had a pH 3.80. The solution was freeze dried to obtain an oil, which was diluted with H₂O and slowly evaporated in an evacuated desiccator. The concentrated thick solution was then placed in the refrigerator. Measured crystals formed from the residue on the freeze drying dish and in solution were [N(CH₃)₄]H₂PO₄·H₂O [74]. After five months, cubic crystals of [N(CH₃)₄]HPO₃F·H₂O were found in the refrigerated solution. Crystals were dried and characterized.

³¹P-NMR (121.5 MHz, crystals in H₂O/D₂O, δ): -3.7 (d, $J(\text{P},\text{F}) = 908$ Hz, HPO₃F⁻), 0.8 (s, H₂PO₄⁻), 2% H₂PO₄⁻.

¹⁹F-NMR (282.4 MHz, crystals in H₂O/D₂O, δ): -74.8 (d, $J(\text{P},\text{F}) = 908$ Hz, HPO₃F⁻).

Anal. Found (Calcd): C 24.81 (25.11), H 7.42 (7.85), N 7.23 (7.32), F 0.2 (H₂O)/9.5 (Seel) (9.94)%.

The system of $[NR_4]/PO_3F$ ($R = H, CH_2CH_3$)

$[NH_2(CH_2CH_3)_2]HPO_3F$ ($M = 173.12$ g/mol)

Diethylammonium hydrogen monofluorophosphate was prepared from Na_2PO_3F (9.5 g, 66 mmol) and $NH(CH_2CH_3)_2$ (4.8 g, 66 mmol) in 83% yield. Crystals were obtained from EtOH with slow addition of Et_2O and refrigeration.

^{31}P -NMR (121.5 MHz, crystals in H_2O/D_2O , δ): -3.7 (d, $J(P,F) = 908$ Hz, HPO_3F^-).

^{19}F -NMR (282.4 MHz, crystals in H_2O/D_2O , δ): -74.8 (d, $J(P,F) = 908$ Hz, HPO_3F^-).

Anal. Found (Calcd): C 27.22 (27.73), N 7.95 (8.09), H 6.72 (7.51), F 0.03 (H_2O)/11.65 (Seel) (10.97)%.

$[NH(CH_2CH_3)_3]HPO_3F$ ($M = 201.18$ g/mol)

Triethylammonium hydrogen monofluorophosphate was obtained using Na_2PO_3F (10 g, 70 mmol) and triethylamine (7.0 g, 69 mmol). The hygroscopic oil was dissolved in EtOH. The saturated solution was stored in the refrigerator. The mixture was then recrystallized from EtOH by adding Et_2O . Beautiful plates were filtered and saved (21% yield).

^{31}P -NMR (121.5 MHz, neut. eluate in H_2O/D_2O , δ): -3.3 (d, $J(P,F) = 904$ Hz, HPO_3F^-), 0.7 (s, $H_2PO_4^-$), 11% $H_2PO_4^-$.

^{19}F -NMR (282.4 MHz, neut. eluate in H_2O/D_2O , δ): -74.7 (dd, $J(P,F) = 904$ Hz, $J(H,F) = 7$ Hz, HPO_3F^-), -126.3 (s, F^-).

Anal. Found (Calcd): C 35.04 (35.79), N 6.83 (6.96), H 7.79 (8.45), F 0.1 (H_2O)/9.2 (Seel) (9.44)%.

The system of $[NH_2(CH_2CH_2)_2NH_2]/PO_3F$

$[NH_2(CH_2CH_2)_2NH_2][HPO_3F]_2$ ($M = 286.11$ g/mol)

Piperazinium hydrogen monofluorophosphate was synthesized from Na_2PO_3F (11 g, 76 mmol) and piperazine (3.0 g, 35 mmol). During neutralization of the dilute H_2PO_3F , the pH was held between 3-4 with a final pH of 2.86. The freeze dried oil was recrystallized from about 5 mL H_2O . Ethanol, 1 mL, was added and a fine precipitate of single crystals for the

piperazonium dihydrogen phosphate, already measured, was obtained. Block crystals of a minor phase found along with crystals of the dihydrogen phosphate were characterized as $[\text{PpizH}_2][\text{HPO}_3\text{F}]_2$.

^{31}P -NMR (121.5 MHz, neut. eluate in $\text{H}_2\text{O}/\text{D}_2\text{O}$, δ): -3.8 (d, $J(\text{P},\text{F}) = 909$ Hz, HPO_3F^-), 0.7 (s, H_2PO_4^-), 23% H_2PO_4^- .

^{19}F -NMR (282.4 MHz, neut. eluate in $\text{H}_2\text{O}/\text{D}_2\text{O}$, δ): -75.2 (d, $J(\text{P},\text{F}) = 909$ Hz, HPO_3F^-).

The system of $[\text{C}(\text{NH}_2)_3] / \text{PO}_3\text{F}$

$[\text{C}(\text{NH}_2)_3]\text{HPO}_3\text{F}$ ($M = 159.07$ g/mol)

Guanidinium hydrogen monofluorophosphate was synthesized using $\text{Na}_2\text{PO}_3\text{F}$ (10 g, 69 mmol) and $[\text{C}(\text{NH}_2)_3]_2\text{CO}_3$ (6.3 g, 35 mmol). The aqueous solution had a pH of <2.6 after cation exchange and complete addition of the carbonate. The freeze dried product (60% yield) was recrystallized in two separate batches. Measured crystals of $[\text{C}(\text{NH}_2)_3]_2\text{SiF}_6$ [75] were obtained from the crystallized residue on the tray. The bulk product was then recrystallized from H_2O (4 mL) with addition of EtOH. The solution was placed in the refrigerator. Crystals did not appear. Crystals of $[\text{C}(\text{NH}_2)_3]\text{HPO}_3\text{F}$ were isolated by the evaporation of a drop of the solution on a glass slide.

^{31}P -NMR (121.5 MHz, residue from tray in $\text{H}_2\text{O}/\text{D}_2\text{O}$, δ): -4.0 (d, $J(\text{P},\text{F}) = 909$ Hz, HPO_3F^-), 0.5 (s, H_2PO_4^-), 28% H_2PO_4^- .

^{19}F -NMR (282.4 MHz, residue from tray in $\text{H}_2\text{O}/\text{D}_2\text{O}$, δ): -74.5 (dd, $J(\text{P},\text{F}) = 909$ Hz, HPO_3F^-), -127.5 (s, F).

Anal. Found (Calcd): C 7.48 (7.54), N 26.24 (26.40), H 4.03 (4.40), F 0.8 (H_2O)/11.1 (Seel) (11.94)%.

$[\text{C}(\text{NH}_2)_3]_2\text{PO}_3\text{F}$ ($M = 218.15$ g/mol)

Guanidinium monofluorophosphate was synthesized by cation exchange using $\text{Na}_2\text{PO}_3\text{F}$ (10.1 g, 70 mmol) and $[\text{C}(\text{NH}_2)_3]_2\text{CO}_3$ (11.9 g, 66 mmol). The neutralized eluate had a pH of 6.21. The freeze dried raw product (90% yield) was dissolved in 5 mL H_2O and the solution filtered. Crystals were isolated by decanting the thick, cloudy solution onto a tile. The dried crystals were characterized.

^{31}P -NMR (121.5 MHz, neut. eluate in $\text{H}_2\text{O}/\text{D}_2\text{O}$, δ): 1.4 (d, $J(\text{P},\text{F}) = 870$ Hz, PO_3F^{2-}), 1.3

(s, H_2PO_4^-), 20% H_2PO_4^- .

^{19}F -NMR (282.4 MHz, neut. eluate $\text{H}_2\text{O}/\text{D}_2\text{O}$, δ): -73.7 (d, $J(\text{P},\text{F}) = 870$ Hz, PO_3F^{2-}).

Anal. Found (Calcd): C 8.97 (11.00), H 4.36 (5.50), N 31.69 (38.51), F 3.5 (H_2O)/10.7 (Seel) (8.71)%.

The system of $\{\text{OC}[\text{NH}(\text{CH}_3)]_2\} / \text{PO}_3\text{F}$

$\{\text{HOC}[\text{NH}(\text{CH}_3)]_2\}\text{HPO}_3\text{F}$ (M = 188.10 g/mol)

The dilute, aqueous solution of monofluorophosphoric acid (eluant: 10 g, 69 mmol of $\text{Na}_2\text{PO}_3\text{F}$) was mixed with N,N'-dimethyl urea (6.1 g, 69 mmol). The pH sank to 0.8 and then rose slightly to 1.5. After freeze drying, the tray of moist raw product was washed with EtOH. The EtOH solution was filtered and left to stand. The tray residue was added to the solution later and crystals were formed and characterized.

^{31}P -NMR (121.5 MHz, neut. eluate in $\text{H}_2\text{O}/\text{D}_2\text{O}$, δ): -4.1 (d, $J(\text{P},\text{F}) = 909$ Hz, HPO_3F^-), 0.5 (s, H_2PO_4^-), 62% H_2PO_4^- .

^{19}F -NMR (282.4 MHz, neut. eluate in $\text{H}_2\text{O}/\text{D}_2\text{O}$, δ): -75.0 (d, $J(\text{P},\text{F}) = 909$ Hz, HPO_3F^-), -127.5 (s, F^-).

Anal. Found (Calcd): C 17.80 (19.14), N 13.80 (14.89), H 5.01 (4.78), F 0.5 (H_2O)/9.4 (Seel) (10.10)%.

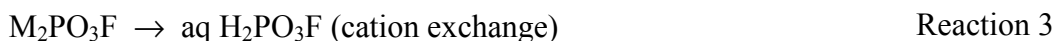
Chapter 3

Synthesis

Methods of synthesis

The hydrogen sulfates studied in [11, 12] were synthesized from sulfuric acid by partial neutralization with the corresponding carbonate, oxide, or hydroxide. The absence of commercially available, pure monofluorophosphoric acid required alternative routes of synthesis for the preparation of the acid and acid salts with little or no impurities. A variety of methods have been used to prepare basic monofluorophosphates in the last 100 years [16]; however, there are fewer possibilities for the synthesis of the hydrogen monofluorophosphates. This is due to the accelerated hydrolysis of the fluorophosphate ion at pH values below 3 and above 9 [19]. Therefore, the two most promising methods of preparation found in the literature were first carried out and evaluated with ^{31}P and ^{19}F NMR.

The method for preparing hydrogen monofluorophosphates via cation exchange [26] started with prepared monofluorophosphates (Reaction 3 and 4). The solution of a monofluorophosphate, $\text{Na}_2\text{PO}_3\text{F}$, $\text{K}_2\text{PO}_3\text{F}$, or $(\text{NH}_4)_2\text{PO}_3\text{F}$, was passed through a chromatography column of a H^+ charged ion-exchange resin. In a second step, the eluate of dilute, aqueous $\text{H}_2\text{PO}_3\text{F}$ was partially neutralized with an equivalent amount of monofluorophosphate (Reaction 4).



The authors characterized the obtained products by paper chromatography, ^{31}P and ^{19}F NMR spectroscopy, elemental analysis, and X-ray powder diffraction. A 0.01 M aqueous solution of these hydrogen monofluorophosphates was reported to have pH 3.8 and thus the equivalence point of the acid to be pH 3.5 [26].

The other method implies direct synthesis of the monofluorophosphoric acid as patented in 1949 [76]. It involved the reaction of P_2O_5 with concentrated HF, in which the H_2O content was ≤ 33 mol%, and yielded variable mixtures of HPO_2F_2 and $\text{H}_2\text{PO}_3\text{F}$ (Reaction 5). The reaction mixture was heated at 358 K for 8 hours to yield a 50:50 mixture of $\text{H}_2\text{PO}_3\text{F}$ and HPO_2F_2 , when $x = 1$.



The products were separated by vacuum distillation; HPO_2F_2 was distilled off, while $\text{H}_2\text{PO}_3\text{F}$ remained in the residue. The product was characterized by elemental analysis.

A comparative evaluation showed the following. In the cation exchange synthesis, significant amounts of phosphate were found in the eluate after cation exchange and neutralization. The synthesis with P_2O_5 and HF resulted in side products: a mixture of monofluorophosphoric, orthophosphoric, polyphosphoric, and difluorodiphosphoric acids was formed when temperatures slightly exceeded 358 K and higher fluorinated products, such as HPF_6 , were obtained when HF was in slight excess. Product separation failed with $\text{H}_2\text{PO}_3\text{F}$ found in both the distillate of HPO_2F_2 and the residue after repeated distillations at several different pressures.

Therefore, the method of cation exchange (Reaction 3 and 4) was adopted and modified for an effective synthesis of the hydrogen monofluorophosphates. The only exception was the attempted synthesis of $\text{NH}_4\text{HPO}_3\text{F}$ by reacting $(\text{NH}_4)_2\text{PO}_3\text{F}$ with NH_4HSO_4 as described in [70]. Although the synthesis of $\text{NH}_4\text{HPO}_3\text{F}$ from $(\text{NH}_4)_2\text{PO}_3\text{F}$ was successful, the relatively low solubility of $\text{NH}_4\text{HPO}_3\text{F}$ made the complete separation of the monofluorophosphate from $(\text{NH}_4)_2\text{SO}_4$ problematic. Repeated washing of the byproduct, $(\text{NH}_4)_2\text{SO}_4$, was required for a complete product separation. Therefore, cation exchange was used in further syntheses of $\text{NH}_4\text{HPO}_3\text{F}$.

Cation exchange was carried out by using either $\text{Na}_2\text{PO}_3\text{F}$ or $(\text{NH}_4)_2\text{PO}_3\text{F}$ as a starting

reagent in first experiments. $(\text{NH}_4)_2\text{PO}_3\text{F}$ was obtained separately by melting uronium phosphate and ammonium hydrogen difluoride together at 443K [70]. Later on, only the commercially available sodium salt was used to reduce the steps of preparation. The acidic eluate was neutralized by a carbonate, hydroxide, or amine instead of a basic monofluorophosphate as described in [26] except for in the syntheses of sodium salts, because $\text{Na}_2\text{PO}_3\text{F}$ was readily available. Amounts of phosphate formed were kept at a minimum by adding an aqueous solution of the base or amine dropwise into the eluate at a rate, at which the monitored pH remained between 3 and 6. In [26], product isolation involved the precipitation of products from an almost completely evaporated aqueous solution with large amounts of nonaqueous solvents, such as Et_2O or EtOH . To improve yields, this working-up procedure was replaced by freeze drying of the solution after partial neutralization. This prevented the condensation of phosphorus and escape of HF during the complete evaporation of the eluate and enabled isolation of the raw products for analysis before recrystallization. Sufficient amounts of raw products were then available for the crystallization experiments described below.

Crystallization

Several methods were used for the crystallization of the freeze dried, raw products to obtain pure, crystalline hydrogen monofluorophosphates for the single crystal structure analysis and further characterization. These included

- slow evaporation in a desiccator
- fractional crystallization with slow evaporation
- crystallization from H_2O by adding EtOH/MeOH
- filtration of an oversaturated aqueous solution and slight evaporation

Slow evaporation in a desiccator of an aqueous solution yielded crystalline batches with approximately the same composition as the original solution—a two phase mixture of the hydrogen monofluorophosphate and hydrogen phosphate. Which compound was the major phase depended on how long the solution was left to stand. The phosphate became the major phase, when the solution was left to stand for longer periods of time.

Fractional recrystallization with slow evaporation was also unsuccessful. A slow, but steady hydrolysis of the HPO_3F^- anion was observed instead of product separation. The filtered and dried fraction of crystals were characterized by XRD and fluoride analysis. The first fraction, a mixture of the MHPO_3F and MH_2PO_4 phases, was similar to that found in the raw product. The XRD patterns of the second fraction showed a very pure phase of the hydrogen phosphate. Fluoride analysis confirmed increased amounts of free fluoride in

each further fraction reflecting the hydrolysis of the HPO_3F^- anion. An initial fluoride content of 0.74% for the raw product increased to 1.46% for the first fraction and to 8.85% in the second fraction.

Therefore, a method of accelerated recrystallization was used. The raw product was dissolved in H_2O , MeOH, or EtOH. A second solvent was then gradually added, MeOH or EtOH for an aqueous solution or Et_2O for a MeOH or EtOH solution, until a precipitate formed. The solution was refrigerated overnight. The alkali metal hydrogen monofluorophosphates and most of the salts with cations containing nitrogen were crystallized from H_2O with EtOH. The compounds with NEt_3 , NHEt_2 , and $\text{N,N}'\text{-dmu}$ were obtained crystalline from EtOH with Et_2O . This method yielded adequate amounts of pure hydrogen monofluorophosphates for a further characterization and worked particularly well for the hydrogen monofluorophosphates with N-containing cations.

The fourth method was also quite successful in yielding pure monofluorophosphates. It involved the filtration of an oversaturated aqueous solution of the raw product. The trick here was to use very little H_2O and lots of product (Sect. 2.3 $\beta\text{-RbHPO}_3\text{F}$). The filtered solution was then left to stand for 1–3 days until crystals of the hydrogen monofluorophosphate were formed. The crystals formed were filtered and dried.

The overall success of recrystallization was directly dependent on the purity of the freeze dried product. Crystal batches with particularly high levels of phosphate impurities were difficult to recrystallize (Sect. 2.3 KHPO_3F). The influence of the cation on recrystallization was also observed and will be discussed later on.

Confirmation of the P–F bond

^{31}P and ^{19}F NMR spectroscopy of aqueous solution and fluoride analysis were used to ensure that fluorine was bonded to the phosphorus atom in the crystalline compounds. The doublet shown in the ^{31}P and ^{19}F NMR spectra verified the existence of the P–F bond in solution. Phase purity was confirmed by the absence or low intensity of the hydrogen phosphate singlet in the ^{31}P spectrum. An integration of the signals, the phosphate singlet and the monofluorophosphate doublet, in the ^{31}P spectrum enabled the approximation of the $\text{H}_2\text{PO}_4^-/\text{HPO}_3\text{F}^-$ ratio. A study of the rate of hydrolysis with a $\text{Na}_2\text{PO}_3\text{F}/\text{H}_2\text{SO}_4$ solution showed that the phosphate signal increased slightly in intensity after about ten days for the solution with pH 3.76 corresponding to the pH of the alkali metal hydrogen monofluorophosphates and to the same extent after one day for pH 2.67 corresponding to the hydrogen monofluorophosphates with N-containing cations. A phosphate singlet was not observed in the spectra of the $\text{Na}_5[\text{N}(\text{CH}_3)_4](\text{PO}_3\text{F})_3 \cdot 18\text{H}_2\text{O}$,

$[\text{NH}_2\text{Et}_2]\text{HPO}_3\text{F}$, and $\beta\text{-NH}_4\text{HPO}_3\text{F}$ crystals. An observed phosphate singlet of very low intensity (2%) was shown in the spectrum of $[\text{N}(\text{Me})_4]\text{HPO}_3\text{F}\cdot\text{H}_2\text{O}$. For other compounds, the neutralized solution or freeze dried powder was characterized by NMR in the absence of a crystalline product. In this case, the overall amount of the phosphate impurity was estimated prior to recrystallization and nothing could be concluded about the crystalline product.

Fluoride analysis was particularly useful in evaluating phase purity by a double determination (Sect. 2.1 Fluoride analysis). Deviations were found between the experimental (Seel) and calculated values of even very pure crystals. Experimental values of the total fluoride content were generally lower than the calculated values by less than 20%, based on small amounts of H_2O and hydrogen phosphate in the sample. Two examples were the fluoride analyses of $[\text{N}(\text{CH}_3)_4]\text{HPO}_3\text{F}\cdot\text{H}_2\text{O}$ and $\text{Na}_5[\text{N}(\text{CH}_3)_4](\text{PO}_3\text{F})_3\cdot 18\text{H}_2\text{O}$ with experimental (calculated) values of 9.5 (9.94) and 6.5 (7.06)%, and a free fluoride content of 0.2 and 0%, respectively. Crystals with free fluoride contents of less than 2% were of high purity. Incomplete fluoride analyses reflected difficulties with hydrolysis and product isolation.

Alkali metal and ammonium hydrogen monofluorophosphates

The alkali metal hydrogen monofluorophosphates were obtained with the compositions, MHPO_3F and $\text{M}_3\text{H}(\text{PO}_3\text{F})_2$. The synthesis of compounds with a M/H ratio of 1:1, MHPO_3F , was rather straight-forward for $\text{M} = \text{NH}_4$ [77], Rb, and Cs [78]. The cesium salt, CsHPO_3F , crystallized easily and could be identified by XRD.

Dimorphism of the NH_4 and Rb compounds made crystallization and product identification by XRD complicated. Therefore, the modifications were confirmed by measuring the cell on the single crystal diffractometer.

After repeated syntheses, the formation of the α and β -modifications of $\text{NH}_4\text{HPO}_3\text{F}$ could be controlled by the $\text{H}_2\text{PO}_3\text{F}/(\text{NH}_4)_2\text{PO}_3\text{F}$ ratio. One experiment also showed that $\beta\text{-NH}_4\text{HPO}_3\text{F}$ could be obtained by recrystallization at 333K (Sect. 2.3 $\beta\text{-NH}_4\text{HPO}_3\text{F}$); the α -modification was isolated after recrystallization of the same raw product at room temperature. An extensive study of this dimorphism could not be carried out within the scope of this thesis, but further investigation thereof are planned. Structure determinations of $\beta\text{-NH}_4\text{HPO}_3\text{F}$ measured at 310 and 180 K were almost identical with only slight deviations in the a lattice constant and P–F bond lengths between the two [77]. A comparison of the simulated powder data of α - and $\beta\text{-NH}_4\text{HPO}_3\text{F}$ and the powder data published for $\text{NH}_4\text{HPO}_3\text{F}$ [26] showed that the data for $\text{NH}_4\text{HPO}_3\text{F}$ [79] could be assigned

to a mixture of both modifications except for three peaks at d -values of 5.30, 4.30, and 3.44 Å. The strongest peaks at 3.71 and 3.49 Å probably belong to the β -modification and suggest that this was the major phase. This is not surprising because the $\text{NH}_4\text{HPO}_3\text{F}$ salt in [26] was obtained at pH 3.8, which would more likely be reached by a 3:2 molar ratio of $\text{NH}_4/\text{PO}_3\text{F}$ as is the case for $\beta\text{-NH}_4\text{HPO}_3\text{F}$.

In comparison with the NH_4 compound, the conditions for the formation of α and $\beta\text{-RbHPO}_3\text{F}$ were not fully understood, but also seemed to be dependent on the $\text{H}_2\text{PO}_3\text{F}/\text{Rb}_2\text{PO}_3\text{F}$ ratio. The modifications could be obtained separately by repeated syntheses. Crystals isolated for both modifications were measured twice at ca. 180 K; the second measurement yielded improved R_I -factors for the structure refinements of both modifications. Crystals of $\beta\text{-RbHPO}_3\text{F}$ seemed to crystallize more easily than those of $\alpha\text{-RbHPO}_3\text{F}$. The structure of $\beta\text{-RbHPO}_3\text{F}$ has been more difficult to interpret. Further investigation could acquire information on a possible phase transition and the thermal stability of each modification, which could not be obtained within the framework of this thesis.

In the case of KHPO_3F , repeated syntheses obtained charges with particularly high amounts of phosphate. Purity could not be improved, thus, making the crystallization and characterization of this compound difficult. Crystallization seemed to be chemically hindered, as if the crystal structure was rather unstable. This was confirmed by the pseudo-orthorhombic twinning of very small crystals (0.1 x 0.1 x 0.1 mm) measured. The simulated powder data agreed with that of the KHPO_3F phase [26, 80].

Crystalline $\text{NaHPO}_3\text{F} \cdot 2.5\text{H}_2\text{O}$ [81] was obtained by the recrystallization of NaHPO_3F [26, 71] from H_2O . The moderate pH (5.5) of $\text{Na}_2\text{PO}_3\text{F}$ enabled the addition of the complete amount of $\text{Na}_2\text{PO}_3\text{F}$ required for the synthesis prior to the collection of the eluate. Thus, neutralization was carried out at a starting pH not higher than 5.5 and yielded a product with very low degree of hydrolysis that recrystallized easily.

Attempts to synthesize acid salts with other M/H ratios resulted in the formation of second modifications of the hydrogen monofluorophosphate, e.g. $\beta\text{-NH}_4\text{HPO}_3\text{F}$, or the basic monofluorophosphates except for $\text{K}_3[\text{H}(\text{PO}_3\text{F})_2]$. This phase was rather impure with a free fluoride content of 11.9% (calculated value of 6.05 and 13.76% for KHPO_3F) probably based on hydrolysis.

Hydrogen monofluorophosphates with N-containing cations

The next system studied was that of the hydrogen monofluorophosphates with organic cations containing nitrogen. In this case, higher yields of crystalline products were

obtained for a complete characterization: elemental analysis, NMR, and XRD. The XRD patterns of these compounds were easier to interpret than those of the alkali metal and NH_4 compounds.

In the first synthesis with tetramethylammonium hydroxide, crystals of $[\text{N}(\text{CH}_3)_4]\text{H}_2\text{PO}_4 \cdot \text{H}_2\text{O}$ [74] were found at first. However, six months later, cubic crystals of the hydrogen monofluorophosphate hydrate (Sect. 4.6.2) could be isolated and characterized completely. The crystals were stable in solution. Both the diethyl and triethylammonium compounds were obtained crystalline in higher yields and could then be characterized completely. The crystallization of the guanidinium acid salt was more difficult; crystals for measurement were, therefore, first formed by the evaporation of a drop of the aqueous solution on the slide. Crystals of a pure product formed later were then characterized.

The isolation of $[\text{PipzH}_2]\text{HPO}_3\text{F}$ was not straight-forward. After a first synthesis, which obtained the hydrogen phosphate, a repeated synthesis yielded single crystals of the hydrogen monofluorophosphate despite significant amounts of phosphate. Further characterization was not possible. Other nitrogen heterocycles, $\text{N,N}'$ -dimethylpiperazine and 1,4-diazabicyclo[2.2.2]octan, were also used as a counterion, but in both cases, single crystals with a high enough quality for measurement could not be isolated.

The $[\text{N,N}'\text{-dmuH}]\text{HPO}_3\text{F}$ compound was obtained in an amazingly pure and crystalline form despite its very low pH of 1.5 in solution. This was confirmed by fluoride analysis, whereas crystals of uronium hydrogen monofluorophosphate could not be isolated.

The mixed salts, $\text{Cs}_3(\text{NH}_4)_2(\text{HPO}_3\text{F})_3\text{PO}_3\text{F}$ [78] and $\text{Na}_5[\text{N}(\text{CH}_3)_4](\text{PO}_3\text{F})_3 \cdot 18\text{H}_2\text{O}$, were both synthesized using partial cation exchange of $(\text{NH}_4)_2\text{PO}_3\text{F}$ and $\text{Na}_2\text{PO}_3\text{F}$, respectively. While the $\text{Na}/[\text{N}(\text{CH}_3)_4]$ was recrystallized with ease forming needles, the Cs/NH_4 salt could not be isolated in high yields. An incomplete fluoride analysis of the Cs/NH_4 compound measured 8.2% free fluoride in the sample, which is lower than the calculated value of 9.16% probably based on the hygroscopicity of the sample and consequent hydrolysis. In comparison to the NH_4/Cs structure, 0% free fluoride was found in needles of the $\text{Na}/[\text{N}(\text{CH}_3)_4]$ compound and a phosphate singlet in the NMR spectrum was not observed for this product.

A final synthesis of the guanidinium compound, $[\text{C}(\text{NH}_2)_3]_2\text{PO}_3\text{F}$, yielded a rather impure product with a experimental free fluoride content of 3.5%; the experimental C, H, N contents also deviated significantly from the theoretical values.

Despite experimental difficulties described here, single crystals were obtained and

measured by single crystal X-ray diffraction. The results of these investigations are treated in the following chapter.

Chapter 4

The Crystal Structures and their Hydrogen Bonding

The crystal structures of the hydrogen monofluorophosphates and basic monofluorophosphates presented here were determined with single crystal X-ray diffraction. The distinction between oxygen and fluorine in the crystal structure was accomplished crystallographically by first refining the structure to a low R_1 -factor while treating all of the atoms on the phosphorus atom as oxygen. Fluorine was then assigned a position on each unique phosphorus atom based on typical P–O/F bond lengths and the location of hydrogen atoms: long distance to phosphorus and no hydrogen atom in its vicinity. The existence of the P–F bond(s) in the structures was supported by NMR and elemental analysis.

The basic structural unit is a distorted (H)PO₃F tetrahedron with P–O and P–F bond lengths that vary. P–O distances in the hydrogen monofluorophosphates differ depending on the hydrogen donor/acceptor functions of the oxygen atoms. In general, two shorter P–O_A distances (around 1.5 Å) are found for the oxygen atoms acting as hydrogen acceptors in the hydrogen bond system. Oxygen atoms not involved in hydrogen bonding exhibit shorter interatomic distances to phosphorus. A longer P–O_DH bond (≈1.55 Å) is observed for the H donor oxygen atom. The P–F distance, for the most part, is longer than the P–O_A and P–O_DH bonds, but shorter than P–F lengths found in the basic

monofluorophosphates. This is due to changes in the P–O bonding. In the structures of the basic monofluorophosphates, all of the oxygen atoms are hydrogen acceptors (O_A); therefore, three P–O bonds have similar distances around 1.5 Å. The P–F distance of about 1.6 Å is longer than the P–F lengths found in the hydrogen monofluorophosphates.

Hydrogen bonding is observed in both the hydrogen monofluorophosphates and basic monofluorophosphates investigated here. Three basic types of hydrogen bonds were observed in the structures. Two weak hydrogen bonds, $O_w-H\cdots O_{(w)}$ and/or $N-H\cdots O$, connect the $(H)PO_3F$ tetrahedra to crystal water (O_w) and/or the N-containing cation in both the hydrogen monofluorophosphate and monofluorophosphate structures. Hydrogen bonds of medium strength are more of an exception and will be discussed, when appropriate. Strong or very strong $O-H\cdots O$ bonds link the HPO_3F tetrahedra to one another in the acid salts. The acid salts were classified according to the structural pattern of these bridged HPO_3F tetrahedra for a discussion and systematic comparison with the hydrogen sulfates. Infinite chains, branched chains, isolated dimers, cyclic dimer, or cyclic tetramers were found in the structures of the hydrogen monofluorophosphates dependent on cation size. The units were then inter-linked by either metal-oxygen/fluorine coordination or weak hydrogen bonds with the crystal water or the cations containing nitrogen.

The crystal structures and their hydrogen bonding are described and compared in the following. Selected crystallographic data from Appendix A.1, the fluoride analysis, when available (Sect. 2.1 and 2.3), and the total bond valency for fluorine, V_F , (Sect. 2.1) are given for each compound/structure in the appropriate section. Atomic coordinates and the equivalent isotropic displacement parameters are listed in Appendix A.2. The bond lengths and hydrogen bonding are provided in each section for that particular compound with supplementary data in Appendix A.3.

4.1 The Structures with Infinite Chains

Infinite chains of HPO_3F tetrahedra were found in the crystal structures of the hydrogen monofluorophosphates with the smaller cations, sodium and diethylammonium, and the piperazinium cation (Tab. 1 and A1). In the structures of $NaHPO_3F \cdot 2.5H_2O$ [81] and $[NH_2Et_2]HPO_3F$, zigzag chains of HPO_3F tetrahedra run parallel to the b -axis ($\angle PPP_{Na} = 72^\circ$, $\angle PPP_{Diet} = 164^\circ$). In comparison, the HPO_3F tetrahedra in the piperazinium structure are connected to each other in the c -direction with $\angle PPP_{Pip} = 101^\circ$. The sodium and piperazinium structures are both monoclinic, whereas the diethylammonium salt

crystallizes in the orthorhombic space group *Pbca*.

Tab. 1 Selected crystallographic data

Formula	NaHPO ₃ F·2.5H ₂ O*	[NH ₂ Et ₂]HPO ₃ F	[PipzH ₂][HPO ₃ F] ₂
Formula weight	167.01	173.12	286.11
Crystal system	<i>Monoclinic</i>	<i>Orthorhombic</i>	<i>Monoclinic</i>
Space group	<i>C2/c</i>	<i>Pbca</i>	<i>P2₁/c</i>
Crystal Size	0.8 x 0.4 x 0.4	0.4 x 0.2 x 0.1	0.6 x 0.4 x 0.1
<i>a</i> /Å	19.112(4)	12.892(4)	6.020(2)
<i>b</i> /Å	5.341(1)	9.530(3)	13.012(3)
<i>c</i> /Å	12.727(3)	13.555(4)	7.285(2)
β /°	110.18(3)	90	95.09(3)
<i>V</i> /Å ³ , <i>Z</i>	1219.4(4), 8	1665.4(9), 8	568.4(3), 2
$\rho_{\text{calc.}}$ /g·cm ⁻³	1.819	1.381	1.672
<i>R</i> _i [<i>I</i> > 2σ(<i>I</i>)]	0.0277	0.0288	0.0251
Analysis			
F (50 mL H ₂ O)	0.3	0.03	-
F (Seel)	9.2	11.65	-
F (calcd)	11.38	10.97	-
<i>V</i> _F	0.95	0.95	0.95

4.1.1 NaHPO₃F·2.5H₂O

The sodium compound, NaHPO₃F·2.5 H₂O [81], was the only hydrate determined for the alkali metal hydrogen monofluorophosphate (Tab. A9, Fig. 1, Tab. 2). The asymmetric unit contains one Na atom, one HPO₃F tetrahedron, and three molecules of water. The Na atom is octahedrally coordinated by four water molecules (Ow4, Ow5, Ow5', and Ow6) and two O atoms from the tetrahedron (O1 and O1') with an average Na–O bond length of 2.406 Å (Tab. 2). The NaO₆ octahedra alternately share one edge involving Ow5 and Ow5' and one face defined by Ow6, O1, and O1' to form chains running along the *c*-axis. The HPO₃F tetrahedron has two short P–OA bonds (1.481(1) Å for P–O1 and 1.503(1) Å for P–O2), a P–ODH (1.563(2) Å for P–O3), and a long P–F bond (1.564(1) Å). The P–O lengths reflect the function of the oxygen atom in the hydrogen bond system as an H acceptor (O1 and O2) or a donor (O3).

Tab. 2 Bond lengths in NaHPO₃F·2.5H₂O (Å)

	d		d		d
Na–O _w 5	2.388(2)	Na–O1	2.397(2)	P–O1	1.481(2)
Na–O _w 6	2.392(2)	Na–O _w 4	2.403(2)	P–O2	1.503(2)
Na–O _w 5'	2.395(2)	Na–O1'	2.458(2)	P–O3	1.563(2)
				P–F	1.564(2)

* The data was refined postpublication.

In the hydrogen bond system (Tab. 3), the HPO_3F -tetrahedra are connected to each other by one short hydrogen bond $\text{O3-H1}\cdots\text{O2}$ (2.566(2) Å), which form columns around the crystallographic 2_1 axis at $\{\frac{1}{4}, y, \frac{1}{4}\}$ (Fig. 1). These columns run in the b -direction as zigzag chains of P-tetrahedra. They are held together by weaker hydrogen bonds (2.791(2) to 2.972(2) Å) with the water molecules to form a three-dimensional network. The hydrogen bond, $\text{O}_w6\text{-H6A}\cdots\text{O1}$, bridges the chains of HPO_3F -tetrahedra together in the a -direction. Hydrogen bonds also link the chains parallel to the c -axis. The O_w atoms act mainly as donors in the hydrogen bonds: $\text{O}_w4\text{-H4A}\cdots\text{O2}$, $\text{O}_w4\text{-H4B}\cdots\text{O}_w3$, $\text{O}_w5\text{-H5B}\cdots\text{O2}$, and $\text{O}_w5\text{-H5A}\cdots\text{O}_w4$. The F atom is not involved in the hydrogen bonding and has a bond valency of 0.95 for the bond to P (Tab. 1). The P-F vertex of the tetrahedron points away from the NaO_6 octahedra (Fig. 1).

Tab. 3 Hydrogen bonding in $\text{NaHPO}_3\text{F}\cdot 2.5\text{H}_2\text{O}$ (Å, °)

D-H...A	d(D-H)	d(H...A)	d(D...A)	$\angle\text{D-H}\cdots\text{A}$
$\text{O3-H1}\cdots\text{O2}$	0.84(3)	1.73(3)	2.566(2)	173(3)
$\text{O}_w4\text{-H4A}\cdots\text{O3}$	0.83(3)	2.17(3)	2.972(2)	164(3)
$\text{O}_w4\text{-H4B}\cdots\text{O2}$	0.76(3)	2.10(3)	2.838(3)	165(3)
$\text{O}_w5\text{-H5A}\cdots\text{O}_w4$	0.86(3)	1.94(3)	2.791(2)	171(3)
$\text{O}_w5\text{-H5B}\cdots\text{O2}$	0.86(3)	2.03(3)	2.880(3)	170(3)
$\text{O}_w6\text{-H6A}\cdots\text{O1}$	0.84(3)	2.14(3)	2.910(3)	152(3)

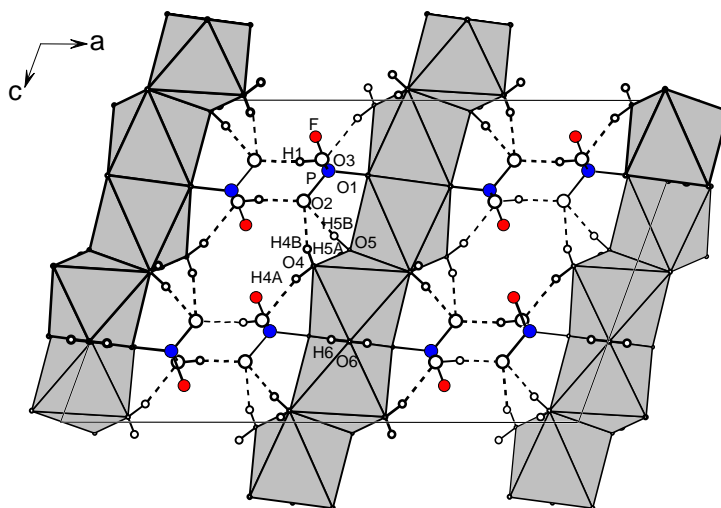


Fig. 1 Structure of $\text{NaHPO}_3\text{F}\cdot 2.5\text{H}_2\text{O}$ looking down the b -axis. The chains of $[\text{NaO}_6]$ units running in the c -direction at $x = 0$ and $\frac{1}{2}$ are represented by gray octahedra. $\text{H}\cdots\text{O}$ bonds are indicated by dashed lines. The P atoms are blue; F atoms are red; H atoms are small open circles; O atoms are larger open circles.

4.1.2 $[\text{NH}_2(\text{CH}_2\text{CH}_3)_2]\text{HPO}_3\text{F}$

The structure of diethylammonium hydrogen monofluorophosphate (Tab. A10, Fig. 2a, b, and c) made up of one crystallographically independent $[\text{NH}_2\text{Et}_2]^+$ cation and HPO_3F^- anion is quite symmetrical due to the high orthorhombic symmetry. Two N–C distances (1.495(3) and 1.496(3) Å) (Tab. 4) are found in the $[\text{NH}_2\text{Et}_2]^+$ cation with equidistant C–C lengths of 1.503(3) Å. The C–H distances range from 0.91(3) to 0.99(2) Å. The cations were found grouped together in layers parallel to the *ac*-plane at $b = \frac{1}{4}$ and $\frac{3}{4}$ (Fig. 2b and c). The HPO_3F tetrahedra demonstrates typical P–O and P–F bond lengths with two short P–O_A distances (1.476(1) and 1.485(1) Å) and two long bonds for P–O_DH and P–F of 1.545(1) and 1.566(1) Å, respectively (Tab. 4).

Tab. 4 Bond lengths in $[\text{NH}_2\text{Et}_2]\text{HPO}_3\text{F}$ (Å)

	d		d		d		d
P1–O1	1.476(1)	N–C1	1.495(3)	C1–H4	0.93(2)	C3–H9	0.96(2)
P1–O2	1.485(1)	N–C3	1.496(3)	C1–H5	0.97(2)	C3–H10	0.96(2)
P1–O3	1.545(1)	C1–C2	1.503(3)	C2–H6	0.91(3)	C4–H11	0.98(3)
P1–F1	1.566(1)	C3–C4	1.503(3)	C2–H7	0.96(2)	C4–H12	0.99(3)
				C2–H8	0.98(2)	C4–H13	0.99(2)

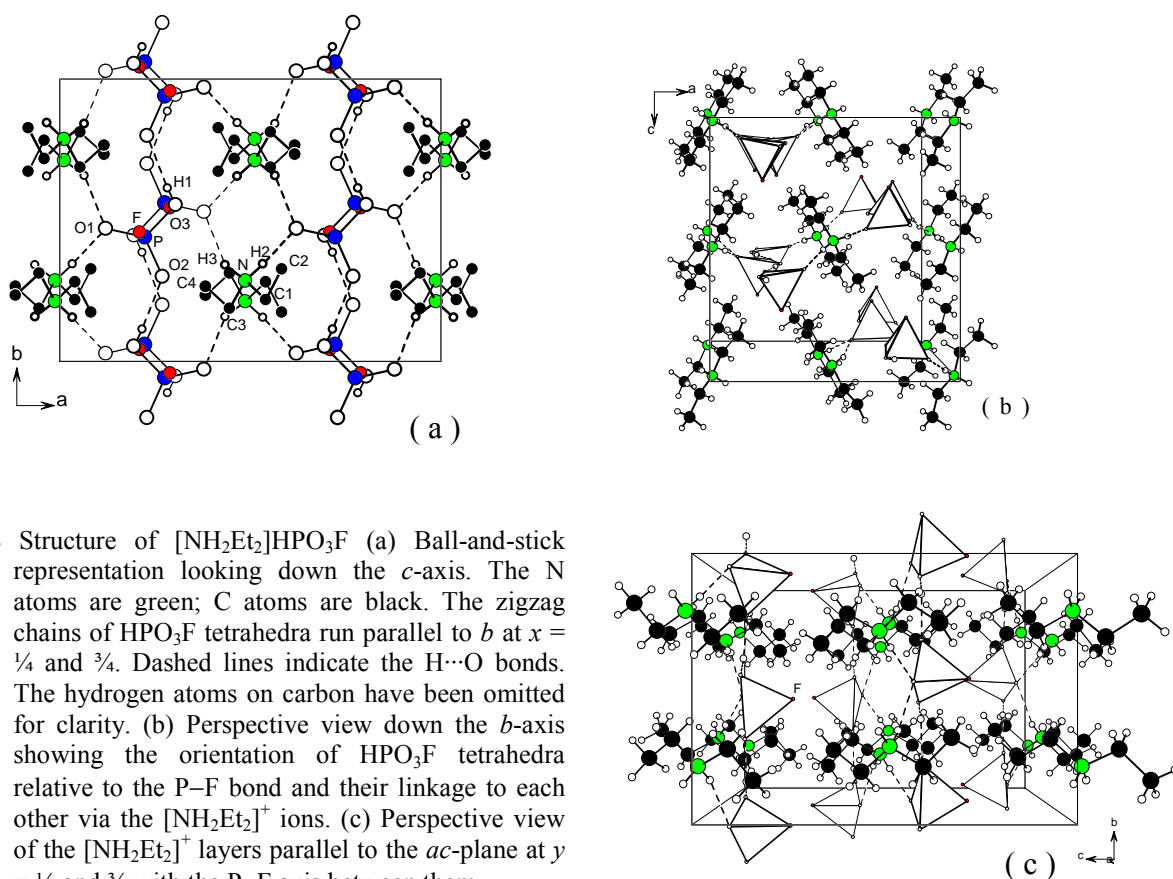


Fig. 2 Structure of $[\text{NH}_2\text{Et}_2]\text{HPO}_3\text{F}$ (a) Ball-and-stick representation looking down the *c*-axis. The N atoms are green; C atoms are black. The zigzag chains of HPO_3F tetrahedra run parallel to *b* at $x = \frac{1}{4}$ and $\frac{3}{4}$. Dashed lines indicate the H···O bonds. The hydrogen atoms on carbon have been omitted for clarity. (b) Perspective view down the *b*-axis showing the orientation of HPO_3F tetrahedra relative to the P–F bond and their linkage to each other via the $[\text{NH}_2\text{Et}_2]^+$ ions. (c) Perspective view of the $[\text{NH}_2\text{Et}_2]^+$ layers parallel to the *ac*-plane at $y = \frac{1}{4}$ and $\frac{3}{4}$ with the P–F axis between them.

The hydrogen bond system (Tab. 5) consists of one short O–H···O bond (O3···O2 2.529(2) Å) and two longer hydrogen bonds (N···O 2.761(2) and 2.837(2) Å). The O···O bridge links the HPO₃F tetrahedra to zigzag chains along the *b*-axis (Fig. 2b). These chains are connected to each other by N···O bonds, N–H2···O1 and N–H3···O1', with each O1 atom hydrogen-bonded to two different [NH₂Et₂]⁺ ions. Although the O1 atom is a twofold hydrogen acceptor in the structure, the P–O1 length is slightly shorter than the P–O2 bond probably due to weaker hydrogen interactions with O1. Each HPO₃F tetrahedra is fixed in the structure by hydrogen bonds to its three oxygen vertices. The fourth vertex of the tetrahedron (P–F axis) lies between the layers of [NH₂Et₂]⁺ ions (Fig. 2c) with the F atom not participating in any other bonds.

Tab. 5 Hydrogen bonding in [NH₂Et₂]HPO₃F (Å, °)

D–H···A	d(D–H)	d(H···A)	d(D···A)	∠D–H···A
O3–H1···O2	0.72(2)	1.81(2)	2.529(2)	173(2)
N–H2···O1	0.90(2)	1.86(2)	2.761(2)	176(2)
N–H3···O1	0.92(2)	2.00(2)	2.837(2)	151(2)

4.1.3 [NH₂(CH₂CH₂)₂NH₂][HPO₃F]₂

The piperazinium structure was the only one determined, in which the cation was a nitrogen heterocycle. The structure of one unique HPO₃F tetrahedron and one-half of a unique piperazinium cation (Tab. A11, Fig. 3a and b) is less symmetrical when compared to that of [NH₂Et₂]HPO₃F. The piperazinium cations (PipzH₂²⁺) are centered around centers of symmetry at {½, ½, 0} (Fig. 3a) with the HPO₃F tetrahedra located in between.

Tab. 6 Bond lengths in [PipzH₂][HPO₃F]₂ (Å)

	d		d		d
P–O1	1.483(1)	N–C1	1.493(2)	C1–H5	0.92(2)
P–O2	1.505(1)	N–C2	1.493(2)	C2–H6	0.92(2)
P–O3	1.549(1)	C1–C2	1.512(2)	C2–H7	0.82(2)
P–F	1.564(1)	C1–H4	0.93(2)		

Bond distances (Tab. 6) are comparable to those found in [NH₂Et₂]HPO₃F. The [PipzH₂]²⁺ cation has two N–C distances of 1.493(2) with a C–C bond length of 1.512(2) Å. C–H bonds are between 0.82(2) and 0.93(2) Å. The P–O_DH and P–F bonds with lengths of 1.549(1) and 1.564(1) Å are similar to those found in [NH₂Et₂]HPO₃F, whereas the P–O_A distances vary with values of 1.483(1) for O1 and 1.505(1) Å for O2. The P–O2 bond is longer than typical P–O_A distances, due to the twofold hydrogen acceptor function of O2 in

the structure.

Three hydrogen bonds build up a structure of interconnected HPO_3F chains running in the c -direction (Tab. 7, Fig. 3a). The zigzag chains of HPO_3F tetrahedra are formed by one short hydrogen bond, $\text{O3-H1}\cdots\text{O2}$, (2.541(2) Å). They are then linked together by one weaker $\text{N}\cdots\text{O}$ hydrogen bond, $\text{N-H2}\cdots\text{O2}$, with a length of 2.822(2) Å and a shorter $\text{N}\cdots\text{O}$ bridge, $\text{N-H3}\cdots\text{O1}$ (2.677(2) Å). The short distance of the $\text{N}\cdots\text{O1}$ bond could be caused by the fact that the O1 atom is only involved in one hydrogen bond as an acceptor. Layers of the $[\text{PipzH}_2]^{2+}$ cations are located parallel to the c -axis at $x = \frac{1}{2}$ with the P–F bond pointed in the opposite direction (Fig. 3b).

Tab. 7 Hydrogen bonding in $[\text{PipzH}_2][\text{HPO}_3\text{F}]_2$ (Å, °)

D–H \cdots A	d(D–H)	d(H \cdots A)	d(D \cdots A)	$\angle\text{D–H}\cdots\text{A}$
$\text{O3–H1}\cdots\text{O2}$	0.73(2)	1.82(2)	2.541(2)	168(3)
$\text{N–H2}\cdots\text{O2}$	0.86(2)	1.97(2)	2.822(2)	170(2)
$\text{N–H3}\cdots\text{O1}$	0.83(2)	1.85(2)	2.677(2)	172(2)

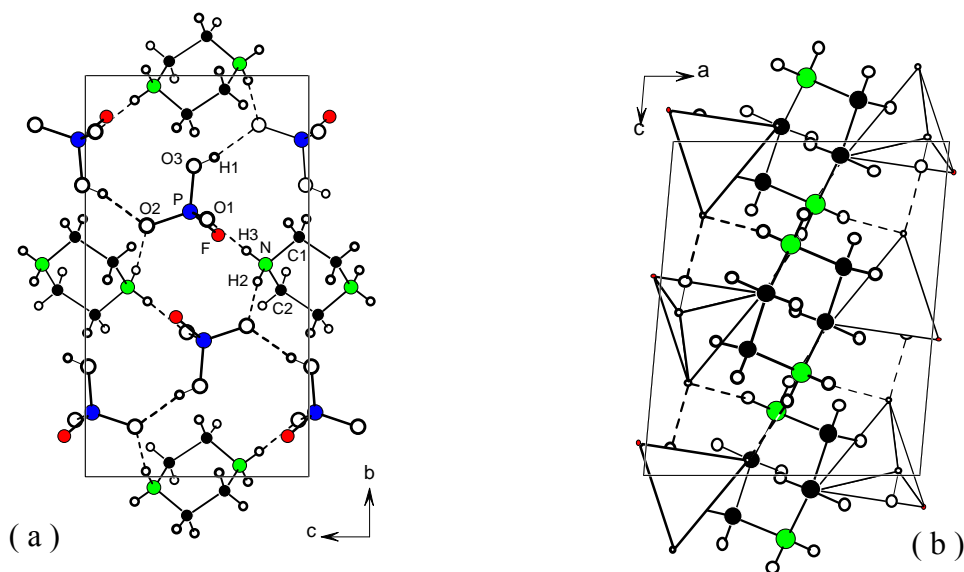


Fig. 3 Structure of $[\text{PipzH}_2][\text{HPO}_3\text{F}]_2$ (a) View along the a -axis with the zigzag HPO_3F chains parallel to the c -direction. (b) Polyhedral representation of the HPO_3F tetrahedra looking down the b -axis. The layer of $[\text{PipzH}_2]^{2+}$ ions is shown at $x = \frac{1}{2}$ with the P–F axis of tetrahedron pointed in the opposite direction.

4.2 The Structure with Branched Chains

Branched chains of HPO_3F tetrahedra were only found in the KHPO_3F structure (Tab. 8 and A2). The structure consists of infinite chains of three different HPO_3F tetrahedra with one branched HPO_3F tetrahedron. The structure exhibited twinning which was not

surprising due to the β angle close to 90° . A R_I -factor of about 20% was reached after solving and refining the structure in the monoclinic space group, $P2_1$. After refinement with the TWIN correction for a pseudo-orthorhombic symmetry, a R_I -factor of 2.14% was achieved with a 0.465:0.535 population ratio for the two orientations.

Tab. 8 Selected crystallographic data

Formula	KHPO₃F
Formula weight	138.08
Crystal system	<i>Monoclinic</i>
Space group	$P2_1$
Crystal Size	0.1 x 0.1 x 0.1
$a/\text{\AA}$	7.273(1)
$b/\text{\AA}$	14.086(3)
$c/\text{\AA}$	7.655(2)
$\beta/^\circ$	90.13(3)
$V/\text{\AA}^3, Z$	784.2(3), 8
$\rho_{\text{calc.}}/\text{g}\cdot\text{cm}^{-3}$	2.339
R_I [$I > 2\sigma(I)$]	0.0214
V_F (F1, F2, F3, F4)	1.09, 1.01, 1.07, 1.15

4.2.1 KHPO₃F

The KHPO₃F structure is composed of four crystallographically unique units of K^+ and HPO₃F[−] ions (Tab. A12, Fig. 4). The potassium atoms, K1, K3, and K4, have an eightfold coordination with both oxygen and fluorine atoms, whereas the K2 atom is only coordinated by seven atoms (1F + 6O). Average K–O lengths are 2.888, 2.814, 2.845, and 2.940 Å for K1, K2, K3, and K4, respectively (Tab. A30). The K1, K2, and K3, atoms located in the vicinity of one of the O–O edges of the HPO₃F tetrahedra of P1, P2, and P3 (Fig. 4) are each bonded to one fluorine atom with K–F lengths of 2.757(3), 3.075(4), and 2.762(3) Å, respectively. The K4 atom positioned near the O–F edge of the HPO₃F tetrahedron of P4 is coordinated by three F atoms with an average K–F length of 2.925 Å.

Tab. 9 P–O and P–F bond lengths in KHPO₃F (Å)

	d		d		d		d
P1–O1	1.483(3)	P2–O4	1.471(4)	P3–O7	1.479(4)	P4–O10	1.463(4)
P1–O2	1.489(4)	P2–O5	1.487(4)	P3–O8	1.504(4)	P4–O11	1.512(4)
P1–O3	1.555(4)	P2–O6	1.568(4)	P3–O9	1.556(3)	P4–O12	1.545(4)
P1–F1	1.565(3)	P2–F2	1.585(3)	P3–F3	1.574(3)	P4–F4	1.568(3)

The four HPO₃F tetrahedra vary slightly in their P–O, P–OH, and P–F lengths (Tab. 9). The P–O_A bonds found in the HPO₃F tetrahedra with P1 have similar lengths of 1.483(3) and 1.489(4) Å; both of these oxygen atoms, O1 and O2, act as hydrogen acceptors in the structure. In the HPO₃F tetrahedra with P3 and P4, only one of the oxygen atoms acts as a

hydrogen acceptor, O8 and O11, with longer P–O bond lengths of 1.504(4) and 1.512(4) Å respectively, whereas the oxygen atoms, O4, O5, O7, and O10, are not involved in hydrogen bonding and have shorter P–O distances between 1.463(4) and 1.487(4) Å. The HPO_3F tetrahedron of P2 due to the absence of a hydrogen acceptor does not have a characteristic P–O_A distance. The P–O_DH bond distances with the oxygen atoms, O3, O6, O9, and O12, range from 1.545(4) to 1.568(4) Å. The P–F bond is the longest bond in each tetrahedron with lengths between 1.565(3) and 1.585(3) Å. The fluorine atoms, F2 and F3, are bonded to one phosphorus and one potassium atom, whereas the F1 and F4 atoms are involved in two K–F and one P–F bonds (Tab. A30).

Tab. 10 Hydrogen bonding in KHPO_3F (Å, °)

D–H...A	d(D–H)	d(H...A)	d(D...A)	∠D–H...A
O3–H1...O11	0.73(2)	1.93(4)	2.590(5)	150(9)
O6–H2...O2	0.80(9)	1.8(1)	2.544(5)	175(9)
O9–H3...O1	0.93(6)	1.60(6)	2.520(5)	169(6)
O12–H4...O8	0.91(6)	1.60(6)	2.497(5)	169(5)

Four short O–H...O hydrogen bonds build up zigzag chains of the three HPO_3F tetrahedra with the P1, P3, and P4 atoms. These O–H...O bonds have O...O lengths between 2.497(5) and 2.590(5) Å. Each of these tetrahedra has one hydrogen donor and at least one hydrogen acceptor oxygen (Tab. 10). The chains run along *b* around the crystallographic 2_1 axis (Fig. 4). The fourth tetrahedra (P2, O4, O5, O6, F2) is connected to the HPO_3F tetrahedra of P1 with the hydrogen bond, O6–H2...O2, to create a branched chain.

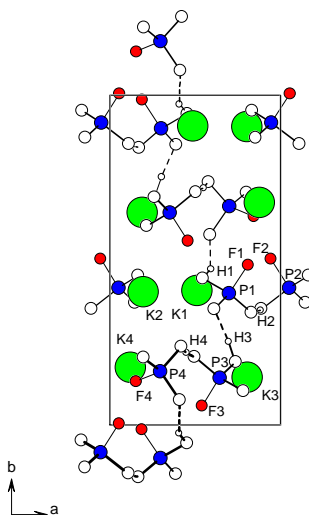


Fig. 4 Structure of KHPO_3F viewed along the *c*-axis showing a branched chain of HPO_3F tetrahedra, which runs parallel to *b* around the crystallographic 2_1 axis at $x = \frac{1}{2}$. Dashed lines indicate the H...O bonds. The K atoms are green.

4.3 The Structure with Isolated Dimers

The structure of $K_3[H(PO_3F)_2]$ uniquely featured isolated dimers of $[H(PO_3F)_2]$ units (Tab. 11 and A2). The $[H(PO_3F)_2]$ unit consisted of two equivalent PO_3F tetrahedra hydrogen-bonded to each other by a symmetrically-disordered hydrogen bond.

Tab. 11 Selected crystallographic data

Formula	$K_3[H(PO_3F)_2]$
Formula weight	314.25
Crystal system	<i>Monoclinic</i>
Space group	<i>C2/c</i>
Crystal Size	0.9 x 0.8 x 0.2
<i>a</i> /Å	7.973(3)
<i>b</i> /Å	11.635(4)
<i>c</i> /Å	9.668(4)
β /°	113.52(4)
<i>V</i> /Å ³ , <i>Z</i>	822.3(5), 4
$\rho_{calc.}/g\cdot cm^{-3}$	2.538
R_I [<i>I</i> >2 σ (<i>I</i>)]	0.0581
Analysis	
F (50 mL H ₂ O)	11.9
F (calcd)	6.05
<i>V_F</i>	1.14

4.3.1 $K_3[H(PO_3F)_2]$

The structure of the potassium hydrogen monofluorophosphate, $K_3[H(PO_3F)_2]$ (Tab. A13, Fig. 5), was the only one characterized with a H/ PO_3F ratio of 0.5. The space group, *C2/c*, yielded a structure model with a R_I -factor over 6%. A decrease in the R_I -factor was achieved after the hydrogen atom initially found on the center of symmetry was assigned a general position within the hydrogen bond geometry.

Tab. 12 Bond lengths in $K_3[H(PO_3F)_2]$ (Å)

	d		d		d		d		d
K1–O1	2.729(4)	K1–O3'	2.860(4)	K2–O1	2.846(4)	K2–O1'	2.953(5)	P1–O1	1.487(4)
K1–O1'	2.729(4)	K1–F	3.096(4)	K2–O2	2.915(5)	K2–O2''	3.084(5)	P1–O2	1.492(4)
K1–O2	2.785(4)	K1–F'	3.096(4)	K2–O2'	2.936(5)	K2–O3	3.150(5)	P1–O3	1.543(4)
K1–O2'	2.785(4)			K2–F	2.942(4)	K2–F'	3.181(4)	P1–F1	1.594(3)
K1–O3	2.860(4)			K2–O1	2.948(5)				

The asymmetric unit consists of two potassium atoms, one PO_3F tetrahedron, and a disordered hydrogen atom. The K1 atom has a special position on the crystallographic C_2 axis (Fig. 5). The potassium atoms, K1 and K2, are bonded to a total of eight and nine oxygen and fluorine atoms, respectively, with average K–O/F lengths of 2.868 (for K1) and 2.995 Å (for K2) (Tab. 12). The PO_3F tetrahedron has two P–O bonds with distances

of 1.487(4) and 1.492(4) Å (Tab. 12). These oxygen atoms, O1 and O2, coordinate the two K^+ ions and do not participate in hydrogen bonding. The O3 atom, which is a half donor and half acceptor in the structure has a distance of 1.543(4) Å to phosphorus. This length is longer than other P–OH distances for oxygen atoms involved in a hydrogen bond as a donor and acceptor ($\frac{1}{2}D + \frac{1}{2}A$) possibly due to further coordination of O3 to the potassium cations. The P–F bond with a length of 1.594(3) Å is also longer than those found in the other hydrogen monofluorophosphates and most likely caused by its extended coordination with four K atoms.

The hydrogen bond system consists of one short, symmetrically-disordered hydrogen bond, $O3-H\cdots O3'$, (2.451(8) Å) (Tab. 13). This O–H \cdots O bond links two equivalent PO_3F tetrahedra together to form an isolated dimer with the formula: $H(PO_3F)_2$. These dimers are positioned around centers of symmetry. Layers of K atoms and two tetrahedra of two separate dimers alternate along the *b*-axis (Fig. 5).

Tab. 13 Hydrogen bonding in $K_3[H(PO_3F)_2]$ (Å, °)

D–H \cdots A	d(D–H)	d(H \cdots A)	d(D \cdots A)	$\angle D-H\cdots A$
$O3-H\cdots O3'$	0.75(2)	1.72(4)	2.451(8)	166(20)

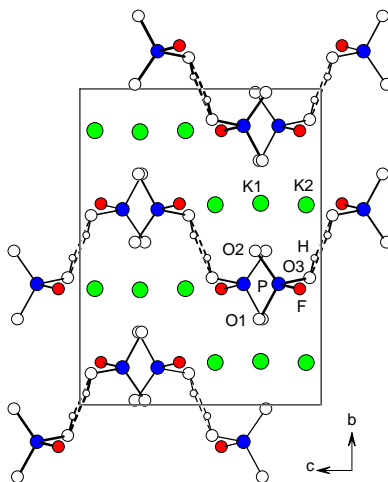


Fig. 5 View of the $K_3[H(PO_3F)_2]$ structure looking down the *a*-axis. The $H\cdots O3'$ bond is indicated with dashed lines. The isolated dimers of $[H(PO_3F)_2]$ are shown positioned around centers of symmetry at $\{\frac{1}{2}, \frac{1}{2}, \frac{1}{2}\}$ with the O1–O2 edges of the PO_3F tetrahedra overlapping each other.

4.4 The Structures with Cyclic Dimers

Cyclic dimers of hydrogen-bonded HPO_3F tetrahedra were also observed in the crystal structures of the hydrogen monofluorophosphates. This type of dimer was found in the

hydrogen monofluorophosphate structures with cesium [78] and the N-containing cations, $[\text{NHEt}_3]^+$, $[\text{C}(\text{NH}_2)_2]^+$, and $\text{N,N}'\text{-dmuH}^+$ (Tab. 14, A3, and A4). The cyclic dimers in the cesium and triethylammonium structures were formed by disordered hydrogen bonds.

Tab. 14 Selected crystallographic data

Formula	CsHPO_3F	$[\text{NHEt}_3]\text{HPO}_3\text{F}$	$[\text{C}(\text{NH}_2)_3]\text{HPO}_3\text{F}$	$[\text{N,N}'\text{-dmuH}]\text{HPO}_3\text{F}$
Formula weight	231.89	201.18	159.07	188.10
Crystal system	<i>Monoclinic</i>	<i>Monoclinic</i>	<i>Monoclinic</i>	<i>Monoclinic</i>
Space group	<i>C2/m</i>	<i>P2₁/n</i>	<i>P2₁/c</i>	<i>P2₁/c</i>
Crystal Size	0.4 x 0.2 x 0.1	0.5 x 0.4 x 0.2	0.24 x 0.08 x 0.04	0.5 x 0.2 x 0.1
<i>a</i> /Å	14.478(8)	10.735(3)	6.780(1)	5.435(1)
<i>b</i> /Å	5.929(3)	8.214(2)	10.089(2)	17.634(4)
<i>c</i> /Å	5.413(2)	11.755(3)	9.389(2)	8.507(2)
$\beta/^\circ$	103.30(4)	91.15(3)	105.77(3)	100.47(3)
<i>V</i> /Å ³ , <i>Z</i>	452.2(4), 4	1036.3(5), 4	618.1(2), 4	801.7(3), 4
$\rho_{\text{calc.}}/\text{g}\cdot\text{cm}^{-3}$	3.406	1.289	1.709	1.558
<i>R_I</i> [<i>I</i> > 2σ(<i>I</i>)]	0.0155	0.0387	0.0449	0.0383
Analysis				
F (50 mL H₂O)	-	0.1	0.8	0.5
F (Seel)	8.1	9.2	11.1	9.4
F (calcd)	8.19	9.44	11.94	10.10
<i>V_F</i>	1.04	0.95	0.98	0.97

4.4.1 CsHPO_3F

The crystal structure of cesium hydrogen monofluorophosphate consists of one crystallographically unique cesium atom and one HPO_3F tetrahedron (Tab. A14). The HPO_3F^- anions are hydrogen-bonded to each other via one unique hydrogen bond to form cyclic dimers with cesium atoms between them (Fig. 6). The cesium, phosphorus, fluorine, and oxygen (O1) atoms are situated on the mirror plane, which gives the structure a symmetrical simplicity.

The cesium atom has a tenfold coordination with one fluorine and nine oxygen atoms with Cs–X distances between 3.030(3) and 3.379(2) Å (Tab. 15). In the HPO_3F -tetrahedron, two different P–O bonds with lengths of 1.477(3) (P–O1) and 1.528(2) Å (P–O2) are observed with a longer distance of 1.577(2) Å between P and F. The O1 atom with a short distance to P does not participate in hydrogen bonding. The distance from phosphorus to the half protonated oxygen atom, O2, is between typical P–O_A and P–O_DH lengths.

Tab. 15 Bond lengths in CsHPO_3F (Å)

d		d		d	
Cs–O1	3.030(3)	Cs–O2'	3.315(2)	P–O1	1.477(3)
Cs–O1'	3.159(1)	Cs–O2''	3.363(2)	P–O2	1.528(2)
Cs–O1''	3.159(1)	Cs–O2'''	3.363(2)	P–F	1.577(2)
Cs–F	3.194(3)	Cs–O2''''	3.379(2)		
Cs–O2	3.315(2)	Cs–O2'''''	3.379(2)		

The disordered hydrogen bond, $\text{O2-H}\cdots\text{O2}'$, with a $\text{O}\cdots\text{O}$ distance of $2.527(2)$ Å (Fig. 6, Tab. 16) links two HPO_3F tetrahedra with each other to form cyclic dimers. The oxygen atom, O2, acts as a half hydrogen donor and half acceptor ($\frac{1}{2}\text{D} + \frac{1}{2}\text{A}$) on the basis of the disordered hydrogen position. Therefore, the tetrahedron can be more accurately written as $[\text{PO}(\text{OH}_{1/2})_2\text{F}]$.

Tab. 16 Hydrogen bonding in CsHPO_3F (Å, °)

D-H \cdots A	d(D-H)	d(H \cdots A)	d(D \cdots A)	$\angle\text{D-H}\cdots\text{A}$
$\text{O2-H}\cdots\text{O2}'$	0.74(2)	1.84(4)	2.527(2)	153.9(1)

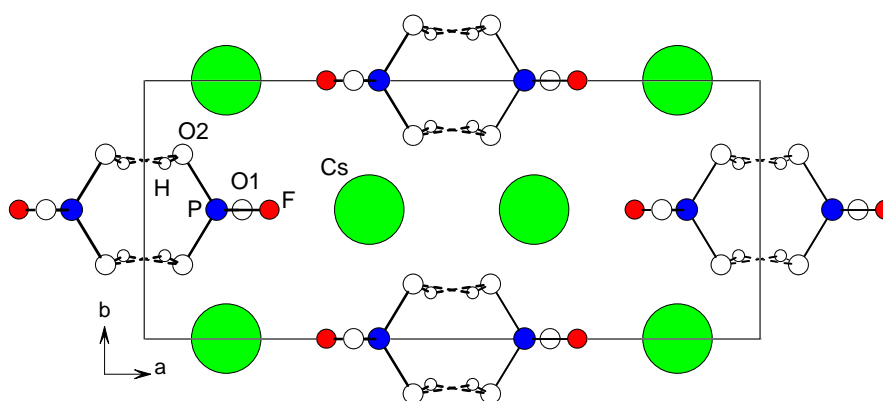


Fig. 6 Structure of CsHPO_3F viewed along the c -axis showing the cyclic dimers of HPO_3F tetrahedra. The Cs atoms are green. Dashed lines indicate the $\text{H}\cdots\text{O2}'$ bond.

4.4.2 $[\text{NH}(\text{CH}_2\text{CH}_3)_3]\text{HPO}_3\text{F}$

The triethylammonium structure contains one unique $[\text{NHEt}_3]^+$ cation and one HPO_3F^- anion (Tab. A15, Fig. 7a and b). Cyclic dimers are formed in the structure by a disordered hydrogen bond. The $[\text{NHEt}_3]^+$ cation has N-C lengths between $1.498(3)$ and $1.532(2)$ Å with C-C distances varying from $1.461(4)$ Å for C1-C2 to $1.521(3)$ Å for C5-C6 (Tab. 17). The C-H bonds have an average length of 1.00 Å (Tab. A31). A typical length of $1.566(2)$ Å is observed in the structure for the P-F distance, whereas inconsistencies are found in the P-O bond lengths. A very short P-O_A distance of $1.452(2)$ Å is found for the P-O1 bond. The other P-O distances of $1.511(2)$ (P-O2) and $1.532(2)$ (P-O3) are much longer between P-O_A and P-O_{DH} lengths. These deviations in the interatomic distances are caused by the $\frac{1}{2}\text{D} + \frac{1}{2}\text{A}$ function of the O2 and O3 atoms. The average P-O _{$\frac{1}{2}\text{D} + \frac{1}{2}\text{A}$} length is 1.523 Å.

Tab. 17 P–X, N–C, and C–C bond lengths in [NHEt₃]HPO₃F (Å)

	d		d		d
P–O1	1.452(2)	N–C1	1.498(2)	C3–C4	1.494(3)
P–O2	1.511(2)	N–C3	1.532(2)	C5–C6	1.521(3)
P–O3	1.534(2)	N–C5	1.522(3)		
P–F	1.566(2)	C1–C2	1.461(4)		

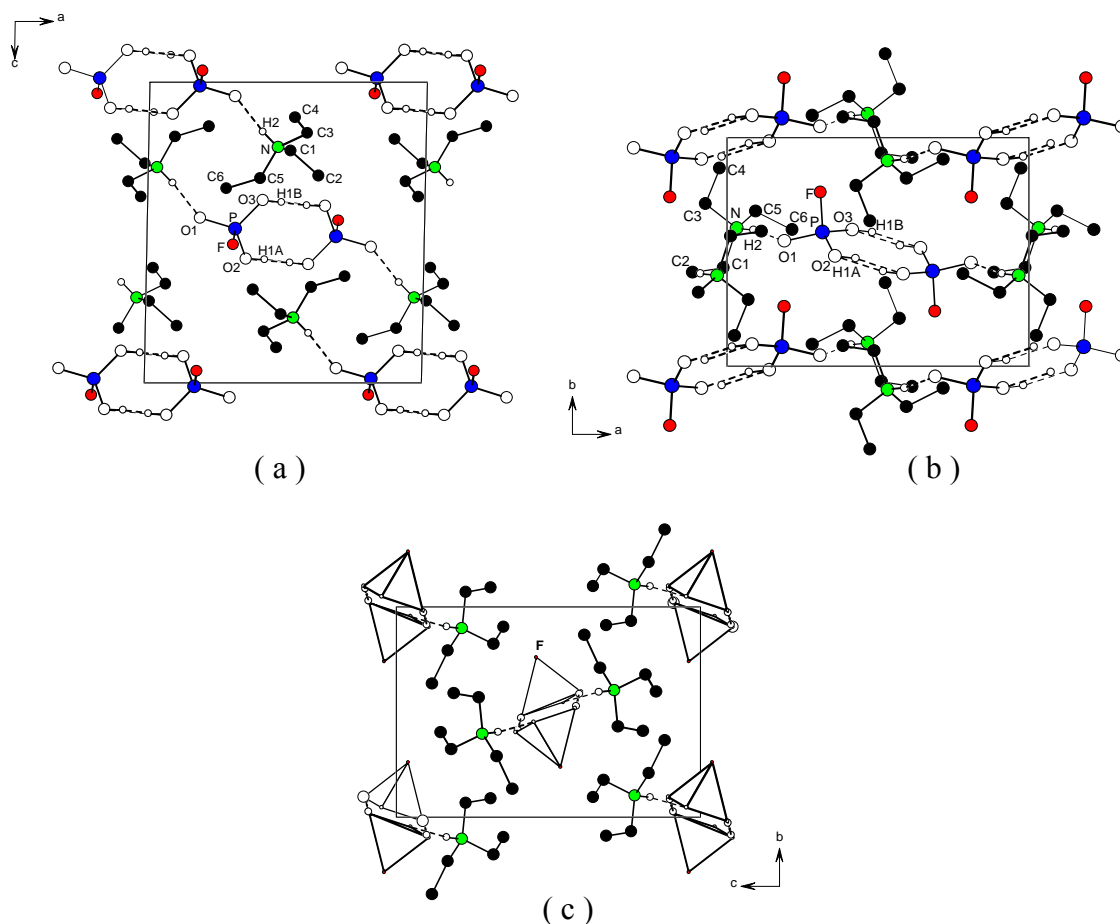


Fig. 7 Structure of [NHEt₃]HPO₃F (a) Ball-and-stick representation viewed along the *b*-axis. The hydrogen atoms on carbon have been omitted for clarity. Dashed lines indicate the H···O bonds. (b) Another view of the structure down the *c*-axis showing the O–H···O bonds with the disordered hydrogen position. (c) Polyhedral representation of the HPO₃F tetrahedra along the *a*-axis showing the direction of the P–F axis relative to the layers of [NHEt₃]⁺ ions at *z* = 1/4 and 3/4.

The HPO₃F tetrahedra are linked to each other to form cyclic dimers in the structure via a short hydrogen bond between O2 and O3, in which the hydrogen atom has a disordered position (Fig. 7a). The tetrahedron can consequently be expressed as [PO(OH_{1/2})₂F]. The disordered hydrogen bond, O2–H1B···O3' and O3–H1A···O2', has a length of 2.515(2) Å (Tab. 18, Fig. 7b). The cyclic dimers are fixed in the structure by a second hydrogen bond, N–H2···O1 (2.622 Å). Each of the three oxygen vertices of the [PO(OH_{1/2})₂F] tetrahedron are hydrogen-bonded to either a second tetrahedron or the [NHEt₃]⁺ cation shown in Fig. 7a.

The fluorine atom on the fourth vertex of the tetrahedron located between the layers of cations at $z = \frac{1}{4}$ and $\frac{3}{4}$ does not participate in additional bonding (Fig. 7c).

Tab. 18 Hydrogen bonding in [NHEt₃]HPO₃F (Å, °)

D–H...A	d(D–H)	d(H...A)	d(D...A)	∠D–H...A
O2–H1A...O3	0.72(4)	1.81(4)	2.515(2)	167(4)
O3–H1B...O2	0.74(2)	1.80(3)	2.515(2)	162(7)
N–H2...O1	0.84(3)	1.78(3)	2.622(2)	169(2)

4.4.3 [C(NH₂)₃]HPO₃F

In the guanidinium hydrogen monofluorophosphate structure, one crystallographically independent unit of a [C(NH₂)₃]⁺ cation and a HPO₃F[−] anion are found (Tab. A16, Fig. 8). The guanidinium cation has C–N lengths between 1.310(4) and 1.339(4) Å. N–H distances vary from 0.78(4) to 0.87(4) Å (Tab. 20). P–O_A lengths of 1.480(2) and 1.479(3) Å are found for the P–O1 and P–O2 bonds, respectively. The P–O3 and P–F have lengths of 1.531(3) and 1.544(3) Å (Tab. 19).

Tab. 19 Bond lengths in [C(NH₂)₃]HPO₃F (Å)

	d		d
P–O1	1.480(2)	C–N1	1.339(4)
P–O2	1.479(3)	C–N2	1.310(4)
P–O3	1.531(3)	C–N3	1.325(4)
P–F	1.544(3)		

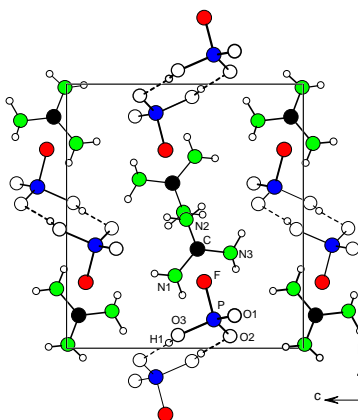


Fig. 8 Ball-and-stick representation of the [C(NH₂)₃]HPO₃F structure viewed along the *a*-axis. The cyclic dimers of HPO₃F tetrahedra are shown linked by the short hydrogen bond, O3–H1...O2. The N–H...O hydrogen bonds are not shown for clarity.

The hydrogen bond system (Tab. 20) in the guanidinium structure involves one short O–H \cdots O hydrogen bond and longer N–H \cdots O bridges. The hydrogen bond, O3–H1 \cdots O2, with a length of 2.562(4) Å connects the HPO₃F tetrahedra to cyclic dimers. The dimers are interlinked to each other by the long N–H \cdots O bridges. Only the nitrogen atoms, N2 and N3, participate in N \cdots O bonds with a range of lengths from 2.920(4) to 3.042(4) Å (Tab. 20). The hydrogen atoms, H2 and H3, on N1 are not involved in hydrogen bonding in the structure. The O1 atom is involved in three N \cdots O hydrogen bonds, whereas O2 participates in the short O \cdots O bond and one long N \cdots O bridge as a hydrogen acceptor.

Tab. 20 Hydrogen bonding in [C(NH₂)₃]HPO₃F (Å, °)

D–H \cdots A	d(D–H)	d(H \cdots A)	d(D \cdots A)	\angle D–H \cdots A
O3–H1 \cdots O2	0.81(5)	1.77(5)	2.562(4)	166(5)
N1–H2	0.84(5)			
N1–H3	0.85(5)			
N2–H4 \cdots O2	0.81(4)	2.17(4)	2.920(4)	155(3)
N2–H5 \cdots O1	0.79(4)	2.18(5)	2.934(4)	161(4)
N3–H6 \cdots O1	0.78(4)	2.14(4)	2.898(4)	163(3)
N3–H7 \cdots O1	0.87(4)	2.27(4)	3.042(4)	149(3)

4.4.4 {HOC[NH(CH₃)₂]}HPO₃F

In the structure of the N,N'-dimethyluronium (N,N'-dmuH) hydrogen monofluorophosphate, a crystallographic unique set of one [N,N'-dmuH]⁺ ion and one HPO₃F[–] anion build up a structure of interconnected cyclic dimers (Tab. A17, Fig. 9). The uronium carbon atom is bonded to one oxygen atom (1.303(3) Å) and two nitrogen atoms (average distance of 1.323 Å) (Tab. 21). Longer N–C bonds are observed between the nitrogen atoms and the methyl groups with lengths of 1.445(3) and 1.466(3) Å. The average C–H length in the structure is 0.94 Å with N–H distances of 0.79(3) and 0.83(3) Å (Tab. 22). The HPO₃F tetrahedron has two short P–O_A lengths of 1.498(2) and 1.492(2) Å with a P–O_DH distance of 1.542(2) Å. The P–F bond length is 1.554(2) Å.

Tab. 21 Bond lengths in [N,N'-dmuH]HPO₃F (Å)

	d		d		d
P–O1	1.498(2)	C1–N1	1.321(3)	C2–H6	0.89(3)
P–O2	1.492(2)	C1–N2	1.325(3)	C2–H7	0.94(3)
P–O3	1.542(2)	N1–C2	1.445(3)	C3–H8	0.97(4)
P–F	1.554(2)	N2–C3	1.466(3)	C3–H9	0.93(5)
C1–O4	1.303(3)	C2–H5	0.99(3)	C3–H10	0.92(4)

The hydrogen bond system in the uronium salt consists of two short O–H \cdots O bonds and two longer N–H \cdots O bridges (Fig.9, Tab. 22). The hydrogen bond, O3–H1 \cdots O2, with a

length of 2.562(2) Å links the HPO_3F tetrahedra to cyclic dimers. The second short hydrogen bond, $\text{O4-H2}\cdots\text{O1}$, (2.488(2) Å) is between the carbonyl oxygen atom, O4, and the HPO_3F tetrahedron. It and the weaker $\text{N-H}\cdots\text{O}$ bonds with lengths of 2.884(3) and 2.942(3) Å connect the dimers to each other. The fluorine atoms are located near the inert part of the organic cation on the *ac*-plane at about $y = 0$ and $\frac{1}{2}$. Layers of the uronium cations are situated at $y = \frac{1}{4}$ and $\frac{3}{4}$ in a parallel plane (Fig. 9).

Tab. 22 Hydrogen bonding in $[\text{N},\text{N}'\text{-dmuH}]\text{HPO}_3\text{F}$ (Å, °)

D-H \cdots A	d (D-H)	d (H \cdots A)	d (D \cdots A)	$\angle\text{OHO}$
$\text{O3-H1}\cdots\text{O2}$	0.88(4)	1.70(4)	2.562(2)	168(4)
$\text{O4-H2}\cdots\text{O1}$	0.97(3)	1.52(4)	2.488(2)	173(3)
$\text{N1-H3}\cdots\text{O2}$	0.79(3)	2.10(3)	2.884(3)	171(3)
$\text{N2-H4}\cdots\text{O1}$	0.83(3)	2.16(3)	2.942(3)	158(2)

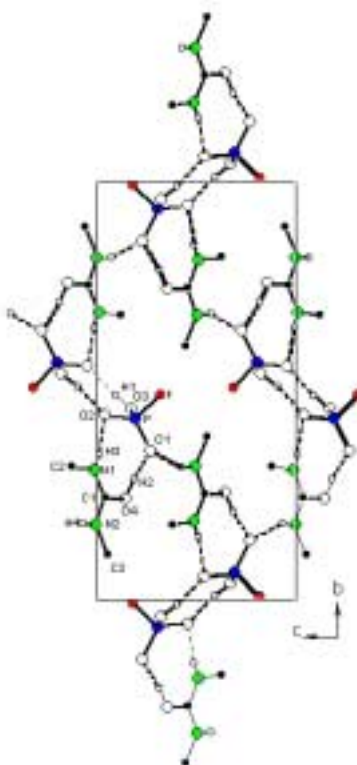


Fig. 9 Cyclic dimers of HPO_3F tetrahedra in the structure of $[\text{N},\text{N}'\text{-dmuH}]\text{HPO}_3\text{F}$ viewed down the *a*-axis. Dashed lines indicate the $\text{H}\cdots\text{O}$ bonds. Hydrogen atoms on carbon are not shown for clarity.

4.5 The Structures with Cyclic Tetramers

Tetramers were formed in the structures with ammonium and rubidium (Tab. 23 and A5). In the case of ammonium, two modifications, α - and β - $\text{NH}_4\text{HPO}_3\text{F}$ [77], were found with cyclic tetrameric units of HPO_3F tetrahedra. Cyclic tetramers were also formed in α - RbHPO_3F isostructural to the α - $\text{NH}_4\text{HPO}_3\text{F}$ structure.

Tab. 23 Selected crystallographic data

Formula	α - $\text{NH}_4\text{HPO}_3\text{F}$	β - $\text{NH}_4\text{HPO}_3\text{F}$	α - RbHPO_3F
Formula weight	117.02	117.02	184.45
Crystal system	0.4 x 0.1 x 0.1	0.7 x 0.6 x 0.4	0.8 x 0.2 x 0.1
Space group	<i>Monoclinic</i>	<i>Triclinic</i>	<i>Monoclinic</i>
Crystal Size	$P2_1/n$	$P\bar{1}$	$P2_1/n$
$a/\text{\AA}$	7.4650(7)	7.481(1)	7.465(2)
$b/\text{\AA}$	15.586(2)	7.511(1)	15.551(8)
$c/\text{\AA}$	7.5785(9)	7.782(1)	7.563(4)
$\alpha/^\circ$	90	84.31(1)	90
$\beta/^\circ$	108.769(9)	84.20(3)	105.38(5)
$\gamma/^\circ$	90	68.67(2)	90
$V/\text{\AA}^3, Z$	834.9(2), 8	404.31(9), 4	846.5(7), 8
$\rho_{\text{calc.}}/\text{gcm}^{-3}$	1.862	1.922	2.894
$R_I [I > 2\sigma(I)]$	0.0376	0.0254	0.0365
Analysis			
F (50 mL H_2O)	14.2	0.4	1.1
F (Seel)	-	15.7	9.4
F (calcd)	16.24	16.24	10.30
$V_F(\text{F1}, \text{F2})$	0.96, 0.95	0.96, 0.95	1.08, 1.12

4.5.1 α - $\text{NH}_4\text{HPO}_3\text{F}$

The α - $\text{NH}_4\text{HPO}_3\text{F}$ structure contains two crystallographically independent NH_4^+ cations and HPO_3F^- anions (Tab. A18, Fig. 10). The NH_4^+ cations have an average N—H bond length of 0.85 Å (Tab. 25). P—O_A lengths vary from 1.487(2) to 1.492(2) with P—O_DH lengths of 1.545(2) and 1.550(2) Å. The P—F bond lengths observed are 1.558(2) and 1.566(2) Å (Tab. 24).

Tab. 24 Bond lengths in α - $\text{NH}_4\text{HPO}_3\text{F}$ and β - $\text{NH}_4\text{HPO}_3\text{F}$ (310 K) (Å)

	α - $\text{NH}_4\text{HPO}_3\text{F}$	β - $\text{NH}_4\text{HPO}_3\text{F}$		α - $\text{NH}_4\text{HPO}_3\text{F}$	β - $\text{NH}_4\text{HPO}_3\text{F}$
P1—O1	1.492(2)	1.486(1)	P2—O4	1.490(2)	1.483(1)
P1—O2	1.487(2)	1.483(1)	P2—O5	1.491(2)	1.488(1)
P1—O3	1.545(2)	1.547(1)	P2—O6	1.550(2)	1.546(1)
P1—F1	1.558(2)	1.563(1)	P2—F2	1.566(2)	1.568(1)

The hydrogen bond system consists of short O—H \cdots O and longer N—H \cdots O bonds. The shorter hydrogen bonds, O3—H1 \cdots O5 and O6—H2 \cdots O2, link two pairs of nonequivalent HPO_3F tetrahedra together to form cyclic tetramers (Fig. 10). They have lengths of

2.535(3) and 2.508(3) Å (Tab. 25). The weaker N—H···O bonds connect the tetramers to each other with N···O distances between 2.800(3) and 2.951(4) Å. The ammonia hydrogen atom, H10, is not involved in the hydrogen bond system. The compound has a calculated density of 1.862 g·cm⁻³. No O—H···F or N—H···F bonds are found in the structure, although a very short distance of 2.731 Å exists between F1 and F2 (\angle P1F1F2 = 118 ° and \angle P2F2F1 = 159°). An H atom was not located between these two F atoms.

Tab. 25 Hydrogen bonding in α -NH₄HPO₃F (Å, °)

D—H···A	d(D—H)	d(H···A)	d(D···A)	\angle D—H···A
O3—H1···O5	0.74(2)	1.82(2)	2.535(3)	166(5)
O6—H2···O2	0.87(4)	1.64(4)	2.508(3)	174(4)
N1—H3···O4	0.92(3)	2.04(3)	2.932(4)	164(3)
N1—H4···O1	0.80(4)	2.22(4)	2.951(4)	152(3)
N1—H5···O1	0.87(4)	2.02(4)	2.863(4)	161(3)
N1—H6···O2	0.84(4)	2.10(4)	2.917(4)	163(3)
N2—H7···O1	0.90(4)	1.99(4)	2.876(4)	164(3)
N2—H8···O4	0.81(4)	2.01(4)	2.800(3)	167(3)
N2—H9···O4	0.84(5)	2.01(5)	2.842(4)	174(4)
N2—H10	0.83(4)			

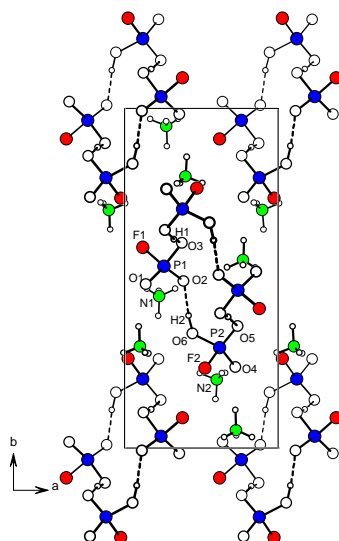


Fig. 10 Structure of α -NH₄HPO₃F viewed along the c-axis with the NH₄⁺ ions and the cyclic tetramers of HPO₃F tetrahedra. Dashed lines indicate the H···O bonds. N—H···O bonds are not shown for clarity.

4.5.2 β -NH₄HPO₃F

The β -NH₄HPO₃F structure was measured at both 180 (Tab. A19) and 310 K (Tab. A20) [77]. The measurement at 310 K probably due to improved crystal quality yielded a more precise structure model than the 180 K measurement. Only slight differences were observed between the two structure refinements [77]; therefore, only the data from the 310 K measurement is presented and discussed here.

The structure contains crystallographically unique units of two NH₄⁺ cations and two

HPO_3F^- anions (Fig. 11). An average N—H bond length of 0.86 Å is found in the structure (Tab. 26). P—O_A lengths are between 1.483(1) to 1.488(1) Å with P—O_DH lengths of 1.547(1) and 1.546(1) Å (Tab. 24). The P—F bond has distances of 1.563(1) and 1.568(1) Å.

Short O—H \cdots O and weaker N—H \cdots O bonds make up the hydrogen bond system. The short O—H \cdots O bonds, O3—H1 \cdots O5 and O6—H2 \cdots O2, link two pairs of the unique HPO_3F tetrahedra to cyclic tetramers (Fig. 11, Tab. 26); they have distances of 2.568(2) and 2.539(2) Å, respectively. The tetramers are interconnected with weaker N—H \cdots O bonds (2.881(2)–3.043(2) Å). All of the ammonium hydrogen atoms participate in hydrogen bonds. The structure had a calculated density of 1.922 g·cm⁻³.

Tab. 26 Hydrogen bonding in $\beta\text{-NH}_4\text{HPO}_3\text{F}$ at 310 K (Å, °)

D—H \cdots A	d(D—H)	d(H \cdots A)	d(D \cdots A)	$\angle\text{D—H}\cdots\text{A}$
O3—H1 \cdots O5	0.73(3)	1.85(3)	2.568(2)	169(3)
O6—H2 \cdots O2	0.75(3)	1.79(3)	2.539(2)	174(4)
N1—H3 \cdots O1	0.88(2)	2.02(2)	2.895(2)	169(2)
N1—H4 \cdots O4	0.84(3)	2.06(3)	2.881(2)	165(2)
N1—H5 \cdots O1	0.83(3)	2.13(3)	2.919(2)	160(2)
N1—H6 \cdots O2	0.88(3)	2.15(3)	2.899(2)	142(2)
N2—H7 \cdots O4	0.84(3)	2.07(3)	2.904(2)	176(2)
N2—H8 \cdots O4	0.82(3)	2.27(3)	3.043(2)	159(2)
N2—H9 \cdots O5	0.90(3)	2.15(3)	3.004(2)	159(2)
N2—H10 \cdots O1	0.89(2)	2.07(2)	2.964(2)	175(2)

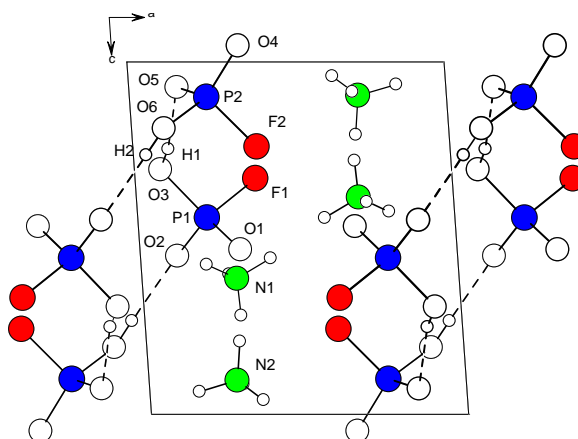


Fig. 11 View of $\beta\text{-NH}_4\text{HPO}_3\text{F}$ looking down the b -axis with the tetrameric hydrogen-bonded phosphorus tetrahedra and the NH_4^+ ions. The H \cdots O bonds are indicated by dashed lines. N—H \cdots O bonds are not shown for clarity.

4.5.3 α -RbHPO₃F

The α -RbHPO₃F structure (Tab. A21, Fig. 12) isotypic to α -NH₄HPO₃F (Fig. 10) has two crystallographic unique units of Rb⁺ and HPO₃F⁻ ions (Fig. 12). The Rb atoms are coordinated with a total of nine oxygen and fluorine atoms, Rb1 (8 O + 1 F) and Rb2 (6 O + 3 F), with average lengths of 3.057 and 3.049 Å, respectively (Tab. A32). The HPO₃F tetrahedra have three different P–O bonds: P–O, P–O_A, and P–O_DH. The P–O bonds are short with lengths of 1.477(5) and 1.479(5) Å for O1 and O4, respectively, which are only involved in the Rb coordination (Tab. 27). The O2 and O5 atoms act as hydrogen acceptors in the hydrogen bonds and have interatomic distances to phosphorus of 1.499(4) and 1.493(4) Å (P–O_A). The P–O_DH distances are practically identical for the HPO₃F tetrahedra with 1.556(5) and 1.557(6) Å, whereas the P–F bond lengths vary between the tetrahedra: 1.571(4) and 1.586(4) Å.

Tab. 27 P–O and P–F bond lengths in α -RbHPO₃F (Å)

	d		d
P1–O1	1.477(5)	P2–O4	1.479(5)
P1–O2	1.499(4)	P2–O5	1.493(4)
P1–O3	1.556(5)	P2–O6	1.557(6)
P1–F1	1.571(4)	P2–F2	1.586(4)

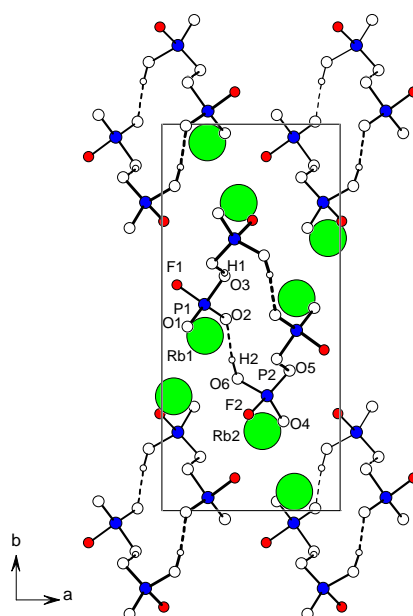


Fig. 12 Structure of α -RbHPO₃F looking down the c-axis with the Rb⁺ ions and the cyclic tetramers of hydrogen-bonded HPO₃F tetrahedra. Dashed lines indicate the H···O bonds. The Rb atoms are green.

The hydrogen bond system consists of two short O–H \cdots O hydrogen bonds, which connect the tetrahedra to cyclic tetramers identical to those found in α -NH₄HPO₃F. The bonds, O3–H1 \cdots O5 and O6–H2 \cdots O2, have lengths of 2.561(6) and 2.486(7) Å (Tab.28).

Tab. 28 Hydrogen bonding in α -RbHPO₃F (Å, °)

D–H \cdots A	d(D–H)	d(H \cdots A)	d(D \cdots A)	\angle D–H \cdots A
O3–H1 \cdots O5	0.75(2)	1.83(3)	2.561(5)	160(10)
O6–H2 \cdots O2	0.8(1)	1.7(1)	2.486(7)	169(9)

4.6 The Complex Structures and Hydrates

More complex structures were found for compositions other than MHPO₃F (Tab. 29 and Tab. 30, A6, and A7). Structures with mixed cations were determined for compounds with Cs⁺ and NH₄⁺ ions and Na⁺ and [N(CH₃)₄]⁺ ions. Both HPO₃F and PO₃F tetrahedra were observed in the structure with cesium and ammonium, Cs₃(NH₄)₂(HPO₃F)₃(PO₃F) [78]. Structures of basic salts were determined for: the decahydrate of Na₂PO₃F [81], Na₅[N(CH₃)₄](PO₃F)₃·18H₂O, and [C(NH₂)₃]₂PO₃F (Tab. 30). The structures described here are more complex and can not be described by a certain type of structural feature formed by the hydrogen-bonded HPO₃F tetrahedra.

Tab. 29 Selected crystallographic data

Formula	Cs ₃ (NH ₄) ₂ (HPO ₃ F) ₃ (PO ₃ F)	[N(CH ₃) ₄] ₂ HPO ₃ F·H ₂ O
Formula weight	829.72	191.14
Crystal system	<i>Monoclinic</i>	<i>Cubic</i>
Space group	<i>P2₁/c</i>	<i>P2₁3</i>
Crystal Size	0.6 x 0.6 x 0.6	0.8 x 0.8 x 0.24
<i>a</i> /Å	20.619(4)	9.691(2)
<i>b</i> /Å	12.076(2)	9.691(2)
<i>c</i> /Å	15.856(3)	9.691(2)
β /°	102.58(2)	90
<i>V</i> /Å ³ , <i>Z</i>	3853(1), 8	910.1(3), 4
$\rho_{\text{calc.}}$ /gcm ⁻³	2.860	1.395
<i>R</i> _{<i>I</i>} [<i>I</i> > 2 σ (<i>I</i>)]	0.0466	0.0239
Analysis		
F (50 mL H ₂ O)	8.2	0.2
F (Seel)	-	9.5
F (calcd)	9.16	9.94
<i>V</i> _F	1.04-1.09	0.96

Tab. 30 Selected crystallographic data

Formula	Na ₂ PO ₃ F·10H ₂ O	Na ₅ [N(CH ₃) ₄](PO ₃ F) ₃ ·18H ₂ O	[C(NH ₂) ₃] ₂ PO ₃ F
Formula weight	324.11	807.3	218.15
Crystal system	<i>Monoclinic</i>	<i>Triclinic</i>	<i>Monoclinic</i>
Space group	<i>P2₁/c</i>	<i>P$\bar{1}$</i>	<i>Cm</i>
Crystal Size	0.5 x 0.5 x 0.4	0.4 x 0.2 x 0.1	0.6 x 0.5 x 0.4
<i>a</i> /Å	11.380(3)	6.438(2)	13.201(3)
<i>b</i> /Å	10.234(2)	13.438(4)	7.291(1)
<i>c</i> /Å	13.051(4)	19.520(5)	11.680(2)
<i>α</i> /°	90	89.38(3)	90
<i>β</i> /°	106.49(3)	88.84(3)	119.72(3)
<i>γ</i> /°	90	88.18(3)	90
<i>V</i> /Å ³ , <i>Z</i>	1457.4(7), 4	1687.5(8), 6	976.3(3), 4
<i>ρ</i> _{calc.} /gcm ⁻³	1.477	1.589	1.484
<i>R</i> _I [<i>I</i> > 2σ(<i>I</i>)]	0.0266	0.0306	0.0424
Analysis			
F (50 mL H ₂ O)	-	0	3.5
F (Seel)	-	6.5	10.7
F (calcd)	-	7.06	8.71
<i>V</i> _F	0.91	0.92, 0.94, 0.94	0.94, 0.95

4.6.1 Cs₃(NH₄)₂(HPO₃F)₃(PO₃F)

The structure of Cs₃(NH₄)₂(HPO₃F)₃(PO₃F) (Tab. A22 and A23, Fig. 13a and b) is made up of a complex network of HPO₃F and PO₃F tetrahedra held together by cesium atoms and hydrogen bonds. The PO₃F tetrahedron (P8, O22, O23, O24, F8) is disordered around the P–F axis (Tab. 31). The three disordered oxygen atoms have two orientations with occupancies refined to 0.65(2) and 0.35(2) for the major and minor components, respectively. The asymmetric unit contains six Cs⁺ and four NH₄⁺ cations and two PO₃F²⁻ and six HPO₃F⁻ anions. Two types of hydrogen bonds, O–H···O and N–H···O, link the different structural units together to form a three-dimensional structure (Fig. 13b). Five of the six crystallographically independent cesium atoms are coordinated by twelve atoms (fluorine and oxygen). The cesium atom, Cs1, has an elevenfold coordination. The Cs–O and Cs–F distances range from 3.005(6) to 3.750(6) Å (Tab. A33).

Tab. 31 P–O and P–F bond lengths in Cs₃(NH₄)₂(HPO₃F)₃PO₃F (Å) for the PO₃F tetrahedra

d		d		d	
P7–O19	1.503(5)	P8–O22	1.49(1)	P8–O22A	1.50(2)
P7–O20	1.487(5)	P8–O23	1.43(1)	P8–O23A	1.53(2)
P7–O21	1.490(5)	P8–O24	1.52(1)	P8–O24A	1.49(1)
P7–F7	1.574(4)	P8–F8	1.544(5)		

Two different types of PO₃F tetrahedra are found in the structure for the eight crystallographically independent tetrahedra. The P–O bond lengths vary depending on the type of tetrahedron. The PO₃F tetrahedron of P7 with three short P–O bonds (average

length of 1.493 Å) and one long P–F bond (1.574(4) Å) is a PO₃F tetrahedron (Tab. 31). The bonding of the PO₃F tetrahedron of P8 with three short P–O lengths is difficult to discuss because of the higher esd's caused by tetrahedral disordering. All of the oxygen atoms of the two PO₃F tetrahedra were hydrogen acceptors (O_A) in O···O (Tab. 33) and N···O hydrogen bonds (Tab. A34).

Tab. 32 P–O and P–F bond lengths in Cs₃(NH₄)₂(HPO₃F)₃PO₃F (Å) for the HPO₃F tetrahedra

	d		d		d
P1–O1	1.482(5)	P2–O4	1.488(5)	P3–O7	1.481(5)
P1–O2	1.480(6)	P2–O5	1.480(6)	P3–O8	1.474(5)
P1–O3	1.544(5)	P2–O6	1.544(6)	P3–O9	1.559(5)
P1–F1	1.580(4)	P2–F2	1.571(5)	P3–F3	1.576(5)
P4–O10	1.486(5)	P5–O13	1.468(6)	P6–O16	1.473(6)
P4–O11	1.482(5)	P5–O14	1.477(5)	P6–O17	1.479(5)
P4–O12	1.551(5)	P5–O15	1.538(6)	P6–O18	1.547(6)
P4–F4	1.577(4)	P5–F5	1.559(6)	P6–F6	1.568(5)

The other six tetrahedra (Tab. 32) have only two short P–O_A bonds (average length: 1.479 Å) instead of three and are characterized as HPO₃F tetrahedra. The two oxygen atoms with short P–O_A lengths in the HPO₃F tetrahedra are hydrogen acceptors in the N–H···O hydrogen bonds. The third oxygen atom in each of these six HPO₃F tetrahedra has a long interatomic distance to P, which is between 1.538(6) and 1.559(5) Å (O3, O6, O9, O12, O15, and O18) with an average length of 1.547 Å. These oxygen atoms are protonated and participate in hydrogen bonding to the PO₃F tetrahedra as hydrogen donors (O_D) (Tab. 33). The P–F bonds range from 1.559(6) to 1.580(4) Å (Tab. 32).

Tab. 33 O–H···O hydrogen bonding in Cs₃(NH₄)₂(HPO₃F)₃PO₃F (Å, °)

	d(D–H)	d(H···A)	d(D···A)	∠D–H···A
O3–H1···O20	0.65(5)	1.88(4)	2.501(7)	162(6)
O6–H2···O22A	0.68(6)	1.88(5)	2.50(1)	140(10)
O6–H2···O22	0.68(6)	1.95(5)	2.47(2)	155(7)
O9–H3···O21	0.68(4)	1.88(4)	2.531(8)	176(7)
O12–H4···O19	0.7(1)	1.8(1)	2.503(7)	160(10)
O15–H5···O24	0.69(5)	1.88(7)	2.57(2)	150(10)
O15–H5···O24A	0.69(5)	1.70(7)	2.37(2)	156(5)
O18–H6···O23	0.69(7)	1.80(9)	2.44(1)	150(10)
O18–H6···O23A	0.69(7)	1.98(7)	2.67(2)	167(13)

A total of 22 O···O and N···O hydrogen bonds create an elaborate three-dimensional network in the structure (Fig. 13b). The O–H···O bonds are short with lengths between 2.44(1) and 2.67(2) Å and connect the HPO₃F tetrahedra to the PO₃F tetrahedra (Tab. 33). The N–H···O bonds (2.735(8)–2.86(2) Å; Tab. A34) then interlink these groups

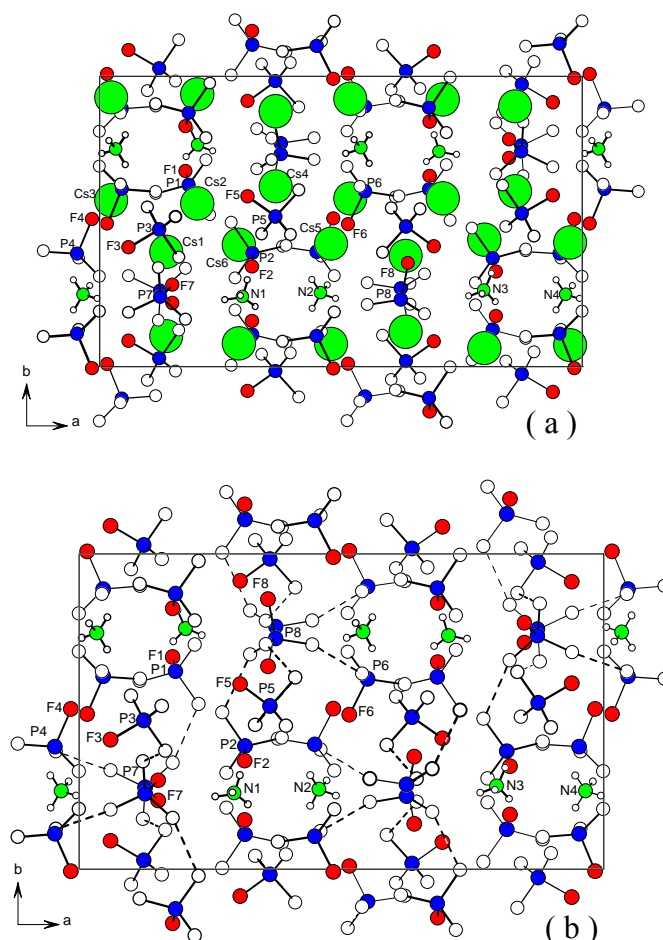


Fig. 13 Projection of the $\text{Cs}_3(\text{NH}_4)_2(\text{HPO}_3\text{F})_3(\text{PO}_3\text{F})$ structure along the c -axis. Only one orientation (major component) of the disordered P8 tetrahedron is shown. (a) The Cs atoms are large green circles; smaller green circles represent the N atoms. The hydrogen bonds are not shown for clarity. (b) The hydrogen-bonded layers of $(\text{NH}_4)_2\text{PO}_3\text{F}$ and HPO_3F -tetrahedra are shown in and around the ac -plane. The Cs atoms, H atoms, and $\text{N}-\text{H}\cdots\text{O}$ bonds are not shown for clarity. Dashed lines indicate the $\text{H}\cdots\text{O}$ bonds between the PO_3F and HPO_3F tetrahedra.

of HPO_3F and PO_3F tetrahedra; these bonds are not shown in Fig. 13b. In general, the structure of $\text{Cs}_3(\text{NH}_4)_2(\text{HPO}_3\text{F})_3(\text{PO}_3\text{F})$ can be considered as two sets of structural units: 2 NH_4^+ and PO_3F^{2-} (**I**) and Cs^+ and HPO_3F^- (**II**). The **I** units are found very close to the ac -plane at $y = 1/4$ and $3/4$, whereas the units of **II** are arranged between them around parallel planes at $y = 0$ and $1/2$ (Fig. 13b). For every complete set of **I**, there are three sets of **II**, thus the compound can be written as: $3\text{CsHPO}_3\text{F}\cdot(\text{NH}_4)_2\text{PO}_3\text{F}$. These layers, alternate in the b -direction and are linked together by hydrogen bonds. Each of the PO_3F -tetrahedra (**I**) is hydrogen-bonded to three HPO_3F tetrahedra of **II**. Taking the strongest interaction in the structure, $\text{O}-\text{H}\cdots\text{O}$, into consideration, the structure can also be characterized by thick, alternating layers parallel to the bc -plane shown in Fig. 13b. The thick layers running in the b -direction both have the composition of $3\text{CsHPO}_3\text{F}\cdot(\text{NH}_4)_2\text{PO}_3\text{F}$, but are

crystallographically different. The layer centered around $x = \frac{1}{2}$ consists of the disordered PO_3F tetrahedron of P8 hydrogen-bonded to the HPO_3F tetrahedra of P2, P5, and P6 with the N1, N2, and Cs4–6 atoms. The second layer at $x = 0$ includes the $(\text{H})\text{PO}_3\text{F}$ tetrahedra of P1, P3, P4, and P7, and the atoms, N3, N4, and Cs1–3. The layers have two different orientations for their three hydrogen bonds. Two of the hydrogen bonds on the PO_3F tetrahedron of P7 have a similar orientation to the *ac*-plane, whereas the third branches out to the other side of the PO_3F plane. The hydrogen bonds between the PO_3F tetrahedron of P8 and the HPO_3F units, on the other hand, are all directed to the same side of the plane. This is not affected by the disordering in the PO_3F tetrahedra of P8 except for a slight rotation of the bonds around the P–F bond.

4.6.2 $[\text{N}(\text{CH}_3)_4]\text{HPO}_3\text{F}\cdot\text{H}_2\text{O}$

The tetramethylammonium hydrogen monofluorophosphate monohydrate (Tab. A24) was found to contain the following crystallographically independent units: one HPO_3F tetrahedron, one molecule of crystal water, and one $[\text{NMe}_4]^+$ cation. Its structure (Fig. 14a and b) is quite unique due to its cubic symmetry. The phosphorus, fluorine, oxygen ($\text{O}_{\text{w}2}$ and $\text{O}_{\text{w}2\text{A}}$), nitrogen, and carbon (C1) atoms all have special positions on the crystallographic C_3 axis (Fig. 14a). The threefold symmetry in the structure is shown in Fig. 14b looking down the crystallographic C_3 axis. Disordered oxygen and hydrogen positions were observed for both the PO_3F tetrahedron and the molecule of crystal water. The tetrahedron was disordered around the P–F axis with two orientations. The occupancies of the major and minor components were refined to 0.888(4) and 0.112(4), respectively ($\text{O}1$ and $\text{O}1\text{A}$). The position of the oxygen atom of the crystal water, $\text{O}_{\text{w}2}$, was also disordered with the same occupancies for the major and minor components. The hydrogen positions given represent the corresponding hydrogen atom, H5A or H5B, for the major orientation of the oxygen atom, $\text{O}1$ or $\text{O}_{\text{w}2}$, respectively. The minor components of the hydrogen atom positions were neglected. Only the major component of the disordered oxygen and hydrogen positions is discussed and shown in Fig. 14a and b.

The $[\text{NMe}_4]^+$ cation contains two different N–C bonds with lengths of 1.496(3) and 1.493(1) Å (Tab. 34) with an average C–H distance of 0.945 Å. The HPO_3F tetrahedron has one short P–O length of 1.500(1) Å ($\text{O}1$) and one long P–F bond with a distance of 1.563(1) Å.

Tab. 34 Bond lengths in $[\text{N}(\text{CH}_3)_4]\text{HPO}_3\text{F}\cdot\text{H}_2\text{O}$ (Å)

	d		d	
P–O1	1.500(1)	C1–H1	0.94(2)	
P–F	1.563(1)	C2–H2	0.96(2)	
P–O1A	1.485(8)	C2–H3	0.93(2)	
N–C1	1.496(3)	C2–H4	0.95(2)	
N–C2	1.493(1)	O1A–H5A	1.07(9)	
		O _w 2A–H5B	0.92(3)	

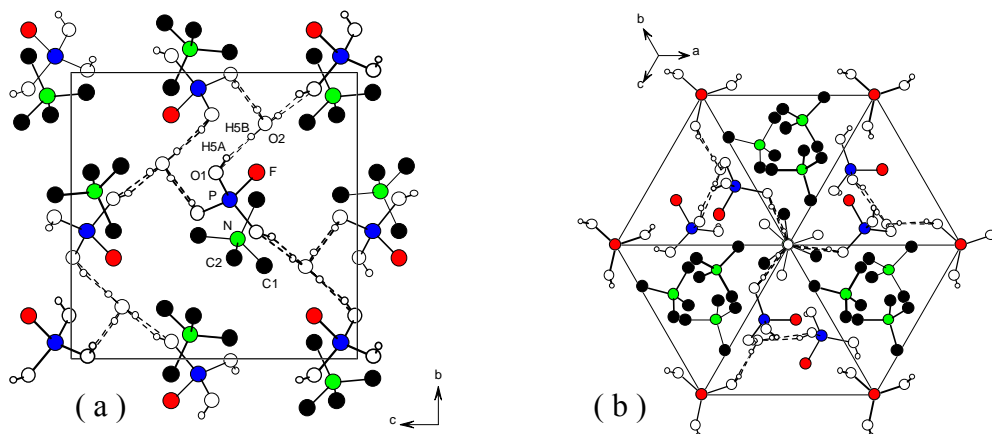


Fig. 14 Structure of $[\text{N}(\text{CH}_3)_4]\text{HPO}_3\text{F}\cdot\text{H}_2\text{O}$ (a) Ball-and-stick representation of the HPO_3F tetrahedra with the molecule of crystal water and $[\text{NMe}_4]^+$ ions viewed along the a -axis. The minor component of the oxygen positions of the PO_3F tetrahedron and crystal water is not shown. The $\text{H}\cdots\text{O}$ bonds are indicated by dashed lines. (b) View looking down the crystallographic C_3 axis. The molecule of crystal water, $[\text{NMe}_4]^+$ cation, and HPO_3F^- anion are centered on this axis.

The hydrogen bond system consists of one disordered hydrogen bond between the molecule of crystal water and the disordered oxygen atom on phosphorus. The hydrogen bond, $\text{O1}–\text{H5A}\cdots\text{O}_{\text{w}2}$ and $\text{O}_{\text{w}2}–\text{H5B}\cdots\text{O1}$, has an $\text{O}\cdots\text{O}$ distance of 2.637(2) Å. (Tab. 35). Shorter $\text{O}\cdots\text{O}$ distances of 2.551(2) and 2.499(8) Å are observed between these H donor oxygen atoms and the minor components of the disordered oxygen atoms. Each molecule of crystal water is hydrogen-bonded to three equivalent HPO_3F tetrahedra (Fig. 14a).

Tab. 35 Hydrogen bonding in $[\text{N}(\text{CH}_3)_4]\text{HPO}_3\text{F}\cdot\text{H}_2\text{O}$ (Å, °)

D–H \cdots A	d(D–H)	d(H \cdots A)	d(D \cdots A)	$\angle\text{D–H}\cdots\text{A}$
$\text{O1}–\text{H5A}\cdots\text{O}_{\text{w}2}$	0.65(9)	2.02(9)	2.637(2)	160(11)
$\text{O}_{\text{w}2}–\text{H5B}\cdots\text{O1}$	0.70(3)	1.94(3)	2.637(2)	174(3)

4.6.3 Na₂PO₃F·10H₂O

The Na₂PO₃F·10H₂O structure [81] (Tab. A25, Fig. 15a and b) contains the following crystallographically independent atoms and units: two Na atoms, one PO₃F tetrahedron, and ten molecules of water. Eight of the ten O_w atoms participate in the octahedral coordination of the Na atoms. The two alternating NaO₆ octahedra are linked together by edge-sharing (O_w6–O_w7 and O_w8–O_w9) to form chains parallel to the *c*-axis. The Na–O bond lengths range from 2.380(1) to 2.473(1) Å (Tab. 36). The PO₃F-tetrahedron has three short P–O bonds with an average length of 1.508 Å and one long P–F bond (1.6082(9) Å) typical for bonding in a PO₃F tetrahedron.

Tab. 36 Bond lengths in Na₂PO₃F·10H₂O (Å)

	d		d		d
Na1–O _w 5	2.380(1)	Na2–O _w 6	2.373(1)	P–O1	1.5130(9)
Na1–O _w 8	2.398(1)	Na2–O _w 8	2.400(1)	P–O2	1.5069(9)
Na1–O _w 6	2.433(1)	Na2–O _w 11	2.426(1)	P–O3	1.505(1)
Na1–O _w 4	2.445(1)	Na2–O _w 7	2.439(1)	P–F	1.6082(9)
Na1–O _w 7	2.450(1)	Na2–O _w 9	2.440(1)		
Na1–O _w 9	2.473(1)	Na2–O _w 10	2.464(1)		

Tab. 37 Hydrogen bonding in Na₂PO₃F·10H₂O (Å, °)

D–H...A	d(D–H)	d(H...A)	d(D...A)	∠D–H...A
O _w 4–H4A...O1	0.76(2)	2.26(2)	3.023(2)	177(2)
O _w 4–H4B...O _w 10	0.78(2)	2.03(2)	2.790(2)	163(2)
O _w 5–H5A...O3	0.83(2)	1.90(2)	2.727(1)	174(2)
O _w 5–H5B...O _w 11	0.85(3)	1.95(3)	2.790(2)	170(2)
O _w 5–H5C...O _w 11	0.79(7)	1.98(7)	2.771(2)	171(5)
O _w 6–H6A...O2	0.83(2)	1.93(2)	2.753(1)	173(2)
O _w 6–H6B...O _w 13	0.82(2)	2.03(2)	2.827(2)	165(2)
O _w 7–H7A...O3	0.83(3)	2.14(3)	2.952(2)	168(2)
O _w 7–H7B...O _w 12	0.82(2)	2.03(2)	2.851(1)	177(2)
O _w 8–H8A...O2	0.80(2)	1.99(2)	2.767(2)	167(2)
O _w 8–H8B...O _w 12	0.85(2)	1.94(2)	2.783(2)	175(2)
O _w 9–H9A...F	0.79(2)	2.21(2)	3.003(2)	176(2)
O _w 9–H9B...O _w 13	0.81(2)	2.03(2)	2.841(2)	176(2)
O _w 10–H10A...O2	0.82(2)	1.99(2)	2.793(2)	164(2)
O _w 10–H10B...O _w 4	0.80(3)	2.07(2)	2.836(2)	162(2)
O _w 11–H11A...O1	0.78(2)	2.16(2)	2.927(2)	167(2)
O _w 11–H11B...O _w 5	0.83(4)	1.96(4)	2.771(2)	163(2)
O _w 11–H11C...O _w 5	1.05(6)	1.84(6)	2.790(2)	149(5)
O _w 12–H12A...O1	0.87(2)	1.94(2)	2.802(2)	174(2)
O _w 12–H12B...O3	0.80(2)	1.97(2)	2.760(2)	175(2)
O _w 13–H13A...F	0.83(2)	1.90(2)	2.837(2)	172(2)
O _w 13–H13B...O1	0.84(2)	2.08(2)	2.718(2)	149(2)

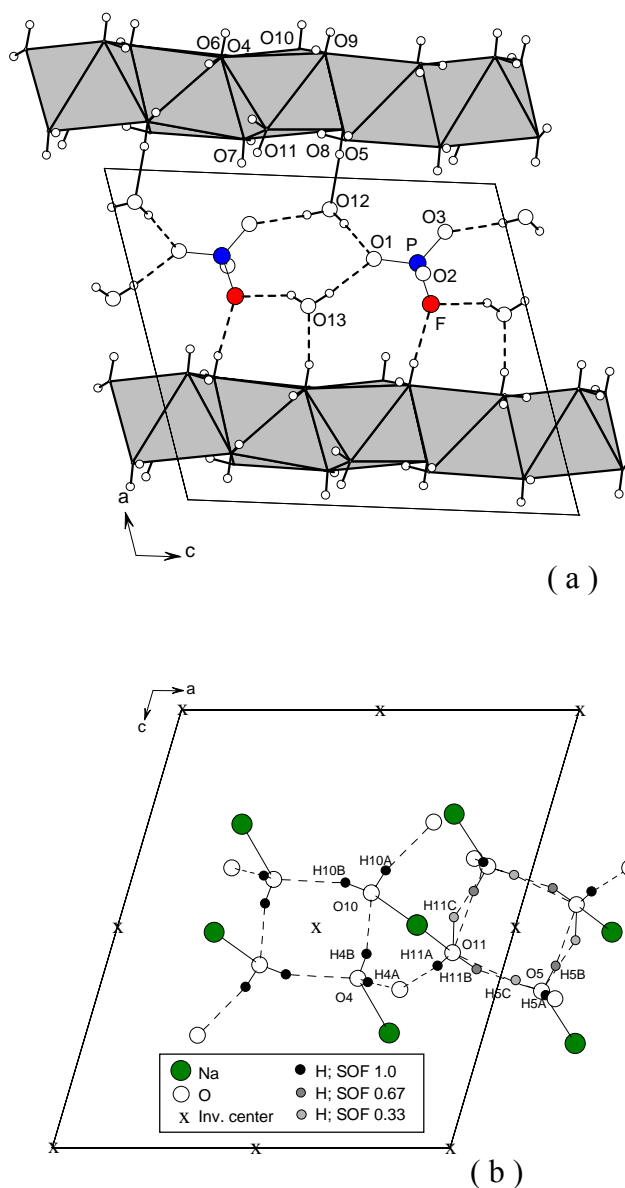


Fig. 15 Structure of $\text{Na}_2\text{PO}_3\text{F} \cdot 10\text{H}_2\text{O}$ (a) View of one layer along the b -axis. The chains of NaO_6 and connected PO_3F tetrahedra run along the c -axis. Only the hydrogen bonds, $\text{O}_w\text{-H}\cdots\text{F}$, and the $\text{O}_w\text{-H}\cdots\text{O}$ bonds between the PO_3F tetrahedra and the $\text{O}_{w12}/\text{O}_{w13}$ molecules are shown. (b) Projection of the two tetramers along the b -axis. The hydrogen bonds and anchoring bonds to the Na and O1 – O3 atoms are shown with the indicated centers of symmetry.

The elaborate system of 20 hydrogen bonds, $\text{O}_w\text{-H}\cdots\text{O}_{(w)}$ and $\text{O}_w\text{-H}\cdots\text{F}$, forms a three-dimensional network with hydrogen atoms supplied by the molecules of crystal water. The hydrogen bonds have lengths between 2.718(2) and 3.023(2) Å (Tab. 37). The acceptor O atoms of the PO_3F -tetrahedron, namely O1, O2, and O3, are hydrogen-bonded to 3, 3, and 4 molecules of crystal water, respectively (Tab. 37). The F atom only participates in two hydrogen bonds to O_{w9} and O_{w13} . The eight water molecules, $\text{O}_{w4}\text{--O}_{w11}$, are hydrogen-

bonded to one of the O/F atoms in the tetrahedron and one O_w atom. The O_w12 and O_w13 water molecules, which are not involved in the Na coordination, connect two PO₃F tetrahedra to each other parallel to the *c*-axis (Fig. 15a). The cyclic tetramers are formed by water molecules, O_w4 with O_w10 and O_w5 with O_w11 via hydrogen bonding around the centers of symmetry at ($\frac{1}{2}$, $\frac{1}{2}$, $\frac{1}{2}$) and (0, 0, $\frac{1}{2}$) (Fig. 15b). The hydrogen bonds, O_w4–H4B···O_w10 and O_w10–H10B···O_w4, form one tetramer. In the second tetramer between O_w5 and O_w11, two disordered hydrogen bonds connect the water molecules to each other. The relative occupancies for the disordered hydrogen positions were refined to values of 0.67 for H5B and H11B and 0.33 for H5C and H11C and then fixed. The disordered bonds are O_w5–H5B···O_w11 and O_w11–H11B···O_w5 with the minor components H11C and H5C, respectively (Fig. 15b). Both hydrogen-bonded ring systems are fixed in the structure by bonds to Na atoms and O atoms of the PO₃F-tetrahedra.

4.6.4 Na₅[N(CH₃)₄](PO₃F)₃·18H₂O

The triclinic structure of sodium tetramethylammonium monofluorophosphate (Tab. A26 and A27) with 18 molecules of crystal water is composed of an elaborate three-dimensional network of O–H···O hydrogen bonds, which forms channels along the *a*-axis for the [NMe₄]⁺ cations (Fig. 16a and b). The asymmetric unit contains five Na atoms, one [NMe₄]⁺ cation, three PO₃F²⁻ anions, and the molecules of crystal water. The hydrogen positions of the methyl groups were calculated. The compound is a basic salt with O_w–H···O_(w) hydrogen bonds. The Na atoms are octahedrally coordinated solely by oxygen atoms to form trimeric units of [Na₃O₁₃] and isolated dimeric units of [Na₂O₈]. Na–O distances range from 2.283(2) to 2.674(2) Å except for the bond Na5–O_w13 with a length of 2.801(2) Å (Tab. A35). Average Na–O distances (Tab. 38) are comparable for all five of the NaO₆ octahedra despite the short Na5–O_w25 and long Na5–O_w13 bonds.

Tab. 38 Avg. Na–O bond lengths in Na₅[N(CH₃)₄](PO₃F)₃·18H₂O (Å)

	d
Na1	2.449
Na2	2.404
Na3	2.446
Na4	2.441
Na5	2.447

The [Na₃O₁₃] units in the structure build up infinite chains with the three NaO₆ octahedra, Na1, Na2, and Na3, running in the *b*-direction at *z* = $\frac{1}{2}$. The Na1 and Na3 octahedra are

connected to equivalent octahedra by edge-sharing on centers of symmetry with the oxygen atoms, O16/O16' (for Na1) and O28/O28' (for Na3) (Fig. 16a). The third NaO₆ octahedron, Na2, connects these Na1 and Na3 "dimers" to each other by face-sharing. The faces are defined by the oxygen atoms: O18, O12, O19 for Na1 and O14, O17, O19 for Na3. The second unit of Na atoms, [Na₂O₈], is somewhat questionable based on the vertex-sharing involving four common atoms (O13, O23, O24, O26). This unit consists of the Na4 and Na5 octahedra, which are linked by oxygen atoms to one another to form isolated dimers located around the center of symmetry at ($\frac{1}{2}$, $\frac{1}{2}$, 0) (Fig. 16a). The Na–Na interatomic distance in these dimers is 3.272 Å. One of the four atoms shared is that of the oxygen atom, O_w13, which has an exceptionally long distance to Na5 (2.801(2) Å) compared to the other structures with NaO₆ units. The NaO₆ octahedron of Na5 also has the shortest Na–O distance in the structure: 2.283(2) Å for Na5–O_w25. An interesting feature of this NaO₆ octahedron is that one of the PO₃F oxygen atoms, O4, is involved in the Na coordination (Fig. 16a), while one of the molecules of crystal water, O_w15, does not participate in the metal coordination.

The [NMe₄]⁺ cation (Fig. 16b) has N–C bonds with distances between 1.494(4) and 1.506(3) Å and a calculated C–H bond length of 0.98 Å for the methyl groups (Tab. A35). The three PO₃F tetrahedra each have three short P–O_A distances between 1.498(2) and 1.518(2) Å with an average length of 1.509 Å (Tab. 39). These distances correspond to a PO₃F tetrahedron, in which all of the oxygen atoms are hydrogen acceptors in the hydrogen bond system. Two different interatomic distances of 1.580(2) and 1.599(2) are found between the P and F atoms in the structure. The long P–F bond (1.599(1) Å) explains the significantly shorter P–O1 length of 1.498(2) Å in the PO₃F tetrahedron of P1.

Tab. 39 P–O and P–F bond lengths in Na₅[N(CH₃)₄](PO₃F)₃·18H₂O (Å)

	d		d		d
P1–O1	1.498(2)	P2–O4	1.507(2)	P3–O7	1.505(2)
P1–O2	1.504(2)	P2–O5	1.510(2)	P3–O8	1.508(2)
P1–O3	1.517(2)	P2–O6	1.512(2)	P3–O9	1.518(2)
P1–F1	1.599(2)	P2–F2	1.580(2)	P3–F3	1.580(2)

The hydrogen bond system of predominantly longer O–H \cdots O bonds (Tab. A36, Fig. 16b) creates a complicated three-dimensional network with channels for the [NMe₄]⁺ cations. The O_w–H \cdots O_(w) hydrogen bonds have O \cdots O distances ranging from 2.706(3) to 2.988(3) Å with an exceptionally short bond, O_w27–H27A \cdots O3: O \cdots O distance of 2.677(3) Å. Two hydrogen atoms, H19B and H26A, are not involved in hydrogen bonds. The oxygen atoms,

O_A , from the PO_3F tetrahedra except for O4 and O8 participate in 2–3 hydrogen bonds. The O4 atom is not only involved in two hydrogen bonds, but also bonded to the Na5 atom; the oxygen atom, O8, is a fourfold hydrogen acceptor. The water molecules, O_w11 , O_w13 , and O_w20 – O_w22 , are both hydrogen donors and acceptors and coordinate the Na^+ cations. The O_w15 atom functions as an hydrogen acceptor and donor in four hydrogen bonds, but does not coordinate a Na atom. All of the other O_w atoms coordinate the Na^+ ions and act exclusively as hydrogen donors in the structure.

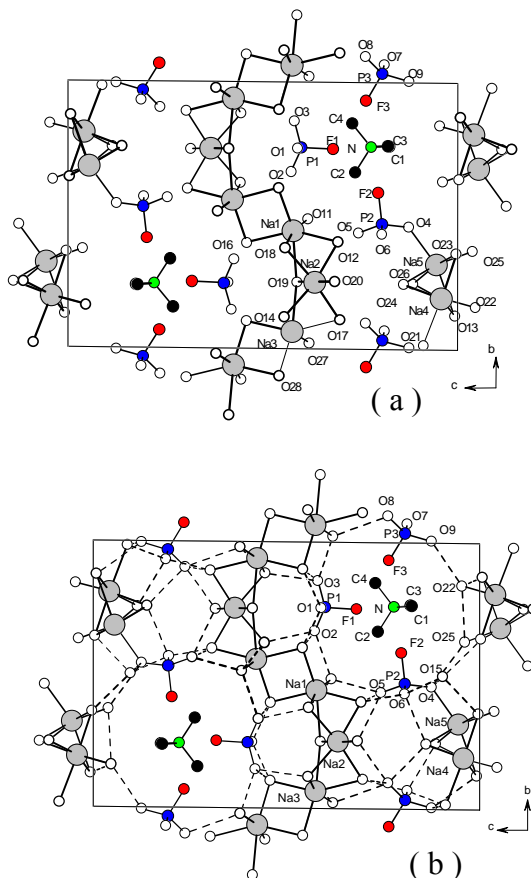


Fig. 16 Structure of $Na_5[N(CH_3)_4](PO_3F)_3 \cdot 18H_2O$ (a) Ball-and-stick representation along the a -axis. The infinite chains of $[Na_3O_{13}]$ are shown running in the b -direction with the isolated dimers $[Na_2O_8]$. The hydrogen atoms were omitted and hydrogen bonds are not shown for clarity. The Na atoms are gray. (b) $O_w \cdots O_w$ hydrogen bonding indicated by dashed lines. The organic cations are seen in the channels at $(x, 1/4, 3/4)$ and $(x, 3/4, 1/4)$. The hydrogen atoms have been omitted for clarity.

The most interesting feature of this structure is the formation of channels at $(x, 1/4, 1/4)$ and $(x, 3/4, 3/4)$ (Fig. 16b) for the $[NMe_4]^+$ cations. These channels are formed by the NaO_6 octahedra and the PO_3F tetrahedra connected indirectly to each other via hydrogen bonds (a) to crystal water. The channels can be characterized by the P–F vertex of the three PO_3F tetrahedra directed towards the organic cation. The other three oxygen vertices face outwards to participate in the hydrogen bonding. The size of the channel can be estimated

by the F...O and F...F interatomic distances, 5.47 for F1...O22, 5.75 for F1...O25, 3.171 for F1...F2, 2.96 for F1...F3, and 4.70 Å for F2...F3, not considering the covalent radii. Fluorine's nonparticipation in hydrogen bonding is very well demonstrated by this structure.

4.6.5 $[\text{C}(\text{NH}_2)_3]_2\text{PO}_3\text{F}$

The guanidinium monofluorophosphate structure with the space group *Cm* (Tab. A28) consists of PO_3F tetrahedra hydrogen-bonded to the guanidinium cations via N–H...O bonds. The asymmetric unit consists of three $[\text{C}(\text{NH}_2)_3]^+$ cations and two PO_3F^{2-} anions (Fig. 17a and b). The atoms: P1, P2, F1, F2, C1, C2, O1, O3, N2 and N3, all have special positions on the mirror plane.

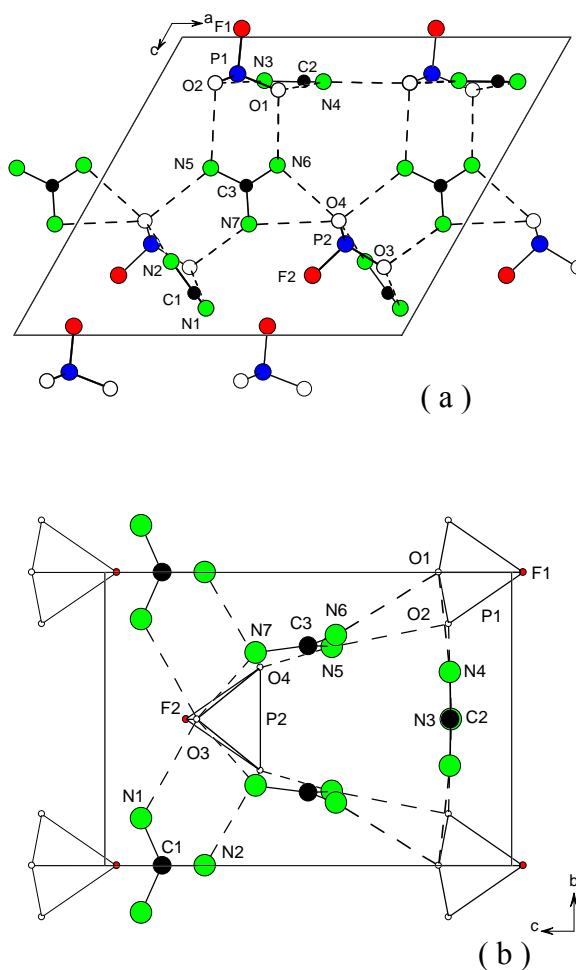


Fig. 17 Structure of $[\text{C}(\text{NH}_2)_3]_2\text{PO}_3\text{F}$ (a) Ball-and-stick representation looking down the *b*-axis. Dashed lines indicate the H...O hydrogen bonds. The hydrogen atoms have been omitted for clarity. (b) Polyhedral representation of the HPO_3F tetrahedra along the *a*-axis showing the P–F bond orientation relative to the hydrogen bonds.

The guanidinium cations have C–N distances between 1.310(7) and 1.334(4) Å with an average length of 1.324 Å (Tab. 40). The N–H bond lengths had an average distance of 0.86 Å (Tab. 41). Short P–O bonds with similar lengths were found in each PO₃F tetrahedra: 1.505(3) and 1.509(2) for the P1 tetrahedra and 1.504(2) Å for the P2 tetrahedra. In comparison with the P–O bonds, the distance between P and F vary between the tetrahedra with lengths of 1.575(3) and 1.567(3) Å.

Tab. 40 Bond lengths in [C(NH₂)₃]₂PO₃F (Å)

d		d		d		d		d	
P1–O1	1.505(3)	P2–O3	1.504(4)	C1–N1	1.334(4)	C2–N4	1.330(4)	C3–N7	1.324(5)
P1–O2	1.509(2)	P2–O4	1.504(2)	C1–N2	1.310(7)	C3–N5	1.326(5)		
P1–F1	1.575(3)	P2–F2	1.567(3)	C2–N3	1.327(7)	C3–N6	1.318(5)		

The hydrogen bond system of N–H⋯O bridges is somewhat complicated, because of the three different guanidinium cations in the structure. Long N–H⋯O bonds with N⋯O distances between 2.820(4) and 3.128(4) Å connect the PO₃F tetrahedra to the guanidinium cations (Tab. 41, Fig. 17a). These N⋯O bridges build up a three-dimensional network of hydrogen bonds (Fig. 17b). The direction of the P–F axis in the PO₃F tetrahedra of P1 is quite easy to recognize. Here, the bond is pointed directly towards the carbon atom of the C1 guanidinium cation where no hydrogen bonds are found (Fig. 17b). The P–F bond in the PO₃F tetrahedra of P2 lies between the hydrogen bonds, O3⋯N1 and O3⋯N7 as shown in Fig. 17b.

Tab. 41 Hydrogen bonding in [C(NH₂)₃]₂PO₃F (Å, °)

D–H⋯A	d(D–H)	d(H⋯A)	d(D⋯A)	∠D–H⋯A
N1–H1A⋯O3	0.86(2)	2.06(2)	2.911(4)	175(4)
N1–H1B⋯O2	0.84(2)	2.24(3)	2.989(4)	148(4)
N2–H2⋯O4	0.87(2)	2.02(2)	2.884(3)	175(4)
N3–H3⋯O2	0.86(2)	2.07(2)	2.914(4)	166(4)
N4–H4A⋯O2	0.90(4)	2.05(4)	2.920(4)	162(4)
N4–H4B⋯O1	0.85(2)	2.10(2)	2.942(4)	171(5)
N5–H5A⋯O2	0.85(2)	2.19(3)	2.978(4)	155(5)
N5–H5B⋯O4	0.86(2)	2.10(2)	2.949(4)	168(4)
N6–H6A⋯O1	0.87(7)	2.18(7)	3.000(5)	158(6)
N6–H6B⋯O4	0.87(2)	1.96(2)	2.820(4)	169(4)
N7–H7A⋯O3	0.86(2)	2.18(2)	3.007(5)	163(5)
N7–H7B⋯O4	0.86(2)	2.37(3)	3.128(4)	148(4)

4.7 The Structure of β-RbHPO₃F

The structural clarification of β-RbHPO₃F has been somewhat problematic. A first single crystal X-ray diffraction measurement yielded a basic structural model for the *P*2₁/*n* space

group with a R_I -factor over 5%. One disordered hydrogen position was found between two equivalent oxygen atoms with an occupancy of 0.5. A lower R_I -factor of 3.64% was achieved by a second measurement; however, the second hydrogen atom could not be found.

^{19}F , ^{31}P , and ^1H MAS NMR spectra showed two separate signals for the F, P, and H nuclei with signal ratios of 3:7, 4:6, and 3:7, respectively (Appendix A.4). Two doublets in both the ^{19}F and ^{31}P spectra confirmed the presence of two nonequivalent PO_3F tetrahedra in the structure. A singlet at 0.7 ppm with an area of 5% was also found in the ^{31}P spectrum for the phosphate impurity. The ^1H spectrum showed one broad signal at 13.0 ppm for a hydrogen atom involved in a strong hydrogen bond (60-70%) and one sharp signal at 5.9 ppm for a weakly bonded hydrogen atom (30-40%). The ^1H signal ratio of ca. 2:1 correlated with that of phosphorus. Based on these results showing two nonequivalent PO_3F tetrahedra, the single crystal data was then solved and refined for the noncentrosymmetric space groups, Pn and $P2_1$. Both refinements included strong correlations of the heavier atoms and difficulties were encountered when the displacement parameters were refined anisotropically. Thus, the centrosymmetric space group was assumed to be correct. The different P and F surroundings found by the MAS NMR measurements can most likely be explained by a statistical O/F disordering of the O3 and F positions on phosphorus, which generates two different phosphorus tetrahedra. Second harmonic generation measurements could help determine whether the structure is centrosymmetric or noncentrosymmetric, but could not be carried out within the scope of this thesis.

Tab. 42 Selected crystallographic data

Formula	$\beta\text{-RbHPO}_3\text{F}$
Formula weight	184.45
Crystal system	<i>Monoclinic</i>
Space group	$P2_1/n$
Crystal Size	0.2 x 0.2 x 0.2
$a/\text{\AA}$	7.5157(8)
$b/\text{\AA}$	7.7244(7)
$c/\text{\AA}$	7.5582(8)
$\beta/^\circ$	104.29(1)
$V/\text{\AA}^3, Z$	425.21(7), 4
$\rho_{\text{calc.}}/\text{gcm}^{-3}$	2.877
$R_I [I > 2\sigma(I)]$	0.0352
Analysis	
F (50 mL H_2O)	0.5
F (Seel)	9.3
F (calcd)	10.30
V_F	1.07

Thus, the $P2_1/n$ structure was refined further with an O/F disorder in both the F and O3 positions on phosphorus based on the NMR measurements and implied by the almost identical bond lengths of 1.539(4) (P–O3) and 1.540(5) Å (P–F). The relative occupancies for these positions were refined and fixed as 0.7 and 0.3 for O3/F (major component) and FA/O3A (minor component), respectively, which correspond to the signal ratios found in the MAS NMR spectra. The R_I -factor decreased to 3.52% (Tab. 42 and A8). A short distance was found between the O3 and F positions.

The structure of β -RbHPO₃F (Tab. A29, Fig. 18) has one unique Rb atom and one HPO₃F tetrahedron. The Rb atom has an eightfold coordination with bonds to seven oxygen atoms and one fluorine atom. Distances range from 2.868(4) to 3.358(4) Å (Tab. 43). The HPO₃F tetrahedron has a P–F distance that strongly deviates from those in the structures described previously (Tab. 43). The bond between the P and O1 atoms has a length of 1.485(4) Å, typical for oxygen atoms only participating in the metal coordination in the structure. The exact functions of the other O atoms in the structure is more difficult to define. The P–OH_{1/2} bond (O2) has a length of 1.513(4) Å. This atom, O2, is involved in the only hydrogen bond found in the structure with a disordered hydrogen position (occupancy 0.5) as a hydrogen acceptor and donor ($\frac{1}{2}A + \frac{1}{2}D$). The other positions on phosphorus, O3/FA and F/O3A, have almost identical interatomic distances to the P atom of 1.538(4) and 1.541(4) Å, respectively. These distances are relatively long for a P–O bond and very short for a P–F bond, when compared to the other structures. This is probably due to the O/F disorder.

Tab. 43 Bond lengths in β -RbHPO₃F (Å)

	d		d		d
Rb–O1	2.868(4)	Rb–O2	3.049(4)	P–O1	1.485(4)
Rb–O1′	2.882(4)	Rb–O3′/FA′	3.054(4)	P–O2	1.513(4)
Rb–O1′′	2.966(4)	Rb–O2′	3.154(4)	P–O3/FA	1.538(4)
Rb–O3/FA	2.973(4)	Rb–F/O3A	3.358(4)	P–F/O3A	1.541(4)

The hydrogen bond system (Tab. 44) consists of one short, symmetrically-disordered hydrogen bond between two equivalent HPO₃F tetrahedra. An O2⋯O2′ distance of 2.560(8) Å was found. A second hydrogen bond between the O3/FA and F/O3A positions of two HPO₃F tetrahedra is implied by the short distance between these two positions shown by the red dashed lines in Fig. 18. The O3/FA and F/O3A positions have a distance of 2.672(6) Å with the following angles: $\angle PFO3 = 115.9(2)^\circ$ and $\angle PO3F = 130.9(2)^\circ$. These values strongly indicate a hydrogen bond, yet a hydrogen atom could not be found. Thus, a new type of structure is formed that has not been observed for either the metal

hydrogen phosphates or the pure monofluorophosphates.

Tab. 44 Hydrogen bonding in β -RbHPO₃F (Å, °)

D–H...A	d(D–H)	d(H...A)	d(D...A)	∠D–H...A
O2–H...O2'	0.75(2)	1.84(6)	2.560(8)	160(20)
O3...F			2.672(6)	

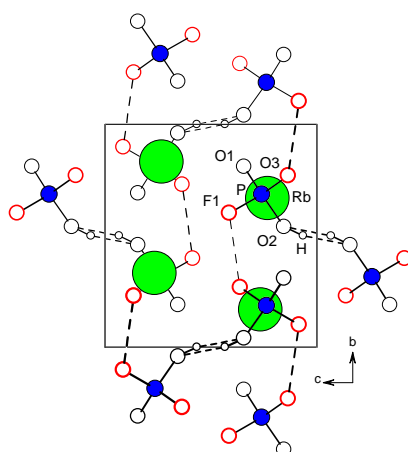


Fig. 18 View of the structure of β -RbHPO₃F looking down the a -axis. The black dashed lines indicate the symmetrically-disordered H...O bond between H and O2'. The implied hydrogen bond between the O3/FA and the F/O3A positions (indicated by the red-outlined open circles) is shown with red dashed lines. The Rb atoms are green.

4.8 Summary

The crystal structures of the hydrogen monofluorophosphates and basic monofluorophosphates were determined for the alkali metal and N-containing cations. The structures vary in their structural features, but have similarities in their bonding overall, which are summarized here.

Infinite chains of hydrogen-bonded HPO₃F tetrahedra (Sect. 4.1) are found in the structures of NaHPO₃F·2.5H₂O (Na), [NH₂Et₂][HPO₃F], and [PipzH₂][HPO₃F]. The zigzag chains are held together by longer hydrogen bonds, O_w–H...O_(w) (Na) and N–H...O (Diet and Pipz). The sodium atom is octahedrally coordinated solely with oxygen atoms to form chains of NaO₆ octahedra. In all three structures, the P–F vertex of the tetrahedron is pointed away from the hydrogen bond system.

The potassium compounds feature unique structural patterns of branched chains in KHPO₃F and isolated dimers in K₃[H(PO₃F)₂] (Sect. 4.2 and 4.3). In KHPO₃F, three different, short and very short O–H...O bonds form chains of HPO₃F tetrahedra with a

short O–H \cdots O bond between the chain and the branched tetrahedron. The isolated dimers in $K_3[H(PO_3F)_2]$ are made up of two equivalent PO_3F tetrahedra bonded to each other via a strong, symmetrically-disordered O–H \cdots O bond. The potassium cations have a 7–9 coordination with both oxygen and fluorine atoms.

In comparison to the structural patterns in the potassium structures, structures with cyclic dimers (Sect. 4.4) have been found in numerous compounds with Cs, $[NEt_3]$, $[C(NH_2)_3]$, and $[N,N'\text{-dmu}]$ as cations. Short O–H \cdots O hydrogen bonds link the HPO_3F tetrahedra to dimers; disordered hydrogen positions are only observed in $CsHPO_3F$ and $[NH_4]HPO_3F$. The HPO_3F dimers are then fixed by the Cs coordination in $CsHPO_3F$ and longer N–H \cdots O bonds in the other structures. The Cs atom is coordinated by O and F atoms. In the structures with N-containing cations, the P–F bond is pointed either between layers of cations in $[NH_4]HPO_3F$ or towards the inert part of the cation: the C atom in $[C(NH_2)_3]HPO_3F$ or a methyl group in $[N,N'\text{-dmuH}]HPO_3F$.

The α and β -modifications of NH_4 and the structure of α - $RbHPO_3F$ isotypic to α - NH_4HPO_3F are made up of cyclic tetramers (Sect. 4.5). These tetramers are defined by two unique HPO_3F tetrahedra connected alternately to tetramers with two short, unique O–H \cdots O bonds. The tetrameric units are bonded to each other in the structure by either longer N–H \cdots O or Rb–X bonds. The Rb^+ ion has a nine-fold coordination with O and F atoms.

The complex structures described in Sect. 4.6 feature structural aspects not observed in the hydrogen monofluorophosphates with the composition, $MHPO_3F$. In the $Cs_3(NH_4)_2(HPO_3F)_3(PO_3F)$, tetrahedra of PO_3F and HPO_3F are found with short O–H \cdots O bonds linking them together. The hydrate structures, $[N(CH_3)_4]HPO_3F \cdot H_2O$, $Na_2PO_3F \cdot 10H_2O$, and $Na_5[N(CH_3)_4](PO_3F)_3 \cdot 18H_2O$, vary as much in their compositions as in their systems of hydrogen bonds. A hydrogen bond with a disordered hydrogen position is found between the HPO_3F tetrahedra and the O_w atom in $[NMe_4]HPO_3F \cdot H_2O$. In the $Na_2PO_3F \cdot 10H_2O$ structure with $O_w\text{--}H\cdots O_{(w)}$ bonds, the fluorine atom acts as a two-fold hydrogen acceptor in long $O_w\text{--}H\cdots F$ bonds. Both of these bonds have lengths similar to those found for the weaker N–H \cdots O and $O_w\text{--}H\cdots O_{(w)}$ hydrogen bonds. The elaborate hydrogen bond system in the structure of the mixed salt, $Na_5[NMe_4](PO_3F)_3 \cdot 18H_2O$, forms channels for the $[NMe_4]^+$ ions with the P–F bond directed towards the inert C atom of the cation. The structure of $[C(NH_2)_3]_2PO_3F$ is rather asymmetrical with two nonequivalent PO_3F tetrahedra hydrogen-bonded to three $[C(NH_2)_3]^+$ ions with longer N–H \cdots O bonds.

The β -modification of RbHPO_3F is the only structure found with O/F disordering. Here, one symmetrically-disordered hydrogen bond held two equivalent PO_3F tetrahedra together. A suspiciously short distance is observed between the O/F disordered position on phosphorus, but the corresponding hydrogen atom could not be located.

In general, three types of hydrogen bonding are found in the structures. Short and very short hydrogen bonds link the $(\text{H})\text{PO}_3\text{F}$ tetrahedra to one another, while longer hydrogen bonds are found between the $(\text{H})\text{PO}_3\text{F}$ tetrahedra and the crystal water or cations containing nitrogen. Hydrogen bonds with lengths in between are found for a $\text{N}-\text{H}\cdots\text{O}$ bond in $[\text{PipzH}_2]\text{HPO}_3\text{F}$ and $[\text{NHET}_3]\text{HPO}_3\text{F}$ and $\text{O}_w-\text{H}\cdots\text{O}$ and $\text{O}_w-\text{H}\cdots\text{O}_w$ bonds in $\text{Na}/[\text{NMe}_4]$, $\text{Na}_2\text{PO}_3\text{F}\cdot 10\text{H}_2\text{O}$, and $[\text{NMe}_4]\text{HPO}_3\text{F}\cdot\text{H}_2\text{O}$. Fluorine is involved in two hydrogen bonds in the $\text{Na}_2\text{PO}_3\text{F}\cdot 10\text{H}_2\text{O}$ structure as a hydrogen acceptor. This is not observed in any other structure. In several structures, single hydrogen atoms do not participate in the hydrogen bond system: two hydrogen atoms in $[\text{C}(\text{NH}_2)_3]\text{HPO}_3\text{F}$ and $\text{Na}_5[\text{N}(\text{CH}_3)_4](\text{PO}_3\text{F})_3\cdot 18\text{H}_2\text{O}$ and one hydrogen atom in the $\alpha\text{-NH}_4\text{HPO}_3\text{F}$.

The total calculated bond valency of fluorine, V_F , varies in the compounds. The V_F values are between 0.94 and 0.97 for the structures with N-containing cations in comparison to the alkali metal structures, in which V_F is 0.91 for $\text{Na}_2\text{PO}_3\text{F}\cdot 10\text{H}_2\text{O}$ and 0.95 (Na) to 1.15 (K) for the MHPO_3F compounds with $\text{M} = \text{Na}, \text{K}, \text{Rb}, \text{and Cs}$. This difference is also demonstrated by the mixed salts, $\text{Cs}_3(\text{NH}_4)_2(\text{HPO}_3\text{F})_3(\text{PO}_3\text{F})$ and $\text{Na}_5[\text{N}(\text{CH}_3)_4](\text{PO}_3\text{F})_3\cdot 18\text{H}_2\text{O}$, with fluorine valencies of 1.04-1.09 and 0.92-0.94, respectively.

Chapter 5

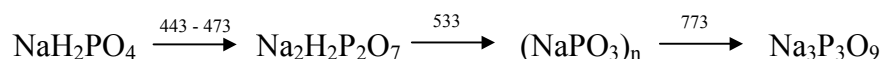
Thermal Analysis

The crystallographic study of the hydrogen monofluorophosphates lead to investigations on the thermal behavior of a select number of these compounds. The existence of first-order phase transitions [82] similar to those found in the hydrogen sulfates was also examined. Compounds were selected for measurement depending on their composition and structure. The results provide an overview of the thermal decomposition for the different types of substance in this class of compounds. The investigations on the thermal behavior of the sodium compounds, NaHPO_3F and $\text{NaHPO}_3\text{F} \cdot 2.5\text{H}_2\text{O}$, gave insight on the influence of the crystal water on the salt's thermal decomposition. The study of the CsHPO_3F compound was of particular interest based on phase transitions found for the isoelectronic CsHSO_4 , a well-known proton conductor [2]. The hydrogen monofluorophosphate with an organic cation and a structure similar to CsHPO_3F , $[\text{NHEt}_3]\text{HPO}_3\text{F}$, was also investigated thermally.

Thermal studies have been carried out on the monofluorophosphates, $\text{CaPO}_3\text{F} \cdot 2\text{H}_2\text{O}$ [21, 22], $\text{SrPO}_3\text{F} \cdot \text{H}_2\text{O}$ [23, 24], and $\text{Mg}(\text{NH}_4)_2(\text{PO}_3\text{F})_2 \cdot 2\text{H}_2\text{O}$ [25] and the hydrogen monofluorophosphate, KHPO_3F [26, 27]. The decomposition of the basic monofluorophosphates yielded the diphosphate, $\text{M}_2\text{P}_2\text{O}_7$ ($\text{M} = \text{Sr}, \text{Ca}$), as the end product, whereas KHPO_3F decomposed to the *cyclo*-triphosphate, $\text{K}_3[\text{P}_3\text{O}_9]$. In the case of KHPO_3F , condensation reactions began at 413 K with the release of HF rather than H_2O

[27]. At this temperature, unreacted KHPO_3F was found along with the *cyclo*-triphosphate. A variation in decomposition was observed, when KHPO_3F was heated directly to temperatures above 463 K. In this case, an array of polyphosphates with and without fluorine: $\text{K}_n[\text{P}_n\text{O}_{3n-1}\text{F}_2]$, $\text{K}_{n+1}[\text{P}_n\text{O}_{3n}\text{F}]$, and $\text{K}_n[\text{P}_n\text{O}_{3n+1}]$ were obtained by the escape of both HF and H_2O [27]. The basic monofluorophosphate, $\text{CaPO}_3\text{F}\cdot 2\text{H}_2\text{O}$, was studied with MS-coupled thermogravimetry [21]. The MS gas analysis showed the release of H_2O^+ , HF^+ , and POF_2^+ , a fragment of POF_3 , at different stages throughout the decomposition of the Ca salt. Fluorination of the solid sample with gaseous HF resulted in the formation of small amounts of POF_3 , which was observed by the IC curve of m/z 85 for POF_2^+ .

The KH_2PO_4 compound decomposes to the end product of metaphosphate, KPO_3 , above 573 K [83]. The sodium phosphate, NaH_2PO_4 , decomposes to $\text{Na}_2\text{H}_2\text{P}_2\text{O}_7$ between 473 and 513 K [84] according to the following path of decomposition [85]:



Three stable, crystalline phases of NaPO_3 exist, which give identical solutions [19]. Thus, the thermal study of the hydrogen monofluorophosphates should contribute to an understanding of their decomposition and could show similarities to the hydrogen phosphates or KHPO_3F , or, in the case of the hydrate, the $\text{CaPO}_3\text{F}\cdot 2\text{H}_2\text{O}$. The thermal behavior of the compounds, NaHPO_3F , $\text{NaHPO}_3\text{F}\cdot 2.5\text{H}_2\text{O}$, CsHPO_3F , and $[\text{NHEt}_3]\text{HPO}_3\text{F}$, were studied in N_2 or air with a TA-MS skimmer coupled system described in Sect. 2.1 Differential Thermal Analysis. The results of these thermal investigations are presented here.

5.1 The Sodium Salts: NaHPO_3F and $\text{NaHPO}_3\text{F}\cdot 2.5\text{H}_2\text{O}$

The compounds, NaHPO_3F and $\text{NaHPO}_3\text{F}\cdot 2.5\text{H}_2\text{O}$, had three and four step decompositions, respectively (Fig. 19a and b). In both cases, decomposition was complete by 673 K. The initial temperatures of decomposition varied between the compounds. Dehydration of $\text{NaHPO}_3\text{F}\cdot 2.5\text{H}_2\text{O}$ started immediately after heating, whereas the anhydrous salt was stable up to about 373 K. The decompositions of the sodium compounds were simulated and the intermediate and end products were characterized by H and F elemental analysis, XRD, ^{31}P and ^{19}F NMR (when soluble), and IR to understand the distinct steps of decomposition.

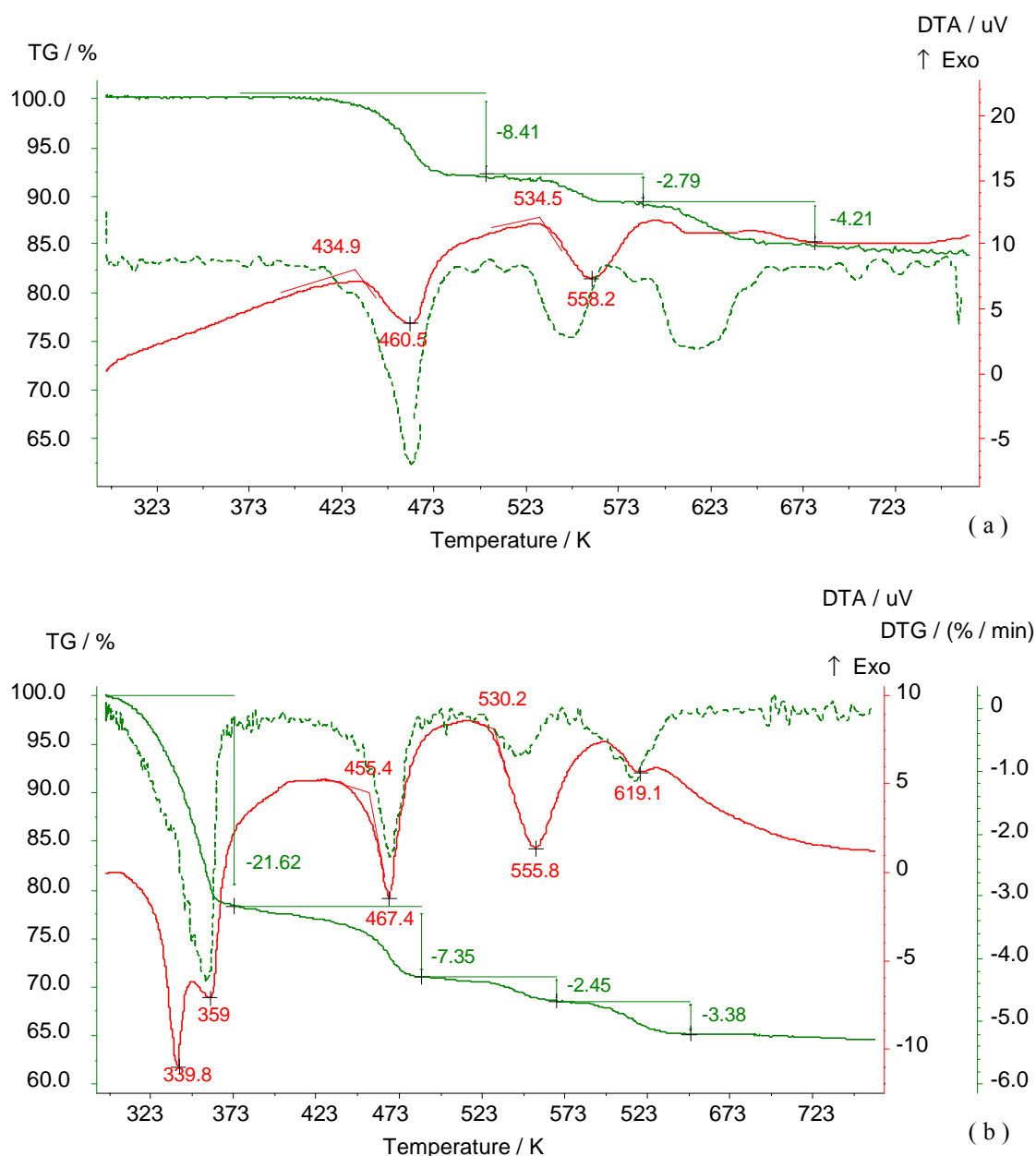


Fig. 19 STA curves for (a) NaHPO₃F and (b) NaHPO₃F·2.5H₂O both in N₂ showing the respective three and four step decompositions.

5.1.1 The Thermal Behavior of NaHPO₃F

The hydrogen monofluorophosphate, NaHPO₃F, decomposes in a three step process with a total mass loss of 15.41% (1.04 mg, 8.5 mmol). Endothermic effects are observed between ca. 423-483, 523-573, and 598-648 K (Fig. 19a). The IC curves, m/z 17 (OH⁺), 18 (H₂O⁺), 19 (F⁺), and 20 (HF⁺), show three corresponding maxima for these intervals (Fig. 20a). Therefore, the loss of mass in the samples can be explained by the simultaneous release of H₂O and HF up to 673 K. The formation of PO₂F₃ was only confirmed for the first step of

decomposition by the detected maxima between 423 and 498 K in the IC curves of m/z 50 (PF^+) and 47 (PO^+), both fragments of POF_3 [21] (Fig. 20b). However, the absolute amount of these fragments is significantly less than the others due to the smaller scale of 10^{-12} A (Fig. 20b). The quantitative interpretation of the data showed a total mass loss of 0.24 (0.013 mmol) and 1.01 mg (0.053 mmol) for H_2O and HF, respectively (Tab. 45), which corresponds to yields of 23.6 and 96.1 %, respectively.

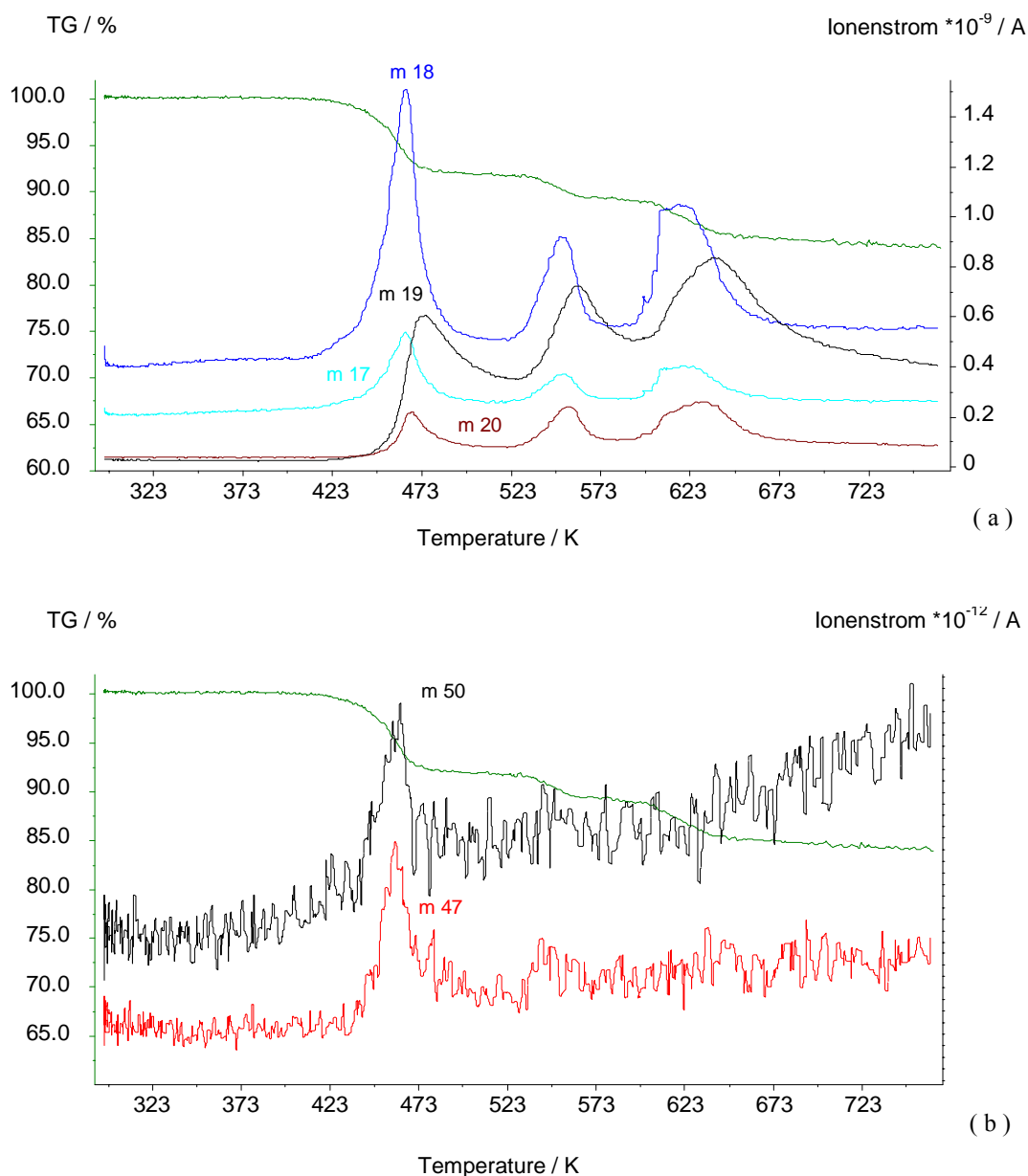


Fig. 20 Measured IC and TG curves of NaHPO_3F . (a) Maxima are observed for the IC curves, m/z 17 (OH^+), 18 (H_2O^+), 19 (F^+), and 20 (HF^+) for each of the endothermic processes. (b) The IC curves of m/z 50 (PF^+) and 47 (PO^+) showing a maximum for the first step of decomposition.

Tab. 45 Quantitative interpretation of the IC curves, m/z 18 and 19, for NaHPO_3F postcalibration

	T [K] ^a	Δm (TG) [mg]	A [10^{-6} A·s]	$m_{\text{H}_2\text{O}}$ (PTA) [mg] ^b	m_{HF} (PTA) [mg] ^c
Δm_1	372...506	0.57	0.165		
Δm_2	506...591	0.19	0.044		
Δm_3	591...683	0.28	0.094		
$\Sigma \Delta m_i$		1.04	0.303	0.24	1.01

^a Integration limits for the calculation of the area, A^b Calculated with $A=0.792 \cdot 10^6$ mg/A·s from the calibration with NaHCO_3 in N_2 ^c Calculated with $A=5.172 \cdot 10^6$ mg/A·s from the calibration with $\text{NaHF}_2 \cdot 0,12 \text{ H}_2\text{O}$ in N_2 ; with the partial area of 372-683K calculated as one

Simulated experiments were carried out at 498, 573, and 673 K. The elemental analyses showed a reduction in the hydrogen contents with increasing temperature (Tab. 46). The amount of free fluoride remained constant except for a higher value of 1.1 % found in the sample heated to 498 K. On the other hand, the total fluoride contents (Seel) diminished steadily as the temperature increased. Thus, it seems P–F bonds are broken gradually resulting in the stepwise release of HF throughout the entire process, which is supported by the three maximums found for m/z 19 and 20 shown in Fig. 20a. The final Seel value of 1.1 % obtained after the sample was heated to 673 K indicated the almost complete release of fluoride in the form of HF or POF_3 . The "absence" of H ($0.025 \approx 0\%$) implies a hydrogen-free end product.

Tab. 46 Elemental analysis of NaHPO_3F at RT and after being heated to the indicated temperature

T/K	RT [exp.(calcd)]	498	573	673
H /%	0.7 (0.82)	0.44	0.045	0.025
F (50 mL H_2O / Seel) / %	0.3 / 13.0 (15.57)	1.1 / 7.9	0.4 / 3.4	0.5 / 1.1

While the elemental analyses were quite effective in showing what escaped from the melt, the identification of the products or residue formed after heating was characterized by ^{31}P and ^{19}F NMR and XRD. The NMR spectra after heating to 498 K showed that several products of condensation were obtained in the first step of decomposition, which was also observed in [27]; in the second step (573 K), no new products were formed (Tab. 47). The ^{31}P NMR spectra were identical for 498 and 573 K except for a change in the product ratios. The major phase at 498 K was the stable diphosphate anion, $\text{H}_2\text{P}_2\text{O}_7^{2-}$, with 47%. The triphosphate anion, $(\text{P}_3\text{O}_9)^{3-}$, indicated by the singlet at ca. -20 ppm was obtained in 81% in the mixture at 573 K and was the end product at 673 K. The low H contents (0.045%) found at 573 K agrees with the NMR data, which shows that the hydrogen-free anions, $\text{P}_2\text{O}_5\text{F}_2^{2-}$ and $\text{P}_3\text{O}_9^{3-}$, account for 90% of the phosphorus species obtained at this

temperature.

Tab. 47 ^{31}P NMR data (δ) for the products obtained after heating NaHPO_3F to the indicated temperature; J is given in parenthesis with the product ratios in %

T/K	RT	%	498	%	573	%	673
HPO_3F^-	-3.6 (d, 908 Hz)	81					
H_2PO_4^-	0.8 (s)	19					
$\text{H}_2\text{P}_2\text{O}_7^{2-}$			-10.0 (s)	47	-9.8 (s)	4	
$\text{HP}_2\text{O}_6\text{F}^{2-}$			-10.1 (s), -16.9 (d, 933 Hz)	18	10.0 (s), -16.8 (d, 931 Hz)	4	
$\text{P}_2\text{O}_5\text{F}_2^{2-}$			-17.8 (dt, $J_{\text{PF}} = 940$, $J_{\text{PF}'} = 8$ Hz)	11	-17.7 (dt, 940 Hz)	10	
$\text{P}_3\text{O}_9^{3-}$			-20.9 (s)	13	-20.7 (s)	81	-20.8 (s)
?			-13.2 (s)	3	-13.1 (s)	1	

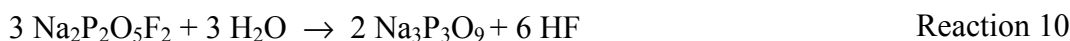
The double triplet found at $-17.8/-17.7$ ppm for the temperatures, 498 and 573 K, was assigned to the difluorodiphosphate anion, $\text{P}_2\text{O}_5\text{F}_2^{2-}$ [86], with the corresponding double triplet at -73.7 ppm with $J_{\text{FP}} = 942$ and $J_{\text{FP}'} = 10$ Hz in the ^{19}F spectra. A second doublet found in the ^{31}P and ^{19}F spectra at $-16.9/-16.8$ and -74.0 ppm, respectively, with $J_{\text{PF}} = 933$ Hz implied a second, fluorinated, condensated phosphate in the melt. The chemical shift of the doublet similar to that of the $\text{P}_2\text{O}_5\text{F}_2^{2-}$ anion and the singlet at -10.1 ppm in the ^{31}P spectra suggest the intermediate $\text{HP}_2\text{O}_6\text{F}^{2-}$ anion [87, 88], which was also formed in the decomposition of KHPO_3F , when initially heated to temperatures above 463 K [27]. The singlet observed at $-13.2/-13.1$ ppm for 498/573 K, respectively, could not be interpreted. XRD confirmed the *cyclo*-triphosphate, $\text{Na}_3\text{P}_3\text{O}_9$ [89, 90], as the end product. The patterns measured for 573 and 673 K were identical except for weak peaks at 21.4, 25.8, 27.9, and 31.1 Å (573 K) due to the incomplete decomposition of the intermediates at 573 K. The pattern measured for the melt heated to 498 K could not be interpreted because of the numerous phases present (Tab. 47).

The following can be concluded about the path of decomposition:

- complete decomposition of NaHPO_3F to condensated products was observed in the first step before 498 K
- condensation reactions and the release of HF and H_2O (mass loss) seem to be synergetic
- two fluorinated diphosphates, $\text{HP}_2\text{O}_6\text{F}^{2-}$ and $\text{P}_2\text{O}_5\text{F}_2^{2-}$, were obtained as intermediates
- the end product of decomposition was the *cyclo*-triphosphate, $\text{Na}_3\text{P}_3\text{O}_9$.

The following reactions can be understood as a rough schema for the stepwise decomposition of NaHPO_3F , but are not mechanistic and other products and combinations can not be ruled out.

Above 498 K



Overall without consideration of the minimal loss of H_2O and formation of fluorinated diphosphates:



The decomposition of anhydrous NaHPO_3F resembles that of KHPO_3F reported in [27] with identical end products. The diphosphate, $\text{Na}_2\text{H}_2\text{P}_2\text{O}_7$, which is more stable than that of the potassium, is also found as an intermediate product.

5.1.2 The Thermal Behavior of $\text{NaHPO}_3\text{F} \cdot 2.5\text{H}_2\text{O}$

The decomposition of $\text{NaHPO}_3\text{F} \cdot 2.5\text{H}_2\text{O}$ involved four steps with endothermic effects between RT-373, 448-473, 530-573, and 598-633 K (Fig. 19b) [91]. The total mass loss of 34.8% was higher than that found for NaHPO_3F . The IC curves for m/z 17 (OH^+), 18 (H_2O^+), 19 (F^+), and 20 (HF^+) are shown in Fig. 21a and b. The release of HF was not observed until the second step of decomposition at temperatures of about 473 K and continued on with two additional maxima up to 723 K (Fig. 21a), whereas dehydration started immediately after heating and was even observed in the dry gas flow at RT (Fig. 21b). Therefore, the removal and addition of crystal water from the structure was examined.

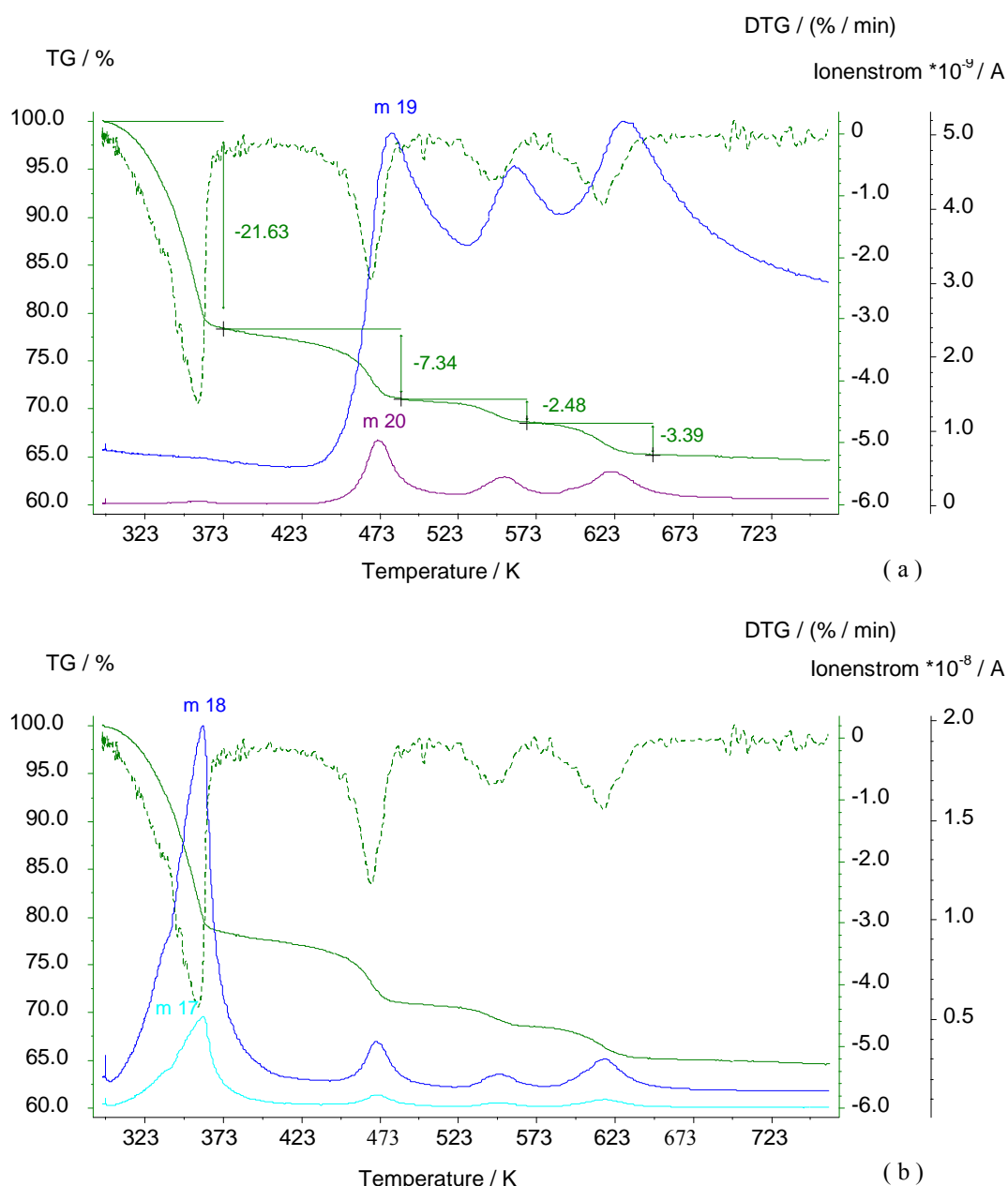


Fig. 21 Measured IC curves with the TG and DTG graphs of $\text{NaHPO}_3\text{F}\cdot 2.5\text{H}_2\text{O}$ (a) for m/z 19 (F^+) and 20 (HF^+) and (b) for m/z 17 (OH^+) and 18 (H_2O^+)

The 2.5 moles of crystal water could be completely removed after $\text{NaHPO}_3\cdot 2.5\text{H}_2\text{O}$ was left to stand in vacuum at RT for 12 h. The ease with which the crystal water can be removed without heating was confirmed by XRD; the pattern of the treated $\text{NaHPO}_3\cdot 2.5\text{H}_2\text{O}$ was identical to that of NaHPO_3F [71]. Experiments in air showed that 1.7 moles of crystal water, which corresponded to a mass increase of 25.5%, could be recovered by simply leaving the sample to stand in air over a period of 6 d. The experimental and theoretical changes in mass for both experiments are given in (Tab. 48).

Tab. 48 Behavior of $\text{NaHPO}_3\text{F} \cdot 2.5\text{H}_2\text{O}$ at RT

	12 h Vacuum	In air
Change in mass /% (calcd)	-28.8 (26.95)	+25.5 (36.88)

Inconsistencies due to immediate dehydration were observed in the total amount of mass lost during thermal decomposition. The loss of crystal water accounted for 97.1% of the total mass loss in the first stage of decomposition. After that, the fraction of H_2O responsible for the total mass loss decreased significantly with the simultaneous release of HF and other species above 473 K (Tab. 49).

Tab. 49 Quantitative interpretation of the IC curves, m/z 18, postcalibration for $\text{NaHPO}_3\text{F} \cdot 2.5\text{H}_2\text{O}$

	T [K] ^a	Δm (TG) [mg]	A [10^{-6} A·s]	Δm (PTA) [mg] ^b	$\frac{\Delta m(\text{PTA})}{\Delta m(\text{TG})} 100\%$
Δm_1	29...150	2.76	5.415	2.68	97.1
Δm_2	160...240	0.94	0.272	0.13	13.8
Δm_3	250...306	0.31	0.081	0.04	12.9
Δm_4	306...392	0.43	0.227	0.11	25.6

^a Integration limits for the determination of the area, A

^b Calculated with $A=0.496 \cdot 10^6$ mg/A·s ($\pm 3\%$) from the calibration with NaHCO_3 in air

^c Fraction of H_2O in the TG step, Δm_i

Information on the products formed during decomposition was acquired by simulated experiments carried out at 393, 493, and 673 K. Again, the H contents decreased with higher temperatures (Tab. 50) as in the case of NaHPO_3F . However, inconsistencies were observed in the fluoride analyses. The total fluoride contents increased initially from 9.2 to 11.7% at 393 K before decreasing to a final value of 1.0% very similar to the 1.1% found for NaHPO_3F . At 393 K, 92% of the entire fluoride in the sample was found as free fluoride in the melt. This and the two singulets in the ^{19}F spectra (Tab. 52) imply that the fluoride does not immediately escape the melt in the form of HF, although the P–F bond has been broken; maxima in the IC curves for HF and F were first observed at about 473 K (Fig. 21a). The release of HF after heating to 493 K correlated with (a) a reduction in the amount of free fluoride to 39 %, (b) the disappearance of the singulet at –151 ppm in the ^{19}F spectra, and (c) the observed maximum in Fig. 21a.

Tab. 50 Elemental analysis of $\text{NaHPO}_3\text{F} \cdot 2.5\text{H}_2\text{O}$ at RT and after being heated to the indicated temperature

T/K	12 h Vacuum [exp.(calcd)]	RT [exp.(calcd)]	393	493	673
H /%	0.9 (0.82)	3.3 (3.59)	2.3	0.9	0.02
F (50 mL H_2O / Seel)/ %	0.1 / 14.2 (15.57)	0.3 / 9.2 (11.38)	10.8 / 11.7	2.7 / 6.9	0.1 / 1.0

The presence of the HPO_3F^- and H_2PO_4^- anions was detected in the melt at 393 and 493 K by ^{31}P NMR (Tab. 51). The ^{31}P spectrum of the melt heated to 393 K showed that the $\text{HPO}_3\text{F}^-/\text{H}_2\text{PO}_4^-$ signal ratio was reversed when compared with the spectrum of the RT product; equivalent amounts of the HPO_3F^- and H_2PO_4^- anions are found in the melt at 493 K. A strong singlet at -10.0 ppm confirmed the condensation of phosphorus and the presence of the $\text{H}_2\text{P}_2\text{O}_7^{2-}$ anion as the major product in the second step of decomposition (493 K) identical to NaHPO_3F melt at 498 K. On the other hand, a doublet in the ^{19}F spectra was observed for the HPO_3F^- anion throughout the decomposition and two singlets were observed for the melt heated to 393 K (Tab. 52) not observed in the decomposition of NaHPO_3F . The singlet at -151 ppm was assigned to HF not yet released from the melt [92]. The other singlet at -131 ppm ($\{\text{F1}\}$) could not be interpreted. An analysis of the product ratios in the ^{19}F spectra shows that the majority of fluorine is in the form of HF at 393 K (73%), but at higher temperatures, HF leaves the melt (the singlet at -151 ppm disappears) and HPO_3F^- becomes the major product containing fluoride. Interestingly enough, the signal ratio of $\text{HPO}_3\text{F}^-/\{\text{F1}\}$ remains approximately constant from 393 to 493 K with a value of ca. 2.4.

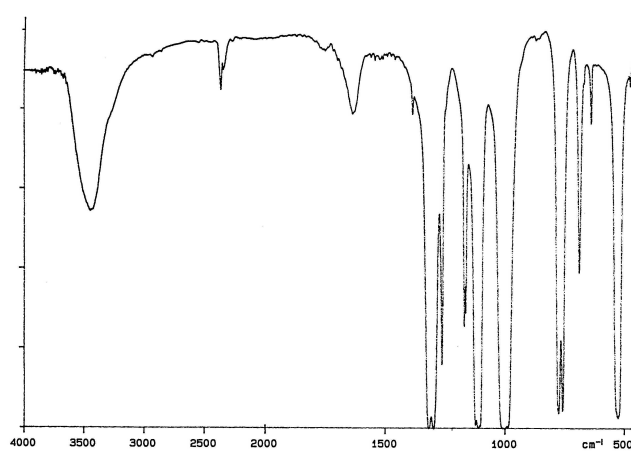
Tab. 51 ^{31}P NMR data (δ) for $\text{NaHPO}_3\text{F}\cdot 2.5\text{H}_2\text{O}$ and the products obtained after heating to the indicated temperature; J_{PF} is given in parenthesis with the product ratios in %

T/K	12 h Vacuum	%	RT	%	393	%	493	%
HPO_3F^-	-3.6 (d, 908 Hz)	90	-3.7 (d, 909 Hz)	89	-3.8 (d, 908 Hz)	9	-3.7(d, 909 Hz)	22
H_2PO_4^-	0.8 (s)	10	0.7 (s)	11	0.8 (s)	91	0.7 (s)	22
$\text{H}_2\text{P}_2\text{O}_7^{2-}$							-10.0(s)	56

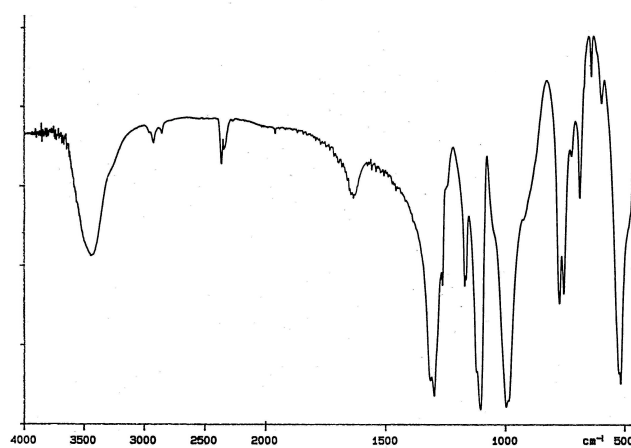
Tab. 52 ^{19}F NMR data (δ) for $\text{NaHPO}_3\text{F}\cdot 2.5\text{H}_2\text{O}$ and the products obtained after heating to the indicated temperature; J_{PF} is given in parenthesis

T/K	12 h Vacuum	RT	393	%	493	%
HPO_3F^-	-74.9 (d, 908 Hz)	-74.8 (d, 909 Hz)	-74.8 (d, 904 Hz)	19	-74.8(d, 904 Hz)	71
$\{\text{F1}\}$			-131 (s)	8	-131 (s)	29
HF^-			-151 (s)	73		

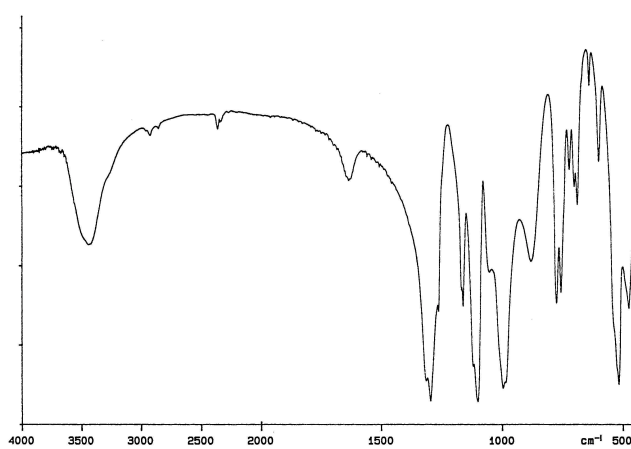
The XRD patterns measured for the tempered melts were difficult to interpret except for the pattern of the melt heated to 673 K. This pattern could be assigned to a monoclinic (NaPO_3) phase [93] and not the *cyclo*-triphosphate as in the case of NaHPO_3F . Interestingly enough, the IR spectra were identical for $\text{NaHPO}_3\text{F}\cdot 2.5\text{H}_2\text{O}$ and NaH_2PO_4 , both tempered to 673 K; the spectrum of the end product of anhydrous NaHPO_3F varied (Fig. 22).



(a)



(b)



(c)

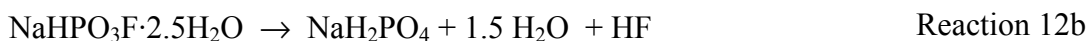
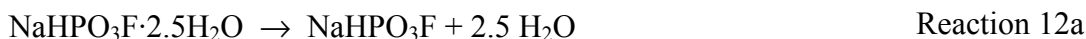
Fig. 22 IR spectra for the tempered (a) NaHPO_3F , (b) $\text{NaHPO}_3\text{F} \cdot 2.5\text{H}_2\text{O}$, and (c) NaH_2PO_4 (673 K).

The following can be concluded about the decomposition of $\text{NaHPO}_3\text{F}\cdot 2.5\text{H}_2\text{O}$:

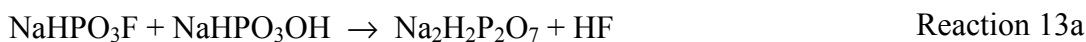
- formation of additional phosphate due to hydrolysis of the P–F bond was observed along with the presence of free-fluoride species (HF) in the melt at 393 K
- the release of HF and formation of condensation products are synergetic and occur at temperatures higher than 393 K
- the phosphates, H_2PO_4^- and $\text{H}_2\text{P}_2\text{O}_7^{2-}$, act as intermediates
- the end product, a monoclinic NaPO_3 phase, is identical to the end product of the NaH_2PO_4 decomposition.

With this information, the following nonmechanistic reactions can be formulated for the decomposition of $\text{NaHPO}_3\text{F}\cdot 2.5\text{H}_2\text{O}$ demonstrating the simultaneous release of HF and H_2O ; again, other products could not be ruled out.

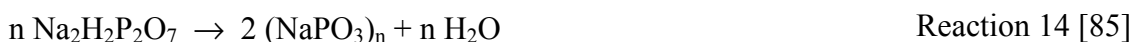
Up to 393 K



Ongoing



At 673 K



5.1.3 Comparison

The NaHPO_3F and $\text{NaHPO}_3\text{F}\cdot 2.5\text{H}_2\text{O}$ both have stepwise decompositions, yet the intermediate and end products formed during these processes vary. The crystal water in $\text{NaHPO}_3\text{F}\cdot 2.5\text{H}_2\text{O}$ was released between RT and 373 K during an additional stage of decomposition. Differences in the intermediate and final products formed were based on the hydrolysis of the P–F bond with crystal water in $\text{NaHPO}_3\text{F}\cdot 2.5\text{H}_2\text{O}$ and the direct heating of NaHPO_3F to over 463 K. The fluorinated diphosphates, $\text{Na}_2\text{H}_2\text{P}_2\text{O}_5\text{F}_2$ and $\text{Na}_2\text{HP}_2\text{O}_6\text{F}$, the diphosphate, $\text{Na}_2\text{H}_2\text{P}_2\text{O}_7$, and the *cyclo*-triphosphate, $\text{Na}_3\text{P}_3\text{O}_9$, were formed in the first step of decomposition for NaHPO_3F with traces of them still existing in the melt tempered to 573 K. In the case of the hydrate, only the anions of H_2PO_4^- and

$\text{H}_2\text{P}_2\text{O}_7^{2-}$, were found during the decomposition of the hydrate, because decomposition of $\text{NaHPO}_3\text{F}\cdot 2.5\text{H}_2\text{O}$ involved the formation of phosphate. The complete reaction of the HPO_3F^- anion prior to 498 K was implied by the absence of the corresponding doublet in the ^{31}P spectrum of the tempered NaHPO_3F , whereas the HPO_3F^- anion was observed in the spectrum of $\text{NaHPO}_3\text{F}\cdot 2.5\text{H}_2\text{O}$ tempered to 493 K. The release of HF and condensation reactions took place at temperatures above 393 K for both Na compounds. This agrees with the findings in [27] that condensation reactions began at 413 K. Thus, it seems that while the NaHPO_3F condensates directly, the hydrate is first hydrolyzed; condensation then takes place with phosphate and monofluorophosphate explaining the absence of fluorinated diphosphates and the end product identical to that of the NaH_2PO_4 . This discrepancy could also be based on the different paths of decomposition and consequent varying heating regimes, which has also been commented on in [27].

Not only do the courses of decomposition, but also the end products formed differ for NaHPO_3F and $\text{NaHPO}_3\text{F}\cdot 2.5\text{H}_2\text{O}$. In the case of NaHPO_3F , a *cyclo*-triphosphate was formed. The hydrate decomposed to the corresponding metaphosphate, $(\text{NaPO}_3)_n$, identical to the end product of the NaH_2PO_4 below 773 K [85].

5.2 The Thermal Behavior of CsHPO_3F

The cesium hydrogen monofluorophosphate was measured in air between RT and 773 K. Endothermic maxima were found at 452 and 507 K (Fig. 23).

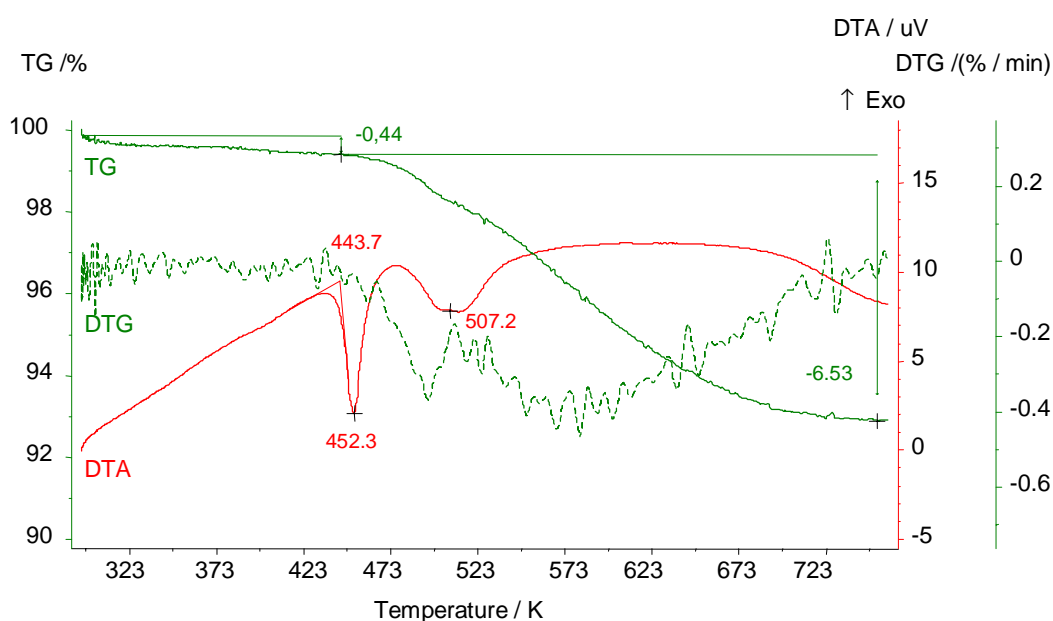


Fig. 23 STA graphs measured for CsHPO_3F showing a total loss of mass at 6.97%.

In comparison with the hydrogen sulfate [2], a first-order phase transition was not observed. CsHPO_3F melts at 443.7 K and then decomposes directly to the end product at 748 K without forming stable intermediates. Thus, the decomposition of the cesium compound is quite different from that observed for the sodium salts. The release of HF was much more gradual than in the case of the sodium compounds and began around 398 K continuing up to 748 K (Fig. 24a). On the other hand, the temperature range, in which H_2O escaped the melt, was narrower (between 448 and 673 K) (Fig. 24a). A short break was observed for both species at 507 K (endothermic effect) (Fig. 24a). The formation of the fluorination product, POF_3 , above 473 K was confirmed by the maximum for m/z 47 (PO^+) and 88 (PF_3^+) [21] shown in Fig. 24b.

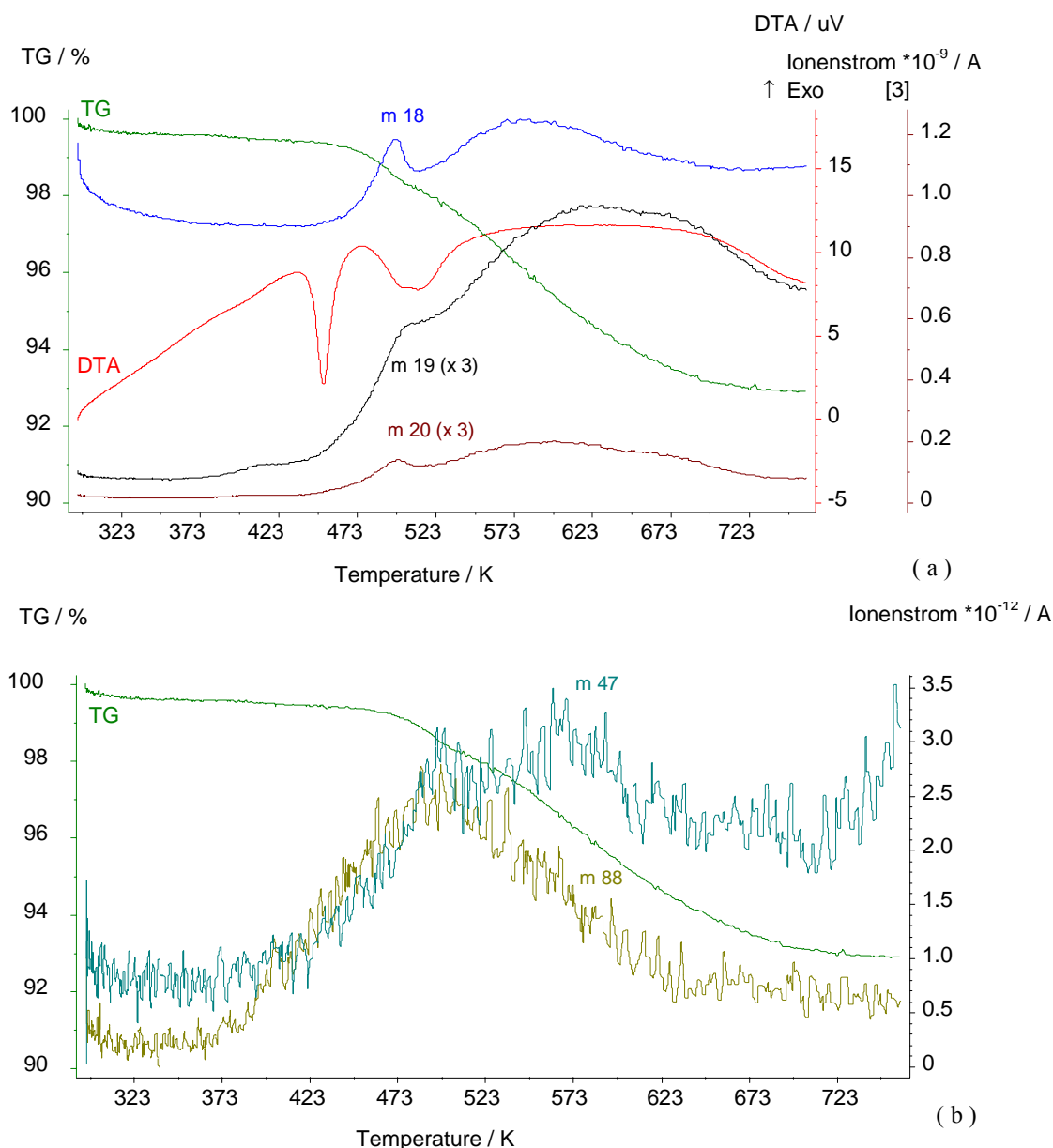


Fig. 24 IC graphs for (a) m/z 18 (H_2O^+), 19 (F^+), and 20 (HF^+) and (b) m/z 47 (PO^+) and 88 (PF_3^+) shown with the DTA and TG data of CsHPO_3F .

The hydrogen phosphate, CsH_2PO_4 , is reported to undergo dehydration at ca. 508 K [85] and $(\text{CsPO}_3)_n$ is synthesized by the dehydration of CsH_2PO_4 [85]. Based on the similar behavior of KHPO_3F [27], and NaHPO_3F , it can be assumed that CsHPO_3F decomposes to form the *cyclo*-triphosphate, $\text{Cs}_3\text{P}_3\text{O}_9$ (Reaction 15). A total mass loss of 8.62% (1.56 mg) corresponds to the condensation of the hydrogen monofluorophosphate to the *cyclo*-triphosphate with the release of HF shown in Reaction 15. The total mass loss (6.97 %, 1.27 mg) found amounts to 81% of the theoretical value.



Again, the occurrence of H_2O is not considered in the overall reaction for the thermal degradation of CsHPO_3F . However, it can be assumed that small amounts of H_2O are released as in the decomposition of NaHPO_3F supported by the formation of fluorinated diphosphates.

5.3 The Thermal Behavior of $[\text{NH}(\text{CH}_2\text{CH}_3)_3]\text{HPO}_3\text{F}$

The thermal behavior of $[\text{NHEt}_3]\text{HPO}_3\text{F}$ was investigated between RT–993 K and was quite different than that of the alkali metal hydrogen monofluorophosphates (Fig. 25).

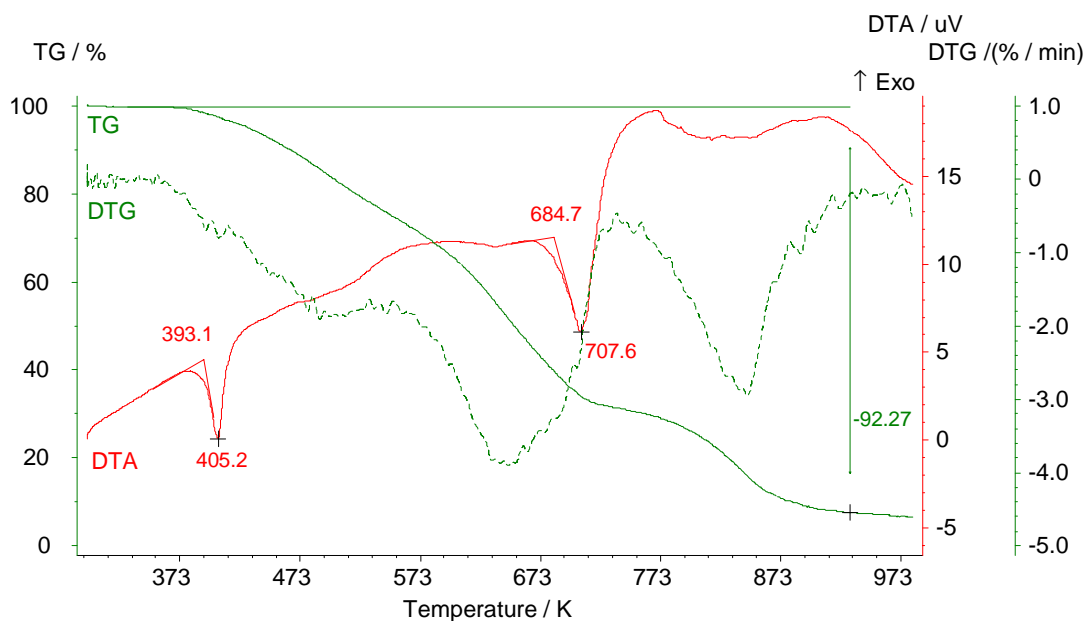


Fig. 25 STA graphs of $[\text{NHEt}_3]\text{HPO}_3\text{F}$ showing the progression (course) of decomposition.

The steps of decomposition are less distinct than in the case of the sodium compounds. The first endothermic effect, the melting point, is lower than that of the cesium salt and was

observed at 393.1 K. In succeeding steps of decomposition up to 684 K, exothermic and endothermic processes overlap each other. A pronounced endothermic process then occurs at 684 K, which corresponds to the decomposition of the organic cation (Fig. 26a). Above this temperature, indistinct exothermic processes take place.

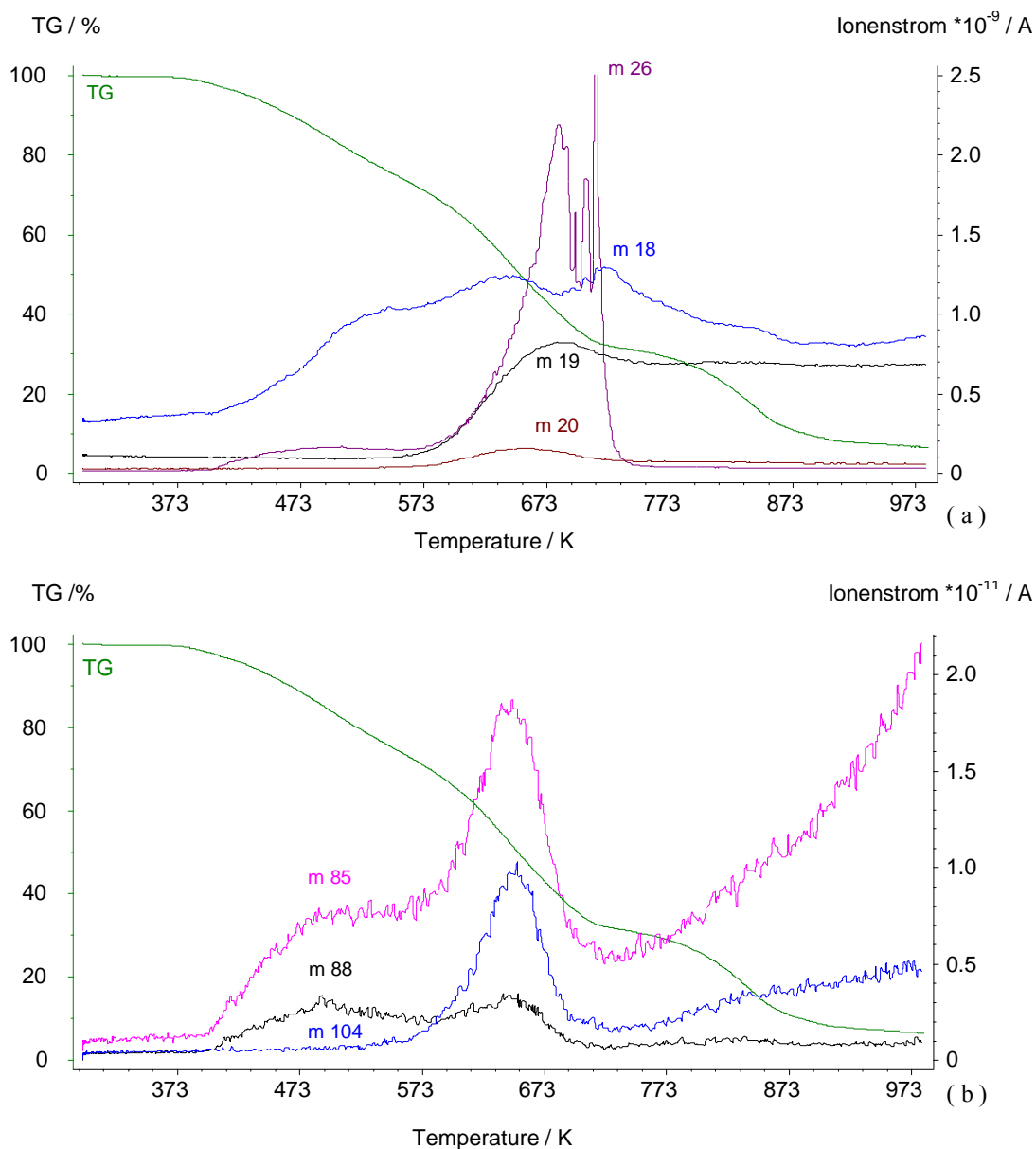


Fig. 26 IC curves of [NHEt₃]HPO₃F for (a) m/z 18 (H₂O⁺), 19 (F⁺), 20 (HF⁺), 26 (C₂H₂⁺) and (b) m/z 88 (PF₃⁺), 104 (POF₃⁺), and 85 (POF₂⁺)

The emission of HF first began at 531 K, a higher temperature than for the alkali metal hydrogen monofluorophosphate (ca. 473 K), whereas dehydration was observed immediately after melting (393.1 K) (Fig. 26a). An integral quantitative analysis of the TG graph for the entire path of decomposition (331 to 931 K) found a total mass loss of

92.27% (10.71 mg, 0.053 mmol) much higher than those found for the alkali metal compounds (Tab. 53). In comparison with the alkali metal hydrogen monofluorophosphate, an end product, such as a triphosphate or metaphosphate, was not observed based on the absence of a stabilizing cation, instead a small amount of a black residue was left over. Both the organic cation and the HPO_3F^- anion seem to decompose and escape the melt as diverse volatile products. This is reflected by small H_2O and HF fractions (7 and 17%, respectively) of the total mass lost. The secondary formation of POF_3 due to the presence of HF in the melt was confirmed with the observation of various POF_3 fragments [21]: PO , PF , PF_2 , PF_3 , POF_3 , and POF_2 . Only those of PF_3 , POF_3 , and POF_2 are shown in Fig. 26b; the points of release vary. These fragments were not as abundant in the decompositions of the alkali metal hydrogen monofluorophosphates. The formation of POF_3 was also supported by the constant release of fluorine (m/z 19) above 723 K (Fig. 26a).

Tab. 53 Quantitative interpretation of the TG graph and IC curves, m/z 18 and 19

	T [K]	A [10^{-6} A·s]	m (PTA) [mg/mmol]	m_{TG} [mg/mmol]
$\Delta m_{\text{H}_2\text{O}}$	402...931	0.941	0.74 / 0.041	
Δm_{HF}	531...931	0.356	1.82 / 0.096	
Δm_{total}	330...683			10.71 / 0.053

5.4 Summary

The thermal behavior of NaHPO_3F , $\text{NaHPO}_3\text{F} \cdot 2.5\text{H}_2\text{O}$, CsHPO_3F , and $[\text{NHEt}_3]\text{HPO}_3\text{F}$ are quite different depending on the cation and presence of crystal water in the structure. The sodium salts, NaHPO_3F and $\text{NaHPO}_3\text{F} \cdot 2.5\text{H}_2\text{O}$, both have decompositions involving three and four steps, respectively. The anhydrous salt initially decomposed to the intermediate condensation products, $\text{Na}_2\text{H}_2\text{P}_2\text{O}_5\text{F}_2$, $\text{Na}_2\text{HP}_2\text{O}_6\text{F}$, $\text{Na}_2\text{H}_2\text{P}_2\text{O}_7$, and $\text{Na}_3\text{P}_3\text{O}_9$, after heating to 498 K with the *cyclo*-triphosphate, $\text{Na}_3\text{P}_3\text{O}_9$, as the end product at 673 K. On the other hand, the decomposition of the hydrate, $\text{NaHPO}_3\text{F} \cdot 2.5\text{H}_2\text{O}$, involves the initial release of the crystal water and the formation of the corresponding phosphate, NaH_2PO_4 (393 K). After that, HF escapes the melt and condensation occurs forming the diphosphate, $\text{Na}_2\text{H}_2\text{P}_2\text{O}_7$. A metaphosphate, $(\text{NaPO}_3)_n$, was obtained as the end product, which was identical to the decomposition product of NaH_2PO_4 . The cesium compound, CsHPO_3F , melts at 443.7 K and then decomposes directly to the end product without the formation of stable intermediates. The decomposition of $[\text{NHEt}_3]\text{HPO}_3\text{F}$ is similar to the CsHPO_3F . Melting occurs at 373.1 K and then the compound decomposes gradually with a break at 707.6 K. A black residue was left over as the final product based on an almost complete loss of mass (92.27 %).

Tab. 54 Observed temperatures for the escape of HF and H₂O (K)

	NaHPO ₃ F	NaHPO ₃ F·2.5H ₂ O	CsHPO ₃ F	[NHEt ₃]HPO ₃ F
HF release				
Initial temperature	448	448	473	531
First maximum	473	473	498	673
H ₂ O release				
Initial temperature	423	RT	473	393
First maximum	<473	<373	<498	>473 (broad)

The following two types of decomposition were observed:

- Na compounds: stepwise decomposition
- Cs and [NHEt₃]: direct decomposition,

yet the compounds can be grouped differently according to the temperature at which H₂O and HF escaped the melt (Tab. 54). The anhydrous salts of Na and Cs have similar behavior with regard to the release of H₂O and HF. A comparison of the hydrate with these anhydrous salts shows that, as expected, H₂O is released from the hydrate at much lower temperatures. HF, on the other hand, escapes the melt of NaHPO₃F·2.5H₂O at temperatures identical to those of NaHPO₃F. The thermal behavior of [NHEt₃]HPO₃F differed from that of the hydrate and anhydrous salts, NaHPO₃F and CsHPO₃F. In this case, H₂O escaped the melt at temperatures lower than those observed for the anhydrous alkali metal salts, while the release of HF started later than that for the MHPO₃F. The broadness of the maximum also suggests another type of mechanism compared with that of the alkali metal compounds.

Chapter 6

Discussion

6.1 A Structural Comparison to the Hydrogen Chalcogenates and Other Oxoacid Salts

The similarity of the basic sulfate and monofluorophosphates due to their isosterism was commented on quite early [18, 94, 95]. Certain basic sulfates and monofluorophosphates are isostructural and do have comparable solubilities [17, 19]. On the other hand, the crystal structures of the hydrogen monofluorophosphates proved to be quite different when compared with those of the hydrogen sulfates. Only a few examples were observed, in which the hydrogen monofluorophosphate / basic monofluorophosphates and the corresponding sulfate were isostructural. Unfortunately, not all of the structures presented in this thesis have an analogous sulfate, whose structure has been previously determined. Thus, the comparison is not complete, yet leads to interesting conclusions about the structural influence of fluorine in the hydrogen and basic monofluorophosphates.

The hydrogen monofluorophosphates with K, Rb, Cs, NH₄

Despite the parallel compositions of MHPO_3F and MHSO_4 with $\text{M} = \text{K, Rb, Cs, NH}_4$, these compounds are not isostructural. In the case of potassium, the orthorhombic structure of KHSO_4 [9, 39] contains cyclic dimers and infinite chains of HSO_4 tetrahedra. Branched

chains like the ones found in KHPO_3F were only observed in $\alpha\text{-NaHSO}_4$ [41].

The Rb structures of both classes of compounds are monoclinic, but have different lattice parameters. They also vary in their patterns of hydrogen-bonded tetrahedra. The structure of RbHSO_4 [8, 96] includes two crystallographically different chains of tetrahedra parallel to the b -axis. This type of structure has not been observed in the hydrogen monofluorophosphate structures. The $\alpha\text{-RbHPO}_3\text{F}$, instead, has tetramers similar to those found in the nonisostructural AgHSO_4 [42, 43]. Yet, the isotypism of the Rb and NH_4 hydrogen sulfates [97] was imitated by the isostructural hydrogen monofluorophosphates: $\alpha\text{-RbHPO}_3\text{F}$ and $\alpha\text{-NH}_4\text{HPO}_3\text{F}$. The $\beta\text{-RbHPO}_3\text{F}$ structure with O/F disordering could not be compared structurally to the hydrogen sulfates, but does have lattice constants comparable to a high-pressure RbHSO_4 modification [98] ($a = 7.354$, $b = 7.354$, $c = 7.758$ Å, $\gamma = 110.84(4)^\circ$), in which the hydrogen positions could also not be determined.

In the room temperature phase of CsHSO_4 [6], the HSO_4 tetrahedra are connected by hydrogen bonds to form chains instead of dimers like those formed in CsHPO_3F . Interestingly enough, some similarity is found between the monoclinic lattice constants of CsHPO_3F and the high-temperature, tetragonal phase, CsHSO_4 ($a = 5.714$ Å and $c = 14.212$ Å) [99].

Analogous to the alkali metal compounds, the α and β modifications of $\text{NH}_4\text{HPO}_3\text{F}$ and those of the hydrogen sulfate, NH_4HSO_4 [7, 100], are not isostructural [77]. The nonferroelectric, RT modification of NH_4HSO_4 [100] does contain two unique, distorted SO_4 tetrahedra linked by two short hydrogen bonds (2.514(6) and 2.598(5) Å), but the units form chains, not tetramers, in the b -direction. A difference between the $\text{NH}_4\text{HPO}_3\text{F}$ and NH_4HSO_4 structures is also seen in the $\text{N}\cdots\text{O}$ hydrogen bonding. In the case of the sulfate, each O atom is involved in one $\text{N}-\text{H}\cdots\text{O}$ bond including the O atoms, which are hydrogen donors in the two $\text{O}-\text{H}\cdots\text{O}$ bonds. In the $\text{NH}_4\text{HPO}_3\text{F}$ structures, the hydrogen donor atoms, O3 and O6, are not acceptors in $\text{N}-\text{H}\cdots\text{O}$ bonds. This and the absence of $\text{N}-\text{H}\cdots\text{F}$ bonds force the other O atoms to participate in more than one hydrogen bond. The only exception is O5 in $\alpha\text{-NH}_4\text{HPO}_3\text{F}$, which is a single acceptor due to the missing hydrogen bond with H10.

Similarities are observed between the α modification of $\text{NH}_4\text{HPO}_3\text{F}$ and the acid salt, $\alpha\text{-(NH}_4)_2\text{SeO}_4(\text{H}_3\text{PO}_4)$ [101]. The lattice constants of these two salts (both $P2_1/n$) are almost identical with $a = 7.540(3)$, $b = 15.516(5)$, $c = 7.741(3)$ Å, and $\beta = 106.75(3)$ for $\alpha\text{-(NH}_4)_2\text{SeO}_4(\text{H}_3\text{PO}_4)$. The structures also have common features. The phosphoric acid adduct consists of tetramers of selenium and phosphorus tetrahedra with a similar

orientation and packing to those in α - $\text{NH}_4\text{HPO}_3\text{F}$. The tetramers in α - $(\text{NH}_4)_2\text{SeO}_4(\text{H}_3\text{PO}_4)$ are then linked to each other along the b -axis by an additional hydrogen bond. This hydrogen bond is imitated in the $\text{NH}_4\text{HPO}_3\text{F}$ structure by the short $\text{F}\cdots\text{F}$ distance (2.731 Å) probably induced by the packing of the tetramers in the structure. The $\text{F}\cdots\text{F}$ distance is longer than the hydrogen bond (2.503(3) Å) in α - $(\text{NH}_4)_2\text{SeO}_4(\text{H}_3\text{PO}_4)$. In the case of the β modifications, the compounds have similar lattice constants, but different space groups.

In comparison to the hydrogen monofluorophosphates with the MHPO_3F composition, some structural similarity was found between the unique hydrogen monofluorophosphate, $\text{K}_3[\text{H}(\text{PO}_3\text{F})_2]$ and the corresponding sulfate. The formula with a M/H ratio of 3:1 was only obtained for the potassium hydrogen monofluorophosphate, whereas it is quite common among the acid sulfates and selenates with the general formula, $\text{M}_3[\text{H}(\text{XO}_4)_2]$: $(\text{NH}_4)_3[\text{H}(\text{SO}_4)_2]$, $\text{Na}_3[\text{H}(\text{SO}_4)_2]$, $\text{K}_3[\text{H}(\text{XO}_4)_2]$, $\text{Rb}_3[\text{H}(\text{XO}_4)_2]$, and $\text{Cs}_3[\text{H}(\text{SeO}_4)_2]$ ($\text{X} = \text{S}$ or Se), which are all isostructural except for the sodium salt. The space group of $\text{K}_3[\text{H}(\text{PO}_3\text{F})_2]$, $C2/c$ ($A2/a$), is identical to that of $\text{K}_3[\text{H}(\text{SO}_4)_2]$ at RT [44], but the compounds have different lattice constants and ratios. In both structures, the K1 atom has a special position; there is only one unique tetrahedron; and the hydrogen bond is situated around the center of symmetry. The hydrogen atom was assigned the special position at (0, 0, $\frac{1}{2}$) in $\text{K}_3[\text{H}(\text{SO}_4)_2]$ instead of a disordered general position as in $\text{K}_3[\text{H}(\text{PO}_3\text{F})_2]$, but hydrogen disordering at RT seemed to be very clear in $\text{K}_3[\text{H}(\text{SO}_4)_2]$ [44]. A refinement with the hydrogen atom position directly on the center of symmetry resulted in an increased R factor for the structure of $\text{Rb}_3\text{H}(\text{SeO}_4)_2$ in [48], which was also observed for the refinement of $\text{K}_3[\text{H}(\text{PO}_3\text{F})_2]$. The hydrogen bond length, $\text{O}\cdots\text{O}$, in $\text{K}_3[\text{H}(\text{PO}_3\text{F})_2]$ of 2.451(8) Å was one of the shortest found for the hydrogen monofluorophosphates presented here and was only slightly shorter than the 2.493(1) Å found in $[\text{K}_3\text{H}(\text{SO}_4)_2]$ [44]. Thus, some common structural features exist between the $\text{K}_3[\text{H}(\text{PO}_3\text{F})_2]$ and $[\text{M}_3\text{H}(\text{XO}_4)_2]$ salts. However, the arrangement of the tetrahedra is much different probably due to fluorine and its limited involvement in the metal coordination in comparison with oxygen. This could account for a variation in the lattice parameters between the hydrogen monofluorophosphate and hydrogen sulfates.

The guanidinium compounds

Differences between the (hydrogen) monofluorophosphates were observed in the structures with not only ammonium and the alkali metal cations, but also guanidinium. Both the guanidinium monofluorophosphate and hydrogen monofluorophosphate are not isostructural with the corresponding sulfate and hydrogen sulfate [35]. The structures of

the basic salts are quite different in symmetry; the structure of the sulfate is cubic ($P4_132$), that of the monofluorophosphate monoclinic (Cm), yet some structural similarities do exist between the two. In both structures, three guanidinium cations and two tetrahedra are found in the asymmetric unit. The tetrahedra have special positions on rotation axes in the sulfate and on the mirror plane in the monofluorophosphate. Two of the guanidinium cations are also situated on a special position with the third in a general position. This also applies to both structures. In addition, the long $N\cdots O$ hydrogen bonds have comparable ranges for the $N\cdots O$ distances of 2.87(1)-3.15(2) Å in the sulfate and 2.911(4)-3.128(4) Å in the monofluorophosphate. One of which is bifurcated in the sulfate. Bifurcated hydrogen bonds were not observed in either the hydrogen monofluorophosphates or basic monofluorophosphates. Instead one of the oxygen atoms participates in two hydrogen bonds to two different nitrogen atoms. In both cases, all of the oxygen atoms participate in hydrogen bonding. As expected, an automatic reduction in symmetry results, when oxygen is replaced by fluorine in the tetrahedra. The non-involvement of fluorine in hydrogen bonding also varied the structural features of the hydrogen bond system with each guanidinium cation connected to three SO_4 tetrahedra in the sulfate and 3–4 PO_3F tetrahedra in the monofluorophosphate.

The acid salts with guanidinium are symmetrically more closely related: both are monoclinic, $P2_1/n$ (sulfate) and $P2_1/c$ (monofluorophosphate), but structurally quite diverse. The SO_4 tetrahedra are hydrogen-bonded to form chains instead of cyclic dimers like those in $[C(NH_2)_3]HPO_3F$. The $O-H\cdots O$ bond is also slightly longer than that observed in the monofluorophosphate (2.623(3) compared to 2.562(4) Å). In addition, each of the O atoms on sulfur participates in two $N\cdots O$ hydrogen bonds independent of its function in the $O-H\cdots O$ hydrogen bonding. In the hydrogen monofluorophosphate, only the O atoms, which do not function as a hydrogen donor in $O-H\cdots O$ bond, participate in the hydrogen bonding to the guanidinium cations. A similar behavior was observed in the ammonium structures. Thus, a noninvolvement of two hydrogen atoms in hydrogen bonding is observed in the structure of the hydrogen monofluorophosphate not seen in the structure of the hydrogen sulfate. This noninvolvement could be caused by the absence of a sufficient amount of hydrogen acceptors in the structure due to the nonparticipation of both the fluorine atom and the hydrogen donor O atoms in the hydrogen bonding. It could also be an effect of the packing (fluorine directed away from the N atoms and hydrogen bonds) making hydrogen bonding with these hydrogen atoms unfavorable. In the hydrogen sulfate, all of the guanidinium hydrogen atoms and all of the O atoms participate in hydrogen

bonding.

Thus, isotypism of the sulfate and monofluorophosphates mentioned in [17, 19] was not reflected in the anhydrous hydrogen sulfates and hydrogen monofluorophosphates. At the most, common structural features were observed between the structures. The presence of fluorine in the structures seemed to play a significant role in the variations found. The comparison of the hydrates, $\text{NaHPO}_3\text{F}\cdot 2.5\text{H}_2\text{O}$, $[\text{N}(\text{CH}_3)_4]\text{HPO}_3\text{F}\cdot \text{H}_2\text{O}$, and $\text{Na}_2\text{PO}_3\text{F}\cdot 10\text{H}_2\text{O}$, to the corresponding sulfates and acid salts also showed the influence of fluorine on the crystal structure.

The hydrates

$\text{NaHPO}_3\text{F}\cdot 2.5\text{H}_2\text{O}$

A hydrate identical to $\text{NaHPO}_3\text{F}\cdot 2.5\text{H}_2\text{O}$ [81] is not known for the sodium hydrogen sulfates: α - NaHSO_4 [41], β - NaHSO_4 [36], or the monohydrate [102]. However, the hydrate of sodium hydrogen monofluorophosphate is isostructural to the phosphite, $\text{NaHPO}_3\text{H}\cdot 2.5\text{H}_2\text{O}$, with the lattice parameters: space group $C2/c$, $a = 19.177(3)$, $b = 5.2869(7)$, $c = 12.672(2)$ Å, $\beta = 109.82(3)^\circ$ with $V = 1208.67(3)$ Å³ and $Z = 8$ [103]. In the hydrogen phosphite, the hydrogen atom on phosphorus does not participate in hydrogen bonding or metal coordination. On the basis of this isostructural behavior, one can assume that the hydrogen (phosphite) and fluorine (monofluorophosphate) atoms have equivalent positions and functions in the structures. This strongly supports the general observation that fluorine does not participate in the hydrogen bonding or sodium coordination in the structure. The comparison of the hydrogen monofluorophosphates to the hydrogen phosphites has been made before in [28] and leads to interesting conclusion about the similarity of hydrogen and fluorine when bonded to phosphorus.

$[\text{N}(\text{CH}_3)_4]\text{HPO}_3\text{F}\cdot \text{H}_2\text{O}$

The cubic tetramethyl ammonium acid salts, $[\text{N}(\text{CH}_3)_4]\text{HPO}_3\text{F}\cdot \text{H}_2\text{O}$ and $[\text{N}(\text{CH}_3)_4]\text{HSO}_4\cdot \text{H}_2\text{O}$ [103], are isostructural with the lattice constants, $a = 9.691(2)$ and $9.750(1)$ Å, respectively. Slight differences in the structure were observed in the disorder of the tetrahedral anion. In the sulfate structure, all of the tetrahedral oxygen atoms have general positions and are disordered, whereas in the monofluorophosphate, the fluorine position on phosphorus has a special position on the C_3 axis and is not disordered. The special position of fluorine is probably caused by the HPO_3F tetrahedral symmetry and the orientation of fluorine away from hydrogen bonding and towards the inert part of the structure: the $[\text{N}(\text{CH}_3)_4]^+$ cation; both of which do not apply to the sulfate structure. The variation in tetrahedral disorder and the nonparticipation of fluorine in the hydrogen

bonding could lead to the observed change in the occupancies of the two orientations of the O_w atom from 0.5/0.5 in the sulfate to 0.888(4)/0.112(4) in the monofluorophosphate. Consequently, the hydrogen atom positions also vary in their disorder between the two structures. These small variations, however, are not significant enough to affect the overall isotypism of the compounds. A similar effect was observed in the decahydrate of sodium monofluorophosphate.

Na₂PO₃F·10H₂O

The decahydrate, $Na_2PO_3F \cdot 10H_2O$ [81], is isostructural with the corresponding sulfate, $Na_2SO_4 \cdot 10H_2O$ (Glauber's salt). The sulfate structure has been studied at room temperature with X-ray [104] and neutron [105] single crystal structure analysis. The P–F bond corresponds to the S–O6 bond in [105]. The bridging of the NaO_6 octahedra and the interconnection of the PO_3F tetrahedra to each other via two water molecules are structural features of both compounds. The lengths of the hydrogen bonds in the sulfate (2.75 to 3.01 Å) [105] are similar to those found in the monofluorophosphate (2.718(2) to 3.023(2) Å). One difference between the two structures is the bond lengths in the tetrahedron. All of the S–O bonds lengths are within the range of 1.4–1.5 Å [105], whereas the PO_3F tetrahedron is distorted with three P–O bonds (1.5 Å) and a P–F bond (1.6 Å).

Differences between the structures were also found in bonding and disorder. In the crystal structure analysis of [104], disordered hydrogen bonds were assumed to be present in both the tetramers with water molecules. The authors correlated the possible disorder in the structure to a residual entropy, which was found earlier experimentally [106]. In the neutron diffraction study [105], the exact positions of the hydrogen atoms were determined. Both the SO_4 tetrahedron and the hydrogen atoms in the ring systems are in fact disordered. The two orientations for the SO_4 tetrahedron are rotated about 30° around one of the S–O bond. The disorder of the rings and tetrahedron was confirmed as the source for the zero point entropy. The occupancies were refined to 0.5 for both positions of the disordered hydrogen atoms in the rings and to 0.753/0.247 for the major and minor configurations of the O atoms on sulfur.

The degree of disorder found in $Na_2PO_3F \cdot 10H_2O$ and $Na_2SO_4 \cdot 10H_2O$ [105] differs slightly affecting the hydrogen bond system. In $Na_2PO_3F \cdot 10H_2O$, disorder is only found in the O_{w5}/O_{w11} tetramer and disordering of the PO_3F tetrahedron is questionable. Although very weak peaks with distances of 1.481, 1.423, and 1.869 Å from the P atom were found shifted 23.2 to 30.2 ° from O2, O3, and F, respectively, this weak disorder is rotated around the P–O1 axis not equivalent to the S–O axis of rotation in the sulfate. An additional

refinement of the occupancies yielded values of about 0.97/0.03 compared to occupancies of 0.753/0.247 in $\text{Na}_2\text{SO}_4 \cdot 10\text{H}_2\text{O}$ [105]. Therefore, the second orientation of the PO_3F tetrahedron was neglected in the final refinement. The disorder of the $\text{O}_{\text{w}5}/\text{O}_{\text{w}11}$ ring also varies from that in $\text{Na}_2\text{SO}_4 \cdot 10\text{H}_2\text{O}$ [105] in its assigned occupancies. The occupancies refined and fixed for the disordered hydrogen atoms are 0.67 and 0.33 instead of an equal distribution between the two positions. One explanation for the discrepancies in disorder between the structures could be the measurement temperature: 160 for $\text{Na}_2\text{PO}_3\text{F} \cdot 10\text{H}_2\text{O}$ and 296.5 K for $\text{Na}_2\text{SO}_4 \cdot 10\text{H}_2\text{O}$ [105].

The structure of $\text{Na}_2\text{SO}_4 \cdot 10\text{H}_2\text{O}$ measured at 180 K [107] has the same type of disorder, but the occupancies vary from those found at RT [105]. The new occupancies of the different configurations were refined to 0.938/0.062 for the tetrahedron and 0.569/0.431 for one of the tetramers. The disorder in the second tetramer (0.5/0.5) is not noticeably influenced by temperature, but the temperature does appear to have a significant effect on the disorder of the SO_4 tetrahedron. Fluorine could be the controlling factor for the variation in disorder of the hydrogen atoms in the tetramer of both structures. The replacement of SO_4 with PO_3F also leads to interesting and subtle variations in the hydrogen bond system. The F atom bonds to two water molecules like that found for the corresponding O atom in sulfate. However, it does not participate in a third bond found in sulfate. Thus, by substituting an O atom with a F atom, the disorder is reduced in the structure and the hydrogen bonding of the water molecules to the PO_3F tetrahedron is slightly varied.

The thermal stabilities of the salts also differed. Glauber's salt, $\text{Na}_2\text{SO}_4 \cdot 10\text{H}_2\text{O}$ melts at 305 K [55], whereas the monofluorophosphates has a lower (incongruent) melting point of 283 ± 2 K suggesting a more unstable structure, which may be expected on the basis of fluorine's unusual involvement in the hydrogen bonding.

6.2 Structural Features

The structural features of the hydrogen-bonded HPO_3F tetrahedra were all types that had been observed before in acid salts of oxoacids, except for that of $\beta\text{-RbHPO}_3\text{F}$ due to O/F disordering. Yet, some variations did exist.

Hydrogen-bonded chains were, interestingly enough, observed in the hydrogen sulfates and selenates of larger cations: Rb^+ [8, 33] and Cs^+ [6, 34]. $[\text{C}(\text{NH}_2)_3]\text{HSO}_4$ also formed chains of HSO_4 tetrahedra. In the case of the hydrogen monofluorophosphates, the smaller

cations, Na^+ and $[\text{NH}_2\text{Et}_2]^+$, form such a pattern, whereas cyclic dimers were formed in the structures with larger cations, Cs^+ and $[\text{NHEt}_3]^+$, and $[\text{C}(\text{NH}_2)_3]$.

The following correlation between cation size and pattern of the hydrogen-bonded HPO_3F tetrahedra was observed:

Na (infinite chains) \rightarrow K (branched chains) \rightarrow Rb/NH_4 (tetramers) \rightarrow Cs (cyclic dimers) with a similar trend for the diethyl and triethylammonium structures.

$[\text{NH}_2\text{Et}_2]$ (infinite chains) \rightarrow $[\text{NHEt}_3]$ (cyclic dimers)

The structural pattern of cyclic dimers found in a variety of the hydrogen monofluorophosphates, CsHPO_3F , $[\text{NHEt}_3]\text{HPO}_3\text{F}$, $[\text{C}(\text{NH}_2)_3]\text{HPO}_3\text{F}$, and $[\text{N}_3\text{N}'\text{-dmuH}]\text{HPO}_3\text{F}$, was not very common for the hydrogen sulfates [32]. The only hydrogen sulfate, which contains cyclic HSO_4 dimers, was $\beta\text{-NaHSO}_4$ [36], which was indirectly confirmed with the determination of the isostructural NaHSeO_4 [37]. The frequent occurrence of this pattern in the hydrogen monofluorophosphate suggests the structural stability of this pattern. Its rarity in the hydrogen sulfates implies the structural influence of fluorine in the hydrogen monofluorophosphates.

6.3 Fluorine

Some general bonding characteristics were observed for the fluorine atom in the structures of the hydrogen and basic monofluorophosphates and seem to have a direct influence on the crystal structure formed. The characteristics included

- coordination of larger metal cations,
- nonparticipation in the $\text{N}\cdots\text{X}$ hydrogen bond system,
- and restricted involvement in $\text{O}_{(\text{w})}\cdots\text{X}$ bonding.

In the structures with sodium and N-containing cations, the fluorine atom is only bound to phosphorus. Metal coordination and $\text{N}\cdots\text{F}$ hydrogen bonds were not observed. Thus, the sodium cations were coordinated solely by oxygen atoms in the hydrates, $\text{NaHPO}_3\text{F}\cdot 2.5\text{H}_2\text{O}$, $\text{Na}_2\text{PO}_3\text{F}\cdot 10\text{H}_2\text{O}$, and $\text{Na}_5[\text{N}(\text{CH}_3)_4]\text{PO}_3\text{F}\cdot 18\text{H}_2\text{O}$. The presence of crystal water and its abundance in two of the sodium structures: the decahydrate and mixed salt, in which more than one sodium cation is present, suggest that crystal water is necessary for cation coordination. The only other hydrate structure found was that of tetramethylammonium. The noninvolvement of fluorine in the metal coordination and presence of crystal water have also been observed in other hydrates, in which the cations have an equivalent or smaller radius than that of Na (Tab. 55), such as $\text{CaPO}_3\text{F}\cdot 2\text{H}_2\text{O}$ [73],

$\text{CuPO}_3\text{F}\cdot 2\text{H}_2\text{O}$ [108], $\text{ZnPO}_3\text{F}\cdot 2.5\text{H}_2\text{O}$ [109], and $\text{Ni}(\text{H}_2\text{O})_6(\text{NH}_4)_2(\text{PO}_3\text{F})_2$ [110]. Therefore, it can be concluded that the crystal water is essential for the complete coordination of the metal and a resulting stabilization of the structure.

Tab. 55 Cation radii [111, 112], number of metal-fluorine bonds per fluorine atoms, avg. M–F distance, avg. P–F distances, and V_F in the alkali metal hydrogen monofluorophosphates (Å)

Structure	$\text{NaHPO}_3\text{F}\cdot 2.5\text{H}_2\text{O}$	KHPO_3F	$\text{K}_3[\text{H}(\text{PO}_3\text{F})_2]$	$\alpha\text{-RbHPO}_3\text{F}$	CsHPO_3F
Cation radius	1.16	1.52	1.52	1.66	1.81
M–F bonds	-	1-2	4	2	1
Avg. d(M–F)	-	2.895	3.079	3.106	3.194(3)
Avg. d(P–F)	1.564(2)	1.573	1.594(3)	1.579	1.577(2)
V_F	0.95	1.01-1.15 1.08 (avg.)	1.14	1.08 and 1.12 1.10 (avg.)	1.04

Anhydrous structures were obtained for the hydrogen monofluorophosphates with larger metal cations, K^+ , Rb^+ , and Cs^+ (Tab. 55); the coordination of these cations was fulfilled by both fluorine and oxygen atoms. The number of M–F bonds found per fluorine atom in the structure varied from 1–4. In the MHPO_3F structures, the fluorine atoms coordinate with 1–2 metal cations, whereas the fluorine atom in the structure of $\text{K}_3[\text{H}(\text{PO}_3\text{F})_2]$ is extensively involved in the coordination of four different potassium cations based on the high M/F ratio. Consequently, the P–F bond is lengthened and the total fluorine bond valency of 1.14 is one of the highest observed. This high valency for fluorine suggests structural instability and explains why this type of acid salt was not obtained for other hydrogen monofluorophosphates, although it is a common composition among the sulfates. The high valencies of the F4 atom in KHPO_3F and F2 in $\alpha\text{-RbHPO}_3\text{F}$ also suggest a chemical instability of these compounds, which was reflected by the pseudo-orthorhombic twinning of KHPO_3F and difficult recrystallization of $\alpha\text{-RbHPO}_3\text{F}$.

The compounds with N-containing cations and sodium have average total bond valencies of fluorine that are less than 1.0 with the exception of 1.06 for $\text{Cs}_3(\text{NH}_4)_2(\text{HPO}_3\text{F})_3(\text{PO}_3\text{F})_2$ due to fluorine coordination of cesium (Tab. 56). The low values (< 1.0) reflect an almost complete valency of fluorine based only on the bond to phosphorus. A similar observation was noted in [73]. Thus, the fluorine atom is content by its bond to phosphorus and is basically isolated in the structure aside from the P–F bond. This "isolation" is demonstrated by the packing of the $(\text{H})\text{PO}_3\text{F}$ tetrahedra in the structures. The P–F bond is often directed towards a location in the structure (indicated with * in Tab. 56), where no hydrogen donors or hydrogen atoms are situated. Consequently, no N–H \cdots F hydrogen bonds were observed. This was illustrated most clearly in the structure of $\text{Na}/[\text{NMe}_4]$ (Fig. 16b), in which the $[\text{NMe}_4]^+$ cation is located in a cavity with the P–F bonds pointed

towards the central N atom of the cation. In the structure of [N,N'-dmuH]HPO₃F, the methyl groups provide an inert space in the structure for the fluorine atoms (P–F bond), which gives the structure added stability and could explain the successful synthesis and analysis of this salt despite its very low pH. The absence of these stabilizing methyl groups and additional hydrogen bonds was probably responsible for the failed synthesis of the uronium hydrogen monofluorophosphate.

Tab. 56 Structures with N-containing cations and the total fluorine bond valency

Structure	V_F (avg.)
[PipzH ₂][HPO ₃ F] ₂ *	0.95
[NH ₂ (CH ₂ CH ₃) ₂][HPO ₃ F]*	0.95
[NH(CH ₂ CH ₃) ₃][HPO ₃ F]*	0.95
[N,N'-dmuH]HPO ₃ F*	0.97
[C(NH ₂) ₃][HPO ₃ F]*	0.98
α -NH ₄ HPO ₃ F	0.96
β -NH ₄ HPO ₃ F (RT)	0.96
[N(CH ₃) ₄][HPO ₃ F·H ₂ O]*	0.96
Cs ₃ (NH ₄) ₂ (HPO ₃ F) ₃ (PO ₃ F) ₂	1.06
Na ₅ [NMe ₄](PO ₃ F) ₃ ·18H ₂ O*	0.93
[C(NH ₂) ₃] ₂ PO ₃ F*	0.95

Similar packing behavior is observed in the structure of NaHPO₃F·2.5H₂O, in which the P–F points away from the O–H···O bond between the HPO₃F tetrahedra and the chains of the NaO₆ octahedron and hence, the O_w–H···O_(w) hydrogen bonds. The fluorine atom does not participate in the O_(w)–H···X hydrogen bonding. This applied to all of the structures presented here regarding the O–H···X bonding between the tetrahedra. This also holds true for almost all of the structures in the case of O_w–H···X bonding except for the decahydrate of Na₂PO₃F. In the Na₂PO₃F·10H₂O structure, two hydrogen bonds are found which do involve fluorine as a hydrogen acceptor. Extended bonding of the fluorine atom has a direct effect on the P–F distance, which has been noticed before in mixed alkali metal monofluorophosphates [113]. Consequently, this structure has the longest P–F distance of 1.6082(9) Å and the lowest bond valency for fluorine (0.91) (hydrogen bonds are not considered in the calculation of the V_F) (Tab. 57). These O–H···F bonds connect the tetrahedron to two different water molecules. The question of why unusual O···F bonds are observed can be answered by considering the hydrate structure of Na₅(NMe₄)(PO₃F)₃·18H₂O. This structure with Na⁺ and [NMe₄]⁺ cations also has a high number of water molecules; however, O···F hydrogen bonds were not observed. Instead two of the hydrogen atoms do not participate in the hydrogen bonding at all, which can be directly derived from the presence of fluorine instead of oxygen on phosphorus. A similar

nonparticipation of individual hydrogen atoms was also observed in the acid salts: α - NH_4HPOF and $[\text{C}(\text{NH}_2)_3]\text{HPO}_3\text{F}$, but is more involved on the basis of $\text{O}-\text{H}\cdots\text{O}$ bonding and will be discussed later. A look at the $\text{F}/\text{H}_2\text{O}$ ratio in the hydrates shows that the $\text{F}/\text{H}_2\text{O}$ ratio has increased from 1:6 in $\text{Na}_5[\text{NMe}_4](\text{PO}_3\text{F})_3\cdot 18\text{H}_2\text{O}$ to 1:10 in the decahydrate. Thus, the high $\text{F}/\text{H}_2\text{O}$ ratio found in the decahydrate is probably the deciding factor for the forced $\text{O}\cdots\text{F}$ bonding. Interestingly enough, $\text{O}\cdots\text{F}$ hydrogen bonding has only been observed in hydrated fluorides and fluorometallate hydrates such as $\text{FeSiF}_6\cdot 6\text{H}_2\text{O}$, where no oxygen atoms are bonded to the central atom [30]. A noted feature of the $\text{O}\cdots\text{F}$ bonds in $\text{Na}_2\text{PO}_3\text{F}\cdot 10\text{H}_2\text{O}$ is their long distances of 2.837(2) and 3.003(2) Å. These $\text{O}\cdots\text{F}$ hydrogen bonds are comparable in length to $\text{O}\cdots\text{F}$ bonds found in the hydrates of the hexafluorosilicates and fluorometallates [114, 30]. The long $\text{O}\cdots\text{F}$ distances and the lower melting point of the salt compared to that of $\text{Na}_2\text{SO}_4\cdot 10\text{H}_2\text{O}$ reflect fluorine's hesistance to participate in additional bonds.

6.4 The Tetrahedral Bonding

Certain trends are observed in the bonding of the $(\text{H})\text{PO}_3\text{F}$ tetrahedron within the hydrogen monofluorophosphates (Group I and II) and basic monofluorophosphates (Group III) shown in Tab. 57. Group I includes the hydrogen monofluorophosphates with N-containing cations; the alkali metal hydrogen monofluorophosphates belongs to Group II. The β - RbHPO_3F and $\text{Cs}_3(\text{NH}_4)_2(\text{HPO}_3\text{F})_3(\text{PO}_3\text{F})_2$ are handled separately based on their unique structural features: O/F disordering and the presence of HPO_3F and PO_3F tetrahedra, respectively. Based on the data in Tab. 57, the average $\text{P}-\text{O}_\text{D}\text{H}$ and $\text{P}-\text{F}$ distance increase from 1.544 and 1.560 for Group I to 1.559 and 1.577 Å for Group II, respectively, because of metal coordination to the oxygen and fluorine atoms. The longest $\text{P}-\text{F}$ distance is observed for the basic monofluorophosphates (Group III, 1.588 Å). A parallel trend is found for the average $\text{P}-\text{O}$ distance from Group I to Group III. Although the metal coordination explains the slightly longer distance found for Group II (1.486 Å) compared to that of Group I (1.482 Å), this does not apply to Group III for compounds with sodium and N-containing cations. In this case, the longer $\text{P}-\text{O}$ distance of 1.508 Å can be attributed to extensive hydrogen bonding.

Tab. 57 Avg. bond distances and V_F for the given structures /Å
(Values were averaged for structures with several bonds.)

Structure	V_F	d(P-F)	d(P-O _D H)	d(P-OH _{disd})	d(P-O)
Group I					
[PipzH ₂][HPO ₃ F] ₂	0.95	1.564(1)	1.549(1)		1.493
[NH ₂ (CH ₂ CH ₃) ₂][HPO ₃ F]	0.95	1.566(1)	1.545(1)		1.481
[NH(CH ₂ CH ₃) ₃][HPO ₃ F]	0.95	1.566(2)		1.523	1.452(3)
[N,N'-dmuH][HPO ₃ F]	0.97	1.554(2)	1.542(2)		1.495
[C(NH ₂) ₃][HPO ₃ F]	0.98	1.544(3)	1.531(3)		1.480
α-NH ₄ HPO ₃ F	0.96	1.562	1.548		1.490
β-NH ₄ HPO ₃ F (RT)	0.96	1.566	1.547		1.485
[N(CH ₃) ₄][HPO ₃ F·H ₂ O]	0.96	1.563(1)		1.500(1)	
Avg.	0.96	1.560	1.544		1.482
Group II					
NaHPO ₃ F·2.5H ₂ O	0.95	1.564(2)	1.563(2)		1.492
KHPO ₃ F	1.08	1.573	1.556		1.486
α-RbHPO ₃ F	1.10	1.579	1.557		1.487
CsHPO ₃ F	1.04	1.577(2)		1.528(2)	1.477(3)
K ₃ [H(PO ₃ F) ₂]	1.14	1.594(3)		1.543(4)	1.490
Avg.	1.06	1.577	1.559		1.486
Group III					
Na ₂ PO ₃ F·10H ₂ O	0.91	1.6082(9)			1.508
Na ₅ [NMe ₄](PO ₃ F) ₃ ·18H ₂ O	0.93	1.586			1.509
[C(NH ₂) ₃] ₂ PO ₃ F	0.95	1.571			1.506
Avg.	0.93	1.588			1.508
β-RbHPO ₃ F	1.07	1.538(4)	1.541(4)	1.513(4)	1.485(4)
Cs₃(NH₄)₂(HPO₃F)₃(PO₃F)₂					
HPO ₃ F	1.09	1.572	1.547		1.479
PO ₃ F	1.06	1.574(4)			1.493

The bond distances in the Cs₃(NH₄)₂(HPO₃F)₃(PO₃F) are inconsistent with these trends. Similar P–F distances of 1.572 and 1.574(4) Å are found for the HPO₃F tetrahedra and nondisordered PO₃F tetrahedron, respectively, and are only slightly shorter than that found in Group II. Both distances are practically identical to the 1.573 distance for KHPO₃F, although that of the PO₃F tetrahedron should theoretically be longer. The P–O_DH distance (1.547 Å), on the other hand, approaches that of the Group I compounds (1.544 Å), which is feasible due to the presence of NH₄⁺ cations in the structure. Differences are seen in the P–O bond lengths: 1.479 averaged for the HPO₃F tetrahedra and 1.493 for the PO₃F tetrahedron. The P–O bond of the HPO₃F tetrahedra has the shortest distance overall and that of PO₃F tetrahedron lies between the average distance found for Group II and Group

III as does the composition of the compound with HPO_3F and PO_3F tetrahedra.

The $\beta\text{-RbHPO}_3\text{F}$ compound demonstrates the shortest P–F bond on the basis of O/F disordering in the structure [115]. The P–O bond distance (P–O1) has an expected distance of 1.485(4) Å, which lies directly between the lengths for Group I and II, the P–O3/FA distance is much longer with a length of 1.538(4) Å. This length is difficult to interpret based on the missing hydrogen atom, but may, at least partially, correspond to a P–O_DH bond. It is only slightly shorter than the average for Group I, but deviates significantly from lengths observed in the alkali metal hydrogen monofluorophosphates (Group II).

The P–OH_{disd} distance for the oxygen atom involved in the disordered hydrogen bond has a distance of 1.513(4) Å in $\beta\text{-RbHPO}_3\text{F}$. The hydrogen atom position is disordered not only in $\beta\text{-RbHPO}_3\text{F}$, but also in the structures of $[\text{NHET}_3]\text{HPO}_3\text{F}$, $[\text{N}(\text{CH}_3)_4]\text{HPO}_3\text{F}\cdot\text{H}_2\text{O}$, $\text{K}_3[\text{H}(\text{PO}_3\text{F})_2]$, and CsHPO_3F predominantly with an occupancy of 0.5. Consequently, the corresponding oxygen atom is both a hydrogen donor and hydrogen acceptor ($\frac{1}{2}\text{D}+\frac{1}{2}\text{A}$) and should have a P–O distance between P–O and P–O_DH lengths. The P–OH_{disd} distances varied from 1.500(1) for the hydrate to 1.543(4) for $\text{K}_3[\text{H}(\text{PO}_3\text{F})_2]$ and are, as expected, all between the P–O and P–O_DH distances of Groups I and II. Similar P–O _{$\frac{1}{2}\text{D}+\frac{1}{2}\text{A}$} distances of 1.523 (averaged) and 1.528(2) Å were found for the $[\text{NHET}_3]\text{HPO}_3\text{F}$ and CsHPO_3F structures, respectively, which both feature cyclic dimers of HPO_3F tetrahedra. The short P–OH_{disd} distance in $[\text{N}(\text{CH}_3)_4]\text{HPO}_3\text{F}\cdot\text{H}_2\text{O}$ can be accounted for by the changed occupancy from 0.5 as in the other structures to 0.33. In the case of $\text{K}_3[\text{H}(\text{PO}_3\text{F})_2]$, the same trend is observed for the P–O _{$\frac{1}{2}\text{D}+\frac{1}{2}\text{A}$} distance as was found for the P–F length. The extensive metal coordination results in a P–O _{$\frac{1}{2}\text{D}+\frac{1}{2}\text{A}$} bond longer than that found in the other structures. The P–O _{$\frac{1}{2}\text{D}+\frac{1}{2}\text{A}$} in $\beta\text{-RbHPO}_3\text{F}$ lies between that found for CsHPO_3F and $[\text{N}(\text{CH}_3)_4]\text{HPO}_3\text{F}\cdot\text{H}_2\text{O}$.

6.5 The Hydrogen Bonding

The hydrogen bonding in the hydrogen monofluorophosphates and basic monofluorophosphates was as diverse as the structural patterns and compositions (Tab. 58). The hydrogen bonds classified as O \cdots O (O–H \cdots O bond between the (H) PO_3F tetrahedra), O_w \cdots O (O_w–H \cdots O bond between the crystal water and the (H) PO_3F tetrahedron), O_w \cdots O_w (O_w–H \cdots O_w bond between molecules of crystal water), and N \cdots O (N–H \cdots O bond between the N-containing cation and the (H) PO_3F tetrahedra) are summarized in (Tab. 58). They

have strengths ranging from very strong (<2.5 Å) to strong (2.5 - 2.65 Å) to medium (2.65 - 2.8 Å) to weak (>2.8 Å) [31].

The HPO_3F tetrahedra were connected to each other with both strong and very strong $\text{O}-\text{H}\cdots\text{O}$ bonds. Very strong bonds were found between the tetrahedra in the potassium salts and $\alpha\text{-RbHPO}_3\text{F}$. The only other very strong hydrogen bond found was between the carbonyl group of the dimethyl uronium cation and the HPO_3F tetrahedron. The bond is one of the shortest seen in the hydrogen monofluorophosphates but not as short as the $2.421(3)$ Å bond in $[\text{OC}(\text{NH}_2)_2]\cdot\text{H}_3\text{PO}_4$ [116]. A medium strength and very strong $\text{O}\cdots\text{O}$ hydrogen bonds observed in Cs/NH_4 structure between the HPO_3F and disordered PO_3F tetrahedra could be due to the PO_3F disorder and based on inaccuracy and high standard deviations, but it is not clear if that is the main reason.

The strong $\text{O}_w\cdots\text{O}$ bond found in $[\text{NMe}_4]\text{HPO}_3\text{F}\cdot\text{H}_2\text{O}$ is the only one of its type and is the result of the disordered hydrogen position between the HPO_3F tetrahedron and the crystal water. This is probably due to the bulky cation preventing the interlinking of the HPO_3F tetrahedra. Another rather exotic hydrogen bond was the strong $\text{N}\cdots\text{O}$ bond in $[\text{NHEt}_3]\text{HPO}_3\text{F}$ which is caused by the low functionality of the oxygen atoms (one function per oxygen atom) in the structure due to the absence of metal coordination and a total of two hydrogen atoms in the structure.

It seems that the strength of the $\text{N}\cdots\text{O}$ bond is inversely proportional to the $\text{H}_\text{N}/\text{H}_{(\text{H})}\text{PO}_3\text{F}$ ratio. In $[\text{NHEt}_3]\text{HPO}_3\text{F}$, the ratio is 1 and a strong bond is observed. In the $[\text{NH}_2\text{Et}_2]$ and $[\text{PipzH}_2]$ structures, one medium and one weak $\text{N}\cdots\text{O}$ bond are found with an increased $\text{H}_\text{N}/\text{H}_{(\text{H})}\text{PO}_3\text{F}$ ratio of 2. Medium and weak $\text{N}\cdots\text{O}$ bonds also occur in the Cs/NH_4 structure, in which a ratio of 8:5 (1.6) exists. In the guanidinium structures with very high $\text{H}_\text{N}/\text{H}_{(\text{H})}\text{PO}_3\text{F}$ ratios, only weak $\text{N}\cdots\text{O}$ bonds are observed. One exception is the structure of the uronium salt, $[\text{N},\text{N}'\text{-dmuH}]\text{HPO}_3\text{F}$. Here, although there are only two H_N hydrogen atoms for the one HPO_3F tetrahedron, only weak $\text{N}\cdots\text{O}$ bonds are found based on the additional hydrogen atom of the carbonyl group. Thus, the functionalities of the oxygen atoms must also be considered (Tab. 59). Four hydrogen acceptor functions are present in the uronium structure, whereas only three are found in the $[\text{NH}_2\text{Et}_2]$ and $[\text{PipzH}_2]$ structures.

Tab. 58 Hydrogen bond distance (X...Y) for the structure sorted by bond type and strength; the structures are listed by type of structural pattern (Å)
The bonds with disordered hydrogen positons are indicated with (di).

[illegible]

Tab. 59 Functions of the (H)PO₃F oxygen and fluorine atoms in the structures

Structure	O1/O4/O7/O10		O2/O5/O8/O11			O3/O6/O9/O12				F1/F2/F3/F4	
	M–O	O _A	M–O	O _A	O _{½D+½A}	M–O	O _A	O _{½D+½A}	O _D	M–F	F _A
Chains											
NaHPO ₃ F·2.5H ₂ O	2	1		3			1		1		
[NH ₂ Et ₂][HPO ₃ F]		2		1					1		
[PipzH ₂][HPO ₃ F] ₂		1		2					1		
Branched Chains											
KHPO ₃ F	1/3/3/3	1/0/0/0	2/3/2/2	1/0/1/1		2/1/2/1			1/1/1/1	2/1/1/2	
Isolated Dimers											
K ₃ [H(PO ₃ F) ₂]	5		5			3		1		4	
Cyclic Dimers											
CsHPO ₃ F	3		6		1					1	
[NH ₂ Et ₂][HPO ₃ F]		1			1			1			
[C(NH ₂) ₃][HPO ₃ F]		3		2					1		
[N,N'-dmuH][HPO ₃ F]		2		2					1		
Tetramers											
α-NH ₄ HPO ₃ F		3/3		2/1					1/1		
β-NH ₄ HPO ₃ F (RT)		3/3		2/2					1/1		
RbHPO ₃ F	2/3		3/2	1/1		2/2			1/1	2/2	
Complex/Hydrate											
Cs ₃ NH ₄ (avg.)	2	1	2	1		3			1	2	
[NMe ₄][HPO ₃ F·H ₂ O]								1			
Na ₂ PO ₃ F·10H ₂ O		4		3			3				2
Na ₅ [NMe ₄]	0/1/0	2/2/3		3/3/4			3/3/3				
[C(NH ₂) ₃] ₂ PO ₃ F		2/2		4/4							
β-RbHPO ₃ F	3		2		1	2				2	

The functionality of the oxygen atom was also helpful in explaining the noninvolvement of individual hydrogen atom in hydrogen bonding. As was mentioned before, in the structures, α -NH₄HPO₃F and [C(NH₂)₃]HPO₃F, single hydrogen atoms were not involved in the hydrogen bond system. The comparison of the α -NH₄HPO₃F to its sulfate analogy made clear that an oxygen atom does not act as both an hydrogen acceptor and donor in different hydrogen bonds in the hydrogen monofluorophosphates. The function of the oxygen atom as a hydrogen donor rules out it's ability to also act as a hydrogen acceptor in the structures of the hydrogen monofluorophosphates. This limitation on the oxygen atom's functions and the nonparticipation of fluorine in the hydrogen bonding leads to the noninvolvement of hydrogen atoms in the hydrogen bond system of the hydrogen monofluorophosphates due to the insufficient amount of hydrogen acceptors. This was confirmed by a complete hydrogen bond system in [C(NH₂)₃]₂PO₃F, in which this limitation is no longer valid.

Chapter 7

Summary and Conclusions

In this thesis, the crystal structures and thermal behavior of hydrogen monofluorophosphates and basic monofluorophosphates with alkali metal and N-containing cations were studied. A comparison to the analogous hydrogen sulfates showed interesting structural variations and differences in thermal behavior.

The preparation of the hydrogen monofluorophosphates varied from that of the hydrogen sulfates on the basis of the hydrolysis of the P–F bond and the instability of the pure acid. Nonetheless, a synthesis and method of recrystallization were developed to obtain pure acid salts in sufficient amounts for further investigations. The synthesis involved cation exchange and freeze drying. Freeze drying enabled the isolation of raw products by avoiding the escape of HF and consequent phosphate condensation. This method of preparation led to the synthesis of the hydrogen monofluorophosphates with the following cations:

- the alkali metals: Na^+ , K^+ , Rb^+ , and Cs^+ ,
- N-containing cations: NH_4^+ , $[\text{NMe}_4]^+$, $[\text{NH}_2\text{Et}_2]^+$, $[\text{NHEt}_3]^+$, $[\text{C}(\text{NH}_2)_3]^+$, $\{\text{HOC}[\text{NH}(\text{CH}_3)_2]\}^+$, and $[\text{H}_2\text{N}(\text{CH}_2\text{CH}_2)\text{NH}_2]^{2+}$,

and the basic monofluorophosphates, $\text{Na}_2\text{PO}_3\text{F} \cdot 10\text{H}_2\text{O}$ and $[\text{C}(\text{NH}_2)_3]_2\text{PO}_3\text{F}$. The following mixed salts were also obtained with partial cation exchange:

- $\text{Cs}_3(\text{NH}_4)_2(\text{HPO}_3\text{F})_3(\text{PO}_3\text{F})_2$
- $\text{Na}_5[\text{NMe}_4](\text{PO}_3\text{F})_3 \cdot 18\text{H}_2\text{O}$.

The crystal structures of these compounds had diverse structural features. The HPO_3F tetrahedra were hydrogen-bonded to chains, dimers, and tetramers in the structures of the hydrogen monofluorophosphates. Extensive hydrogen bonding in the basic monofluorophosphates due to high amounts of crystal water led to more complicated structural motifs.

Limitations on the bonding of fluorine were observed in each of the structures, whether it be metal coordination or hydrogen bonding. The valency of fluorine is filled by its bond to phosphorus and thus, generally, the fluorine atom does not participate in additional bonds. This explains why, for the most part, the hydrogen monofluorophosphates are not isostructural with the hydrogen sulfates. Only three atoms of the tetrahedron instead of four atoms are available for hydrogen bonding, which influences the crystal structure. This was further confirmed by the comparison of the decahydrates, $\text{Na}_2\text{PO}_3\text{F} \cdot 10\text{H}_2\text{O}$ and $\text{Na}_2\text{SO}_4 \cdot 10\text{H}_2\text{O}$, which are consequently isostructural based on two $\text{O}-\text{H} \cdots \text{F}$ bonds formed in $\text{Na}_2\text{PO}_3\text{F} \cdot 10\text{H}_2\text{O}$. These were the only hydrogen bonds found that involved fluorine as an hydrogen acceptor or donor.

The investigations on the thermal behavior of NaHPO_3F , $\text{NaHPO}_3\text{F} \cdot 2.5\text{H}_2\text{O}$, CsHPO_3F , and $[\text{NH}_4\text{Et}_3]\text{HPO}_3\text{F}$ found no first-order phase transitions. Stepwise decompositions were observed for the sodium salts, which was attributed to the formation of stable intermediates identified with simulated experiments. The Cs and $[\text{NH}_4\text{Et}_3]$ compounds demonstrated a direct decomposition postmelting. In general, the release of H_2O from the melt occurred at lower temperatures, while HF escaped at higher temperatures. The temperatures, at which this initially occurred, and the first maximum observed were dependent on the cation and presence of crystal water.

The immediate decomposition of CsHPO_3F after melting differs from that of the hydrogen sulfate, CsHSO_4 , which undergoes several phase transitions before decomposition [2]. This suggests that the sulfate has more structural flexibility on the basis of the four oxygen corners of the tetrahedra. In comparison, the monofluorophosphate is limited in its bonding mobility due to the presence of fluorine on one of the tetrahedral vertices. Therefore, phase transitions are not observed prior to decomposition.

It can be concluded that fluorine functions differently in the crystal structures on the basis of its lower valency. Thus, the difference in valency between fluorine and oxygen affects the

hydrogen bonding of the hydrogen monofluorophosphates and thus prevents the expected isotypy of the isoelectronic hydrogen monofluorophosphates and hydrogen sulfates.

Zusammenfassung

In vorliegender Arbeit wurden Synthese, Kristallstruktur und thermisches Verhalten von sauren und basischen Monofluorophosphate untersucht. Es wurden Salze mit Alkalimetall- und N-haltigen Kationen dargestellt und kristallographisch charakterisiert. Die Strukturen dieser Verbindungen wurden dann mit denen der isoelektronischen Hydrogensulfate verglichen.

Schon die Synthese der Hydrogenmonofluorophosphate unterscheidet sich von der der Hydrogensulfate auf Grund der Hydrolyse der P–F Bindung und der Nichtverfügbarkeit der Säure in reiner Form. Dennoch konnte mit Hilfe des Kationenaustausches und der Gefriertrocknung ein erfolgreicher Syntheseweg entwickelt werden. Die Gefriertrocknung hinderte die Abspaltung von HF und Kondensation des Phosphats und ermöglichte die Isolierung der Rohprodukte. Auf diesem Weg gelang die Darstellung der reinen Verbindungen in höherer Ausbeute, so daß es möglich wurde, die Substanzen mit unterschiedlichen Methoden zu untersuchen.

Hergestellt und kristallographisch untersucht wurden folgende Verbindungen:

- Hydrogenmonofluorophosphate mit
 - Alkalimetallkationen: Na, K, Rb, Cs
 - N-haltigen Kationen: NH_4 , NMe_4 , NH_2Et_2 , NHEt_3 , $[\text{C}(\text{NH}_2)_3]$, $\{\text{HOC}[\text{NH}(\text{CH}_3)]_2\}$, $[\text{H}_2\text{N}(\text{CH}_2\text{CH}_2)\text{NH}_2]$,
- basische Monofluorophosphate: $\text{Na}_2\text{PO}_3\text{F} \cdot 10\text{H}_2\text{O}$ und $[\text{C}(\text{NH}_2)_3]_2\text{PO}_3\text{F}$
- gemischte Salze: $\text{Cs}_3(\text{NH}_4)_2(\text{HPO}_3\text{F})_3(\text{PO}_3\text{F})_2$ und $\text{Na}_5[\text{NMe}_4](\text{PO}_3\text{F})_3 \cdot 18\text{H}_2\text{O}$.

Die Kristallstrukturen zeigen eine Vielzahl an Strukturtypen, definiert durch die Verknüpfung der verzerrten HPO_3F Tetraeder über kurze $\text{O}-\text{H} \cdots \text{O}$ Wasserstoffbrückenbindungen zu Ketten, Dimere oder Tetramere. Diese sind ihrerseits über längere $\text{N}-\text{H} \cdots \text{O}$ und $\text{O}_\text{w}-\text{H} \cdots \text{O}$ Wasserstoffbrückenbindungen verknüpft. Kompliziertere Struktur motive sind in den Strukturen der basischen Monofluorophosphate und der gemischten Salze zu finden.

Allgemein werden nur Wasserstoffbrückenbindungen des Typs $\text{N}-\text{H} \cdots \text{O}$ und $\text{O}-\text{H} \cdots \text{O}$ gefunden, dagegen werden keine $\text{N}-\text{H} \cdots \text{F}$ Bindungen in den Strukturen beobachtet. Auch ist mehrheitlich keine Isotypie zwischen sauren und basischen Monofluorophosphaten einerseits und den entsprechenden Sulfaten andererseits zu finden. Isotyp sind nur die Strukturen $[\text{NMe}_4]\text{HPO}_3\text{F} \cdot \text{H}_2\text{O}$ mit $[\text{NMe}_4]\text{HSO}_4 \cdot \text{H}_2\text{O}$ und $\text{Na}_2\text{PO}_3\text{F} \cdot 10\text{H}_2\text{O}$ mit $\text{Na}_2\text{SO}_4 \cdot 10\text{H}_2\text{O}$.

Interessanterweise wurden genau in einer dieser isotypen Strukturen, nämlich der des $\text{Na}_2\text{PO}_3\text{F} \cdot 10\text{H}_2\text{O}$, als Ausnahme zwei $\text{O}-\text{H} \cdots \text{F}$ Bindungen gefunden. Die $\text{O} \cdots \text{F}$ Abstände liegen im Bereich der Abstände der $\text{O}_w \cdots \text{O}$ Bindungen in der Struktur.

Eine Erklärung für das seltene Auftreten von H-Brücken mit Fluor als Akzeptor ist eine fast vollständige Valenz des Fluors durch seine Bindung zum Phosphor. Mehrere Strukturen widerspiegeln diese Tatsache mit der Orientierung der P–F Bindung. Die Bindung wird nach inerten Stellen, wo kein Metall- oder Wasserstoffatom in der Struktur vorhanden ist, ausgerichtet, um ein weiteres Binden des Fluors (Metallkoordination, Wasserstoffbrückenbindung) zu vermeiden.

Weiterhin wurde das thermische Verhalten der Verbindungen NaHPO_3F , $\text{NaHPO}_3\text{F} \cdot 2.5\text{H}_2\text{O}$, CsHPO_3F und $[\text{NH}_4\text{Et}_3]\text{HPO}_3\text{F}$ untersucht. Dies erfolgte mit dem Ziel, Information über mögliche Phasenübergänge und die unterschiedlichen Zersetzungstypen zu bekommen. Sowohl der Kation wie auch die Anwesenheit von Kristallwasser haben Einfluß auf den thermischen Abbau. Die Na-Verbindungen zeigen eine Zersetzung über mehrere Schritte, die zu unterschiedlichen Endprodukten führt ($\text{Na}_3\text{P}_3\text{O}_9$ für NaHPO_3F und $(\text{NaPO}_3)_n$ für das Hydrat). Im Vergleich dazu zersetzt sich CsHPO_3F nach dem Schmelzen direkt zum Endprodukt, ohne stabile Zwischenprodukte zu bilden. Ähnlich verläuft der thermische Abbau der $[\text{NH}_4\text{Et}_3]$ Verbindung, die sich allerdings mit einem Masseverlust von 92,27%, also ohne Bildung eines signifikanten Endproduktes, vollständig zersetzt. Während des thermischen Abbaus wurde die Freisetzung von HF und H_2O bei allen Verbindungen beobachtet, die sich aber bezüglich der Zersetzungstemperatur und -menge zwischen den Substanzen unterscheiden.

Es wurden keine Phasenübergänge erster Ordnung beobachtet. Dies war insbesondere für CsHPO_3F überraschend, da das isoelektronische Hydrogensulfat mehrere Phasenübergänge aufweist [2]. Das Ausbleiben von Phasenübergängen allgemein und auch für CsHPO_3F wird folgendermassen erklärt. Während das Sulfat Bindungsmöglichkeiten an allen vier Ecken des SO_4 -Tetraeders hat, besitzt der $(\text{H})\text{PO}_3\text{F}$ -Tetraeder nur eine begrenzte Flexibilität wegen der Anwesenheit von Fluor an einer Ecke. Fluor bevorzugt eine "isolierte" Position am Phosphor. Anhand der vorliegenden Ergebnisse kann die Schlußfolgerung gezogen werden, daß Fluor auf Grund seiner niedrigeren Valenz im Vergleich zu Sauerstoff andere strukturelle und funktionelle Charakteristika aufweist. Die Valenzunterschiede zwischen Sauerstoff und Fluor haben einen starken Einfluß auf das Wasserstoffbrückenbindungssystem in den Kristallstrukturen der Hydrogenmonofluorophosphate und folglich auf die "Nicht-Isotypie"

zu den Hydrogensulfaten.

Appendix

A.1 Selected Experimental Data of the Single Crystal Analysis

Tab. A1 The Structures with Infinite Chains

Formula	NaHPO ₃ F·2.5H ₂ O*	[NH ₂ Et ₂]HPO ₃ F	[PipzH ₂][HPO ₃ F] ₂
Formula weight	167.01	173.12	286.11
Crystal system	<i>Monoclinic</i>	<i>Orthorhombic</i>	<i>Monoclinic</i>
Space group	<i>C2/c</i>	<i>Pbca</i>	<i>P2₁/c</i>
Crystal Size	0.8 x 0.4 x 0.4	0.4 x 0.2 x 0.1	0.6 x 0.4 x 0.1
<i>a</i> /Å	19.112(4)	12.892(4)	6.020(2)
<i>b</i> /Å	5.341(1)	9.530(3)	13.012(3)
<i>c</i> /Å	12.727(3)	13.555(4)	7.285(2)
β /°	110.18(3)	90	95.09(3)
<i>V</i> /Å ³ , <i>Z</i>	1219.4(4), 8	1665.4(9), 8	568.4(3), 2
$\rho_{\text{calc.}}$ /g·cm ⁻³	1.819	1.381	1.672
Abs. corr. method/ μ /mm ⁻¹	Numerical/0.499	None, 0.304	None, 0.426
Transmission, min./max.	0.8454, 0.9741		
Diffractometer	STADI-4	IPDS	IPDS
Temperature/K	160(2)	180(2)	180(2)
2 θ range for data collection/°	3.0-60.0	3.3-52.1	3.3-52.1
Reflections collected	1567	11898	4462
Data/restraints/parameters	1388/0/103	1581/1/143	1027/1/101
<i>wR</i> ₂	0.0649	0.0591	0.0686
<i>R</i> _I [<i>I</i> >2 σ (<i>I</i>)]	0.0277	0.0288	0.0251
<i>GOOF</i> (<i>obs.</i>)	1.097	0.871	1.036
$\Delta\zeta_{\text{max.}}$ (eÅ ⁻³), $\Delta\zeta_{\text{min.}}$ (eÅ ⁻³)	0.463, -0.340	0.208, -0.219	0.372, -0.276
CSD-Nummer	411 318		

Tab. A2 The Structures with Branched Chains or Isolated Dimers

Formula	KHPO ₃ F	K ₃ [H(PO ₃ F) ₂]
Formula weight	138.08	314.25
Crystal system	<i>Monoclinic</i>	<i>Monoclinic</i>
Space group	<i>P2₁</i>	<i>C2/c</i>
Crystal Size	0.1 x 0.1 x 0.1	0.9 x 0.8 x 0.2
<i>a</i> /Å	7.273(1)	7.973(3)
<i>b</i> /Å	14.086(3)	11.635(4)
<i>c</i> /Å	7.655(2)	9.668(4)
β /°	90.13(3)	113.52(4)
<i>V</i> /Å ³ , <i>Z</i>	784.2(3), 8	822.3(5), 4
$\rho_{\text{calc.}}$ /g·cm ⁻³	2.339	2.538
Abs. corr. method/ μ /mm ⁻¹	None, 1.642	None, 2.076
Diffractometer	IPDS	IPDS
Temperature/K	180(2)	180(2)
2 θ range for data collection/°	3.5-54.2	3.8-56.3
Reflections collected	5600	3397
Data/restraints/parameters	2745/2/233	742/1/63
<i>wR</i> ₂	0.0395	0.1615
<i>R</i> _I [<i>I</i> >2 σ (<i>I</i>)]	0.0214	0.0581
<i>GOOF</i> (<i>obs.</i>)	0.961	1.108
$\Delta\zeta_{\text{max.}}$ (eÅ ⁻³), $\Delta\zeta_{\text{min.}}$ (eÅ ⁻³)	0.283, -0.270	0.804, -1.160

*Data re-refined postpublication.

Tab. A3 The Structures with Cyclic Dimers

Formula	CsHPO ₃ F	[NH ₄ Et ₃]HPO ₃ F
Formula weight	231.89	201.18
Crystal system	<i>Monoclinic</i>	<i>Monoclinic</i>
Space group	<i>C2/m</i>	<i>P2₁/n</i>
Crystal Size	0.4 x 0.2 x 0.1	0.5 x 0.4 x 0.2
<i>a</i> /Å	14.478(8)	10.735(3)
<i>b</i> /Å	5.929(3)	8.214(2)
<i>c</i> /Å	5.413(2)	11.755(3)
β /°	103.30(4)	91.15(3)
<i>V</i> /Å ³ , <i>Z</i>	452.2(3), 4	1036.3(5), 4
$\rho_{\text{calc.}}$ /g·cm ⁻³	3.406	1.289
Abs. corr. method/ μ /mm ⁻¹	Numerical, 8.439	None, 0.254
Transmission, min./max.	0.1927, 0.4768	
Diffractometer	STADI-4	IPDS
Temperature/K	180(2)	180(2)
2 θ range for data collection/°	5.8-62.0	3.3-52.1
Reflections collected	1025	7678
Data/restraints/parameters	530/1/39	1889/1/181
wR_2	0.0373	0.1051
R_1 [<i>I</i> >2 σ (<i>I</i>)]	0.0155	0.0387
<i>GOOF</i> (<i>obs.</i>)	1.127	1.044
$\Delta\zeta_{\text{max.}}$ (eÅ ⁻³), $\Delta\zeta_{\text{min.}}$ (eÅ ⁻³)	0.654, -0.830	0.349, -0.217
CSD-Nummer	410 932	

Tab. A4 The Structures with Cyclic Dimers

Formula	[C(NH ₂) ₃]HPO ₃ F	{HOC[NH(CH ₃) ₂]}HPO ₃ F
Formula weight	159.07	188.10
Crystal system	<i>Monoclinic</i>	<i>Monoclinic</i>
Space group	<i>P2₁/c</i>	<i>P2₁/c</i>
Crystal Size	0.2 x 0.08 x 0.04	0.5 x 0.2 x 0.1
<i>a</i> /Å	6.780(1)	5.435(1)
<i>b</i> /Å	10.089(2)	17.634(4)
<i>c</i> /Å	9.389(2)	8.507(2)
β /°	105.77(3)	100.47(3)
<i>V</i> /Å ³ , <i>Z</i>	618.1(2), 4	801.7(3), 4
$\rho_{\text{calc.}}$ /g·cm ⁻³	1.709	1.558
Abs. corr. method/ μ /mm ⁻¹	None, 0.410	None, 0.335
Diffractometer	IPDS	IPDS
Temperature/K	180(2)	180(2)
2 θ range for data collection/°	3.3-52.1	3.3-52.1
Reflections collected	5235	6260
Data/restraints/parameters	1166/0/110	1445/0/140
wR_2	0.1094	0.0679
R_1 [<i>I</i> >2 σ (<i>I</i>)]	0.0449	0.0383
<i>GOOF</i> (<i>obs.</i>)	0.977	0.870
$\Delta\zeta_{\text{max.}}$ (eÅ ⁻³), $\Delta\zeta_{\text{min.}}$ (eÅ ⁻³)	0.532, -0.435	0.359, -0.274

Tab. A5 The Structures with Cyclic Tetramers

Formula	α -NH ₄ HPO ₃ F	β -NH ₄ HPO ₃ F	β -NH ₄ HPO ₃ F	α -RbHPO ₃ F
Formula weight	117.02	117.02	117.02	184.45
Crystal system	<i>P2₁/n</i>	<i>P</i> $\bar{1}$	<i>P</i> $\bar{1}$	<i>P2₁/n</i>
Space group	<i>Monoclinic</i>	<i>Triclinic</i>	<i>Triclinic</i>	<i>Monoclinic</i>
Crystal Size	0.4 x 0.1 x 0.1	0.7 x 0.6 x 0.4	0.6 x 0.6 x 0.4	0.8 x 0.2 x 0.1
<i>a</i> /Å	7.4650(7)	7.444(5)	7.481(1)	7.465(2)
<i>b</i> /Å	15.586(2)	7.507(6)	7.511(1)	15.551(8)
<i>c</i> /Å	7.5785(9)	7.778(6)	7.782(1)	7.563(4)
α /°	90	84.41(6)	84.31(1)	90
β /°	108.769(9)	84.51(5)	84.20(3)	105.38(5)
γ /°	90	68.33(6)	68.67(2)	90
<i>V</i> /Å ³ , <i>Z</i>	834.9(2), 8	401.2(5), 4	404.31(9), 4	846.5(7), 8
$\rho_{\text{calc.}}$ /g·cm ⁻³	1.862	1.937	1.922	2.894
Abs. corr. Method/ μ /mm ⁻¹	Psi scan, 0.557	None, 0.580	None, 0.576	Psi scan, 11.964
Transmission, min./max.	0.8512, 0.9991			0.3131, 0.9957
Diffractometer	STADI-4	STADI-4	STADI-4	STADI-4
Temperature/K	180(2)	180(2)	310(2)	180(2)
2 θ range for data collection/°	3.0-55.0	3.0-60.0	3.0-52.0*	3.0-52.0
Reflections collected	3240	1802	3158	2938
Data/restraints/parameters	1629/1/149	1609/0/149	1579/149/0	1469/1/118
<i>wR</i> ₂	0.0818	0.1379	0.0735	0.0694
<i>R</i> _I [<i>I</i> >2 σ (<i>I</i>)]	0.0376	0.0535	0.0254	0.0365
<i>GOOF</i> (<i>obs.</i>)	1.016	1.105	1.018	1.025
$\Delta\zeta_{\text{max.}}$ (eÅ ⁻³), $\Delta\zeta_{\text{min.}}$ (eÅ ⁻³)	0.407, -0.421	0.799, -0.659	0.274, -0.358	0.874, -0.647
CSD-Nummer	411 903	411 901	411 902	

Tab. A6 The Complex Structures and Hydrates

Formula	Cs ₃ (NH ₄) ₂ (HPO ₃ F) ₃ (PO ₃ F)	[N(CH ₃) ₄]HPO ₃ F·H ₂ O	Na ₂ PO ₃ F·10H ₂ O*
Formula weight	829.72	191.14	324.11
Crystal system	<i>Monoclinic</i>	<i>Cubic</i>	<i>Monoclinic</i>
Space group	<i>P2₁/c</i>	<i>P2₁3</i>	<i>P2₁/c</i>
Crystal Size	0.6 x 0.6 x 0.6	0.8 x 0.8 x 0.24	0.5 x 0.5 x 0.4
<i>a</i> /Å	20.619(4)	9.691(2)	11.380(3)
<i>b</i> /Å	12.076(2)	9.691(2)	10.234(2)
<i>c</i> /Å	15.856(3)	9.691(2)	13.051(4)
β /°	102.58(2)	90	106.49(3)
<i>V</i> /Å ³ , <i>Z</i>	3853(1), 8	910.1(3), 4	1457.4(7), 4
$\rho_{\text{calc.}}$ /g·cm ⁻³	2.860	1.395	1.477
Abs. corr. Method/ μ /mm ⁻¹	Numerical, 6.067	None, 0.293	None/0.310
Transmission, min./max.	0.0497, 0.1504		
Diffractometer	IPDS	IPDS	IPDS
Temperature/K	180(2)	180(2)	160
2 θ range for data collection/°	3.8-56.3	5.94-51.24	3.8-56.3
Reflections collected	25658	5989	13174
Data/restraints/parameters	6339/27/546	582/0/65	3039/0/242
<i>wR</i> ₂	0.0976	0.0445	0.0581
<i>R</i> _I [<i>I</i> >2 σ (<i>I</i>)]	0.0455	0.0194	0.0266
<i>GOOF</i> (<i>obs.</i>)	1.187	1.006	1.030
$\Delta\zeta_{\text{max.}}$ (eÅ ⁻³), $\Delta\zeta_{\text{min.}}$ (eÅ ⁻³)	1.428, -1.407	0.111, -0.088	0.318, -0.366
CSD-Nummer	410 933		411 317

Tab. A7 The Complex Structures and Hydrates

Formula	$\text{Na}_5[\text{N}(\text{CH}_3)_4](\text{PO}_3\text{F})_3 \cdot 18\text{H}_2\text{O}$	$[\text{C}(\text{NH}_2)_3]_2\text{PO}_3\text{F}$
Formula weight	807.3	218.15
Crystal system	<i>Triclinic</i>	<i>Monoclinic</i>
Space group	<i>P</i> 1	<i>Cm</i>
Crystal Size	0.4 x 0.2 x 0.1	0.6 x 0.5 x 0.4
$a/\text{\AA}$	6.438(2)	13.201(3)
$b/\text{\AA}$	13.438(4)	7.291(1)
$c/\text{\AA}$	19.520(5)	11.680(2)
$\alpha/^\circ$	89.38(3)	90
$\beta/^\circ$	88.84(3)	119.72(3)
$\gamma/^\circ$	88.18(3)	90
$V/\text{\AA}^3, Z$	1687.5(8), 2	976.3(3), 4
$\rho_{\text{calc.}}/\text{g}\cdot\text{cm}^{-3}$	1.589	1.484
Abs. corr. Method/ μ/mm^{-1}	None, 0.348	None, 0.290
Diffractionmeter	IPDS	STADI-4
Temperature/K	180(2)	180(2)
2θ range for data collection/ $^\circ$	3.5-54.2	6.2-50.0
Reflections collected	15107	1847
Data/restraints/parameters	5634/3/536	1844/12/181
wR_2	0.0535	0.1097
R_1 [$I > 2\sigma(I)$]	0.0306	0.0424
<i>GOOF</i> (obs.)	0.857	1.055
$\Delta\zeta_{\text{max.}}(\text{e}\text{\AA}^{-3}), \Delta\zeta_{\text{min.}}(\text{e}\text{\AA}^{-3})$	0.245, -0.347	0.521, -0.280

Tab. A8 The Structure of β -RbHPO₃F

Formula	$\beta\text{-RbHPO}_3\text{F}$
Formula weight	184.45
Crystal system	<i>Monoclinic</i>
Space group	$P2_1/n$
Crystal Size	0.2 x 0.2 x 0.2
$a/\text{\AA}$	7.5157(8)
$b/\text{\AA}$	7.7244(7)
$c/\text{\AA}$	7.5582(8)
$\beta/^\circ$	104.29(1)
$V/\text{\AA}^3, Z$	425.21(7), 4
$\rho_{\text{calc.}}/\text{g}\cdot\text{cm}^{-3}$	2.877
Abs. corr. Method/ μ/mm^{-1}	Numerical, 11.907
Transmission, min./max.	0.0861, 0.1569
Diffractionmeter	IPDS
Temperature/K	180(2)
2θ range for data collection/ $^\circ$	3.5-54.2
Reflections collected	2291
Data/restraints/parameters	757/1/60
wR_2	0.0827
R_1 [$I > 2\sigma(I)$]	0.0352
<i>GOOF</i> (obs.)	1.002
$\Delta\zeta_{\text{max.}}(\text{e}\text{\AA}^{-3}), \Delta\zeta_{\text{min.}}(\text{e}\text{\AA}^{-3})$	1.038, -0.792

A.2 Atomic Coordinates and Equivalent Isotropic Displacement Parameters (\AA^2)

Tab. A9 $\text{NaHPO}_3\cdot 2.5\text{H}_2\text{O}$

	x	y	z	U_{eq}
Na	0.02129(4)	0.91511(2)	0.37976(6)	0.0148(2)
P	0.16319(2)	0.15824(9)	0.28108(4)	0.0117(2)
O1	0.08393(7)	0.1121(3)	0.2672(1)	0.0166(3)
O2	0.18950(7)	0.0805(3)	0.1870(1)	0.0157(3)
O3	0.18251(8)	0.4378(3)	0.3152(1)	0.0201(3)
F	0.21320(6)	0.0128(3)	0.3872(1)	0.0246(3)
O _w 4	0.12324(8)	0.6499(3)	0.48432(1)	0.0172(3)
O _w 5	0.06758(8)	0.8010(3)	0.0343(1)	0.0172(3)
O _w 6	0	0.5747(4)	0.25	0.0185(4)
H1	0.223(2)	0.484(7)	0.309(3)	0.06(1)
H4A	0.148(1)	0.609(5)	0.444(2)	0.032(7)
H4B	0.148(2)	0.711(5)	0.538(2)	0.030(7)
H5A	0.080(2)	0.657(6)	0.015(2)	0.043(8)
H5B	0.107(2)	0.871(6)	0.079(3)	0.043(8)
H6	0.036(2)	0.478(6)	0.255(3)	0.052(9)

Tab. A10 $[\text{NH}_2\text{Et}_2]\text{HPO}_3\text{F}$

	x	y	z	U_{eq}
P	0.22352(3)	0.05963(4)	0.12262(3)	0.0182(1)
O1	0.1212(1)	0.0290(1)	0.0787(1)	0.0302(4)
O2	0.2702(1)	0.2002(1)	0.1062(1)	0.0324(4)
O3	0.3047(1)	-0.0547(1)	0.0988(1)	0.0327(4)
F	0.2098(1)	0.0427(1)	0.23676(8)	0.0448(3)
N	0.4876(1)	0.2129(2)	0.5140(1)	0.0207(4)
C1	0.5412(2)	0.2819(2)	0.5989(2)	0.0299(5)
C2	0.5830(2)	0.1735(3)	0.6689(2)	0.0421(6)
C3	0.4461(2)	0.3121(2)	0.4381(2)	0.0267(5)
C4	0.3829(2)	0.2343(3)	0.3626(2)	0.0419(6)
H1	0.280(2)	-0.122(2)	0.104(2)	0.033(7)
H2	0.534(2)	0.155(2)	0.485(2)	0.034(6)
H3	0.435(2)	0.157(2)	0.536(2)	0.047(7)
H4	0.492(2)	0.338(2)	0.629(2)	0.030(5)
H5	0.596(2)	0.340(2)	0.571(2)	0.030(5)
H6	0.616(2)	0.215(2)	0.721(2)	0.048(7)
H7	0.632(2)	0.114(2)	0.634(2)	0.049(7)
H8	0.527(2)	0.115(2)	0.696(2)	0.047(6)
H9	0.505(2)	0.359(2)	0.410(2)	0.029(5)
H10	0.406(2)	0.377(2)	0.476(2)	0.040(6)
H11	0.359(2)	0.301(3)	0.312(2)	0.055(7)
H12	0.324(2)	0.186(3)	0.395(2)	0.061(7)
H13	0.427(2)	0.166(2)	0.327(2)	0.054(7)

Tab. A11 $[\text{PipzH}_2][\text{HPO}_3\text{F}]_2$

	x	y	z	U_{eq}
P	0.15681(6)	0.66043(3)	0.53021(5)	0.0153(2)
O1	0.3739(2)	0.6412(1)	0.4547(2)	0.0311(3)
O2	0.1346(2)	0.62421(7)	0.7239(1)	0.0203(3)
O3	0.0786(2)	0.77375(8)	0.5135(2)	0.0227(3)
F	-0.0267(2)	0.60235(7)	0.4048(1)	0.0360(3)
N	0.5382(2)	0.5280(1)	0.1913(2)	0.0172(3)
C1	0.6113(2)	0.5967(1)	0.0440(2)	0.0187(3)
C2	0.3403(2)	0.4650(1)	0.1238(2)	0.0206(3)
H1	0.091(4)	0.796(2)	0.422(3)	0.043(7)
H2	0.643(3)	0.486(2)	0.228(2)	0.025(4)
H3	0.500(3)	0.563(2)	0.279(3)	0.030(5)
H4	0.740(3)	0.632(2)	0.090(3)	0.027(5)
H5	0.499(4)	0.642(2)	0.010(3)	0.033(5)
H6	0.222(3)	0.510(2)	0.101(3)	0.023(4)
H7	0.311(3)	0.426(2)	0.208(3)	0.030(5)

Tab. A12 KHPO₃F

	x	y	z	U _{eq}
K1	0.5100(1)	0.40632(8)	0.1939(1)	0.0162(2)
K2	0.1961(2)	0.40318(8)	0.7212(1)	0.0152(2)
K3	0.8080(2)	0.14393(8)	0.5916(1)	0.0167(3)
K4	0.1210(1)	0.17410(7)	0.0744(2)	0.0157(2)
P1	0.7004(2)	0.39931(9)	0.7144(1)	0.0119(2)
P2	0.0522(2)	0.41638(8)	0.2179(2)	0.0116(3)
P3	0.3543(2)	0.64428(9)	-0.1155(2)	0.0109(3)
P4	0.7018(2)	0.66338(8)	0.4077(2)	0.0137(3)
O1	0.6127(5)	0.3513(3)	0.8652(4)	0.0195(8)
O2	0.8296(5)	0.3413(2)	0.6083(4)	0.0201(9)
O3	0.5457(5)	0.4443(3)	0.6009(5)	0.0251(8)
F1	0.8113(5)	0.4863(2)	0.7860(4)	0.0375(8)
O4	0.1452(5)	0.3715(2)	0.0688(4)	0.0165(8)
O5	0.1657(4)	0.4533(2)	0.3647(4)	0.0189(8)
O6	-0.1111(5)	0.3526(3)	0.2815(5)	0.0282(9)
F2	-0.0571(5)	0.5047(2)	0.1426(4)	0.0367(8)
O7	0.2168(5)	0.6033(2)	-0.2366(4)	0.0181(8)
O8	0.5029(5)	0.7069(3)	-0.1885(5)	0.0183(8)
O9	0.2622(4)	0.6917(2)	0.0458(4)	0.0143(7)
F3	0.4580(4)	0.5588(2)	-0.0267(4)	0.0311(8)
O10	0.8001(5)	0.7052(3)	0.2599(4)	0.0221(9)
O11	0.5869(5)	0.5764(2)	0.3690(5)	0.0290(9)
O12	0.5777(6)	0.7374(3)	0.4983(5)	0.035(1)
F4	0.8442(4)	0.6326(3)	0.5509(4)	0.0332(8)
H1	0.59(1)	0.473(5)	0.536(8)	0.09(3)
H2	-0.12(1)	0.348(7)	0.39(1)	0.109
H3	0.302(8)	0.753(4)	0.066(8)	0.05(2)
H4	0.550(7)	0.719(4)	0.609(7)	0.029

Tab. A13 K₃[H(PO₃F)₂]

	x	y	z	U _{eq}	Occ
K1	0.50	0.63681(1)	0.25	0.0094(5)	
K2	0.4051(3)	0.8672(2)	0.5626(2)	0.0419(6)	
P	0.2898(2)	0.3822(1)	0.3230(2)	0.0056(5)	
O1	0.2775(5)	0.2711(3)	0.2435(5)	0.0135(9)	
O2	0.2184(5)	0.4869(3)	0.2286(5)	0.0126(9)	
O3	0.4794(5)	0.4014(3)	0.4514(5)	0.0137(9)	
F	0.1614(5)	0.3655(3)	0.4124(4)	0.0157(8)	
H	0.50(2)	0.464(4)	0.47(2)	0.016	0.50

Tab. A14 CsHPO₃F

	x	y	z	U _{eq}	Occ.
Cs	0.36639(1)	0.5000	0.59125(3)	0.0196(1)	
P	0.11792(7)	0.5000	0.839(2)	0.0179(2)	
O1	0.1593(2)	0.5000	0.6146(5)	0.0246(6)	
O2	0.0630(1)	0.7137(4)	0.8726(3)	0.0245(4)	
F	0.2034(2)	0.5000	1.0808(4)	0.0355(6)	
H	0.034(4)	0.68(1)	0.96(1)	0.03(2)	0.5

Tab. A15 [NHEt₃]HPO₃F

	x	y	z	U _{eq}	Occ.
P	0.18183(4)	0.08544(6)	0.01316(5)	0.0362(2)	
O1	0.3090(1)	0.0467(2)	0.0479(1)	0.0568(5)	
O2	0.1412(2)	-0.0172(2)	-0.0876(2)	0.0555(5)	
O3	0.0846(1)	0.0965(2)	0.1067(2)	0.0579(5)	
F	0.1894(2)	0.2602(2)	-0.0395(2)	0.0873(6)	
N	1.0329(1)	0.6032(2)	0.2838(2)	0.0340(4)	
C1	0.9881(2)	0.4313(2)	0.2716(3)	0.0566(7)	
C2	0.8854(3)	0.4106(3)	0.1895(3)	0.0723(9)	
C3	0.9285(2)	0.7099(2)	0.3300(2)	0.0385(5)	
C4	0.9748(2)	0.8652(3)	0.3818(2)	0.0521(6)	
C5	1.0953(2)	0.6775(3)	0.1809(2)	0.0451(5)	
C6	1.2163(2)	0.5962(5)	0.1469(3)	0.0610(7)	
H1A	0.074(4)	-0.027(4)	-0.090(3)	0.02(1)	0.5
H1B	0.017(2)	0.090(7)	0.095(6)	0.08(2)	0.5
H2	1.089(2)	0.595(2)	0.335(2)	0.042(6)	
H3	0.956(2)	0.332(2)	0.321(2)	0.026(4)	
H4	1.058(3)	0.369(3)	0.243(2)	0.067(8)	
H5	0.809(3)	0.481(4)	0.209(3)	0.10(1)	
H6	0.864(3)	0.285(4)	0.192(2)	0.077(8)	
H7	0.928(3)	0.443(4)	0.106(3)	0.093	
H8	0.873(2)	0.735(3)	0.266(2)	0.049(6)	
H9	0.883(2)	0.644(3)	0.388(2)	0.050(6)	
H10	0.906(3)	0.928(3)	0.413(3)	0.069(8)	
H11	1.017(3)	0.938(3)	0.324(3)	0.070(8)	
H12	1.036(3)	0.839(4)	0.444(3)	0.076(9)	
H13	1.032(2)	0.675(3)	0.119(2)	0.058(7)	
H14	1.114(2)	0.797(3)	0.198(2)	0.056(7)	
H15	1.266(3)	0.588(3)	0.208(3)	0.066(8)	
H16	1.258(3)	0.652(4)	0.094(3)	0.09(1)	
H17	1.201(3)	0.490(5)	0.126(3)	0.10(1)	

Tab. A16 [C(NH₂)₃]HPO₃F

	x	y	z	U _{eq}
P	0.8442(1)	0.60983(8)	0.12227(9)	0.0228(3)
O1	0.6929(3)	0.6236(2)	0.2091(2)	0.0291(6)
O2	1.0434(4)	0.5456(3)	0.1909(3)	0.0416(7)
O3	0.7411(4)	0.5497(4)	-0.0294(3)	0.065(1)
F	0.8974(5)	0.7512(2)	0.0819(5)	0.089(1)
C	0.3386(4)	0.6249(3)	0.5526(3)	0.0200(7)
N1	0.3315(5)	0.7253(4)	0.4580(4)	0.0340(7)
N2	0.2422(5)	0.5139(3)	0.5065(4)	0.0269(6)
N3	0.4456(5)	0.6396(3)	0.6926(3)	0.0285(7)
H1	0.825(8)	0.520(5)	-0.068(6)	0.07(2)
H2	0.253(7)	0.718(4)	0.372(5)	0.05(1)
H3	0.388(7)	0.799(5)	0.489(5)	0.05(1)
H4	0.163(5)	0.505(3)	0.425(4)	0.019(9)
H5	0.245(6)	0.463(4)	0.570(5)	0.04(1)
H6	0.518(5)	0.701(4)	0.715(4)	0.016(9)
H7	0.457(5)	0.565(4)	0.740(4)	0.023(9)

Tab. A17 $\{\text{HOC}[\text{NH}(\text{CH}_3)_2]_2\}\text{HPO}_3\text{F}$

	X	y	z	U _{eq}
P	0.4653(1)	0.56673(3)	0.19277(7)	0.0239(2)
O1	0.4761(3)	0.64289(9)	0.2717(2)	0.0303(4)
O2	0.2754(3)	0.55796(9)	0.0435(2)	0.0319(4)
O3	0.7314(3)	0.5424(1)	0.1749(2)	0.0345(5)
F	0.4018(3)	0.50873(8)	0.3169(2)	0.0496(5)
O4	1.2574(3)	0.7426(1)	0.6445(2)	0.0375(5)
N1	0.9490(4)	0.8121(1)	0.4879(2)	0.0284(5)
N2	0.9383(4)	0.6813(1)	0.4955(3)	0.0270(5)
C1	1.0484(5)	0.7466(1)	0.5418(3)	0.0243(5)
C2	0.7145(5)	0.8192(2)	0.3774(3)	0.0297(6)
C3	1.0453(7)	0.6083(2)	0.5563(4)	0.0396(7)
H1	0.746(7)	0.512(2)	0.096(5)	0.09(1)
H2	1.340(6)	0.789(2)	0.686(4)	0.06(1)
H3	1.030(5)	0.849(2)	0.511(3)	0.027(7)
H4	0.808(5)	0.683(1)	0.429(3)	0.025(7)
H5	0.685(6)	0.874(2)	0.355(3)	0.054(9)
H6	0.600(5)	0.799(2)	0.428(3)	0.034(7)
H7	0.732(4)	0.794(1)	0.283(3)	0.021(6)
H8	1.066(7)	0.611(2)	0.672(5)	0.08(1)
H9	0.930(8)	0.571(2)	0.517(5)	0.09(1)
H10	1.200(8)	0.608(2)	0.528(4)	0.08(1)

Tab. A18 $\alpha\text{-NH}_4\text{HPO}_3\text{F}$

	x	y	z	U _{eq}
P1	0.2399(1)	0.03512(5)	0.77387(9)	0.0142(2)
P2	0.6215(1)	0.29611(4)	0.7249(1)	0.0155(2)
O1	0.3598(3)	-0.0184(1)	0.6930(3)	0.0202(5)
O2	0.1142(3)	-0.0087(1)	0.8629(3)	0.0223(5)
O3	0.1253(3)	0.1039(2)	0.6368(3)	0.0300(6)
F1	0.3787(3)	0.0897(1)	0.9314(3)	0.0342(5)
O4	0.7232(3)	0.2384(1)	0.6322(3)	0.0197(5)
O5	0.7364(3)	0.3592(1)	0.8632(3)	0.0225(5)
O6	0.4450(3)	0.3369(2)	0.5810(3)	0.0277(5)
F2	0.5264(3)	0.2356(1)	0.8339(3)	0.0315(5)
N1	0.7727(4)	0.5528(2)	0.8033(4)	0.0193(5)
N2	0.6024(4)	0.2009(2)	0.2506(4)	0.0186(5)
H1	0.175(6)	0.114(3)	0.570(5)	0.06(2)
H2	0.419(5)	0.389(3)	0.603(5)	0.03(1)
H3	0.778(4)	0.612(2)	0.802(4)	0.013(7)
H4	0.851(5)	0.531(2)	0.766(5)	0.03(1)
H5	0.773(5)	0.538(2)	0.914(6)	0.029(9)
H6	0.669(6)	0.532(2)	0.737(5)	0.022(9)
H7	0.594(5)	0.143(3)	0.250(5)	0.03(1)
H8	0.637(4)	0.220(2)	0.355(5)	0.016(8)
H9	0.492(7)	0.220(3)	0.208(6)	0.05(1)
H10	0.657(6)	0.221(2)	0.180(6)	0.04(1)

Tab. A19 β -NH₄HPO₃F bei 180 K

	x	y	z	U _{eq}
P1	0.2828(2)	0.7668(2)	0.0577(1)	0.0118(3)
P2	0.2561(2)	0.2616(2)	0.4014(1)	0.0122(3)
O1	0.1828(4)	0.6663(4)	-0.0341(4)	0.0171(7)
O2	0.3862(4)	0.8794(4)	-0.0504(4)	0.0183(7)
O3	0.4203(5)	0.6375(5)	0.1959(4)	0.0236(8)
F1	0.1180(4)	0.9142(4)	0.1698(4)	0.0229(6)
O4	0.1440(4)	0.2003(4)	0.5502(4)	0.0165(7)
O5	0.3509(5)	0.4012(4)	0.4286(4)	0.0177(7)
O6	0.3975(5)	0.0798(5)	0.3129(5)	0.0240(8)
F2	0.1075(4)	0.3647(4)	0.2595(4)	0.0256(7)
N1	0.1990(6)	0.2899(6)	0.8873(5)	0.0162(8)
N2	0.7791(6)	0.2082(6)	0.4029(6)	0.0180(8)
H1	0.38(1)	0.56(1)	0.26(1)	0.07(3)
H2	0.47(1)	0.11(1)	0.24(1)	0.09(3)
H3	0.193(6)	0.274(6)	0.782(7)	0.00(1)
H4	0.286(9)	0.175(9)	0.928(8)	0.03(2)
H5	0.089(7)	0.296(7)	0.947(6)	0.01(1)
H6	0.228(8)	0.392(8)	0.901(7)	0.02(1)
H7	0.66(1)	0.285(9)	0.434(8)	0.03(2)
H8	0.80(1)	0.08(1)	0.411(9)	0.04(2)
H9	0.86(1)	0.224(9)	0.472(9)	0.04(2)
H10	0.793(9)	0.238(9)	0.298(9)	0.03(2)

Tab. A20 β -NH₄HPO₃F bei 310 K

	x	y	z	U _{eq}
P1	0.21852(5)	0.73469(5)	0.44267(5)	0.0198(1)
P2	0.24396(5)	0.23839(5)	0.10035(4)	0.0204(1)
O1	0.3166(2)	0.8352(2)	0.5324(2)	0.0292(3)
O2	0.1160(2)	0.6229(2)	0.5508(2)	0.0313(3)
O3	0.0828(2)	0.8611(2)	0.3052(2)	0.0381(3)
F1	0.3805(2)	0.5886(2)	0.3305(1)	0.0381(3)
O4	0.3536(2)	0.3018(2)	-0.0471(1)	0.0286(3)
O5	0.1518(2)	0.0993(2)	0.0723(2)	0.0304(3)
O6	0.1035(2)	0.4168(2)	0.1891(2)	0.0393(3)
F2	0.3912(2)	0.1372(2)	0.2410(1)	0.0426(3)
N1	0.2991(2)	0.2121(2)	0.6151(2)	0.0259(3)
N2	0.2785(2)	0.7102(2)	0.9033(2)	0.0293(3)
H1	0.111(4)	0.930(4)	0.248(4)	0.064(9)
H2	0.041(5)	0.397(5)	0.265(4)	0.08(1)
H3	0.411(3)	0.198(3)	0.557(3)	0.035(5)
H4	0.305(3)	0.224(3)	0.720(3)	0.041(6)
H5	0.275(4)	0.115(4)	0.603(3)	0.050(7)
H6	0.207(4)	0.315(4)	0.575(4)	0.056(7)
H7	0.296(3)	0.593(4)	0.915(3)	0.047(7)
H8	0.356(4)	0.729(4)	0.959(3)	0.052(7)
H9	0.156(4)	0.779(3)	0.935(3)	0.042(6)
H10	0.295(3)	0.752(3)	0.794(3)	0.039(6)

Tab. A21 α -RbHPO₃F

	x	y	z	U _{eq}
Rb1	0.24359(9)	0.45173(4)	1.22459(7)	0.0159(2)
Rb2	0.06693(9)	0.29538(4)	0.74534(7)	0.0169(2)
P1	0.2415(2)	0.5334(1)	0.7329(2)	0.0113(4)
P2	0.5926(2)	0.2973(1)	0.7197(2)	0.0132(4)
O1	0.1455(6)	0.4763(3)	0.8344(6)	0.019(1)
O2	0.3619(6)	0.4943(3)	0.6239(6)	0.020(1)
O3	0.3532(7)	0.6072(3)	0.8516(6)	0.024(1)
F1	0.0875(6)	0.5838(3)	0.5883(5)	0.0270(9)
O4	0.6814(7)	0.2308(3)	0.6317(5)	0.021(1)
O5	0.7163(6)	0.3612(3)	0.8410(5)	0.016(1)
O6	0.4259(8)	0.3401(4)	0.5789(6)	0.026(1)
F2	0.4890(6)	0.2490(3)	0.8487(5)	0.0261(9)
H1	0.35(1)	0.615(6)	0.949(5)	0.050
H2	0.40(1)	0.389(6)	0.60(1)	0.05(3)

Tab. A22 Non-hydrogen atoms in Cs₃(NH₄)₂(HPO₃F)₃(PO₃F)

	x	y	z	U _{eq}	Occ.
Cs1	0.13882(2)	0.10401(4)	0.01109(3)	0.0244(1)	
Cs2	0.20242(2)	0.93719(3)	0.31106(3)	0.0242(1)	
Cs3	0.97521(2)	0.42686(3)	0.81963(3)	0.0238(1)	
Cs4	0.36551(2)	0.88035(4)	0.99348(3)	0.0294(2)	
Cs5	0.52003(3)	0.57770(4)	0.16689(3)	0.0327(2)	
Cs6	0.28876(3)	0.42022(4)	0.18731(3)	0.0328(2)	
P1	0.18478(9)	0.8735(1)	0.8592(1)	0.0186(4)	
P2	0.31651(9)	0.1094(1)	0.1507(1)	0.0201(4)	
P3	0.12436(9)	0.0277(1)	0.5109(1)	0.0175(4)	
P4	0.04636(9)	0.8883(1)	0.1288(1)	0.0158(3)	
P5	0.36480(9)	0.9827(1)	0.4923(1)	0.0218(4)	
P6	0.55004(9)	0.8957(1)	0.1278(1)	0.0191(4)	
P7	0.12612(8)	0.2397(1)	0.7710(1)	0.0137(3)	
P8	0.37535(9)	0.7689(1)	0.2506(1)	0.0194(4)	
O1	0.2213(3)	0.7880(4)	0.9181(3)	0.028(1)	
O2	0.1163(3)	0.9042(4)	0.8644(4)	0.031(1)	
O3	0.2289(3)	0.9768(4)	0.8596(5)	0.040(2)	
F1	0.1788(3)	0.8269(4)	0.7647(3)	0.041(1)	
O4	0.2815(3)	0.1946(4)	0.0895(3)	0.029(1)	
O5	0.3867(3)	0.0827(4)	0.1516(4)	0.036(1)	
O6	0.2731(3)	0.0044(5)	0.1459(4)	0.040(2)	
F2	0.3159(3)	0.1561(4)	0.2430(3)	0.051(1)	
O7	0.0998(3)	-0.0502(4)	0.4389(3)	0.026(1)	
O8	0.1581(3)	-0.0170(4)	0.5956(3)	0.030(1)	
O9	0.1648(3)	0.1246(4)	0.4825(4)	0.031(1)	
F3	0.0608(3)	0.0895(4)	0.5267(3)	0.038(1)	
O10	0.0005(3)	0.8100(4)	0.0728(3)	0.026(1)	
O11	0.1164(3)	0.8973(4)	0.1207(3)	0.023(1)	
O12	0.0442(3)	0.8730(5)	0.2253(3)	0.030(1)	
F4	0.0160(2)	1.0077(4)	0.1090(3)	0.039(1)	
O13	0.3357(3)	1.0426(5)	0.4125(4)	0.042(2)	
O14	0.3953(3)	1.0463(4)	0.5704(3)	0.034(1)	
O15	0.4128(4)	0.8928(6)	0.4742(4)	0.054(2)	
F5	0.3072(3)	0.9140(5)	0.5158(4)	0.065(2)	
O16	0.6208(3)	0.9136(4)	0.1286(4)	0.035(1)	
O17	0.5129(3)	0.8114(4)	0.0687(3)	0.033(1)	
O18	0.5398(3)	0.8800(6)	0.2208(4)	0.037(1)	
F6	0.5153(3)	1.0098(4)	0.1012(3)	0.039(1)	
O19	0.0603(2)	0.1873(4)	0.7321(3)	0.026(1)	
O20	0.1788(3)	0.1621(4)	0.8148(4)	0.038(1)	
O21	0.1222(3)	0.3417(4)	0.8224(4)	0.038(1)	
F7	0.1510(3)	0.2818(4)	0.6896(3)	0.044(1)	
O22	0.3263(7)	0.8191(9)	0.178(1)	0.038(3)	0.65(2)
O23	0.4451(5)	0.788(1)	0.2597(8)	0.060(4)	0.65(2)
O24	0.3568(8)	0.786(1)	0.3370(7)	0.067(5)	0.65(2)
F8	0.3607(4)	0.6434(4)	0.2453(5)	0.073(2)	
O22A	0.310(1)	0.824(2)	0.213(1)	0.022(4)	0.35(2)
O23A	0.4246(8)	0.771(1)	0.191(1)	0.031(5)	0.35(2)
O24A	0.4079(8)	0.803(2)	0.340(1)	0.037(6)	0.35(2)
N1	0.2959(3)	0.2594(6)	0.4225(5)	0.022(1)	
N2	0.4581(3)	0.2470(5)	0.0872(4)	0.019(1)	
N3	0.7965(3)	0.2634(5)	0.9162(4)	0.019(1)	
N4	0.9655(3)	0.2513(5)	0.0813(4)	0.017(1)	

Tab. A23 Hydrogen atoms in $\text{Cs}_3(\text{NH}_4)_2(\text{HPO}_3\text{F})_3(\text{PO}_3\text{F})$

	x	y	z	U_{eq}
H1	0.209(2)	1.020(3)	0.843(7)	0.049
H2	0.290(3)	-0.034(3)	0.173(6)	0.048
H3	0.155(4)	0.135(6)	0.440(2)	0.037
H4	0.012(5)	0.855(8)	0.228(6)	0.036
H5	0.403(4)	0.877(8)	0.431(3)	0.065
H6	0.509(3)	0.858(8)	0.218(7)	0.045
H7	0.321(3)	0.293(6)	0.413(6)	0.027
H8	0.262(2)	0.271(7)	0.406(6)	0.027
H9	0.305(4)	0.204(3)	0.416(6)	0.027
H10	0.293(5)	0.258(7)	0.467(3)	0.027
H11	0.488(3)	0.266(7)	0.115(5)	0.023
H12	0.470(4)	0.223(7)	0.053(4)	0.023
H13	0.442(4)	0.204(5)	0.104(5)	0.023
H14	0.441(4)	0.297(4)	0.089(6)	0.023
H15	0.791(4)	0.252(7)	0.959(3)	0.022
H16	0.810(4)	0.318(4)	0.918(5)	0.022
H17	0.818(4)	0.225(6)	0.901(5)	0.022
H18	0.767(3)	0.243(7)	0.893(5)	0.022
H19	0.993(3)	0.266(7)	0.116(4)	0.021
H20	0.978(4)	0.223(6)	0.048(4)	0.021
H21	0.948(4)	0.303(4)	0.072(5)	0.021
H22	0.948(4)	0.204(5)	0.092(5)	0.021

Tab. A24 $[\text{N}(\text{CH}_3)_4]\text{HPO}_3\text{F}\cdot\text{H}_2\text{O}$

	x	y	z	U_{eq}	Occ.
P	0.05561(3)	0.05561(3)	0.05561(3)	0.0240(2)	
O1	0.0071(2)	-0.0585(2)	0.1483(2)	0.0451(5)	0.888(4)
F	0.14874(8)	0.14874(8)	0.14874(8)	0.0569(5)	
O1A	0.083(1)	-0.0887(9)	0.099(1)	0.037(3)	0.112(4)
O _w 2	0.1796(2)	0.8204(2)	0.3204(2)	0.0413(7)	0.888(4)
O _w 2A	0.132(1)	0.868(1)	0.368(1)	0.036(4)	0.112(4)
N	1.0840(1)	0.58340(1)	0.9160(1)	0.0228(4)	
C1	1.1731(1)	0.6731(1)	0.8269(1)	0.0300(5)	
C2	0.9448(1)	0.6488(2)	0.9292(2)	0.0439(4)	
H1	1.133(2)	0.674(2)	0.738(2)	0.039(4)	
H2	0.956(2)	0.735(2)	0.976(2)	0.052(5)	
H3	0.893(2)	0.588(2)	0.981(2)	0.064(6)	
H4	0.911(2)	0.659(2)	0.838(2)	0.049(5)	
H5	0.044(9)	-0.076(9)	0.201(9)	0.07(3)	0.296(2)
H6	0.224(3)	0.870(3)	0.348(3)	0.040(8)	0.592(3)

Tab. A25 Na₂PO₃F·10H₂O

	x	y	z	U _{eq}	Occ.
Na1	0.76241(5)	0.11186(4)	0.23800(4)	0.0157(1)	
Na2	0.75240(5)	0.24128(4)	0.49222(4)	0.0165(1)	
P	0.25291(3)	0.13985(3)	0.25237(2)	0.01163(9)	
O1	0.24389(9)	0.18154(9)	0.36111(7)	0.0199(2)	
O2	0.28236(9)	-0.00249(8)	0.24331(7)	0.0215(2)	
O3	0.15381(9)	0.19442(9)	0.16000(7)	0.0221(2)	
F	0.37463(8)	0.21322(8)	0.24354(7)	0.0276(2)	
O _w 4	0.35762(9)	0.4508(1)	0.38698(8)	0.0198(2)	
O _w 5	0.8857(1)	-0.04265(9)	0.35764(8)	0.0197(2)	
O _w 6	0.6478(1)	0.28448(9)	0.12452(7)	0.0176(2)	
O _w 7	0.8947(1)	0.1170(1)	0.11909(8)	0.0193(2)	
O _w 8	0.8532(1)	0.28569(9)	0.35744(7)	0.0176(2)	
O _w 9	0.6232(1)	0.1030(1)	0.35289(8)	0.0219(2)	
O _w 10	0.3867(1)	0.57609(9)	0.58247(8)	0.0216(2)	
O _w 11	0.8622(1)	0.45990(9)	0.05456(8)	0.0213(2)	
O _w 12	0.09908(9)	0.35056(9)	0.44299(8)	0.0187(2)	
O _w 13	0.3965(1)	0.1486(1)	0.56141(8)	0.0242(2)	
H4A	0.330(2)	0.383(2)	0.378(2)	0.031(5)	
H4B	0.354(2)	0.476(2)	0.442(2)	0.054(6)	
H5A	0.872(2)	-0.122(2)	0.3482(2)	0.033(5)	
H5B	0.870(2)	-0.021(2)	0.415(2)	0.018(6)	0.67
H5C	0.959(7)	-0.042(5)	0.376(4)	0.02(1)	0.33
H6A	0.671(2)	0.352(2)	0.160(2)	0.040(5)	
H6B	0.574(2)	0.293(2)	0.098(2)	0.043(6)	
H7A	0.967(2)	0.140(2)	0.140(2)	0.048(6)	
H7B	0.899(2)	0.041(2)	0.102(2)	0.042(5)	
H8A	0.825(2)	0.353(2)	0.330(2)	0.033(5)	
H8B	0.929(2)	0.302(2)	0.382(1)	0.033(5)	
H9A	0.558(2)	0.134(2)	0.327(2)	0.045(6)	
H9B	0.615(2)	0.031(2)	0.375(1)	0.029(5)	
H10A	0.367(2)	0.5445(2)	0.633(2)	0.030(5)	
H10B	0.460(2)	0.571(2)	0.6052(2)	0.052(7)	
H11A	0.834(2)	0.511(2)	0.085(2)	0.041(5)	
H11B	0.934(3)	0.458(3)	0.093(2)	0.031(7)	0.67
H11C	0.839(5)	0.484(5)	-0.027(5)	0.03(1)	0.33
H12A	0.139(2)	0.295(2)	0.416(1)	0.030(4)	
H12B	0.118(2)	0.340(2)	0.506(2)	0.035(5)	
H13A	0.354(2)	0.153(2)	0.499(2)	0.036(5)	
H13B	0.365(2)	0.196(2)	0.598(2)	0.036(5)	

Tab. A26 Non-hydrogen atoms in $\text{Na}_5[\text{N}(\text{CH}_3)_4](\text{PO}_3\text{F})_3 \cdot 18\text{H}_2\text{O}$

	x	y	z	U_{eq}
Na1	0.0006(2)	0.55757(7)	0.57768(5)	0.0180(2)
Na2	0.75154(15)	0.74930(7)	0.63313(5)	0.0157(2)
Na3	0.0146(2)	0.06404(7)	0.42505(5)	0.0180(2)
Na4	0.0846(2)	0.19265(7)	0.04182(5)	0.0184(2)
Na5	0.3565(2)	0.68056(7)	0.94487(5)	0.0206(2)
P1	0.3794(1)	0.24486(4)	0.59976(3)	0.0098(1)
P2	0.3528(1)	0.53017(4)	0.80604(3)	0.0112(2)
P3	0.6190(1)	0.03386(4)	0.19290(3)	0.0106(1)
O1	0.1495(3)	0.2480(1)	0.58915(9)	0.0176(4)
O2	0.4898(3)	0.3347(1)	0.57294(8)	0.0157(4)
O3	0.4869(3)	0.1465(1)	0.58096(8)	0.0164(4)
F1	0.4000(2)	0.2511(1)	0.68110(7)	0.0235(4)
O4	0.4537(3)	0.5415(1)	0.87459(8)	0.0200(4)
O5	0.4792(3)	0.5640(1)	0.74478(8)	0.0198(4)
O6	0.1288(3)	0.5675(1)	0.80512(8)	0.0157(4)
F2	0.3407(3)	0.4139(1)	0.79693(8)	0.0288(4)
O7	0.3960(3)	0.0699(1)	0.18821(8)	0.0187(4)
O8	0.7483(3)	0.0983(1)	0.23695(8)	0.0165(4)
O9	0.7219(3)	0.0061(1)	0.12479(8)	0.0168(4)
F3	0.6088(2)	-0.0674(1)	0.23449(7)	0.0249(4)
O _w 11	0.3342(3)	0.5137(1)	0.61589(1)	0.0182(4)
O _w 12	0.8732(4)	0.5984(1)	0.6927(1)	0.0198(5)
O _w 13	0.7441(3)	0.1275(2)	0.0077(1)	0.0203(4)
O _w 14	0.3497(3)	0.1191(1)	0.4444(1)	0.0179(4)
O _w 15	0.8649(4)	0.5016(2)	0.9041(1)	0.0239(5)
O _w 16	0.1015(4)	0.6031(1)	0.4592(1)	0.0199(4)
O _w 17	0.1294(4)	0.1105(2)	0.3031(1)	0.0206(4)
O _w 18	0.3410(3)	0.3786(1)	0.4430(1)	0.0175(4)
O _w 19	0.1013(3)	0.7484(1)	0.5873(1)	0.0195(4)
O _w 20	0.4144(3)	0.7461(2)	0.6844(1)	0.0176(4)
O _w 21	0.1337(4)	0.0170(1)	0.0882(1)	0.0213(5)
O _w 22	0.3321(3)	0.1603(2)	0.9541(1)	0.0214(4)
O _w 23	0.0281(3)	0.6402(1)	0.9963(1)	0.0207(4)
O _w 24	0.8790(3)	0.2449(2)	0.1393(1)	0.0189(4)
O _w 25	0.5402(4)	0.6294(2)	0.0384(1)	0.0275(5)
O _w 26	0.6389(3)	0.7538(2)	0.8857(1)	0.0231(5)
O _w 27	0.6956(3)	0.0219(1)	0.3804(1)	0.0181(4)
O _w 28	0.8990(3)	0.1033(1)	0.5421(1)	0.0189(4)
N	0.8676(3)	0.2414(1)	0.7782(1)	0.0146(5)
C1	0.6814(4)	0.2377(2)	0.8247(1)	0.0254(7)
C2	0.8614(5)	0.3362(2)	0.7371(2)	0.0260(7)
C3	1.0579(4)	0.2365(2)	0.8210(1)	0.0259(7)
C4	0.8725(4)	0.1543(2)	0.7303(1)	0.0232(6)

Tab. A27 Hydrogen atoms in $\text{Na}_5[\text{N}(\text{CH}_3)_4](\text{PO}_3\text{F})_3 \cdot 18\text{H}_2\text{O}$

	x	y	z	U_{eq}
H1A	0.685(1)	0.1748(6)	0.8506(6)	0.038
H1B	0.5550(4)	0.242(1)	0.7975(2)	0.038
H1C	0.682(1)	0.2935(7)	0.8566(6)	0.038
H2A	0.984(1)	0.3379(6)	0.7065(6)	0.039
H2B	0.861(3)	0.3930(2)	0.7681(3)	0.039
H2C	0.735(1)	0.3396(6)	0.7099(7)	0.039
H3A	1.1819(4)	0.239(1)	0.7912(2)	0.039
H3B	1.062(2)	0.1741(7)	0.8475(7)	0.039
H3C	1.055(2)	0.2930(8)	0.8524(7)	0.039
H4A	0.996(1)	0.1572(7)	0.7001(6)	0.035
H4B	0.747(1)	0.1568(7)	0.7026(6)	0.035
H4C	0.878(3)	0.0921(2)	0.7570(1)	0.035
H11A	0.380(6)	0.522(3)	0.649(2)	0.05(1)
H11B	0.385(5)	0.457(3)	0.607(2)	0.037(9)
H12A	0.957(5)	0.590(2)	0.723(2)	0.036(9)
H12B	0.771(6)	0.579(3)	0.707(2)	0.04(1)
H13A	0.722(5)	0.094(2)	0.039(2)	0.04(1)
H13B	0.778(5)	0.088(2)	-0.020(2)	0.04(1)
H14A	0.392(5)	0.125(2)	0.479(2)	0.03(1)
H14B	0.453(5)	0.090(2)	0.426(2)	0.033(9)
H15A	0.743(5)	0.515(2)	0.893(2)	0.030(9)
H15B	0.942(6)	0.511(2)	0.876(2)	0.03(1)
H16A	0.033(5)	0.646(2)	0.445(2)	0.027(9)
H16B	0.214(5)	0.619(2)	0.448(2)	0.03(1)
H17A	0.030(5)	0.108(2)	0.283(2)	0.024(9)
H17B	0.216(6)	0.093(2)	0.276(2)	0.04(1)
H18A	0.432(6)	0.412(3)	0.426(2)	0.06(1)
H18B	0.373(5)	0.362(2)	0.481(2)	0.030(9)
H19A	0.201(5)	0.745(2)	0.611(2)	0.030(9)
H19B	0.152(6)	0.749(2)	0.549(2)	0.04(1)
H20A	0.432(5)	0.694(3)	0.706(2)	0.04(1)
H20B	0.378(5)	0.787(2)	0.706(2)	0.03(1)
H21A	0.212(5)	0.026(2)	0.117(2)	0.04(1)
H21B	0.011(6)	0.016(2)	0.103(2)	0.04(1)
H22A	0.449(5)	0.152(2)	0.969(1)	0.013(7)
H22B	0.313(5)	0.119(2)	0.932(2)	0.03(1)
H23A	0.063(5)	0.607(2)	1.031(2)	0.031(9)
H23B	-0.035(6)	0.605(3)	0.974(2)	0.05(1)
H24A	0.853(6)	0.201(3)	0.170(2)	0.05(1)
H24B	0.889(5)	0.292(3)	0.157(2)	0.04(1)
H25A	0.550(5)	0.581(3)	0.063(2)	0.04(1)
H25B	0.628(6)	0.662(3)	0.049(2)	0.06(1)
H26A	0.686(7)	0.714(3)	0.864(2)	0.07(2)
H26B	0.623(5)	0.802(3)	0.861(2)	0.03(1)
H27A	0.638(6)	-0.035(3)	0.393(2)	0.05(1)
H27B	0.692(5)	0.036(2)	0.345(1)	0.03(1)
H28A	0.967(7)	0.141(3)	0.557(2)	0.07(1)
H28B	0.769(7)	0.123(3)	0.551(2)	0.06(12)

Tab. A28 $[\text{C}(\text{NH}_2)_3]_2\text{PO}_3\text{F}$

	x	y	z	U_{eq}
P1	0.19730(8)	1.000	0.1253(1)	0.0193(3)
P2	0.72469(9)	1.000	0.6976(1)	0.0211(3)
O1	0.3273(3)	1.000	0.1803(3)	0.0257(8)
O2	0.1534(2)	0.8257(3)	0.1554(2)	0.0254(5)
F1	0.1423(3)	1.000	-0.0291(3)	0.0321(7)
O3	0.8559(3)	1.000	0.7739(3)	0.0274(8)
O4	0.6746(2)	0.8262(3)	0.6205(2)	0.0294(6)
F2	0.6853(3)	1.000	0.8040(3)	0.0400(8)
N1	0.4585(3)	0.8415(4)	0.9121(4)	0.0300(6)
N2	0.3000(4)	1.000	0.7566(4)	0.029(1)
N3	0.7783(4)	1.000	0.1489(5)	0.0281(9)
N4	0.9311(3)	0.8423(4)	0.1523(3)	0.0277(6)
N5	0.7691(3)	0.7556(5)	0.4428(3)	0.0334(7)
N6	0.9367(3)	0.7165(5)	0.4318(3)	0.0322(7)
N7	0.9487(3)	0.7771(5)	0.6295(3)	0.0336(7)
C1	0.4051(4)	1.000	0.8595(5)	0.0219(9)
C2	0.8796(4)	1.000	0.1506(5)	0.024(1)
C3	0.8846(3)	0.7501(5)	0.5008(4)	0.0270(7)
H1A	0.425(3)	0.742(4)	0.873(4)	0.03(1)
H1B	0.525(2)	0.835(6)	0.979(3)	0.04(1)
H2	0.264(3)	1.101(4)	0.720(4)	0.04(1)
H3	0.753(4)	0.895(4)	0.156(4)	0.04(1)
H4A	0.993(3)	0.858(6)	0.141(4)	0.023(9)
H4B	0.897(4)	0.743(4)	0.151(5)	0.05(1)
H5A	0.723(4)	0.761(7)	0.360(2)	0.05(2)
H5B	0.734(3)	0.787(6)	0.486(3)	0.03(1)
H6A	0.902(5)	0.683(9)	0.350(7)	0.07(2)
H6B	1.012(2)	0.702(6)	0.481(3)	0.03(1)
H7A	0.928(4)	0.822(6)	0.682(4)	0.04(1)
H7B	1.023(2)	0.767(5)	0.660(4)	0.03(1)

Tab. A29 $\beta\text{-RbHPO}_3\text{F}$

	x	y	z	U_{eq}	Occ.
Rb	0.09942(7)	0.67077(6)	0.23383(7)	0.0203(3)	
P	0.4166(2)	0.3151(2)	0.7413(2)	0.0228(4)	
O1	0.5212(5)	0.1905(5)	0.6565(6)	0.0227(9)	
O2	0.5306(6)	0.4608(5)	0.8456(6)	0.0258(9)	
O3	0.3067(6)	0.2306(5)	0.8652(6)	0.031(1)	0.70
FA	0.3067(6)	0.2306(5)	0.8652(6)	0.031(1)	0.30
F	0.2676(5)	0.3997(6)	0.5888(5)	0.040(1)	0.70
O3A	0.2676(5)	0.3997(6)	0.5888(5)	0.040(1)	0.30
H	0.53(2)	0.50(2)	0.94(1)	0.048	0.50

A.3 Selected Bond Lengths

Tab. A30 K–X bond lengths in KHPO_3F (Å)

	d		d		d		d
K1–O1	2.738(3)	K2–O4	2.724(3)	K3–O5	2.712(4)	K4–O10	2.660(4)
K1–F3	2.757(3)	K2–O3	2.768(4)	K3–F4	2.762(3)	K4–O4	2.787(4)
K1–O11	2.801(4)	K2–O10	2.793(4)	K3–O7	2.783(4)	K4–F1	2.895(3)
K1–O8	2.810(4)	K2–O5	2.827(3)	K3–O2	2.787(4)	K4–O8	2.906(4)
K1–O4	2.861(4)	K2–O7	2.841(4)	K3–O9	2.902(3)	K4–O7	2.930(4)
K1–O5	2.904(4)	K2–O2	2.933(4)	K3–O11	3.041(4)	K4–F4	2.938(3)
K1–O6	2.934(4)	K2–F1	3.075(4)	K3–O12	3.172(5)	K4–F2	2.943(3)
K1–O3	3.171(4)			K3–O10	3.185(4)	K4–O9	2.944(4)

Tab. A31 C–H bond lengths in $[\text{NHEt}_3]\text{HPO}_3\text{F}$ (Å)

	d		d		d
C1–H3	1.06(2)	C3–H8	0.97(3)	C5–H13	0.99(3)
C1–H4	0.97(3)	C3–H9	1.00(3)	C5–H14	1.02(3)
C2–H5	1.03(4)	C4–H10	0.98(3)	C6–H15	0.89(3)
C2–H6	1.06(3)	C4–H11	1.02(3)	C6–H16	0.90(4)
C2–H7	1.12(4)	C4–H12	1.00(3)	C6–H17	0.92(4)

Tab. A32 Rb–X bond lengths in $\alpha\text{-RbHPO}_3\text{F}$ (Å)

	d		d
Rb1–O2	2.871(5)	Rb2–O4	2.848(4)
Rb1–O4	2.931(5)	Rb2–O2	2.916(5)
Rb1–O5	2.980(5)	Rb2–O4′	2.953(5)
Rb1–O1	2.984(5)	Rb2–F2	2.982(4)
Rb1–O1′	2.988(5)	Rb2–O5	3.070(4)
Rb1–O2′	3.034(5)	Rb2–F1	3.112(4)
Rb1–O6	3.180(5)	Rb2–O3	3.113(5)
Rb1–F1	3.205(4)	Rb2–F2′	3.123(4)
Rb1–O3	3.339(5)	Rb2–O6	3.322(5)

Tab. A33 Cs–X bond lengths in Cs₃(NH₄)₂(HPO₃F)₃PO₃F (Å)

	d		d		d
Cs1–O10	3.072(5)	Cs2–O13	3.136(7)	Cs3–O2	3.122(6)
Cs1–F7	3.109(4)	Cs2–O21	3.167(6)	Cs3–O21	3.191(6)
Cs1–O4	3.130(6)	Cs2–O1	3.184(5)	Cs3–O7	3.205(5)
Cs1–O11	3.133(5)	Cs2–O11	3.187(5)	Cs3–O19	3.292(5)
Cs1–O2	3.313(5)	Cs2–O7	3.237(5)	Cs3–O10	3.312(5)
Cs1–O6	3.333(6)	Cs2–O22A	3.28(2)	Cs3–O12	3.321(6)
Cs1–O9	3.368(6)	Cs2–F1	3.285(5)	Cs3–F3	3.336(5)
Cs1–F4	3.448(5)	Cs2–O12	3.341(6)	Cs3–F3′	3.378(5)
Cs1–O20	3.460(7)	Cs2–O6	3.362(7)	Cs3–O8	3.381(6)
Cs1–F4′	3.604(5)	Cs2–F5	3.497(7)	Cs3–F1	3.388(5)
Cs1–O3	3.678(7)	Cs2–O24	3.61(2)	Cs3–O12′	3.696(6)
		Cs2–O9	3.746(6)	Cs3–F4	3.703(5)
Cs4–O17	3.125(6)	Cs5–O14	3.079(6)	Cs6–O8	3.005(6)
Cs4–O1	3.157(6)	Cs5–O5	3.094(6)	Cs6–O16	3.103(6)
Cs4–O24	3.169(12)	Cs5–O23A	3.13(2)	Cs6–F8	3.117(5)
Cs4–O16	3.202(6)	Cs5–O17	3.211(5)	Cs6–O4	3.123(5)
Cs4–O22	3.28(2)	Cs5–O18	3.368(6)	Cs6–O14	3.193(6)
Cs4–O3	3.346(6)	Cs5–O15	3.377(6)	Cs6–F2	3.325(5)
Cs4–O23A	3.38(2)	Cs5–O23	3.459(14)	Cs6–O3	3.464(7)
Cs4–F6	3.414(5)	Cs5–O13	3.499(7)	Cs6–F5	3.465(6)
Cs4–O5	3.460(6)	Cs5–F2	3.503(6)	Cs6–O20	3.495(7)
Cs4–O15	3.472(8)	Cs5–O15′	3.641(9)	Cs6–O18	3.551(6)
Cs4–O24A	3.53(2)	Cs5–O24A	3.65(2)	Cs6–O9	3.710(6)
Cs4–F6′	3.550(5)	Cs5–O23′	3.713(14)	Cs6–F7	3.750(6)

Tab. A34 N–H...O hydrogen bonding in $\text{Cs}_3(\text{NH}_4)_2(\text{HPO}_3\text{F})_3\text{PO}_3\text{F}$ (Å, °)

	d(D–H)	d(H...A)	d(D...A)	∠D–H...A
N1–H7...O16	0.70(8)	2.11(8)	2.771(9)	168(10)
N1–H8...O20	0.69(4)	2.15(7)	2.802(9)	156(10)
N1–H9...O13	0.69(5)	2.09(5)	2.758(9)	172(10)
N1–H10...O4	0.72(5)	2.09(6)	2.785(9)	163(10)
N2–H11...O23	0.70(6)	2.22(7)	2.83(1)	153(9)
N2–H11...O24A	0.75(2)	2.21(6)	2.84(2)	160(9)
N2–H12...O17	0.69(8)	2.08(7)	2.758(8)	162(10)
N2–H13...O5	0.69(7)	2.11(8)	2.792(8)	176(10)
N2–H14...O14	0.72(6)	2.18(6)	2.798(8)	169(10)
N3–H15...O1	0.72(6)	2.07(6)	2.800(8)	177(9)
N3–H16...O8	0.73(5)	2.15(5)	2.832(8)	171(9)
N3–H17...O11	0.74(8)	2.06(7)	2.791(8)	170(9)
N3–H18...O22	0.65(6)	2.08(6)	2.83(1)	178(9)
N3–H18...O22A	0.65(6)	2.11(7)	2.86(2)	163(9)
N4–H19...O19	0.72(6)	2.11(6)	2.837(8)	170(9)
N4–H20...O10	0.71(8)	2.10(7)	2.786(8)	160(9)
N4–H21...O7	0.75(6)	1.99(6)	2.734(8)	172(9)
N4–H22...O2	0.73(7)	2.03(8)	2.783(8)	166(9)

Tab. A35 Na–O, N–C, and C–H bond lengths in $\text{Na}_5[\text{N}(\text{CH}_3)_4](\text{PO}_3\text{F})_3 \cdot 18\text{H}_2\text{O}$ (Å)

d		d		d		d	
Na1–O _w 11	2.343(2)	Na2–O _w 20	2.373(2)	Na3–O _w 27	2.336(2)	Na4–O _w 22	2.351(2)
Na1–O _w 18	2.376(2)	Na2–O _w 18	2.382(2)	Na3–O _w 14	2.342(2)	Na4–O _w 24	2.394(2)
Na1–O _w 16	2.399(2)	Na2–O _w 14	2.399(2)	Na3–O _w 28	2.383(2)	Na4–O _w 26	2.428(2)
Na1–O _w 12	2.438(2)	Na2–O _w 19	2.406(2)	Na3–O _w 28'	2.446(2)	Na4–O _w 23	2.451(2)
Na1–O _w 16	2.466(2)	Na2–O _w 17	2.422(2)	Na3–O _w 17	2.555(3)	Na4–O _w 13	2.492(2)
Na1–O _w 19	2.674(2)	Na2–O _w 12	2.442(2)	Na3–O _w 19	2.616(2)	Na4–O _w 21	2.531(2)
Na5–O _w 25	2.283(2)	N–C1	1.491(4)	C1–H1C	0.98	C3–H3C	0.98
Na5–O _w 26	2.369(3)	N–C2	1.497(3)	C2–H2A	0.98	C4–H4A	0.98
Na5–O4	2.390(2)	N–C3	1.497(3)	C2–H2B	0.98	C4–H4B	0.98
Na5–O _w 23	2.398(2)	N–C4	1.504(3)	C2–H2C	0.98	C4–H4C	0.98
Na5–O _w 24	2.443(2)	C1–H1A	0.98	C3–H3A	0.98		
Na5–O _w 13	2.801(2)	C1–H1B	0.98	C3–H3B	0.98		

Tab. A36 Hydrogen bonding in Na₅[N(CH₃)₄](PO₃F)₃ (Å, °)

D–H...A	D–H	H...D	D...A	∠DHA
O _w 11–H11A...O5	0.72(2)	2.09(3)	2.798(3)	171(3)
O _w 11–H11B...O2	0.84(3)	1.87(3)	2.710(3)	171(3)
O _w 12–H12A...O6	0.81(3)	1.98(3)	2.788(3)	172(3)
O _w 12–H12B...O5	0.76(4)	2.02(4)	2.764(3)	165(3)
O _w 13–H13A...O9	0.78(4)	2.03(4)	2.797(3)	169(3)
O _w 13–H13B...O _w 21	0.78(3)	2.02(4)	2.796(3)	178(3)
O _w 14–H14A...O3	0.73(3)	2.13(3)	2.856(3)	174(3)
O _w 14–H14B...O _w 27	0.83(4)	1.99(4)	2.823(3)	178(3)
O _w 15–H15A...O4	0.83(3)	1.93(3)	2.755(3)	176(3)
O _w 15–H15B...O6	0.74(4)	1.98(4)	2.706(3)	166(3)
O _w 16–H16A...O1	0.77(3)	1.94(3)	2.706(3)	177(3)
O _w 16–H16B...O2	0.79(4)	2.05(4)	2.842(3)	174(3)
O _w 17–H17A...O8	0.76(3)	2.05(3)	2.806(3)	175(3)
O _w 17–H17B...O7	0.79(4)	2.07(4)	2.843(3)	165(3)
O _w 18–H18A...O _w 11	0.81(4)	2.00(5)	2.802(3)	176(4)
O _w 18–H18B...O2	0.79(3)	1.99(3)	2.780(3)	171(3)
O _w 19–H19A...O _w 20	0.80(3)	2.01(3)	2.794(3)	168(3)
O _w 19–H19B	0.81(4)			
O _w 20–H20A...O5	0.82(3)	1.92(3)	2.729(3)	173(3)
O _w 20–H20B...O8	0.73(3)	2.05(3)	2.774(3)	174(3)
O _w 21–H21A...O7	0.77(3)	1.96(3)	2.723(3)	170(3)
O _w 21–H21B...O9	0.84(4)	1.91(4)	2.740(3)	171(3)
O _w 22–H22A...O _w 13	0.81(3)	2.08(3)	2.890(3)	178(3)
O _w 22–H22B...O9	0.72(2)	2.05(2)	2.763(3)	174(3)
O _w 23–H23A...O _w 15	0.84(3)	1.97(3)	2.790(3)	165(3)
O _w 23–H23B...O _w 15	0.77(4)	2.09(4)	2.843(3)	166(4)
O _w 24–H24A...O8	0.85(4)	2.02(4)	2.861(3)	171(3)
O _w 24–H24B...O6	0.73(3)	2.04(4)	2.754(3)	169(3)
O _w 25–H25A...O4	0.80(4)	2.04(4)	2.841(3)	174(3)
O _w 25–H25B...O _w 22	0.76(4)	2.41(4)	2.973(3)	132(3)
O _w 26–H26A	0.74(4)			
O _w 26–H26B...O7	0.80(3)	1.97(4)	2.765(3)	171(3)
O _w 27–H27A...O3	0.90(4)	1.78(4)	2.677(3)	177(3)
O _w 27–H27B...O8	0.71(2)	2.29(2)	2.988(3)	167(3)
O _w 28–H28A...O1	0.74(4)	2.01(4)	2.743(3)	175(4)
O _w 28–H28B...O3	0.89(4)	1.91(5)	2.790(3)	170(3)

A.4 ^{19}F , ^{31}P , and ^1H MAS NMR Data and Spectra

Tab. A37 ^{19}F MAS NMR data

Comp.	δ_{iso} (ppm) ± 0.5 ppm	δ_{aniso} (ppm) ± 5 ppm	η ± 0.1	Linewidth (ppm) ± 0.5 ppm	area % $\pm 0.5\%$
d	-68.5	-67	0.0	2.0	26.4
e	-70.8	-128	0.4	2.0	27.5
c	-72.7	-54	1.0	1.3	23.8
f	-75.0	-121	0.4	1.0	22.3

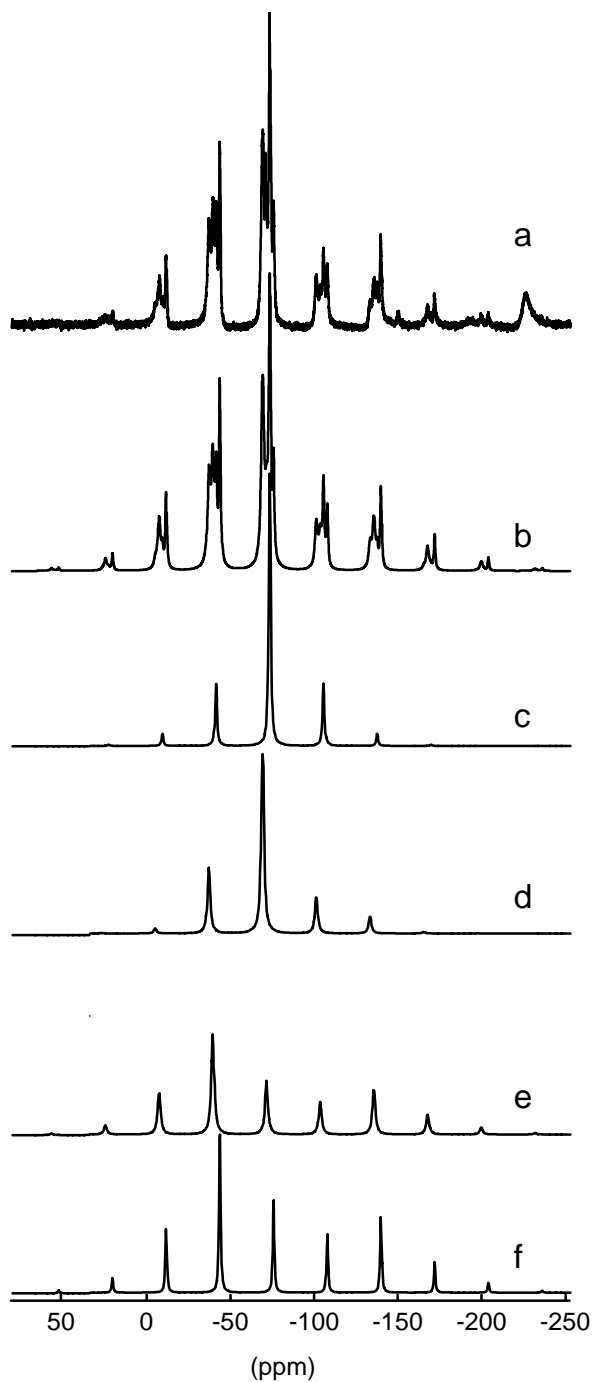
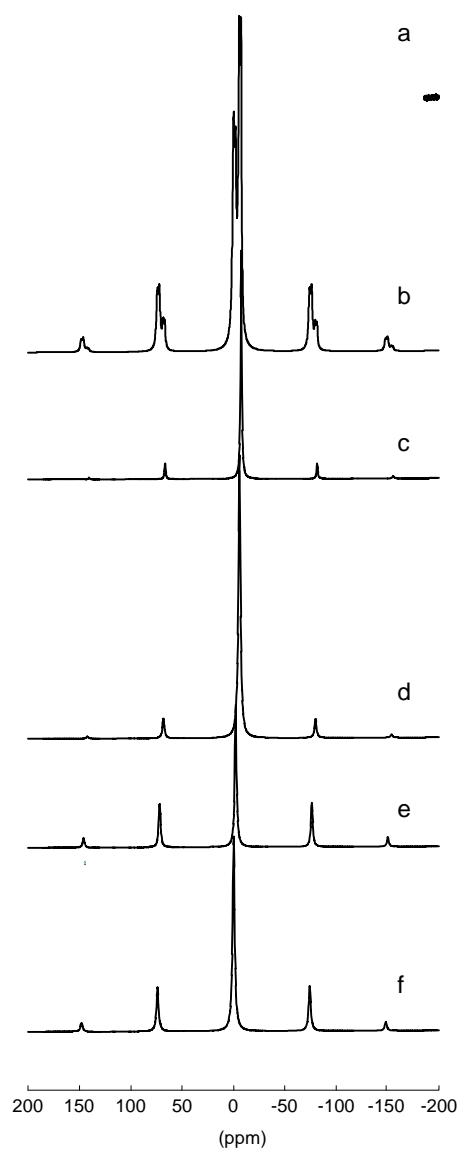


Fig. A1 ^{19}F MAS NMR spectra

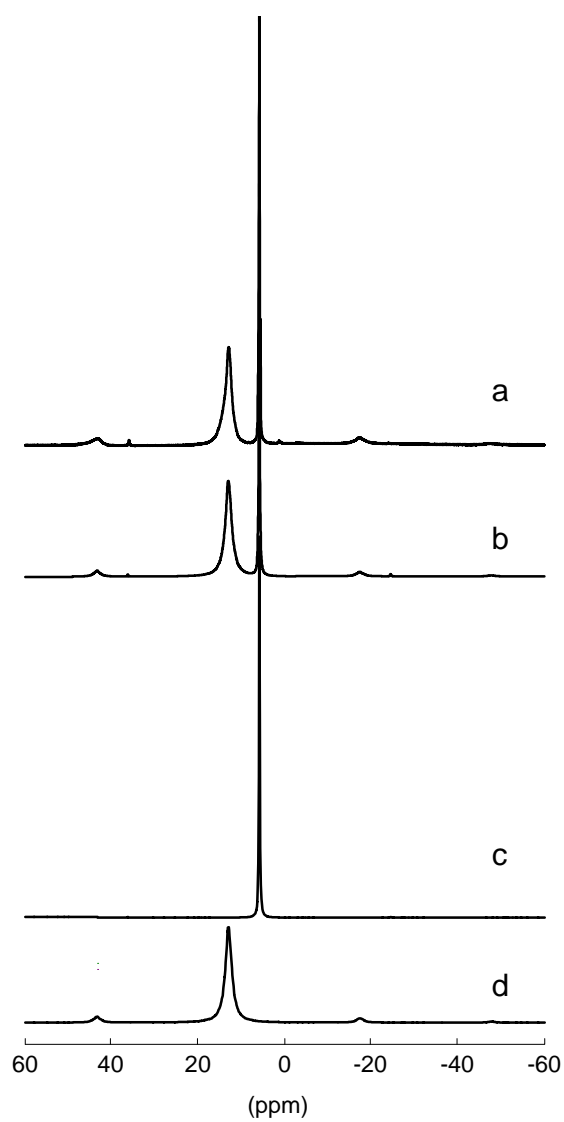
Tab. A38 ^{31}P MAS NMR data

Comp.	δ_{iso} (ppm) ± 0.5 ppm	δ_{aniso} (ppm) ± 5 ppm	η ± 0.1	Linewidth (ppm) ± 0.5 ppm	area % $\pm 0.5\%$
d	-7.5	-75	0.8	1.3	15.1
e	-5.9	-75	0.8	2.3	33.9
c	-2.3	-133	1.0	1.8	19.3
f	-0.3	-119	1.0	2.4	31.7

**Fig. A2** ^{31}P MAS NMR spectra

Tab. A39 ^1H MAS NMR data

Comp.	δ_{iso} (ppm) ± 0.5 ppm	δ_{aniso} (ppm) ± 5 ppm	η ± 0.1	Linewidth (ppm) ± 0.5 ppm	area % $\pm 0.5\%$
c	13.0	-27	0.8	1.8	69.8
d	5.9	-6	0.8	0.2	30.2

**Fig. A3** ^1H MAS NMR spectra

References

1. K. D. Kreuer, Proton Conductivity: Materials and Applications. *Chem. Mater.* **8** (1996) 610.
2. A. I. Baranov, L. A. Shuvalov, N. M. Schagina, Superior conductivity and phase transitions in CsHSO₄ and CsHSeO₄ crystals. *JETP Lett.* **36** (1982) 459.
3. C. J. P. Grotthus, *Ann. Chim.* **58** (1806) 54.
4. K. D. Kreuer, A. Rabenau, W. Weppner, Vehikel-Mechanismus, ein neues Modell zur Deutung der Leitfähigkeit schneller Protonenleiter. *Angew. Chem.* **94** (1982) 224.
5. T. Muiri, A. Daoud, P. Gravereau, Crystal structure and vibrational study of mixed rubidium-caesium hydrogen sulphate Cs_{0.1}Rb_{0.9}HSO₄. *J. Alloys Compd.* **205** (1994) 21.
6. K. Itoh, T. Ukeda, T. Ozaki, E. Nakamura, Redetermination of the Structure of Caesium Hydrogensulfate. *Acta Crystallogr.* **C46** (1990) 358.
7. R. Pepinsky, K. Vedam, S. Hoshino, Y. Okaya, Ammonium Hydrogen Sulfate: A New Ferroelectric with Low Coercive Field. *Phys. Rev.* **111** (1958) 1508.
8. K. Itoh, H. Ohno, S. Kuragaki, Disordered Structure of Ferroelectric Rubidium Hydrogen Sulfate in the Paraelectric Phase. *J. Phys. Soc. Jpn.* **64** (1995) 479-84.
9. F. Payan, R. Haser, On the Hydrogen Bonding in Potassium Hydrogen Sulphate. Comparison with a Previous Crystal Structure Determination. *Acta Crystallogr.* **B32** (1976) 1875-9.
10. E. Kemnitz, C. Werner, S. I. Troyanov, Structural Chemistry of alkaline metal hydrogen sulfates. A review of new structural data. Part II. Hydrogen Bonding Systems. *Eur. J. Solid State Inorg. Chem.* **33** (1996) 581-96.
11. A. Stiewe, Strukturchemische Untersuchungen an sauren Oxosalzen. Ph.D. Thesis: Humboldt University, Berlin, Germany, 2000.
12. C. Werner, Strukturaufklärung von Hydrogensulfaten der Alkali- und Erdalkalimetalle. Ph.D. Thesis: Humboldt University, Berlin, Germany, 2000.
13. N. Wiberg, *Lehrbuch der Anorganische Chemie*; 101st ed., Walter de Gruyter: Berlin, Germany, 1995; p 133.
14. R. F. Weinland, J. Alfa, Über ein Fluorsulfat und ein Fluorphosphat des Kaliums bzw. Rubidium. *Ber. Dtsch. Chem. Ges.* **B31** (1898) 123-6.
15. R. F. Weinland, J. Alfa, Über fluorierte Phosphate, Sulfate, Selenate, Tellurate und Dithionate. *Z. Anorg. Chem.* **21** (1899) 43.

16. W. Lange, The Chemistry of the Fluoro Acids of Fourth, Fifth, and Sixth Group Elements. In *Fluorine Chemistry*; J. H. Simons, Ed.; Academic Press: New York, 1950; Vol. 1, pp 140-9.
17. D. A. Palgrave, Fluorophosphoric Acids and the Fluorophosphates. In *A comprehensive treatise on inorganic and theoretical chemistry*; J. W. Mellor, Ed.; Longmans, Green, and Co.: London, 1971; Vol. 8 (Suppl. 3), pp 843-71.
18. W. Lange, Über die Monofluorophosphorsäure und die Ähnlichkeiten ihrer Salze mit den Sulfaten. *Ber. Dtsch. Ges. Chem.* **B62** (1929) 793-801.
19. J. R. van Wazer, Ed., *Phosphorus and its Compounds*; Interscience Publishers: New York, 1958; Vol. 1, pp 803-17.
20. W. Granier, J. Durand, L. Cot, Composés oxyfluorés du phosphore V. *Rev. Chim. Min.* **12** (1975) 147-55.
21. K. Heide, D.-H. Menz, C. Schmidt, L. Kolditz, Zur thermischen Zersetzung von $\text{CaPO}_3\text{F} \cdot 2\text{H}_2\text{O}$. *Z. Anorg. Allg. Chem.* **520** (1985) 32-8.
22. V. Q. Kinh, G. Montel, Sur la décomposition du monofluorophosphate de calcium et la formation du pyrophosphate de calcium alpha métastable. *Compt. rend.* **249** (1959) 117-9.
23. D.-H. Menz, K. Heide, C. Kunert, C. Mensing, L. Kolditz, Zur thermischen Zersetzung von $\text{SrPO}_3\text{F} \cdot \text{H}_2\text{O}$. *Z. Anorg. Allg. Chem.* **540/541** (1986) 191-7.
24. V. Q. Kinh, G. Montel, Sur la transformation par chauffage du monofluorophosphate de strontium en fluoroapatite. *Compt. rend.* **252** (1961) 3809-11.
25. D.-H. Menz, L. Kolditz, Synthese und thermisches Verhalten von $\text{Mg}(\text{NH}_4)_2(\text{PO}_3\text{F})_2 \cdot 2\text{H}_2\text{O}$. *Z. Chem.* **25** (1985) 189-90.
26. J. Neels, H. Grunze, Darstellung von Alkalihydrogenmonofluorophosphaten. *Z. Anorg. Allg. Chem.* **360** (1968) 284-92.
27. J. Neels, H. Grunze, Kondensationsvorgänge beim Erhitzen von Kaliumhydrogenmonofluorophosphat, $\text{K}[\text{HPO}_3\text{F}]$. *Z. Chem.* **18** (1978) 373.
28. A. K. Idrissi, M. Rafiq, P. Gougeon, R. Guerin, Anilinium Hydrogen Monofluorophosphate, $\text{C}_6\text{H}_8\text{N}^+ \cdot \text{HPO}_3\text{F}^-$. *Acta Crystallogr.* **C51** (1995) 1359-61.
29. N. N. Greenwood, A. Earnshaw, *Chemistry of the Elements*; 1st ed., VCH Verlagsgesellschaft: Weinheim, 1990; p 63. translated by K. Hückmann
30. A. F. Wells, *Structural Inorganic Chemistry*; 5th ed., Clarendon Press: Oxford, 1984; p 357.

31. P. Gilli, V. Bertolasi, V. Ferretti, G. Gilli, Covalent Nature of the Strong Homonuclear Hydrogen Bond. Study of the O-H...O System by Crystal Structure Correlation Methods. *J. Am. Chem. Soc.* **116** (1994) 909-15.
32. E. Kemnitz, S. I. Troyanov, Hydrogen Bonding Systems in Acid Metal Sulfates and Selenates. *Advances in Molecular Structure Research*; M. Hargittai, I. Hargittai; Jai Press Inc.: London, 1998; Vol. 4, pp 79-115.
33. I. P. Makarova, E. E. Rider, V. A. Sarin, I. P. Aleksandrova, V. I. Simonov, Neutron structure studies of the ferroelectric and paraelectric phases of rubidium acid selenate. *Kristallografiya* **34** (1989) 853-61.
34. J. Baran, T. Lis, Structure of cesium hydrogen selenate. *Acta Crystallogr.* **C43** (1987) 811-3.
35. P. Dera, A. Katrusiak, M. Szafranski, Structures of Diguanidinium Sulfate and Guanidinium Hydrogen Sulfate. *Pol. J. Chem.* **74** (2000) 1637-44.
36. E. J. Sonneveld, J. W. Visser, A New Modification of Sodium Hydrogensulphate. *Acta Crystallogr.* **B34** (1978) 643-5.
37. M. A. Zakharov, S. Troyanov, V. B. Rybakov, L. A. Aslanov, E. Kemnitz, *Kristallografiya* **44** (1999) 448.
38. N. G. Hainovsky, Yu. T. Pavlukhim, E. Hairetdinov, *Solid State Ionics* **20** (1986) 249.
39. F. A. Cotton, B. A. Frenz, D. L. Hunter, The Structure of Potassium Hydrogen Sulfate. *Acta Crystallogr.* **B31** (1975) 302-5.
40. J. Baran, T. Lis, Structure of potassium hydrogenselenate. *Acta Crystallogr.* **C42(3)** (1986) 270-2.
41. C. Werner, S. Troyanov, E. Kemnitz, H. Worzala, Hydrogen sulfate with disordered hydrogen atoms-synthesis and structure of $\text{Li}[\text{H}(\text{HSO}_4)_2](\text{H}_2\text{SO}_4)_2$ and refinement of the structure of $\alpha\text{-NaHSO}_4$. *Z. Anorg. Allg. Chem.* **622** (1996) 337-42.
42. D. B. Dell'Amico, F. Calderazzo, F. Marchetti, St. Merlino, *Chem. Mater.* **10** (1998) 524.
43. A. Stiewe, S. Troyanov, E. Kemnitz, Synthesis and crystal structure of metal(I) hydrogen sulfates $\text{Ag}(\text{H}_3\text{O})(\text{HSO}_4)_2$, $\text{Ag}_2(\text{HSO}_4)_2(\text{H}_2\text{SO}_4)$, AgHSO_4 , and $\text{Hg}_2(\text{HSO}_4)_2$. *Z. Anorg. Allg. Chem.* **625** (1999) 329.
44. Y. Noda, S. Uchiyama, K. Kafuku, H. Kasatani, H. Terauchi, Structure Analysis and Hydrogen Bond Character of $\text{K}_3(\text{HSO}_4)_2$. *J. Phys. Soc. Jpn.* **59** (1990) 2804-10.
45. M. Ichikawa, S. Sato, M. Komukae, T. Osaka, Structure of Ferroelastic $\text{K}_3\text{H}(\text{SeO}_4)_2$. *Acta Crystallogr.* **C48** (1992) 1569-71.

46. S. Fortier, M. E. Frasier, R. D. Heyding, Structure of Trirubidium Hydrogenbis(sulfate), $\text{Rb}_3\text{H}(\text{SO}_4)_2$. *Acta Crystallogr.* **C41** (1985) 1139-41.
47. I. P. Makarova, I. A. Verin, N. M. Shchagina, Crystal structure of rubidium selenate ($\text{Rb}_3\text{H}(\text{SeO}_4)_2$). *Kristallografiya* **31** (1986) 178-80.
48. R. Melzer, R. Sonntag, K. S. Knight, $\text{Rb}_3\text{H}(\text{SeO}_4)_2$ at 4K by Neutron Powder Diffraction. *Acta Crystallogr.* **C52** (1996) 1061-3.
49. M. Ichikawa, T. Gustafsson, I. Olovsson, Structural Study of the low-temperature phase transition in tricesium deuterium diselenate. *Acta Crystallogr.* **B48** (1992) 633-9.
50. R. Sonntag, R. Melzer, K. S. Knight, Determination of the hydrogen position in $\text{Cs}_3\text{H}(\text{SeO}_4)_2$ at 483 K. *Physica B* **234-236** (1997) 89-91.
51. W. Joswig, H. Fuess, G. Ferraris, Neutron Diffraction Study of the Hydrogen Bond in Trisodium Hydrogenbissulphate and a Survey of Very Short O-H...O Bonds. *Acta Crystallogr.* **B38** (1982) 2798-2801.
52. S. Suzuki, A. Makita, The Crystal Structure of Triammonium Hydrogen Disulphate, $(\text{NH}_4)_3\text{H}(\text{SO}_4)_2$. *Acta Crystallogr.* **B34** (1978) 732-5.
53. N. A. Tikhomirova, L. A. Shuvalov, L. I. Dontsova, L. G. Bulatova, L. Z. Potikha, Dynamics of domain structure in collinear ferroelectric crystals TGs and GASH. *Kristallografiya* **31(6)** (1986) 1152-9.
54. R. F. Baggio, M. A. R. De Benyacar, B. O. Perazzo, P. K. De Perazzo, Crystal Structure of ferroelectric guanidinium uranyl sulfate trihydrate. *Acta Crystallogr.* **B33** (1977) 3495-9.
55. Römpp Lexikon Chemie, Version 2.0 [CD-ROM]; Georg-Thieme Verlag: Stuttgart/New York, 1999.
56. F. Seel, E. Steigner, I. Burger, Determination of fluorine. *Angew. Chem.* **76(12)** (1964) 532-4.
57. W. Herrendorf, Ph. D. Thesis, University of Karlsruhe, Karlsruhe, Germany. Intergrated in *X-Shape Program: Crystal Optimization for Numerical Absorption Correction*; Revision 1.01, (Stoe & Cie GmbH Deutschland): Darmstadt, 1996.
58. G. M. Sheldrick, *SHELXS-86: Program for Crystal Structure Determination*; University of Göttingen, Göttingen, Germany, 1990.
59. G. M. Sheldrick, *SHELXS-97: Program for Crystal Structure Determination*; University of Göttingen, Göttingen, Germany, 1990.
60. G. M. Sheldrick, *SHELXL-93: Program for the Refinement of Crystal Structures*;

- University of Göttingen, Göttingen, Germany, 1993.
61. G. M. Sheldrick, *SHELXL-97: Program for the Refinement of Crystal Structures*; University of Göttingen, Göttingen, Germany, 1997.
 62. N. E. Brese, M. O'Keefe, Bond-Valence Parameters for Solids. *Acta Crystallogr.* **B47** (1991) 192.
 63. I. D. Brown, Chemical and Steric Constraints in Inorganic Solids. *Acta Crystallogr.* **B48** (1992) 553-72.
 64. L. Pauling, The principles determining the structure of complex ionic crystals. *J. Am. Chem. Soc.* **51** (1929) 1010-26.
 65. PCPDFWIN, Version 1.30 [CD-ROM], International Centre of Diffraction Data: Newtown Square, Pennsylvania, USA, 1997.
 66. J. O. Hill, *For Better Thermal Analysis III, Special Edition of the International Confederation for Thermal Analysis (ICTA)*; 1991.
 67. K. Heide, *Dynamische Thermische Analysenmethoden*; VEB Deutscher Verlag für Grundstoffindustrie: Leipzig, 1982.
 68. H. K. Cammenga, W. Eysel, E. Gmelin, W. Hemminger, G. W. H. Höhne, S. M. Sarge, The temperature calibration of scanning calorimeters. Part 2. Calibraton substances. *Thermochim. Acta* **219** (1993) 333-42.
 69. W. Hemminger, H. K. Cammenga, *Methoden der Thermischen Analyse*; Springer-Verlag Berlin: Heidelberg, 1989.
 70. U. Schülke, R. Kayser, Herstellung von Fluorophosphaten, Difluorophosphaten, Fluorophosphaten und Fluorophosphiten in fluoridhaltigen Harnstoffschmelzen. *Z. Anorg. Allg. Chem.* **600** (1991) 221-6.
 71. PDF-No. 21-1120, Ref. 26.
 72. PDF-No. 18-1215, Ref. Ferguson, Nielsen, Monsanto Research Corporation, Dayton, Ohio, USA; Private Communication, 1963.
 73. A. Perloff, The Crystal Structures of Hydrated Calcium and Ammonium Monofluorophosphates: $\text{CaPO}_3\text{F}\cdot 2\text{H}_2\text{O}$ and $(\text{NH}_4)_2\text{PO}_3\text{F}\cdot \text{H}_2\text{O}$. *Acta Crystallogr.* **C53** (1997) 2183-91.
 74. N. Ohama, M. Machida, Y. Kunifuji, Structure of tetramethylammonium dihydrogen orthophosphate monohydrate. *Acta Crystallogr.* **C43** (1987) 962-4.
 75. A. Waskowska, Diguanidinium hexafluorosilicate. *Acta Crystallogr.* **C53** (1997) 128-30.
 76. W. Lange, Method of Production of Anhydrous Monofluorophosphoric Acid. U. S. Patent

- 2,408,785 , Oct. 8, 1946.
77. H. A. Prescott, S. I. Troyanov, E. Kemnitz, Two Modification of $\text{NH}_4\text{HPO}_3\text{F}$: Synthesis and Crystal Structure. *Z. Anorg. Allg. Chem.* **629** (2002) in press.
 78. H. A. Prescott, S. I. Troyanov, E. Kemnitz, The crystal structures of two hydrogen monofluorophosphates: CsHPO_3F and $\text{Cs}_3(\text{NH}_4)_2(\text{HPO}_3\text{F})_3(\text{PO}_3\text{F})_2$. *Z. Kristallogr.* **215** (2000) 240-5.
 79. PDF-No. 21-0374; Ref. 26.
 80. PDF-No. 21-0987; Ref. 26.
 81. H. A. Prescott, S. I. Troyanov, E. Kemnitz, The Synthesis and Crystal Structures of Two New Hydrated Sodium Monofluorophosphates: $\text{NaHPO}_3\text{F} \cdot 2.5\text{H}_2\text{O}$ (I) and $\text{Na}_2\text{PO}_3\text{F} \cdot 10\text{H}_2\text{O}$ (II) . *J. Solid State Chem.* **156** (2001) 415-21.
 82. A. R. West, *Grundlage der Festkörperchemie*; VCH Verlagsgesellschaft: Weinheim, 1992; translated by M. Hartweg und U. Hartweg
 83. G. Liptay, *Atlas of Thermoanalytical Curves*; Akadémiai Kiadó: Budapest, 1975; Vol. 4, No. 205.
 84. J. E. Macintyre, F. M. Daniel, V. M. Stirling, Eds., *Dictionary of Inorganic Compounds*; Chapman & Hall: London, 1992.
 85. D. E. C. Corbridge, *Phosphorus: An Outline of its Chemistry, Biochemistry, and Technology*; 4th ed., Elsevier: Oxford, 1990; p 231.
 86. H. Falius, Darstellung von Dikalium-difluorodiphosphat durch thermische Reaktion von Tetraphosphatdekaoxid mit Kaliumfluorid. *Angew. Chem.* **80** (1968) 616.
 87. P.A. Bernstein, F. A. Hohurst, M. Eisenberg, D. D. DesMarteau, Preparation of Pure Difluorophosphoric Acid and mu-Oxo-bis(phosphoryl difluoride). *Inorg. Chem.* **10(7)** (1971) 1549-51.
 88. W. E. Hill, D. W. A. Sharp, C. B. Colburn, NMR Spectra of Pyrophosphoryl Tetrafluoride and mu-Oxobis(thiophosphoryl Difluoride). *J. Chem. Phys.* **50(2)** (1960) 612-5.
 89. PDF-No. 11-648, Ref: P. de Wolff, Technische-Physische Dienst, Delft, The Netherlands, ICDD Grant-in-Aid.
 90. H. M. Ondik, The structures of anhydrous sodium trimetaphosphate, Na_3O_9 , and the monohydrate, $\text{Na}_3\text{P}_3\text{O}_9 \cdot \text{H}_2\text{O}$. *Acta Crystallogr.* **18** (1965) 226-32.
 91. H. A. Prescott, M. Feist, J. Przewdziaak, E. Kemnitz, The Thermal Behavior of $\text{NaHPO}_3\text{F} \cdot 2.5\text{H}_2\text{O}$. *Abstracts of Papers*; **2001**, 13th European Symposium on Fluorine Chemistry, Bordeaux, France, 1-P93.

92. C. C. Addison, J. W. Bailey, S. H. Bruce, M. F. A. Dove, R. C. Hibbert, N. Logan, Chemistry in Fuming Nitric Acids-I. NMR Spectroscopic Study of PF_5 , HPO_2F_2 , and P_4O_{10} in the Solvent System 44 wt.% N_2O_4 in 100% HNO_3 . *Polyhedron* **2** (1983) 651-6.
93. PDF-No. 11-650, Ref: P. de Wolff, Technische-Physische Dient. Delft, The Netherlands, ICDD Grant-in-Aid.
94. P. D. Ray, Isomorphism and chemical homology. *Nature* **126** (1930) 310-11.
95. H. C. Goswami, On the Study of some Monofluorophosphates and their Analogy and Isomorphism with Sulphates. *J. Indian Chem. Soc.* **14** (1937) 660.
96. J. P. Ashmore, H. E. Petch, The Structure of RbHSO_4 in its Paraelectric Phase. *Can. J. Phys.* **53** (1975) 2694-702.
97. R. Pepinsky, K. Vedam, Ferroelectric transition in RbHSO_4 . *Phys. Rev.* **117** (1960) 1502.
98. T. Asahi, K. Hasebe, Crystal structure of the high pressure phase of RbHSO_4 . *J. Phys. Soc. Jpn.* **65** (1996) 3233.
99. V. Varma, N. Ragavittal, C. N. R. Rao, A Study of Superionic CsHSO_4 and $\text{Cs}_{1-x}\text{Li}_x\text{HSO}_4$ by Vibrational Spectroscopy and X-ray Diffraction. *J. Solid State Chem.* **106** (1993) 164-73.
100. R. J. Nelmes, An X-ray Diffraction Determination of the Crystal Structure of Ammonium Hydrogen Sulphate above the Ferroelectric Transition. *Acta Crystallogr.* **B27** (1971) 272-81.
101. S. I. Troyanov, I. V. Morozov, M. Reehius, E. Kemnitz, Synthesis of Two Modifications of $(\text{NH}_4)_2\text{SeO}_4(\text{H}_3\text{PO}_4)$ and Their Crystal Structure as Probed by X-ray and Neutron Diffraction. *Russ. J. Inorg. Chem.* **44** (1999) 1924.
102. M. Catti, G. Ferraris, M. Franchini-Angela, Hydrogen bonding in the crystalline state. $\text{NaHSO}_4 \cdot \text{H}_2\text{O}$ (Matteuccite), a pseudosymmetric crystal structure. *Atti Accad. Sci. Torino, Cl. Fis., Mat. Nat.* **109** (1975) 531-45.
103. S. I. Troyanov, Humboldt University, Berlin, Germany, Private Communication, 2001.
104. H. W. Ruben, D. H. Templeton, R. D. Rosenstein, I. Olovsson, Crystal structure and entropy of sodium sulfate decahydrate. *J. Am. Chem. Soc.* **83** (1961) 820-4.
105. H. A. Levy, G. C. Lisensky, Crystal structures of sodium sulfate decahydrate (Glauber's salt) and sodium tetraborate decahydrate (borax). Redetermination by neutron diffraction. *Acta Crystallogr* **B34** (1978) 3502-10.
106. G. Brodale, W. F. Giauque, Heat of hydration of sodium sulfate. Low-temperature heat

- capacity and entropy of sodium sulfate decahydrate. *J. Am. Chem. Soc.* **80** (1958) 2042-4.
107. Structural Information has been deposited at the Fachinformationszentrum Karlsruhe, D-76344 Eggenstein-Leopoldshafen, Germany under the depository number: CSD-No. 411348.
108. M. Zeibig, B. Wallis, F. Möwius, M. Meisel, Darstellung und Kristallstruktur von Kupfer(II)-monofluorophosphat-Dihydrat $\text{CuPO}_3\text{F}\cdot 2\text{H}_2\text{O}$. *Z. Anorg. Allg. Chem.* **600** (1991) 231.
109. J. Durand, A. Larbot, L. Cot, M. Duprat, F. Dabosi, Etude Structurale de $\text{ZnPO}_3\text{F}\cdot 2.5\text{H}_2\text{O}$ Nouvel Inhibiteur de Corrosion. *Z. Anorg. Allg. Chem.* **504** (1983) 163-72.
110. M. Berraho, C. K'Rha, A. Vegas, M. Rafiq, Structure of $\text{Ni}(\text{H}_2\text{O})_6(\text{NH}_4)_2(\text{PO}_3\text{F})_2$. *Acta Crystallogr.* **C48** (1992) 1350-52.
111. R. D. Shannon, C. T. Prewitt, Effective ionic radii in oxides and fluorides. *Acta Crystallogr.* **B25** (1969) 925-46.
112. R. D. Shannon, C. T. Prewitt, *Acta Crystallogr.* **A32** (1976) 751.
113. J. Duran, W. Garnier, L. Cot, J. L. Galigné, Etudes Structurales de Composés Oxyfluorés du P(V).III. Structure Cristallin de $\text{NaK}_3(\text{PO}_3\text{F})_2$. *Acta Crystallogr.* **B31** (1975) 1533-5.
114. G. Rother, Synthese, Struktur und thermisches Verhalten von Fluorometallaten(III) mit organischen N-haltigen Kationen. Ph.D. Thesis: Humboldt University, Berlin, Germany, 1998.
115. A. Vij, X. Zhang, K. O. Christe, Crystal structure of $\text{F}_2\text{NO}^+\text{AsF}_6^-$ and method for extracting meaningful geometries from oxygen/fluorine disordered crystal structures. *Inorg. Chem.* **40** (2001) 416.
116. E. C. Kostanek, W. R. Busing, A Single-Crystal Neutron-Diffraction Study of Urea-Phosphoric Acid. *Acta Crystallogr.* **B28** (1972) 2454.

Lebenslauf

Name: Hillary Anne Prescott

Geburtsort: San Francisco, California, USA

Geburtsdatum: 07.09.1971

Schulbesuch

1976 – 1982 Miraloma Elementary School, San Francisco, California

1982 – 1985 Aptos Middle School, San Francisco, California

1985 – 1989 Lick-Wilmerding High School, San Francisco, California
Abschluß: High School Diploma

Studium

1989 - 1991 Undergraduate Studies at the University of California, Davis
Studiengang: B.S. Chemistry

1991 - 1992 Studienaustauschprogramm der University of California mit der
Georg-August Universität, Göttingen
Studiengang: Diplom-Chemie

1992 - 1998 Chemiestudium an der Freie Universität, Berlin
Diplomarbeit an der BAM (Adlershof)
Abschluß: Diplom-Chemie

1998 – 2001 Promotion an der Humboldt-Universität zu Berlin im Institut für
Anorganische Chemie bei Prof. Dr. E. Kemnitz

Hiermit erkläre ich, daß ich die vorliegende Arbeit selbständig und nur unter Verwendung der angegebenen Literatur und Hilfsmittel angefertigt habe.

Berlin, 01.09.2001

Hillary A. Prescott